Sustainable engineering treatment for highly alkaline chromate contaminated groundwater

Samuel James Fuller

Submitted in accordance with the requirements for the degree of
Doctor of Philosophy

The University of Leeds

School of Civil Engineering
School of Earth and Environment

November 2013

The candidate confirms that the work submitted is his own, except where work which has formed part of jointly-authored publications has been included. The contribution of the candidate and the other authors to this work has been explicitly indicated below. The candidate confirms that appropriate credit has been given within the thesis where reference has been made to the work of others.

All three results chapters presented in this study have been prepared for publication in peer reviewed journals. Due to the collaborative nature of research, various stakeholders have contributed to their production. The extent of their involvement as well as the status of each journal paper is established below.

Chapter 4 – Chromate reduction in highly alkaline groundwater by zero valent iron: Implications for its use in a permeable reactive barrier.

Submitted to *Industrial and Chemical Engineering Research* in February 2013 and published April 2013.

S. J. Fuller	Principle author, Reduction experiments, surface reaction experiments, reaction rate analysis, SEM and XPS.
D. I. Stewart	Reaction rate analysis, SEM, XPS and extensive manuscript review.
I. T. Burke	SEM, XPS and extensive manuscript review.

Chapter 5 – Extracellular electron transport mediated Fe(III) reduction by a community of alkaliphilic bacteria that use flavins as electron shuttles.

Submitted to *Applied and Environmental Microbiology* July 2013 and published online prior to print October 2013.

S. J. Fuller	Principle Author, microcosm experiments, agar plate experiments, analysis of bacteria growth, DNA extraction, cloning and sequencing of the 16s rRNA gene, Mallard analysis, MOTHUR analysis, construction of the phylogenic tree and SEM analysis.
D. McMillan	Isolation and characterisation of riboflavin. Resin extraction, fluorescence spectroscopy, electrochemical assays and HPLC analysis.

M. Renz	Assisted D. McMillan in isolation and characterisation of riboflavin.
M. Schmidt	Assisted D. McMillan in HPLC analysis of riboflavin.
I. T. Burke	Extensive manuscript review.
D. I. Stewart	Extensive manuscript review, guidance on cloning and sequencing techniques.

Chapter 6 – Bio reduction of Hexavalent Chromium by Alkaliphilic Bacteria Recovered from a Chromite Ore Processing Residue Disposal Site.

Submitted to *Geomicrobiology* November 2013

S. J. Fuller	Principle Author, microcosm reduction experiments analysis of bacteria growth, DNA extraction, cloning and sequencing of the 16s rRNA gene, Mallard analysis, MOTHUR analysis, construction of the phylogenic tree.
I. T. Burke	Extensive manuscript review.
D. McMillan	Isolation and characterisation of riboflavin. Resin extraction, Fluorescence spectroscopy.
D. I. Stewart	Extensive manuscript review, guidance on cloning and sequencing techniques.

Acknowledgements

I would like to thank Doug Stewart and Ian Burke for their help, guidance and support throughout the previous three years. This project would not have been possible without their input. I would also like to thank Duncan McMillan for his pioneering work identifying and characterising the riboflavin secreted from my samples. Similar thanks extend to Phil Studds and Mark Bell of Ramboll UK who allowed access to the study site in West Yorkshire. I would also like to acknowledge the assistance provided by all the staff and colleagues who have helped me in a technical capacity throughout the previous three years. This includes Sheena Bennett, David Elliot and Mick Marsden for their advice and support in the laboratories, Ben Johnson, Eric Condliffe and Richard Walshaw for their assistance with XPS and SEM and Rachel Gasior, Lesley Neve and Mark Whittaker who aided with ICP-OES, XRF and XRD respectively. I would like to thank all my friends who have made university life such a special and fulfilling time. Special thanks go to my family who have supported me along the way. Finally I would like to thank Julia Baldwin for the love and support offered throughout my PhD.

This project has been funded by the University of Leeds John Henry Garner scholarship as well as The School of Civil Engineering.

Abstract

Chromite ore processing residue (COPR), a waste product from chromium extraction, is highly alkaline and is toxic due to the soluble Cr(VI) it contains. Unregulated dumping during the previous century led to many sites being contaminated with this waste. As Cr(VI) migrates in groundwater flows, reduction to less toxic and insoluble Cr(III) seems a prudent remediation strategy. Zero valent iron permeable reactive barriers (ZVIPRBs) and biobarriers are both capable of in-situ reduction reactions and were thus investigated for their suitability to treat COPR impacted sites.

Reduction of Cr(VI) by ZVI was possible at pH 12 however the rate was slow and unsustained. Amending pH resulted in increased reaction rates only in the acidic range (<pH 4). Comparative experiments showed that reduction from simple Cr(VI) solutions occurred quicker and for longer than from COPR leachate. Investigative surface analysis of ZVI exposed to both liquors revealed that whilst each sample harboured Cr(III), the iron exposed to COPR leachate had many other solutes precipitated on the surface (chiefly Ca and Si). These precipitates were blocking potential reaction sites, leading to premature inhibition of the iron. Thus whilst ZVI will reduce Cr(VI) at high pH, inhibition reactions may make a ZVIPRB prohibitively expensive.

A community of alkaliphilic Fe(III)-reducing bacteria (principally *Tissierella*, *Clostridium XI* and *Alkaliphilus* sp.) have been isolated from highly alkaline soil found beneath a 19th century COPR site. This community was able to reduce soluble Fe(III) into Fe(II) in anaerobic alkaline media – an important process as Fe(II) can reduce Cr(VI) abiotically. Bacterial growth occurred contemporaneously with the accumulation of riboflavin, a soluble electron shuttle. Bacteria grown in media spiked with riboflavin reduced Fe(II) at a faster rate and with less lag. Due to the link between iron reduction and flavin concentration, it is likely that riboflavin has an import role in extracellular metal reduction by this alkaliphilic community.

In Fe(III) growth media spiked with chromate, Cr(VI) reduction was recorded in media where the initial chromate concentration was up to 8500µmol.L^{-1}. Population data shows that as Cr(VI) is introduced into the growth media the diversity of the community is reduced as the Tissierella, sp. appear to have a low tolerance for Cr(VI). Cr(VI) reduction was also observed in media with Cr(VI) as the sole electron donor, although growth in this media was weak.

The only species to be able to use Cr(VI) as the sole electron donor were Clostridium XI. Both the original Fe(III)-reducing consortium, and the Cr(VI)-reducing *Clostridium XI* sp. were also able to reduce solid phase Fe(III) contained within aquifer material from the site from which they were isolated. Growth of the Fe(III)-reducing consortium on solid phase iron favoured a single species of Tissierella which released riboflavin; probably because this electron shuttling compound can mediate reduction of the extracellular solid phase iron.

Results from this study indicate that biobarriers hold significant promise for the successful treatment of COPR impacted sites. It shows that bioreduction of Cr(VI) can occur as a direct enzymatically mediated process, but this process may not support long term growth. Cr(VI) reduction also occurs as part of Fe(III)/Fe(II) cycling that does support long term growth, even in the presence of high Cr(VI) concentrations. Therefore, it is likely that the indirect mechanism involving microbial Fe(III) reduction will be the more important mechanism for reducing Cr(VI) mobility a at COPR impacted sites.

Abbreviations

ADP	Adenosine Diphosphate
AMP	Adenosine Monophosphate
ATP	Adenosine Triphosphate
BET	Brunauer-Emmett-Teller analysis
CACs	Calcium Aluminium Chromium Oxide Hydrates
COPR	Chromate Ore Processing Residue
CV	Cyclic Voltammograms
DNA	Deoxyribonucleic acid
dNTPs	Deoxynucleoside triphosphates
EDX	Energy-dispersive X-ray spectroscopy
EDTA	Ethylenediaminetetracetic acid
FMN	Flavin Mono Nucletide
FAD	Flavin Adenine Dinucleotide
HDPE	High-Density Polyethylene
HPLC	High Performance Liquid Chromatography
HVOC	Halogenated Volatile Organic Compound
ITS	Internal Transcribed Spacer
MOPS	(*N*-morpholino)propanesulfonic acid
nZVI	Nano Zero Valent Iron
OTU	Operational Taxonomic Unit
PCR	Polymerase Chain Reaction
PTFE	Polytetrafluoroethylene
PRB	Permeable Reactive Barrier
RDP	Ribosomal Database Project
RISA	Ribosomal Integenic Spacer Analysis
RNA	Ribonucleic Acid

SAM	Self-Assembled Monolayer
SEM	Scanning Electron Microscopy
TBE	TRIS, Borate, EDTA, buffer
TSG	Template Stripped Gold
TRIS	Tris (hydroxymethyl) aminomethane ($(HOCH_2)_3CNH_2$)
USEPA	United States Environmental Protection Agency
WHO	World Health Organisation
XPS	X-ray photoelectron spectroscopy
ZVI	Zero Valent Iron
ZVIPRB	Zero Valent Iron Permeable Reactive Barrier

Table of Contents

List of Tables

List of Figures

Chapter 1 **Introduction, Aims and Objectives**

1.1 Introduction

Chromium has many uses in the modern world including in metallurgy, tanning leather and pigments leading to a worldwide consumption of 19.5 million tonnes per year (Guertin et al., 2004, Papp, 2010). In the environment, chromium rarely exists in its elemental form thus the majority is extracted from chromite ore. The principle technique utilised in the 20th century was called the high lime extraction process. Chromite ore was roasted at up to 1500°C in the presence of sodium carbonate and lime which allowed the oxidation of Cr(III) into Cr(VI); which was subsequently extracted out in solution (Darrie, 2001). Chromate Ore Processing Residue (COPR) is the waste material left over from this process. COPR is highly alkaline (pH 12+) and still retains up to 7% of chromium; around 25% of which being in the Cr(VI) state (Hillier et al., 2003, Chrysochoou et al., 2010, Stewart et al., 2010). This represents a problem as Cr(VI) is toxic and carcinogenic to humans and being soluble is highly mobile within water flows (Shayne, 1989). On the other hand Cr(III) is an essential mineral for humans and in neutral to alkaline solutions precipitates as insoluble hydroxides (Anderson, 1989, Rai et al., 1989). Before the problems with this waste were recognised, the majority was used as cheap construction fill or dumped in unlined waste heaps (Chrysochoou et al., 2010, Stewart et al., 2007, Stewart et al., 2010). Thus whilst this process has mostly been superseded by other methods, there is a legacy in this country and abroad of historic COPR sites where soluble Cr(VI) is leaching away from the waste and contaminating large areas of land downstream (Whittleston et al., 2011, Stewart et al., 2007, Wang et al., 2007, Farmer et al., 2006).

Currently there is no consensus on the most appropriate method with which to treat such a site. Traditional remediation strategies generally relied on removing the waste from site and any treatment occurring externally. However Cr(VI) bearing dust has been identified as the principal risk associated with the waste, meaning that removal via excavation would be dangerous and prohibitively expensive. Therefore the only viable treatment options are those which leave the waste in-situ and treat any leachate leaving the site. Strategies that reduce the Cr(VI) to Cr(III) seem the

most prudent approach due to the environmentally favourable characteristics displayed by Cr(III) compounds. The remediation field has benefitted from numerous advances in technology over recent years. Of these, the two techniques which hold most promise for highly alkaline COPR sites are the permeable reactive barrier (PRB) and the biobarrier. Both are non-intrusive to the waste and allow the treatment of contaminated ground flows via a reductive mechanism – essential for COPR sites. This study aimed to investigate the suitability of using such technologies for the treatment of highly alkaline COPR waste so that if the results were successful a practicing engineer would be able to prescribe such technologies in the field. With that in mind, the following aims and objectives were highlighted in order for that to be addressed.

1.2 Zero Valent Iron Permeable Reactive Barriers: Aims and Objectives

Aim:- To investigate the suitability of a zero valent iron PRB for the treatment of highly alkaline COPR leachate.

Whilst pursuing this aim, the following hypotheses and objectives were considered.

Hypothesis:- The reaction between ZVI and Cr(VI) results in Cr(VI) removal at rates that are sufficiently fast to be useful in an engineering solution.

Objective:- Investigate the rate at which ZVI reduces Cr (VI) from COPR leachate at different solid solution ratios in order to develop a rate equation which describes the reaction.

Hypothesis:- Lowering the pH of the leachate will result in an increased reduction rate of Cr(VI) by ZVI.

Objective:- Investigate how the reduction rate of Cr(VI) changes with change in pH.

Hypothesis:- The rate at which ZVI reduces Cr(VI) in alkaline conditions will be affected by passivation and inhibition reactions of the iron.

Objective:- Investigate the surface chemistry of the iron when placed in highly alkaline COPR leachate in order to determine the passivation and inhibition reactions that have occurred.

Hypothesis:- The rate at which ZVI reduces Cr(VI) from COPR leachate in alkaline conditions will be affected by other solutes within the leachate.

Objective:- Investigate how solutes within COPR affect the reduction rate between Cr(VI) and zero valent iron.

1.3 Biobarriers Aims: and Objectives

Aim:- To investigate the suitability of a biobarrier for the treatment of highly alkaline COPR leachate.

In order to achieve the aim, the following hypotheses and objectives were considered.

Hypothesis:- Indigenous alkaliphile Fe(III) reducing Bacteria isolated from a soil stratum beneath a historic COPR site are able to tolerate and reduce Cr(VI).

Objective:- Investigate the microbial growth of a stable consortium of alkaliphile Fe(III) reducing bacteria in the presence of varying concentrations of Cr(VI).

Hypothesis:- Alkaliphile Fe(III) reducing bacteria are able to respire using Cr(VI) as the sole terminal electron acceptor without the presence of Fe(III).

Objective:- Investigate growth of the same bacteria population in media containing Cr(VI) as the sole electron acceptor.

Hypothesis:- The bacteria population present will favour some electron donors compared to others.

Objective:- Investigate how the growth of the bacteria population is affected when grown with differing electron donors.

Hypothesis:- Changes to the media in which the bacteria population are grown (including the introduction of Cr(VI)) will result in changes to that population.

Objective:- Investigate how the bacteria population changes when grown in differing growth media and in varying Cr(VI) concentrations .

Hypothesis:- Understanding the reductive mechanisms of the bacteria population will allow engineers to tailor the electron donors and specific metabolites needed in order to help the growth of the bacteria.

Objective:- Investigate the reductive mechanisms of the same bacteria population including electron transfer mechanisms.

Hypothesis:- Alkaliphile Fe(III) reducing bacteria will be able to grow using solid Fe(III) minerals contained within natural soils as the terminal electron acceptor.

Objective:- Investigate the growth and electron transfer mechanism of the bacteria population in media with soil Fe(III)- material as the sole electron acceptor.

1.4 Thesis Structure

A thorough literature review highlighting the most recent knowledge in this field is followed by a detailed materials and methods section. Three results chapters follow which have all been prepared for external peer reviewed publication. The thesis is finalised with a Summary and conclusion chapter which highlights the key findings of this study and suggests possible future work which could follow on. Copies of the associated peer reviewed publications are included in an appendix.

1.5 References

Alowitz, M. J. & Scherer, M. M. 2002. Kinetics of Nitrate, Nitrite, and Cr(VI) Reduction by Iron Metal. *Environ. Sci. Technol.,* 36**,** 299-306.

Anderson, R. A. 1989. Essentiality of chromium in humans. *Sci. Total Environ.,* 86**,** 75-81.

Chang, L.-Y. 2005. Chromate reduction in wastewater at different pH levels using thin iron wires—A laboratory study. *Environ. Prog.,* 24**,** 305-316.

Chrysochoou, M., Dermatas, D., Grubb, D., Moon, D. & Christodoulatos, C. 2010. Importance of Mineralogy in the Geoenvironmental Characterization and Treatment of Chromite Ore Processing Residue. *J. Geotech. Geoenviron. Eng.,* 136**,** 510-521.

Darrie, G. 2001. Commercial Extraction Technology and Process Waste Disposal in the Manufacture of Chromium chemicals From Ore. *Environ. Geochem. Health,* 23**,** 187-193.

Farmer, J. G., Paterson, E., Bewley, R. J. F., Geelhoed, J. S., Hillier, S., Meeussen, J. C. L., Lumsdon, D. G., Thomas, R. P. & Graham, M. C. 2006. The implications of integrated assessment and modelling studies for the future remediation of chromite ore processing residue disposal sites. *Sci. Total Environ.,* 360**,** 90-97.

Fiuza, A., Silva, A., Carvalho, G., de la Fuente, A. V. & Delerue-Matos, C. 2010. Heterogeneous kinetics of the reduction of chromium (VI) by elemental iron. *J. Hazard. Mater.,* 175**,** 1042-1047.

Gheju, M. & Iovi, A. 2006. Kinetics of hexavalent chromium reduction by scrap iron. *J. Hazard. Mater.,* 135**,** 66-73.

Guertin, J., Jacobs, J. A. & Avakian, C. P. 2004. *Chromium(VI) Handbook*, Taylor & Francis.

Harish, R., Samuel, J., Mishra, R., Chandrasekaran, N. & Mukherjee, A. 2012. Bio-reduction of Cr(VI) by exopolysaccharides (EPS) from indigenous bacterial species of Sukinda chromite mine, India. *Biodegradation,* 23**,** 487-496.

Hillier, S., Roe, M. J., Geelhoed, J. S., Fraser, A. R., Farmer, J. G. & Paterson, E. 2003. Role of quantitative mineralogical analysis in the investigation of sites contaminated by chromite ore processing residue. *Sci. Total Environ.,* 308**,** 195-210.

Liu, C., Gorby, Y. A., Zachara, J. M., Fredrickson, J. K. & Brown, C. F. 2002. Reduction kinetics of Fe(III), Co(III), U(VI), Cr(VI), and Tc(VII) in cultures of dissimilatory metal-reducing bacteria. *Biotechnol. Bioeng.,* 80**,** 637-649.

Papp, J. F. 2010. 2010 Minerals Yearbook, Chromium. *United States Geological Survey*.

Rai, D., Eary, L. E. & Zachara, J. M. 1989. Environmental chemistry of chromium. *Sci. Total Environ.,* 86**,** 15-23.

Shayne, C. 1989. Acute and chronic systemic chromium toxicity. *Sci. Total Environ.,* 86**,** 149-157.

Stewart, D. I., Burke, I. T., Hughes-Berry, D. V. & Whittleston, R. A. 2010. Microbially mediated chromate reduction in soil contaminated by highly alkaline leachate from chromium containing waste. *Ecol. Eng.,* 36**,** 211-221.

Stewart, D. I., Burke, I. T. & Mortimer, R. J. G. 2007. Stimulation of Microbially Mediated Chromate Reduction in Alkaline Soil-Water Systems. *Geomicrobiol. J.,* 24**,** 655 - 669.

Wang, T., He, M. & Pan, Q. 2007. A new method for the treatment of chromite ore processing residues. *J. Hazard. Mater.,* 149**,** 440-444.

Whittleston, R. A. 2011. *Bioremediation of chromate in alkaline sediment-water systems.* PhD thesis, University of Leeds.

Whittleston, R. A., Stewart, D. I., Mortimer, R. J. G., Tilt, Z. C., Brown, A. P., Geraki, K. & Burke, I. T. 2011. Chromate reduction in Fe(II)-containing soil affected by hyperalkaline leachate from chromite ore processing residue. *J. Hazard. Mater.,* 194**,** 15-23.

Chapter 2 **Literature review**

2.1 Chromium and the COPR problem

2.1.1 **Chromium: An Introduction**

Chromium is a transitional metal taking its name from the Greek *Chroma* meaning colour, due to the many different colours of its compounds. Chromium was formally discovered as the mineral Crocite ($PbCrO_4$) in 1761 and isolated in its elemental form in 1797 (Guertin et al., 2004). It is the 16th most abundant compound in the universe, 7th most in the earth and 32nd most in the human body (Cervantes et al., 2001). The distribution of Cr within the earth is heterogeneous, dependent on the presence of specific Cr containing minerals however typical content ranges from 0.1 to 0.3 $mg.kg^{-1}$ (Dhal et al., 2013b). The first recorded human use was by the Chinese over 2000 years ago, who coated the weapons of their terracotta army in chromium oxide in order to prevent rust and allow them to keep their edge (Liu et al., 2011). In modern life, chromium has a vast array of uses including in the manufacture of stainless steel, chrome plating, metal strengthening, colourant in dyes, tanning, wood preservation and in catalysts (Guertin et al., 2004), which leads to an estimated worldwide annual production of 19.5 million tonnes of chromium containing material (Papp, 2010). Chromium exists in the range of oxidation states between -2 to +6 however in the natural environment it typically only exists in its two most thermodynamically stable forms, +3 and +6 (Kotaś and Stasicka, 2000).

2.1.2 **Chromium: Impact on Human Health and the Environment.**

The two environmentally significant oxidation states of chromium, +3 and +6, have wildly different effects on human health and the wider environment. Cr(III) is rated as non-toxic and is considered an essential nutrient for humans; vital for glucose and lipid metabolism (Anderson, 1989). The recommended daily intake is currently set at 50 to 200µg (Anderson, 1989). Cr(III) is considered to be safe to humans as it is rarely transported through cell membranes, meaning that Cr(III) is unlikely to be absorbed by cells directly (Leonard and Lauwerys, 1980).

On the other hand Cr(VI) is toxic, carcinogenic, mutagenic and an irritant (Shayne, 1989). Hexavalent chromium can easily cross cell membranes and once inside is quickly reduced to its trivalent form. The Cr(III) produced can then bind with intercellular components, leading to mutations and formation of cancerous cells (Leonard and Lauwerys, 1980). The toxic nature of Cr(VI) was first documented in 1827 in a medical report listing the development of dermatitis and ulcers on the skin of workers producing potassium dichromate, a brilliant yellow dye (Cumin, 1827). Subsequently there have been many reports documenting the ailments suffered by those working with Cr(VI) compounds, including the perforation of nasal septa, increased incidence of cancer of the respiratory tract and skin problems such as dermatitis and sores (Leonard and Lauwerys, 1980, Shayne, 1989).

The main exposure pathway for humans has been identified as insoluble Cr(VI) containing dust, inhaled directly into the lungs. The dust particles are sparingly soluble so remain in the lung for a long time, leading to large scale ingress of Cr(VI) into the surrounding cells. The World Health Organisation made an estimation that the additional risk of developing lung cancer after a lifetime of exposure to 1 $\mu g.m^3$ airborne Cr(VI) was 4×10^{-2} (World Health Organisation, 2000). Dermal exposure to Cr(VI) salts is likely to produce irritative or corrosive responses on the skin (Shayne, 1989). Other effects can include allergic reactions or the onset of dermatitis. Cr(VI) ingested orally offers the most acute danger to human health, with death likely to follow after consumption of as little as 1 to 3g chromic acid (Leonard and Lauwerys, 1980). Along with the corrosive effects on the upper gastro intestinal tract, ingestion of enough hexavalent compounds will lead to nephrotoxicity and death (Shayne, 1989). Although being the most dangerous exposure pathway, oral consumption is very rare.

The effects of chromium compounds on animals have been extensively studied, most notably on laboratory rats. Effects are much the same as in humans with Cr(VI) causing mutations and cancer in cells (Costa, 1997). Fish exposed to Cr(VI) show behavioural changes, chromium accumulation within body tissue, damage to gills, kidneys and livers and at high enough concentrations, death. For example exposure of the Indian freshwater fish *Channa Puntatus* to 40 $mg.l^{-1}$ potassium dichromate resulted in severe tissue damage to the gills, kidneys and liver; and in some cases death (Mishra and Mohanty, 2008). Behaviour changes were also

observed including hyperactivity and loss of balance. Cr(VI) exposure to Dab and Mullet caused respiratory problems, discolouration and increased instances of swimming to the surface by the fish (Taylor et al., 1985).

Studies have shown that both Cr(VI) and Cr(III) appear to be toxic to plants leading to negative effects such as poor germination, decrease in root length, lower growth heights and reduced foliage (Shanker et al., 2005). A study measuring the algae population in a chromium impacted river showed that upstream of the contamination grew 8 different species, which reduced to 3 species immediately downstream from the waste (Breeze, 1973). The algae population had not recovered a further 1.5km down river. Comparing the impact of waterborne Cr(VI) and Cr(III) on the growth of *Lolium Perenne* seeds showed the toxicity of both compounds to be comparable, however the introduction of soil vastly reduced the toxicity of Cr(III), possibly as it formed hydroxide and organic complexes within the soil which limited the attack on the plant (Breeze, 1973). Thus trivalent chromium compounds are greatly preferable compared to Cr(VI) from a health and environmental stand point.

2.1.3 **Chromium Production and Chromate Ore Processing Residue**

Naturally occurring elemental chromium is very rare, thus the majority has to be extracted from mineral ores before use. Chromite ore is the name given to the range of spinel materials that are the main source of chromium worldwide. Although primarily composed of chromium, iron and oxygen ($FeO.Cr_2O_3$), substitutions within the crystal lattice allow impurities to change the chemical composition of the ore. For example FeO can be replaced by magnesium oxide, and Cr_2O_3 by aluminium or ferric oxide so Chromite is often given the chemical formula $(Mg,Fe)(Al,Cr,Fe)_2O_3$ (Breeze, 1973). The ore has typical Cr_2O_3 content of 15 to 65% (Darrie, 2001), and FeO content of 10 to 26% (Leonard and Lauwerys, 1980). Major sources of chromite are found in South Africa, Russia, Kazakhstan, USA, India, and Turkey (Papp, 2010).

Highly alkaline Chromate Ore Processing Residue (COPR) is the waste product from an antiquated method of extracting chromium from chromite ore; dubbed the high lime extraction process. The first commercial extraction process was developed around 1810 and involved oxidising chromium (III) contained within the ore with

potassium nitrate. The ore was crushed, mixed with the KNO_3 and then roasted at 1100 to 1500°c. This process yielded soluble potassium chromate which could be leached out in solution (Darrie, 2001). Subsequent technological advances first replaced potassium nitrate with sodium carbonate and then in 1845, lime was added to the reactor mix (Darrie, 2001). Lime improved the yield of chromate as it stopped the reactants from fusing, allowing better penetration of the mixture by oxygen and therefore greater oxidation of the Cr(III). The 'high lime' process was born and utilised the following two step reaction:

$$4FeCr_2O_4 + 8Na_2CO_3 + 7O_2 \rightarrow 8Na_2CrO_4 + 2Fe_2O_3 + 8CO_2$$

(2.1)

$$2Na_2CrO_4 + H_2SO_4 \rightarrow Na_2Cr_2O_7 + Na_2SO_4 + H_2O$$

(2.2)

This method was used universally until around 1960 when further technological advances allowed lime free methods to be developed; namely utilising coke or silicothermic and aluminothermic reactions to oxidise the Cr(III) (Guertin et al., 2004). The majority of western chromium producing countries started to switch techniques around this time, however around 40% of total Cr production is still done using the high lime method of extraction; predominantly in Russia, China and other developing countries (Darrie, 2001).

COPR is a highly complex material which can contain a number of different compounds, dependent on the initial reactor mix in the processing plant, the source and chemical composition of the Chromite Ore, and how the residue has been treated post processing. Major elements include Mg, Ca, Si, Fe, Al, S and Na (Geelhoed et al., 2002) which combine to create a number of different compounds, most of which can be categorised into three main groups.

Unreacted materials from the extraction process are the principal constituents of COPR, with up to 70% being Chromite Ore (Hillier et al., 2003). Lime, is also present, usually in the hydrated form Portlandite ($Ca(OH)_2$) (Chrysochoou et al., 2010). The second group include Brownmillerite (Ca_2FeAlO_5), Periclase (MgO) and Larnite (Ca_2SiO_4) which are all phases formed in the high temperatures of the

extraction reactor (Hillier et al., 2003). The third group contains, but is not limited to, Brucite ($Mg(OH)_2$), Calcite, Arogonite ($CaCO_3$), Ettringite ($Ca_6Al_2(OH)_{12}(SO_4)_3$), Calcium aluminium chromium oxide hydrates (CACs) ($Ca_4Al_2(CrO_4)(OH)_{12}.nH_2O$, n= 3, 6, 8), Hydrogarnet ($Ca_3Al_2(OH)_{12}$), Hydrocalumite ($Ca_4Al_2Cl_2(OH)_{12}.6H_2O$) and Hydrocalcite ($Mg_6Al_2(CO_3)(OH)_{16}.4H_2O$) which are assumed to have formed either during the leaching phase of extraction or post processing due to weathering and hydration reactions (Hillier et al., 2003, Chrysochoou et al., 2009).

Once removed from the processing plant hydration reactions onset by the weathering of Brownmillerite, Periclase and Portlandite appear to control the chemical composition of COPR. Chrysochoou et al. analysed the mineralogy of COPR samples from the same processing plant deposited in the same location. They found that although being placed in the same locality, different waste horizons in the waste pile had wildly different chemical compositions. COPR from lower in the ground had up to 45% brownmillerite and 3% periclase. COPR from nearer the surface and subject to increased levels of weathering contained only 2.4% brownmillerite and zero periclase, the main compounds found being hydrogarnet (34%), CACs (12.8%), and hydrocalcites (11.2%); all hydration products (Chrysochoou et al., 2009). Brucite, ettringite, argonite, vaterite and dolomite are also thought to be formed via weathering of brownmillerite, periclase and portlandite in the presence of common groundwater solutes (Chrysochoou et al., 2009). As well as these typical minerals listed, COPR can also contain many other compounds although not in any significant quantity and usually site specific, for example when mixed with other industrial waste from the same chemical plant (Breeze, 1973).

Inefficient oxidation and leaching during the extraction process results in usually 2 to 7% chromium remaining in the waste, with up to 25% of the total being Cr(VI) (Hillier et al., 2003, Weng et al., 1994, Burke, 1991). Of the Cr(III) present, 60 to 70% is contained within unreacted chromite ore. The rest is associated with other common COPR minerals such as brownmillerite, hydrogarnet, hydrocalumite and ettringite that are all known to be able to substitute Cr(III) for Fe and Al within their mineral structure (Hillier et al., 2003, Kindness et al., 1994, Battle et al., 1991).

The hexavalent chromium contained within COPR can be associated with a number of the pre-mentioned mineral phases such as ettringite, hydrocalumite, CACs and possibly hydrogarnet. CrO_4^{2-} can replace the SO_4^{2-} within ettringite and can be

incorporated as the anion in hydrocalcumite (Palmer, 2000). In the case of hydrogarnet, replacement of the SiO_4^{4-} tetrahedral by Cr(VI) anions is theoretically possible but this substitution has not yet been confirmed (Hillier et al., 2003). Other Cr(VI) containing phases found in COPR deposits include the chromium salts, Calcium Chromate ($CaCrO_4$), Calcium aluminochromate ($3CaO.Al_2O_3.CaCrO_4$), tribasic calcium chromate ($Ca_3(CrO_4)_2$) and ferric chromate ($Fe(OH)CrO_4$) (Burke, 1991, Sreeram and Ramasami, 2001). Many of these Cr(VI) containing compounds are sparingly soluble in water which could account for the exceedingly high levels of Cr(VI) still retained by many historic COPR waste sites.

Apart from its large chromium content, the other defining feature of COPR is a hyper alkaline pH, usually >12 (Chrysochoou et al., 2010, Stewart et al., 2010). This is a direct consequence of the presence of lime containing minerals from the reaction process. Thus COPR waste suffers from the dual problems of being highly caustic due to its alkaline pH and extremely toxic due to its Cr(VI) content.

Pore water recovered from COPR deposits has shown that Cr(VI) is leachable from within the waste. COPR Leachate recovered from a site in northern England had a Cr(VI) concentration of 600 $\mu mol.l^{-1}$ and a pH of 12.3, (Stewart et al., 2007) whilst a similar site in West Yorkshire has pore water containing 990 $\mu mol.l^{-1}$ Cr(VI), with a pH of 12.2 (Whittleston et al., 2011b). Leachate collected from boreholes downstream of a COPR site in Glasgow had a Cr content of up to 125 $mg.l^{-1}$, between 64 to 98% of which was in the +6 oxidation state with the pH of the samples ranging from 11.7-12.3 (Farmer et al., 2002). In order to determine the extent of environmentally mobile Cr within solid phase COPR, many leaching tests have been done on the waste. When leaching with acid, Weng et al. adjusted the pH of COPR in the presence of simulated rainwater and found that only 1% of the total chromium contained within COPR was extractable; an amount recorded throughout the pH range of 2.5 to 12 (Weng et al., 1994). Others have reported that the amount of Cr(VI) released increased in neutral to moderately alkaline conditions (Tinjum et al., 2008). When conducting these tests it was found that large quantities of acid were required in order to lower the pH of the COPR due to its huge buffering capacity (Tinjum et al., 2008). Thus efforts to release all available Cr from environmental deposits of COPR using acid would be problematic and uneconomic due to the sheer volume required.

A lack of any passable contaminated waste strategy, combined with little understanding of the toxic nature of the Cr(VI) contained within waste, led to much of the historically produced COPR being dumped in the easiest and cheapest place possible. Usually this meant either in industrial waste tips close to the production facility, or sold as a construction fill due to its resemblance to a sandy soil; ideal as a foundation material (Chrysochoou et al., 2010, Burke, 1991, Breeze, 1973, Stewart et al., 2010, Stewart et al., 2007). Indeed taking into account other sources of Cr(VI) contamination, it is considered one of the top 20 contaminants by the USA Superfund (Dhal et al., 2013b). Many COPR deposits are poorly managed and allow unrestricted groundwater access to the site. Once leachate has left a COPR waste site in such groundwater flows, the chromium it contains can have many different fates within the environment.

2.1.4 **Aqueous Geochemistry of Chromium**

2.1.4.1 The Chromium Cycle

The oxidation state and thus solubility of chromium within the environment is controlled by a well-defined cycle of reactions called the chromium cycle (see Figure 2.1). Cr(III) and Cr(VI) are the only forms of chromium stable within the environment (Kotaś and Stasicka, 2000) and a number of (sometimes simultaneous) reactions cycle the metal between these oxidation states (Dhal et al., 2013b). Cr(VI) is the most mobile, reactive and mobilised form of chromium within the environment (Bartlett, 1991). As such, large concentrations of Cr(VI) are usually only found directly from a chromate polluting source or from the oxidation of a Cr(III) source (Bartlett, 1991, Richard and Bourg, 1991). Once within the ground, naturally occurring Fe(II) and organic matter present within soils will reduce the Cr(VI) into Cr(III), producing a variety of different compounds depending on the geochemistry of the ground (Whittleston et al., 2011b, James, 1996). Some Cr(III) will react with citric acid to form chromic citrate, which is soluble and therefore mobile (Dhal et al., 2013b). Finally naturally occurring manganese oxides will oxidise the Cr citrate, forming Cr(VI) compounds, with a direct correlation existing between the amount of oxidised Cr(III) and the Mn oxide content of a soil (Bartlett and James, 1979). Thus a finely tuned balance between the amount of organic matter and Fe(II) on one hand

and manganese oxides on the other, will ultimately determine the oxidation state of chromium within the environment.

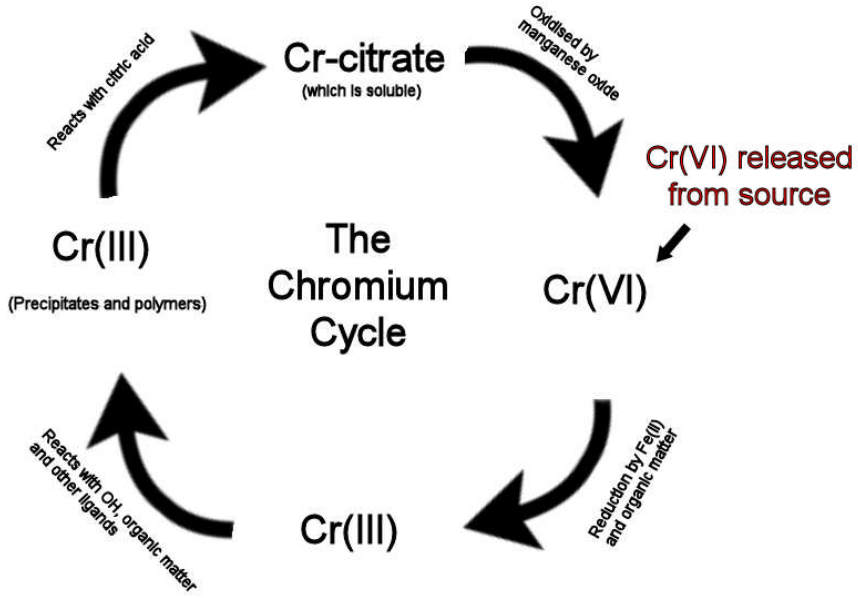

Figure 2.1: Simplified diagram of the chromium cycle in the environment. Adapted from (Dhal et al., 2013b, Bartlett, 1991).

2.1.4.2 Cr(VI)

The requirement for oxidising conditions and high pH (Figure 2.2) means that finding significant quantities of Cr(VI) in the environment is unlikely, and any such presence is highly likely to be from an anthropogenic source (Richard and Bourg, 1991). The exact Cr(VI) species is dependent on pH and Cr concentration. In acidic conditions, dichromate ($Cr_2O_7^{2-}$), and bichromate ($HCrO_4^-$) dominate however chromic acid (H_2CrO_4) is also possible between pH 1 to 3 (Tandon et al., 1984). Above pH 6.5, chromates (CrO_4^{2-}) are expected to be the sole Cr(VI) phase (Figure 2.3). The majority of Cr(VI) compounds are highly soluble in water at any pH, meaning that they are exceedingly mobile in groundwater and have the potential to spread far from source (Kotaś and Stasicka, 2000). There are however notable exceptions such as Cr(VI) salts with a divalent cation, like zinc, barium and lead chromates which buck this trend (Guertin et al., 2004, UK Environmental Agency, 2002). Once in solution, sorption and redox reactions will ultimately control Cr(VI)'s fate.

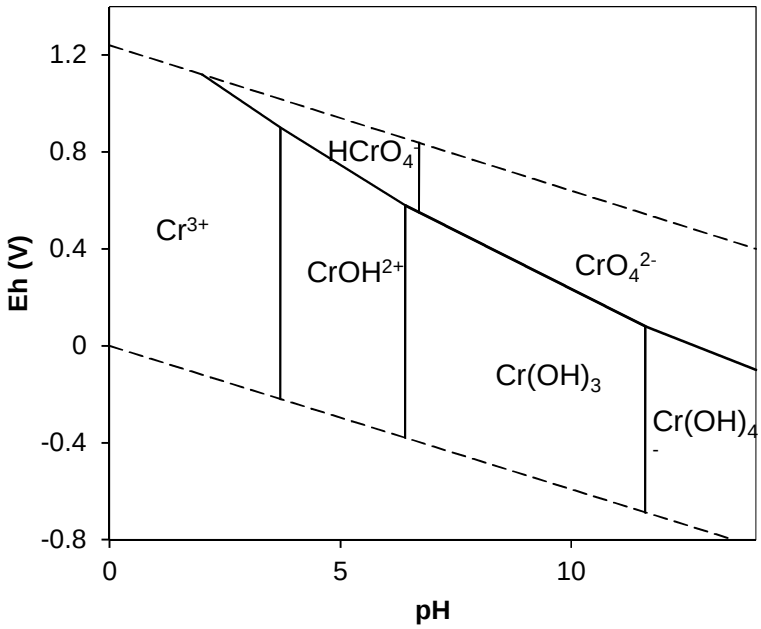

Figure 2.2: Pourbaix diagram highlighting the expected chromium compounds within the stability field of water. Redrawn from that presented by Rai et al. (Rai et al., 1989).

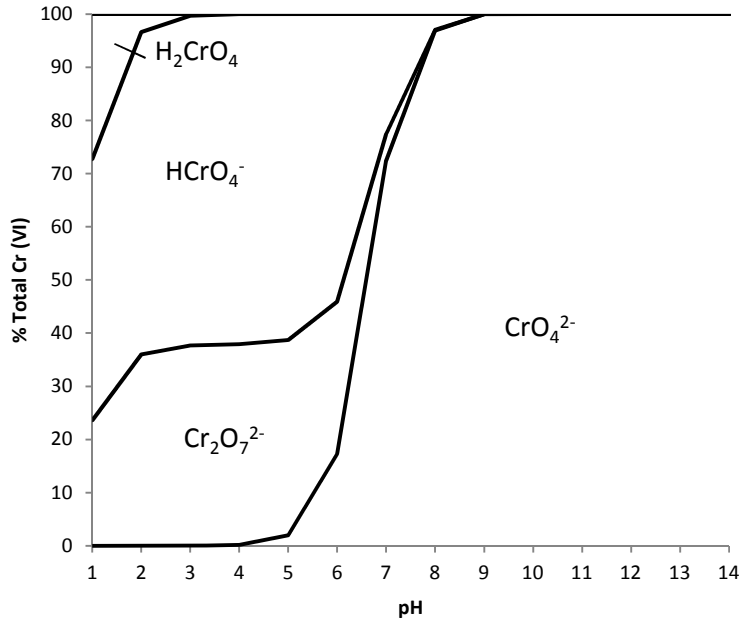

Figure 2.3: Cr(VI) species as a % of total when concentration is $1x10^{-2}$ $mol.l^{-1}$ in the pH range 1 to 14. Produced using data published by (Tandon et al., 1984).

As demonstrated by the chromium cycle redox reactions control the form of Cr within the environment. These reactions are those when an electron is passed from one compound to another in order to drive a chemical reaction, thereby changing the oxidation state of both reactants in the process. Many elements show vastly different physical and chemical properties dependent on their oxidation state thus changing from one state to another can result in notable changes in solubility or reactivity.

The instability of Cr(VI) in liquors with low redox potentials (see Figure 2.2), means that within normal environmental conditions it is likely to be reduced. Many naturally occurring materials and compounds are able to reduce Cr(VI) including elemental and ferrous iron, reduced sulphides and organic matter, usually resulting in the formation of Cr(III) (Deng and Stone, 1996, Buerge and Hug, 1999, Graham et al., 2006, Fiuza et al., 2010, Dhal et al., 2013b). Of these, the most significant on COPR sites are likely to be organic matter and iron minerals as they are both abundant within the subterranean environment.

Organic substances such as humic acids, proteins and carbohydrates are all capable of reducing Cr(VI) to Cr(III) however these reactions appear to be dependent on acidic conditions (Dhal et al., 2013b). Other matter such as hydroquinones are also able to reduce Cr(VI) (James, 1996). Obviously the incidence of organic matter within soils decreases with depth, thus these reactions will only be significant near the surface. Reduction by organic matter appears to create soluble chelated Cr(III) compounds which may be amenable to reoxidisation (Fendorf and Li, 1996).

Whilst both Fe(0) and Fe(II) can reduce Cr(VI), Fe(0) is unlikely to be found in the natural environment due to its propensity to oxidise. Fe(II) is present in a number of stable minerals such as magnetite, vivianite and siderite. Fe(II) is able to reduce Cr(VI) quickly in neutral to acidic conditions however this reaction slows in the alkaline pH range due to the formation of passivating Fe(III) phases (He and Traina, 2005, Buerge and Hug, 1999, Fendorf and Li, 1996). This reaction generates insoluble Cr(III) hydroxides which are stable and generally unavailable for reoxidisation.

Sorption reactions can have a major effect on the mobility of compounds within a subsurface. They bind with compounds in a solution (the adsorbate) to a physical surface (the adsorbant), resulting in an accumulation of adsorbate on that surface. This can be achieved via physisorption, chemisorption or as a result of electrostatic attraction. Many different minerals found in soils can adsorb Cr(VI); mainly those that have exposed inorganic hydroxyl groups on their surface (Rai et al., 1989). Hematite (Fe_2O_3), goethite (α-FeOOH) and alumina (α-Al_2O_3) all adsorb high levels of Cr(VI) in acidic conditions, however for each material the rate of sorption dramatically reduces as pH is increased above neutral (Ajouyed et al., 2009). Grossl et al. reported 100 $mmol.kg^{-1}$ Cr(VI) adsorption by goethite at pH 5, an effect that was completely nullified when pH was increased to 10 (Grossl et al., 1997). Rai et al. found that adsorption of Cr(VI) on amorphous iron oxide effectively stopped above pH 8 (see Figure 2.4.3) (Rai and Zachara, 1986). The reduction in sorption capacity with increased pH is typical adsorption behaviour for anionic species in solution and is possibly due to competition for sorption sites between the chromate ions and OH^-. Once a material has a high proportion of negatively charged OH^- adhered to its surface, the electrostatic charge created will repel the similarly charged CrO_4^{2-} anion, making chromate sorption less likely. For example the point

of zero charge for an alluvium sample collected from beneath a Cr(VI) impacted area was reported as pH 8.35, a level above which adsorption rates will be low (Stollenwerk and Grove, 1985). In the hyper alkaline conditions found near COPR sites, the high concentration of OH^- ions will make sorption of Cr(VI) on soil minerals unlikely and is probably the primary reason as to why it is so easy for it to propagate far from these sites within groundwater flows. As leachate migrates away from a site, the pH of the liquor is likely to reduce due to buffering by soil minerals. If the pH lowers to around neutral, sorption reactions may become significant in Cr(VI) removal from solution.

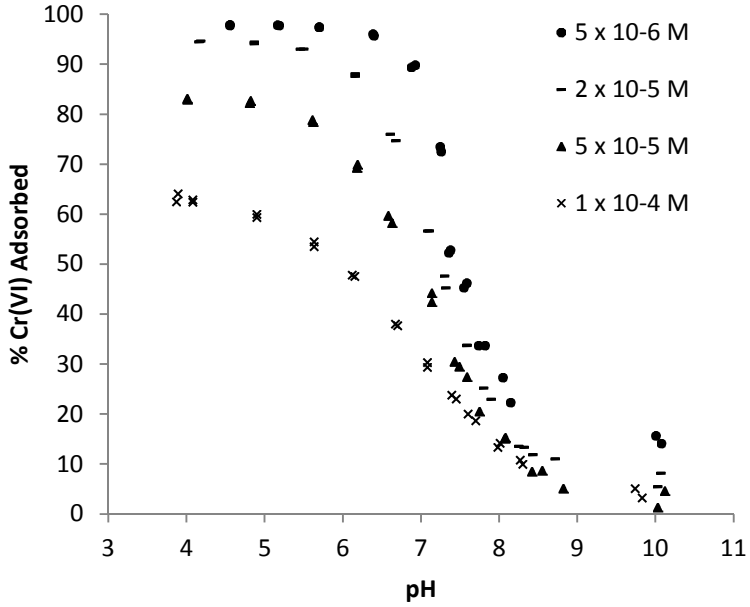

Figure 2.4: Percentage of total Cr(VI) adsorbed on 0.87 x 10^{-3} M amorphous iron oxide ($Fe_2O_3.H_2O$ (am)) for a range of different chromate concentrations. Produced using data published by (Rai and Zachara, 1986).

2.1.4.3 Cr(III)

Trivalent chromium in the aqueous environment exists mostly as stable (oxy)hydroxides, the most common of which are $CrOH^{2+}$, $Cr(OH)_2^{+}$, $Cr(OH)_3$ and $Cr(OH)_4^{-}$; usually formed via hydrolysis. Other Cr(III) compounds include $Cr_2(OH)_2^{4+}$, $Cr_3(OH)_4^{5+}$ and $Cr_4(OH)_6^{6+}$ but are not found in significant quantities (Rai et al., 1987). In the alkaline pH range Cr(III) will precipitate as the highly insoluble $Cr(OH)_3$. For liquors with pH >11.5 $Cr(OH)_4^{-}$ is likely to be the dominant species which is soluble in water (Rai et al., 1989).

In the natural environment Cr(III) will be adsorbed on a range on materials including soil, clay minerals, sand and Fe and Mn oxides in moderately acidic conditions (Griffin et al., 1977, Richard and Bourg, 1991). Griffin et al. found that Cr(III) adsorption on kaolinite was significant between pH 3 to 5, however as pH was increased to 4.5, Cr(III) started to precipitate as a hydroxide phase and above pH 6 precipitation accounted for all Cr(III) removal from solution (Griffin et al., 1977). Thus in the highly alkaline conditions found near COPR sites, the main removal mechanism of Cr(III) in solution is likely to be precipitation.

The high redox potential of the Cr(III)/(VI) couple means only two naturally occurring reagents can oxidise Cr(III) to Cr(VI); oxygen and manganese oxides (Rai et al., 1989). Atmospheric oxygen has been reported to oxidise a limited quantity of Cr(III) at pH >9 (Bartlett and James, 1979). Whittleston reported that 1.5% of total Cr was remobilised as Cr(VI) by O_2 from a pH 11 soil sample incubated aerobically for 60 days (Whittleston, 2011). Schroeder et al. similarly reported that <2% Cr(III) was oxidised by O_2 over a pH range of 5.9 to 9.9 when incubated for two weeks in aerobic conditions (Schroeder and Lee, 1975). They also found that by increasing the temperature from 22°C to 45°C Cr(III) oxidation occurred ten times faster, indicating a high activation energy for this reaction (Schroeder and Lee, 1975). As the rate of the reaction between Cr and O is very slow at room temperature, any available Cr(III) is much more likely to be amenable to faster reactions such as sorption/precipitation (Richard and Bourg, 1991, Schroeder and Lee, 1975). Thus it is unlikely that dissolved O_2 in groundwater will cause large scale oxidation of Cr(III) to Cr(VI) in the neutral to alkaline pH range.

Manganese oxides are the only other naturally occurring oxidisers of Cr(III). As highlighted earlier, the amount of oxidised Cr(III) is directly proportional to the amount of manganese oxide within that soil (James, 1996). Bartlett and James (1979) were surprised by the extent of Cr(VI) produced when adding Cr(III) compounds to a number of different soil samples containing Mn oxide. However Fendorf and Zasoski found that although very efficient in highly acidic solution, manganese oxide mediated oxidation of Cr(III) hydroxides slowed significantly when pH was raised above 5, possibly as Cr(III) precipitates when pH is raised (Fendorf and Zasoski, 1992). The sorption of common groundwater cations such as Ca and Mg on Cr(III) hydroxides can also slow their oxidation by manganese oxide indicating that this reaction may require a sorption step to proceed (Schroeder and Lee, 1975). This being the case, the reaction is unlikely to be significant at neutral and alkaline pH or in the presence of common groundwater constituents and thus any Cr(III) phase is likely to be highly stable in any near COPR subsurface environment.

2.1.5 **COPR – A problem for West Yorkshire and beyond**

Of particular interest to this study is a historic COPR waste site located in West Yorkshire that is in need of a remediation solution (Figure 2.5). The origin of the waste has never been confirmed; however near to its locality were many historical industrial mills, the first being founded in 1849. One of these was a dye works; one of the major consumers of chromium within the 19th century. This being the case, the waste could just have easily been transported onsite from further afield. A historical map drawn in 1890s shows the waste already in place onsite (see Figure 2.52.5), thus the waste is most likely between 120 to 160 years old. Situated at the base of a valley, between a canal on the upper slope and a river in the valley basin, the waste was dumped on the original flood plain built up to form a protrusion from the valley side approximately 1.8 ha in size (Stewart et al., 2010). The sites exact location will not be disclosed by this study due to the negative social and economic impact publication would cause on the nearby inhabitants.

Many surveys have been carried out on the site in order to determine the extent of the waste and as such is pockmarked with numerous boreholes, some screened directly into the waste, some screened into the soil below (Whittleston et al., 2011b).

A typical site profile consists of 0.5m topsoil, on top of 8m COPR, above 2.5m of clay with 8m of gravelly clay underneath (Stewart et al., 2010). Borehole logs indicate that the 2.5m layer of clay may be the original alluvial plain next to the river, pre-deposition of COPR on site. Within the COPR layer is a perched water table, possibly as a result of the limited permeability of the clay layer beneath. It is not known whether the water is entering the site solely due to rainfall, from leaks from the canal, due to pre-existing groundwater flows or any combination of the three. The majority of the site is now covered in grasses, foliage and numerous small trees however on the lower edge, the gradient is such that in patches, the topsoil has eroded and the waste has become exposed, regularly leading to the accumulation of yellow coloured seepage after rainfall. (Figure 2.7)

Despite being in place for >120 years, COPR samples taken from the site still contained 1.27% w/w Cr with 119.1 $mg.kg^{-1}$ Cr(VI) leachable with diH_2O (Stewart et al., 2010, Whittleston et al., 2011b). Similarly, leachate taken from a borehole directly screened into the waste, and which is used in this study, had a high Cr(VI) concentration of 994 $\mu mol.l^{-1}$ and a pH of 12.2 (Whittleston et al., 2011b). Soil samples taken from a clay layer directly below the waste contained 0.3% Cr and topsoil directly adjacent to the waste contained 0.5% Cr confirming the migration of Cr away from the site (Whittleston et al., 2011b).

The only measures to mitigate public exposure to the waste are to fence off the areas where the COPR has become exposed and to construct a drainage ditch along the southern edge of the site to stop leachate contaminating the cricket club next door. After extended rainfall yellow seeps are seen flowing from the side of the pile, into and down the drainage ditch straight into the river. Previous monitoring of the effluent within the drainage ditch has shown it to have a pH of 9.0 to 12.0 and a Cr(VI) content of 131 to 225 $\mu mol.l^{-1}$ (Stewart et al., 2010).

All COPR leachate used in this study was recovered from borehole 5 in March 2009. BH5 was advanced during a commercial site investigation conducted in 2002 and is screened directly into the waste (see Figure 2.6 for location) (Whittleston et al., 2011a). Its position near the south west edge of the site ensures that the leachate will have been within the waste for some time and concentrations of Cr(VI) are likely to be highest. Alluvial material used in this study was recovered from the same site (see Figure 2.6 for excavation location) (Stewart et al., 2010).

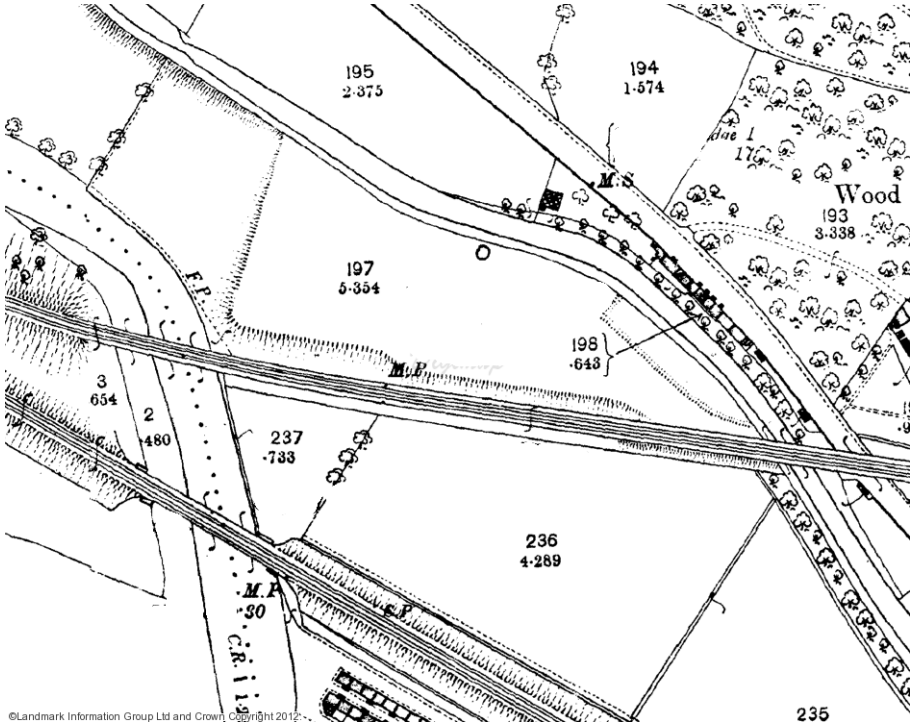

Figure 2.5: 1890s map of West Yorkshire COPR waste site.

In the UK there are many other sites similar to the one in West Yorkshire; all remnants of historical chromium manufacturing. The area around Glasgow in particular has a high frequency of chromium impacted locations as between 1830 to 1968 over 2 million tonnes of COPR from the local chemical plant were used as construction fill (Farmer et al., 2002, Farmer et al., 2006). Another site of interest lies near Bolton where several hundred thousand tonnes of COPR covering ≈ 8.1 ha remains as a remnant of chromate salt manufacture from 1880 to 1968 (Breeze, 1973, Gemmell, 1973, Stewart et al., 2007).

Figure 2.6: Detailed map showing the site in West Yorkshire. The red dot highlights Borehole 5 which was used to recover leachate from within the waste. The blue dot indicates the area where the alluvial material was recovered from.

Figure 2.7: (A) and (B) show the drainage ditch to the south of the site at differing times of the year. (C), (D), (E) and (F) show the exposed COPR waste which has been fenced off to stop public ingress.

Further afield, areas in the USA have some of the highest frequency of COPR contaminated land, including Maryland, New Jersey, New York and Ohio (Chrysochoou et al., 2010). Of these the contamination in New Jersey has been extensively studied as three processing plants in Hudson County, operating between 1905 to 1976, produced approximately 2.75 million tons of

COPR waste material which was subsequently sold and used as a cheap fill or diking material (Kitsa et al., 1992, Chrysochoou et al., 2009, Burke, 1991). It is estimated that as much as 125 x 10^6 kg of Cr has been dispersed, generally in highly populated areas around the county (Katz and Salem, 1994). A study in 1994 identified 130 contaminated sites with total Cr concentrations ranging between 5 to 19000 $mg.kg^{-1}$, with Cr(VI) concentrations from 0.5 $mg.kg^{-1}$ up to 780 $mg.kg^{-1}$ (Katz and Salem, 1994).

Additional countries around the world where COPR has been reported as a problem include France where a 150000m^3 COPR slag heap has been identified and India where COPR contaminated mud has been reported to contain as much as 16000ppm Cr(VI) (Sreeram and Ramasami, 2001, Loyaux-Lawniczak et al., 2001). In China it has been reported that roughly 1 million tonnes of highly alkaline COPR is still produced annually, adding to a reported stockpile of 6 million tonnes already kept in storage heaps (Wang et al., 2007). The high lime process is still practised by many countries including Kazakhstan and Russia, (Darrie, 2001) therefore it is assumed that there are also stocks of untreated COPR in these countries awaiting treatment.

Thus, contamination by highly alkaline COPR is a worldwide problem which will continue to be exacerbated until the high lime method of chromium is completely phased out. There are already many sites in the UK and around the world where COPR is present, leaching highly soluble Cr(VI) into the proximate subsurface with little to no regard of the potential hazard of Cr(VI) and the inherent risk to the wider public. Historically this did not represent a problem and sites were left with little or no attempt made to remediate them. Nowadays with more insight into the health and environmental risks posed by waterborne Cr(VI), there has been identified a need to stop this from occurring. In the UK, environmental quality standards in accordance with the EU Water Framework state the maximum amount of Cr(VI) within freshwater should not exceed 5 to 50 $\mu g.l^{-1}$ dependent on water hardness and 15 $\mu g.l^{-1}$ for saltwater (UKTAG, 2008). The world health organisation have set a maximum permissible level of Chromium in drinking water as 0.05 $mg.l^{-1}$,(World Health Organisation, 2003) whereas the USEPA sets a slightly

higher limit of 0.1 $mg.l^{-1}$ (USEPA, 1998). Both of these limits are in total chromium rather than toxic Cr(VI) due to problems with analytical methods and the varied speciation of chromium in solution. In order to meet such water quality standards there is a need to develop a viable remediation strategy for highly alkaline COPR waste sites such as the one in West Yorkshire, as currently there is no recognised method to deal with such waste.

Traditional practice for other hazardous wastes would be to employ a dig and treat method whereby the harmful waste is removed from site and then treated externally; however as COPR dust is a direct hazard to human health, excavation would be highly problematic and expensive. Strategies whereby the waste is left in place, capped to reduce water ingress, and the leachate leaving the site is treated would be more appropriate. It has been shown above that Cr(VI) is toxic and highly mobile in the environment, whereas Cr(III) is an essential mineral that precipitates as insoluble hydroxides which are immobile in the subsurface. Thus a redox reaction whereby the Cr(VI) within the leachate is reduced to Cr(III) hydroxides would be the preferred method of treatment. Of all the remediation strategies available, two have been identified as being the most suitable for treatment of highly alkaline COPR; The permeable reactive barrier and the biobarrier.

2.2 Potential COPR Treatment Options

2.2.1 **Permeable Reactive Barriers**

Permeable Reactive Barriers (PRBs) are a relatively new remediation strategy designed to treat contaminated groundwater flows in situ. They compromise of reactive zone placed in the subsurface which treats a contaminated groundwater plume as it passes through, resulting in only clean effluent downstream of the barrier (see Figure 2.8 (Morrison, 2002)). PRBs can achieve this in a number of different ways, dependent on the contaminant and the material of the barrier. The three principal techniques employed are degradation (the decomposition of contaminants), precipitation

(formation of insoluble compounds within the barrier) or sorption (contaminants adsorb to the barrier material) (Roehl, 2005).

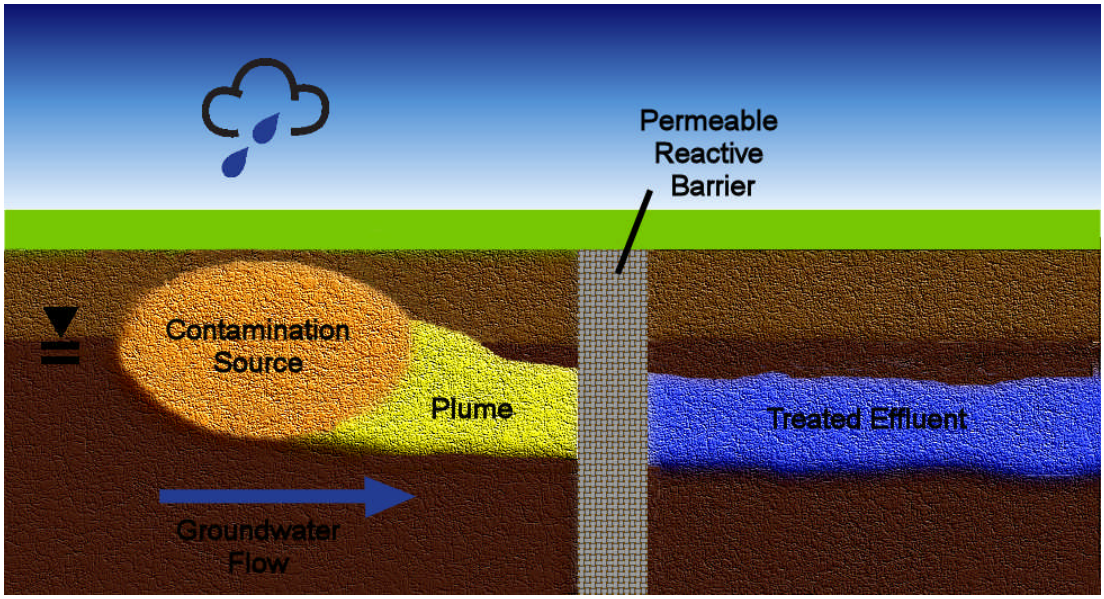

Figure 2.8: Schematic cross-section of a permeable reactive barrier

PRBs allow the treatment of potentially toxic wastes without the need to disturb the main source of the contaminant; a vital requirement for the treatment of COPR. They are seen as a fit and forget solution as after installation only periodical checking of the effluent is required to ensure the barriers continued viability. The increased safety and lack of on-going cost is what makes PRBs such an attractive remediation technique.

Currently there are two main designs which have been implemented on site, the continuous wall and funnel and gate systems. Continuous wall PRBs have a reactive zone that runs for the length of the contamination site whereas funnel and gate systems use impermeable shuttering to redirect the ground flow towards permeable reactive gates (Roehl, 2005, Morrison, 2002). Other designs have been suggested including creating reactive columns in the ground by injecting barrier material into the ground to create reactive wells (Morrison, 2002). Whatever the design, PRBs have to be constructed so that there is a natural hydraulic gradient allowing the

groundwater to flow through them with a residence time within the barrier long enough so that the remediation process can be completed.

Many different materials have been suggested as suitable for use in a PRB in order to treat a range of different soluble contaminants (the most common are listed in Table 1 and 2). The actual material used depends on the required removal technique and also any permeability requirements.

Potential Treatable Contaminants	Examples
Trace Metals	Chromium, Nickel, Uranium, Cadmium
Methanes	Tetrachloromethane
Ethanes	Trichloroethane
Ethenes	Tetrachloroethene
Propanes	Dichloropropane
Aromatics	Benzene, Toluene

Table 2.1: Potential treatable contaminants by PRBs (Xendis, 2002).

Potential PRB Materials
Zero Valent Iron
Activated Carbon
Limestone
Zeolites
Sodium Dithionite
Copper
Wood Chips

Table 2.2: Potential PRB materials (Xendis, 2002).

The potential for in-situ remediation using ‘iron walls’ was first realised by researchers at the University of Waterloo (Gillham and O'Hannesin, 1994, O'Hannesin and Gillham, 1998). A trial iron barrier, treating an artificial trichloroethene plume, was constructed in 1991 in order to prove their concept (O'Hannesin and Gillham, 1998). The concept was proved sound with dechlorination of trichloroethene still occurring 5 years after barrier placement (O'Hannesin and Gillham, 1998). This work led to the construction of numerous trial and experimental PRBs as well as full-scale barriers to treat many different groundwater contaminants. The first full scale barrier was constructed in 1994 in Sunny Vale California (Powell, 1998). 220 tonnes of zero valent iron were used in a funnel and gate configuration for the treatment of halogenated volatile organic compounds (HVOCs) emanating from a semiconductor manufacturing site (USEPA, 1999). 5 years later the PRB was still fully functioning with pore water samples from within the barrier displaying concentrations of HVOCs below the maximum contaminant level for drinking water as set by the Californian State (USEPA, 1999). A second iron barrier was installed in 1996 to treat a neutral pH Cr(VI) plume in a US coast guard support centre. Eight years later chromate levels within the effluent were below 5 $\mu g.l^{-1}$ (Wilkin et al., 2005). By 1998 thirteen full scale PRBs had been installed, 12 of them in the USA, mainly treating chromates and chlorinated hydrocarbons at neutral pH (Powell, 1998). Since then, the range of contaminants for which a barrier has been constructed and the choice of barrier material have greatly increased. For example an experimental zero valent iron barrier was installed in Pécs, Hungary for the treatment of Uranium leaching from mine tailings in the area (Csővári et al., 2005). After construction of the barrier, uranium concentrations downstream of the barrier were 100x less than upstream. An adsorption barrier was constructed in 1999 out of activated carbon in order to treat many waterborne organic contaminants from a historic tar factory in Austria (Niederbacher and Nahold, 2005). After three years use, 40kg of contaminants had been removed from ground flows and the barrier was still operating successfully after 5 years.

Over 200 barriers have now been constructed, in order to treat a range of different subsurface contaminants. There are now enough examples of PRBs that have been successfully running for a number of years to prove that the concept is sound and they are a viable remediation strategy. Although many PRBs have been built in order to treat Cr(VI) in neutral and acidic pH conditions, none have been built in the hyperalkaline pH as found near a COPR site thus far.

2.2.2 **Zero Valent Iron Barriers and Chromate**

Many different materials are able to reduce Cr(VI) leached from alkaline COPR into its trivalent state (e.g. Fe^0, nano Fe^0, $FeSO_4$, CaSx, $Na_2S_2O_4$, $FeCl_2$ and citric acid (Dhal et al., 2013b)). Of these materials identified, zero valent iron (ZVI) holds the most promise as a possible PRB material. ZVI is one of the most popular choices as it is cheap, readily available and comes in a range of sizes; from large pellets which can be used to construct a physical barrier in the ground, to nano zero valent iron (nZVI) which can be stabilised in a binder and pumped into the ground to create a reactive zone (Du et al., 2012). ZVI is easily oxidised to Fe(II) and (III) due to its high redox potential making it ideal for applications where a contaminant can be treated by a reduction reaction; such as Cr(VI) to Cr(III). Upon entering a ZVIPRB, Cr(VI) is reduced by the ZVI resulting in the formation of an insoluble Cr(III) compound, which would fall out of solution be retained within the barrier or soils close by.

ZVIPRBs have already been utilised as a treatment for Cr(VI) contamination in acidic and moderately alkaline conditions and much work has been done already to characterise the reduction reaction between the two (Cantrell et al., 1995, Chang, 2005, Lai and Lo, 2008, Melitas et al., 2001, Wilkin et al., 2005). A number of different equations have been suggested as the reaction pathway such as:

$$\boldsymbol{CrO_4^{2-} + Fe^0 + 8H^+ \rightarrow Fe^{3+} + Cr^{3+} + 4H_2O}$$

(2.3)

$$(1-x)Fe^{3+} + (x)Cr^{3+} + 2H_2O \rightarrow Fe_{(1-x)}Cr_xOOH + 3H^+$$

(2.4)

And:

$$CrO_4^{2-} + Fe^0 + 4H_2O \rightarrow Cr(OH)_3 + Fe(OH)_3 + 2OH^-$$

(2.5)

$$xFe(OH)_3 + (1-x)Cr(OH)_3 \rightarrow (Fe_xCr_{1-x})(OH)_3$$

(2.6)

In either case the reduced chromium forms a Cr(III) hydroxide or a mixed Fe(III)/Cr(III) hydroxide which in the alkaline environment of COPR leachate would fall out of solution. The kinetics of this reaction have been studied extensively and a number of different rate equations have been suggested. In the aqueous environment, the reaction between the two should take the form:

$$-\frac{d[Cr(VI)]}{dt} = -kA[Cr(VI)]^{\alpha}[H^+]^{\beta}$$

(2.7)

Where A is equal to the surface area of ZVI and α and β denoting the order in which each reaction occurs. If it is assumed that during the reaction, the amount of iron available and the solution pH stays constant, then a pseudo rate equation can be used. Equation (9) can then be simplified to:

$$-\frac{d[Cr(VI)]}{dt} = k_{obs}[Cr(VI)]^{\alpha}$$

(2.8)

This rate equation has been used by many to describe the rate of reaction between ZVI and Cr(VI) (Alowitz and Scherer, 2002, Cantrell et al., 1995). A number of different orders of reaction have been suggested for α from 0 to 1 (Melitas et al., 2001, Qian et al., 2008, Gould, 1982). Those who have used order of reaction of 0.5 in [Cr(VI)] state that it may be due to a rate-limiting step involving the interruption of electron transfer between the ZVI and Cr(VI)

(Melitas et al., 2001). Most research thus far has said α = 1 and therefore equation 10 becomes a pseudo first order reaction (Gheju and Iovi, 2006, Qian et al., 2008). If a pseudo first order reaction is used, integration of equation 10 yields the following to describe the removal of Cr(VI) from solution.

$$[Cr(VI)] = [Cr(VI)]_o e^{-k_{obs}t} \quad (2.9)$$

Although simple, a pseudo rate equation of this type may not fully describe the behaviour of the reaction as some have noted that it only held true for the initial reduction reaction and made no account of other processes which may affect the reaction later on (Cantrell et al., 1995). Similarly it does not account for any changes in pH or loss of iron.

2.2.2.1 Effect of pH on the ZVI/Cr(VI) reaction

In acidic conditions the reaction between ZVI and Cr(VI) is extremely quick with Cr(VI) being continuously reduced as long as there is sufficient iron available to continue the reaction (Fiuza et al., 2010). As the Cr(VI) is reduced any reaction products precipitate away from the iron surface, allowing further reaction with the iron below (Fiuza et al., 2010).

Under alkaline conditions this reaction occurs at a much slower rate and in some cases will not occur at all. Chang showed that thin iron wires can fully reduce 10mg.l^{-1} Cr(VI) from pH 3 liquor within 30 hours, whereas only 4mg.l^{-1} Cr(VI) was removed after 72 hours from pH 10 liquor (Chang, 2005). Similarly Fiuza et al. disclosed that at pH 1, Cr(VI) reduction happens almost instantaneously whereas at pH 10 the reduction rate is vastly slower (Fiuza et al., 2010). Alowitz et al. reported the rate coefficient reduced as pH was increased from 5.5 – 9.0 (Alowitz and Scherer, 2002). The reason for the slow reaction rate in alkaline conditions has not been conclusively established however there are a few theories as to why it occurs.

All hydrated oxides allow the exchange of ions from a liquid to the oxide surface via adsorption reactions. Thus adsorption of H^+/OH^- ions on that surface can determine its electrical chemical density (Noh and Schwarz, 1989). In acidic conditions H^+ ions dominate. Therefore surfaces within

acidic liquids adsorb more H^+ cations than OH^- anions; inducing a positive electric charge across the surface. In alkaline conditions, increased sorption of the hydroxide anion (OH^-) onto the surface will result in a negative electrostatic charge on that surface. The point at which the surface charge is zero is called the point of zero charge (PZC), and is the point at which charges from the sorbed H^+ and OH^- cancel one another out (Noh and Schwarz, 1989). The (PZC) for iron and its (hydr)oxides generally occurs between pH 6 to 8 (Silva, 1995). Thus in alkaline conditions an iron surface will be dominated by adsorbed OH^- anions, causing a net negative charge which will electrostatically repulse the similarly negatively charged chromate anion. This will minimise the possibility of the Fe and Cr(VI) coalescing in order to react. As pH increases to the hyper alkaline levels seen in COPR, OH^- concentration in the liquor and iron surface will also increase, leading to an exacerbation of the repulsive effect and a slowing of the reaction between ZVI and Cr(VI).

Another theory for the slow reaction rate in alkaline solutions could be due to changes in the solubility of Fe^{2+} as pH increases. Powell et al. speculated that the reaction between ZVI and Cr(VI) occurs at sites of surface or chemical imperfections, allowing the formation of a corrosion cell and corresponding anodic and cathodic regions. Dissolution of Fe^{2+} from the anodic areas causes a build-up of positive charge, attracting the negatively charged chromate anion to the iron surface where it is subsequently reduced (Powell et al., 1995). In alkaline conditions, Fe^{2+} is sparingly soluble; (Langmuir, 1997) thus the corrosion cell may not be able to form and the electromagnetic attraction bringing the two reactants together would not exist.

Although these two theories would account for slow short term reaction rates, over a long time frame, the majority of Cr(VI) within a solution would still be expected to be reduced. Long term complete loss of reaction could be due to inhibition or passivation of the iron surface itself.

2.2.2.2 Iron Corrosion and Inhibition

Due to its high oxidation potential, iron is very likely to oxidise when placed in any alkaline environment containing water. This can occur aerobically or anaerobically and can lead to the formation of a number of different iron oxides and hydroxides on the surface, blocking potential reaction sites below. Aerobic corrosion of iron can happen in the ground in areas close to the surface where O_2 has leached into the groundwater from the atmosphere. ZVI reacts with O_2 and water to produce Fe^{2+}:

$$2Fe + O_2 + 2H_2O \rightarrow 2Fe^{2+} + 4OH^- \quad (2.10)$$

Fe(II) is unstable in normal aqueous conditions and will further react to form one of a number of different iron (hydr)oxides dependent on the conditions in the ground; the most common being goethite ($Fe(OH)_3$ or haematite (Fe_2O_3):

$$Fe^{2+} + 0.25O_2 + 2.5H_2O \rightarrow Fe(OH)_3 + 2H^+ \quad (2.11)$$

Or:

$$Fe^{2+} + 2OH^- \rightarrow Fe(OH)_2 \quad (2.12)$$

$$4Fe(OH)_2 + O_2 \rightarrow 4H_2O + 2Fe_2O_3 \quad (2.13)$$

Haematite can further react to create a passivating layer on the iron surface of Fe_3O_4 or a hydrated Fe_2O_3 (Schrebler Guzmán et al., 1979). In reality there is usually minimal O_2 present in groundwater below the surface as it will readily react with many chemicals present in soil or be consumed by biological processes (Lovley, 2001). As such, in any ZVIPRB, anaerobic

corrosion of the iron is much more likely to occur. Anaerobic iron corrosion starts due to the oxidative action of water: (Reardon, 1995)

$$Fe + 2H_2O \rightarrow Fe^{2+} + 2OH^- + H_2$$

(2.14)

Being environmentally unstable, Fe(II) will generally transform into $Fe(OH)_2$:

$$Fe^{2+} + 2OH^- \rightarrow Fe(OH)_2$$

(2.15)

Although stable, without the presence of oxygen $Fe(OH)_2$ is predicted to further thermodynamically transform into magnetite via the Schikorr reaction (Reardon, 1995).

$$3Fe(OH)_2 \rightarrow Fe_3O_4 + H_2 + 2H_2O$$

(2.16)

Magnetite formation from the ferrous cation can also occur in highly alkaline conditions via precipitation (Odziemkowski et al., 1998):

$$3Fe^{2+} + 4H_2O \rightarrow Fe_3O_4 + 6H^+ + H_2$$

(2.17)

Dissolution of Fe(II) from within the precipitated magnetite will allow it to react with Cr(VI), however this has been shown to be very slow in the alkaline pH range due to the further formation of other iron oxides such as goethite and maghemite (He and Traina, 2005). In the presence of common groundwater anions such as Cl^-, CO_3^{2-} and SO_4^{2-}, $Fe(OH)_2$ can also transform into a number of green rusts (Roh et al., 2000).

$$4Fe(OH)_2 + Cl^- \rightarrow Fe_3^{2+}Fe^{3+}(OH)_8Cl + e^-$$

(2.18)

$$6Fe(OH)_2 + CO_3^{2-} + 2H_2O \rightarrow \left[Fe_4^{2+}Fe_2^{3+}(OH)_{12}\right][CO_3 \cdot 2H_2O] + 2e^-$$

(2.19)

$$6Fe(OH)_2 + SO_4^{2-} + 2H_2O \rightarrow \left[Fe_4^{2+}Fe_2^{3+}(OH)_{12}\right][SO_4 \cdot 2H_2O] + 2e^-$$

(2.20)

Dependent of the ground conditions these green rusts can further react to form maghemite, magnetite, lepidocrocite or goethite (Myneni et al., 1997).

As well as the formation of iron oxides blocking available reaction sites on the iron surface, other compounds can react with the iron, inhibiting it from reacting or corroding further. These inhibitors can be classed into groups by the way the inhibition works as either anodic, cathodic or adsorption inhibitors (Evans and Winterbottom, 1948). Chromate ions themselves are one of the most effective compounds at inhibiting the reactivity of an iron surface (Evans and Winterbottom, 1948) and before the toxic nature of them was realised, they were regularly added to water in order to minimise the corrosion of pumping equipment and pipes. In neutral conditions, Cr(VI) reacting with Fe(II) released from anodic sites on the iron surface, forms Fe(III) and mixed Fe(III)/Cr(III) oxides (Melitas et al., 2001). This unreactive layer prevents the release of further Fe(II) into solution and blocks access to the unreacted iron below. The inhibiting effect is exacerbated with increasing chromate concentration (Melitas et al., 2001). The Fe(III)/Cr(III) oxide layer appears to be self-healing as long as there is continuous exposure of the surface to chromates which explains the effectiveness with which it inhibits iron (Evans and Winterbottom, 1948). It has not been reported as to whether these chromium containing oxides are formed at hyper alkaline pH. The formation of soluble Fe(II) at high pH is unlikely, thus the initial step which drives this reaction may be missing. However it has already been shown above how iron will readily oxidise in alkaline conditions; often incorporating ions which were present in solution, thus it is expected that a similar Fe(III)/Cr(III) oxide layer would be able to form at high pH.

Silicates are regarded as another excellent inhibitor of iron and are regularly utilised to protect iron and steel subject to aqueous conditions (Lahodny-Sarc

and Kastelan, 1981). Silica is naturally present in groundwater with levels usually ranging between 5 to 85ppm,(Langmuir, 1997) however much greater concentrations could be found in COPR leachate due the hyper alkaline pH found at such sites. In acidic and neutral sodium silicate solutions, the rate of inhibition occurs at a similar rate to diH_2O. However as pH is raised to >10, inhibition of iron in the sodium silicate solution quickly becomes significant. The apparent activation pH coincides with the pH at which silicate ions start to become soluble (≈pH 10),(Langmuir, 1997) thus it has been surmised that a reaction between silicate ions with the iron surface is the main inhibition mechanism. Armstrong et al. postulated that this occurs in a multiple stage process with the formation of iron hydroxides which subsequently react with silicate ions to create an inhibiting layer (Armstrong and Zhou, 1988). Iron pipes exposed to 50mg.l^{-1} SiO_2 for 4 months, developed a scale on the surface containing 7% by weight silica (Rushing et al., 2003). Carbon steel exposed to 100ppm SiO_3^{2-} developed a surface comprising of Fe_2O_3, FeO and Fe with the formation of metal silicates in oxygenated solution and SiO_x in anaerobic conditions (Jiann-Ruey et al., 1991). Iron exposed to $CaSiO_3$ developed a surface coating of $Fe_2(SiO_3)_3$ (Armstrong and Zhou, 1988). Thus silicates will readily react with an iron surface to form a Si containing Fe oxide which will cover the elemental iron beneath. As well as these two materials discussed, many other inorganic soluble compounds are able to inhibit iron to some extent, including nitrates, phosphates and carbonates (Evans and Winterbottom, 1948).

The above just touches the surface of iron corrosion science and is intended to show how complex iron corrosion in the natural environment can be. As many ZVIPRBs have been in situ for a number of years, material recovered from these barriers has been assessed to determine the actual corrosion products created on the iron. ZVI from a barrier used for the reductive treatment of radionuclides and chlorinated organic compounds showed numerous different corrosion products including amorphous iron hydroxides, green rusts and the hydrated iron oxides, akaganeite (β-FeOOH), goethite (α-FeOOH) and lepidocrocite (γ-FeOOH) (Roh et al., 2000). Iron used in a PRB to reduce Cr(VI) from a chrome plating shop in neutral conditions for 20

months had ferrous sulphide as the main corrosion product as well as unidentified iron oxides, hydroxides and oxy-hydroxides (Puls et al., 1999). Other iron PRBs have reported the formation of goethite, magnetite, maghemite, hematite, Cr-Fe-hydroxide, green rusts and siderite as corrosion products (Gerlach et al., 2000). In total there are 16 iron oxides (Cornell and Schwertmann, 2006) and numerous iron containing compounds that can form under different geochemical conditions. Similarly there are many common environmental compounds which will inhibit an iron surface to some extent. Some will form a continuous coating on the iron surface, such as the self-healing ferric chromic oxide formed in chromate solutions; completely blocking the iron beneath and disabling its ability to react. Others will precipitate away from the surface or form non-continuously such as magnetite (which is prone to stress cracking), allowing fresh iron underneath to be able to react.

The above shows how hard it is to predict the exact nature and effect of passivation on iron within any subsurface environment due to the many different reactions it could be subject to, without actually placing the iron in situ. The viability of a ZVIPRB depends on the irons ability to continue to react with the chosen waste product at fast enough rates for the contaminant to be removed within the barrier itself. It is currently not known whether the ZVI/Cr(VI) reaction occurs in the hyperalkaline conditions found near COPR sites at fast enough rates for this to be possible. If this reaction does occur at such a high pH it is not known how long this reaction will occur for or whether it will succumb to the effects of inhibition and passivation. If a ZVIPRB is to be prescribed as a remediation solution for highly alkaline COPR waste, answers to these questions must be found.

2.2.3 **Bio Remediation.**

Bio remediation has been proposed as an alternative technique to a PRB for the treatment of soluble contaminants within the subsurface. Utilising the native population of bacteria present within a soil to interact with, and treat a contaminant could be an elegant and cheap way to remediate sites such as

those containing COPR. Many bacteria respire by a process called dissimilatory reduction whereby an electron is taken from an organic substrate electron donor, utilised by the bacteria to drive internal processes, and then expelled to an external source which is reduced. By promoting the growth of such bacteria in a contaminated subsurface with the introduction of excess electron donor, the electrons released from the bacteria's natural respiration could be used to treat a range of contaminants that require a reduction reaction to remediate them (See Figure 2.9). At the time of writing, many laboratory scale experiments have shown bioremediation to work effectively for a number of contaminants. Push-pull tests have also been developed to test biological processes on site. They inject a cocktail of tracers and reactive solutes into an aquifer via a pre-existing borehole (the push), wait for bacteria within the aquifer to metabolise, before pumping the mixture from the same well in order to analyse it (the pull) (Kleikemper et al., 2002). These have given good indication that augmenting an aquifer can result in the desired reductive effect (e.g. sulphate reduction (Schroth et al., 2001, Kleikemper et al., 2002)) however currently no full-scale biobarrier has been specified to treat a polluted site. If proved viable, bioremediation would be ideal for the treatment of COPR waste as minimal ground disruption would be required.

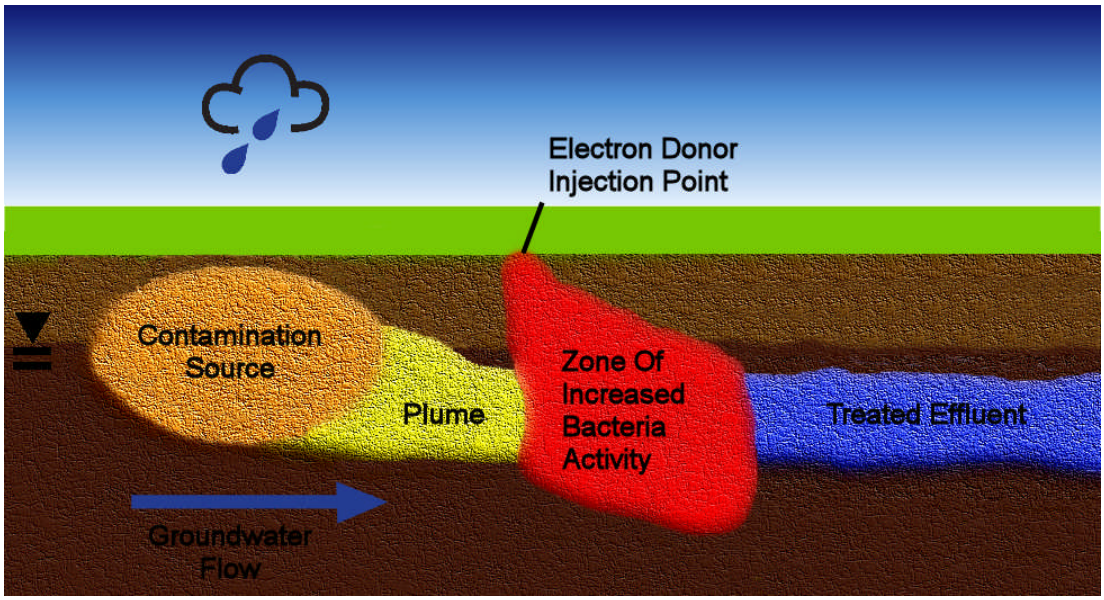

Figure 2.9: Schematic cross-section of a biobarrier

2.2.3.1 Bacteria

Bacteria are single cell prokaryotes that were among some of the first cellular organisms to live on this planet. Ranging from 1 to 2 µm in size, bacteria come in numerous shapes and colours and show wildly different physical features. Today there are estimated to be in the region of 4 to 6 $x10^{30}$ bacteria cells living on the earth (Whitman et al., 1998) and can be found in nearly every habitat conceivable, ranging from frozen lakes in Antarctica (Priscu et al., 1999), to acidic hot vents at the bottom of the ocean (Muyzer et al., 1995). Bacteria thrive in milder conditions such as soil where it has been estimated that 1 gram could contain around $10x10^{10}$ cells and as many as 10000 different bacteria species (Maier et al., 2000). Bacteria also call the bodies of most living creatures home, as well as a wide variety of plants and can be both helpful and destructive to their hosts. In short they are almost ubiquitous wherever you look.

Although bacteria have adapted to many different environments, COPR waste sites offer a particularly harsh environment in which to live. The combination of anaerobic, highly alkaline and toxic conditions will strain even the hardiest bacteria and only those successfully adapted will survive. Thus

it is not known whether a bio remediation strategy would be suitable for such sites.

2.2.3.2 Chromium and its effect on Bacteria

Cr(III) is generally not thought to be toxic to bacteria cells as it forms insoluble hydroxides, which are very unlikely to be able to diffuse through the cell wall and thus cannot affect the inner workings of the cell (Cervantes et al., 2001). As for most metazoa, Cr(VI) is toxic and mutagenic to prokaryotes. Due to this fact Cr(VI) contaminated soil usually has few bacteria in it, all of which have developed a resistance to the toxic metal (Dhal et al., 2013b, Cervantes and Silver, 1992). Cr(VI) can easily pass through bacteria cell walls via the sulphate transport system (Daulton et al., 2007). Once inside the periplasm, Cr(VI) is quickly reduced and the Cr(III) created, bonds with many intracellular compounds such as DNA and reductases that facilitated the reduction reaction (Dhal et al., 2013b, Wang and Shen, 1997, Cervantes and Silver, 1992). This process can lead to mutations caused by the disruption of DNA and consequently cell death.

Bacteria which are able to live in the presence of Cr(VI) have usually developed significant changes to their cells in order to cope with the toxic stress caused by the metal. Those strains determined as Cr(VI) resistant appear to accumulate less Cr within the cell than those less adapted (Cervantes and Silver, 1992). Some bacteria achieve this via the presence of ChrA plasmids which cause changes to their cell wall. These non-chromosomal DNA sequences allow the expression of protein structures within the wall that are able to facilitate the outward transfer of Cr(VI) anions from within the cell before they are reduced (Cervantes and Silver, 1992). This plasmid has been found in a number of Cr(VI) resistant strains and closely resembles other plasmids such as the ArsB plasmid which causes the expression of cell structures which allow the extrusion of arsenite from several species of bacteria, suggesting that they create cell structures that work in a similar way (Cervantes et al., 2001). Cr(VI) resistance and the ability to reduce Cr(VI) are not mutually inclusive as some bacteria have been shown to be resistant to Cr(VI) but are unable to reduce it and *vice versa* (Cervantes et al., 2001).

2.2.3.3 Alkaliphiles

Any bacteria living in or near a COPR waste site will have to be suitably adapted to high pH. Alkaliphiles are classed as bacteria that require alkaline conditions in which to live, usually pH 8 to 11, with optimum growth occurring around pH 10. They can be classified as either alkaliphiles, haloalkaliphiles (which also require high salinity) or facultative alkaliphiles (are most comfortable in neutral conditions but are tolerant of alkaline conditions) (Horikoshi, 1999). Alkaliphiles have been isolated from naturally occurring high pH environments such as eutrophic soda lakes and areas of $Ca(OH)_2$ dominated groundwater as well as neutral environments such as soil (Grant et al., 1990, Zavarzina et al., 2006, Zhilina et al., 2009). There are many types of bacteria now classed as alkaliphiles and they have shown a great diversity in the adaptions made to be able to live in the alkaline environment.

In order to live in high pH conditions, alkaliphiles have had to evolve a number of survival mechanisms. Many common, intercellular compounds such as *Bacillus sp.* protoplasts become unstable in the presence of increased OH^- concentrations, thus adaptations to alkaliphiles' cell walls which prevent the intrusion of the hydroxyl ion have been identified as a key feature that allows survival at high pH (Horikoshi, 2001). Analysis of said strain's cell walls have revealed acidic polymers such as galacturonic and aspartic acid which promote a negative electric charge across them. The charge repels hydroxide ions whilst maintaining the ability to adsorb other vital ions such as sodium and hydronium ions (Horikoshi, 2001, Horikoshi, 1999). Repelling OH^- allows alkaliphiles to maintain a cytoplasmic neutral pH which can be within 0.5 pH units of many neutrophillic bacteria and in some cases up to 2 pH units lower than the external pH (Horikoshi, 2001). This process allows the normal functioning of many enzymes that work optimally around neutral pH.

2.2.3.4 Anaerobic Dissimilatory Reduction of Metals

In order to grow and replicate, bacteria need to take in energy from an external source. They do this in a number of different ways including via fermentation and dissimilatory aerobic and anaerobic respiration. The success of a bioremediation scheme relies on those bacteria that reduce minerals as they respire. The most common respiratory process which facilitates this is anaerobic dissimilatory respiration.

Dissimilatory respiration starts with the oxidation of an external organic substrate known as an electron donor. The electron released from the oxidation reaction is diffused across its cell membrane, causing an electrochemical and pH difference between inside and outside the cell. This electrochemical difference is called the proton motive force which the cell uses to pump a proton through its membrane that can be used to synthesise adenosine triphosphate (ATP) from compounds such as adenosine diphosphate (ADP) and adenosine monophosphate (AMP). ATP is the primary compound that bacteria use to transport energy around the cell. Once metabolised, ATP is cycled back into the precursor compounds ADP and AMP, and a cyclic relationship is developed which can shuttle energy around the cell *ad infinitum*, as long as there is sufficient electron donor to keep the process going.

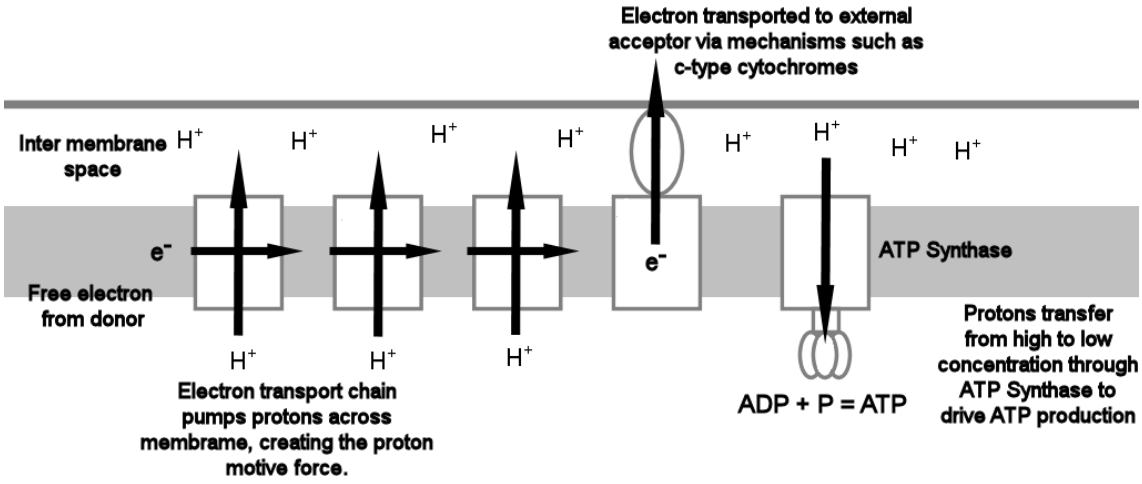

Figure 2.10: Schematic showing how the electron transport chain maintains the proton motive force in order to drive the production of ATP.

Once used, the electron is expelled from the bacteria to an external electron acceptor, which is then reduced. Bacteria have developed many different ways in which to achieve this, both internally and externally to the cell. Many bacteria have developed specific reductases within their cell wall which facilitate the reduction of external phases on contact. For example the species *Shewanella Putrefaciens* and others from the *Geobactor* genus include *c*-type cytochromes bound within their cell wall membrane which are able to facilitate direct electron transfer to Fe(III) phases (Lovley, 2000, Lovley, 2008, Bae and Lee, 2013). These *c*-type cytochromes are also able to act as capacitors which allow electron transfer to continue without the presence of external electron acceptors for up to 8 minutes, a possible reason for *Geobactor's* apparent resilience (Lovley, 2008). Conductive appendages (so called 'nanowires') emanating from bacteria cells and creating a direct link to the external electron acceptor have also been proposed as a method which some bacteria use to transfer electrons extracellularly. Strains including *Shewanella oneidensis, Pelotomaculum thermopropionicum* and *Methanothermobacter thermoautotropicus* all construct these nanowires which are 50 to >150 nm in diameter and can

range >10 µm away from the cell wall (Gorby et al., 2006). This being the case, definitive proof of reductive action via these structures is so far absent and their application confirmed by circumstantial evidence only (Lovley, 2008). Several species of bacteria facilitate non-contact reduction by utilising naturally occurring or self-produced soluble electron carriers that shuttle the electron from the cell to a remote electron acceptor in the proximate environment. Exogenous electron shuttles include humic acids and quinones whereas riboflavin, flavin mononucleotide and flavin adenine dinucleotide have all been identified as bacterially secreted shuttles (Bae and Lee, 2013). Bacteria such as *Shewanella sp.* can reduce poorly crystalline Fe(III) phases away from the cell via the creation and secretion of these soluble flavin based electron carriers (von Canstein et al., 2008, Marsili et al., 2008). Other bacteria such as *Geobacter metallireducens* are able to utilise exogenous electron shuttles resulting in quicker and more sustained Fe(III) reduction (Williamson et al., 2013, Bae and Lee, 2013). Intracellular reduction has been identified in some bacteria strains such as *Shewanella Putrefaciens* CN32, which transport the terminal electron acceptor within the cell walls; apparently storing it until the time it is to be used in so called ‘lungs’ (Glasauer et al., 2007, Lovley, 2008). This is thought to be an advantage to the bacteria as they can stockpile deposits of electron acceptor for times of depleted reserves.

In aerobic conditions the likely terminal electron acceptor will be oxygen as the O_2/H_2O reduction couple has the highest redox potential, meaning that more energy is released to the bacteria cell during the process. In aqueous environments, oxygen is quickly consumed via aerobic respiration and many other geochemical processes so that the majority of the subsurface is completely anaerobic (Schmitz, 2006). In such circumstances, the terminal electron acceptor can be numerous different compounds. Ideally bacteria will hope to respire on the compounds which release the maximum energy once reduced, thus those electron acceptors with the highest reduction potentials would be expected to be utilised first. In reality a bacteria will utilise the electron acceptor which they are most adapted to using and which is available in the near environment, thus the order in which compounds are used in the ground may not follow the order of reductive potential. The most

common compounds on which bacteria respire include nitrate, nitrite, iron(III), manganese(IV), sulphate, sulphur and carbon dioxide (Rabus, 2006, Lovley, 1991, Nealson and Saffarini, 1994, Gao et al., 2009). Although uncommon in the subsurface other materials such as uranium(VI), arsenic(V), chromium(VI), technetium(VII) and selenium(VI) can also be reduced via dissimilatory reduction (Liu et al., 2002, Lovley and Phillips, 1994, Abdelouas et al., 1998, Lovley, 1993). It is quite common for dissimilatory bacteria to be able to use multiple different compounds as the terminal electron acceptor. That said, many subterranean bacteria which respire using metals and minerals as the terminal electron acceptor have developed to be incompatible with growth in aerobic conditions and are thus dubbed anaerobes. Currently over 200 genera of obligate anaerobic microorganisms that have been identified (Schmitz, 2006). It is thought that when exposed to the atmosphere, the reductive processes that allow them to respire anaerobically, reduce oxygen into compounds such as O_2^-, H_2O_2 and OH which are ultimately toxic to the cell (Schmitz, 2006).

2.2.3.5 Dissimilatory Iron Reduction

Of all the electron acceptors utilised by bacteria, iron may be the most important as it is almost ubiquitous in soil minerals and a huge range of different bacteria genera have been found to be able to respire on it. Bacterial reduction of Fe(III) is thought to be one of the earliest bacteria processes on the earth as all of the bacteria closely related to the last common ancestor of all bacteria are able to reduce Fe(III) coupled with the oxidation of hydrogen (Lovley, 2006, Madeline et al., 1998). Estimates state the Fe(III) reduction is responsible for anywhere between 10-100% of organic substrate oxidation in the subsurface (Lovley, 2006). Dissimilatory reduction of Fe(III) is one of the main influences on the distribution and mineralogy of iron and also controls the fate of other trace metals, nutrients and degradation of organic matter (Lovley, 2006). Due to their ubiquity, numerous bacteria have been isolated and characterised which reduce Fe(III) in alkaline conditions as high as pH 11 (for example *Alkaliphilus metalliredigens,* (Roh et al., 2007) *Alkaliphilus peptidofermentans,* (Zhilina et

al., 2009) *Bacillus sp.,* (Pollock et al., 2007) *Anaerobranca californiensis*, (Gorlenko et al., 2004) *Geoalkalibacter ferrihydriticus*, (Zavarzina et al., 2006) *Anoxynatronum sibiricum,* (Garnova et al., 2003) *Tindallia magadii,* (Kevbrin et al., 1998) and *Clostridium beirjerinckii,* (Dobbin et al., 1999)).

Biogenically mediated reduction of Fe(III) to Fe(II) may be important from a remediation standpoint as ferrous iron is able to reduce a number of common waterborne contaminants including Cr(VI). Once Fe(II) has been produced, it is then able to react with any waterborne contaminants present, via an abiotic reductive reaction. Fe(II) is very capable of reducing Cr(VI) via the following reaction (Fendorf and Li, 1996):

$$\boldsymbol{H_xCrO_4^{x-2} + 3Fe^{2+} + iH_2O \leftrightarrow Cr(OH)_y^{3-y} + 3Fe(OH)_z^{3-z} + jH^+}$$

(2.21)

Where i=(y+3z) and j=(x+y+3z). The rate of this reaction slows in alkaline conditions, possibly due to the limited solubility of Fe(II) at elevated pH (Langmuir, 1997).

Although production of soluble Fe(II) is possible, reduction of Fe(III) in alkaline conditions is more likely to result in precipitation of Fe(II) containing mineral phases. Magnetite, Siderite Vivianite and Green rusts are all potential terminal Fe(II) containing minerals (Lovley et al., 1987, Veeramani et al., 2011, Zachara et al., 2002, Williamson et al., 2013). Magnetite is one of the most commonly found Fe(II) containing minerals and is thought to form when bacteria secrete Fe(II) which then reacts with Fe(III) oxyhydroxide from the environment (Bazylinski and Frankel, 2000). Magnetite can reduce Cr(VI) under many different conditions, however He et al. found that the reduction capacity of magnetite in alkaline conditions is <20% of that in acidic and neutral conditions due to the formation of Fe(III) phases on the magnetite surface which block access to the Fe(II) below (He and Traina, 2005).

Poorly crystalline Fe(III) oxides such as Ferrihydrite are seen as readily available for bacterial reduction whereas other more crystalline Fe(III) oxides such as Goethite and haematite are less amenable to reduction (Lovley, 1991, Zachara et al., 2002). Reduction of these crystalline minerals does

occur however a combination of factors such as surface area, structure, thermodynamics and ability to sorb Fe(II) on the surface all affect how bioavailable they are (Zachara et al., 2002).

2.2.3.6 Microbial Chromium Reduction

Although not a common groundwater constituent, many bacteria have been identified as being able to reduce Cr(VI) to Cr(III), both aerobically and anaerobically, usually resulting in the formation of chromium (III) hydroxides (Lovley, 1993, Wang, 2000):

$$CrO_4^{2-} + H^+ + 3^{e-} + 4H_2O \rightarrow Cr(OH)_3 + 3H^+ + H_2O \quad (2.22)$$

Strains identified which are able to do this include. *Enterobacter cloacae,* (Harish et al., 2012) *Desulfovibrio vulgaris, (Lovley and Phillips, 1994) Bacillus sp*., (Dhal et al., 2013a), *Pyrobaculum islandicum,* (Lloyd and Lovley, 2001) *Shewanella Putrefaciens* and *Shewanella alga* (Liu et al., 2002). Very few bacteria have been identified which will reduce Cr(VI) in the alkaline pH range (e.g. *Halomonas sp.* (VanEngelen et al., 2008), *Alkaliphilus metalliredigens* (Ye et al., 2004) and *Leucobacter sp.* (Zhu et al., 2008)). There is some evidence of reduction achieved via multiple reactions including intermediary Cr phases. *Pseudomonas ambigua G-1* produces an enzyme which reduces Cr(VI) to Cr(III) via a two-step process. First Cr(VI) is reduced to an intermediate Cr(V) phase before being reduced to Cr(III) (Suzuki et al., 1992). Whilst these bacteria have been identified to reduce Cr(VI), the link between sustained cell growth using Cr(VI) as the sole electron acceptor has only been proved in a few cases (Daulton et al., 2007). This strongly suggests that the ability to do this is highly specialised and probably the majority of Cr(VI) reduction occurs unintentionally due to other respiration pathways.

Removal from aerobic liquors is generally slower than those with anaerobic conditions, possibly due to the preference to respire with oxygen as the terminal electron acceptor (Wang, 2000). Similarly, the presence of certain heavy metals and sulphate seems to limit the effectiveness of Cr(VI)

reduction which could be problematic for removal from industrial waste streams.(Nealson and Saffarini, 1994).

2.2.3.7 Bacteria at the West Yorkshire COPR site

Much work has already been done by the research group at the University of Leeds in order to characterise the bacteria that live near to the historic COPR site in West Yorkshire of interest to this study.

Soil samples were recovered from a clay layer below the COPR waste which was directly accessible by leachate from the waste above. Mineralogical analysis of the soil samples confirmed that up to 40% of iron within the samples were Fe(II). This was accompanied by the accumulation of Cr(III) compounds within the soil. It was surmised that bacteria present in this clay layer were able to withstand the toxic effects of Cr(VI) in order to reduce Fe(III). The produced Fe(II) was reducing the Cr(VI) abiotically. In effect, the clay layer was performing as a natural biobarrier. Incubating similar soils recovered from close to the historic waste site with leachate from the same site resulted in a pH drop in the microcosms from 12.2-11.7 coupled with Cr(VI) reduction of 990 to 0 $\mu mol.L^{-1}$ after 30 days (Whittleston et al., 2011a).

Cloning and sequencing of the bacteria population within the soil revealed bacteria from the Proteobacteria, Firmicutes and Bacteriodetes phyla which represented 52%, 19% and 16% of the total respectively (the remaining 13% were unable to be assigned) (Whittleston et al., 2011a). A population was isolated from these soils and repeatedly grown in alkaline anaerobic Fe(III) containing (AFC) media (see Chapter 3 for details). These bacteria showed the ability to rapidly and continually reduce soluble Fe(III) citrate to a precipitated Fe(II) phase. After repeated growth cycles the population had changed so that 91% of the sequences were Firmicutes, 2% Proteobacteria and 7% unassigned (Whittleston et al., 2011a). The bacteria population used within this study are direct descendants of this community isolated from the COPR waste site soils. They have been repeatedly grown in AFC media since initial inoculation

Thus whilst COPR waste sites and their proximity represent a unique set of conditions that create an extremely harsh environment in which bacteria have

to live, previous work has shown that a biobarrier has the potential to successfully treat such a site.

2.3 References

Abdelouas, A., Lu, Y., Lutze, W. & Nuttall, H. E. 1998. Reduction of U(VI) to U(IV) by indigenous bacteria in contaminated ground water. *J. Contam. Hydrol.,* 35**,** 217-233.

Ajouyed, O., Hurel, C., Ammari, M., Allal, L. B. & Marmier, N. 2009. Sorption of Cr(VI) onto natural iron and aluminum (oxy)hydroxides: Effects of pH, ionic strength and initial concentration. *J. Hazard. Mater.,* 174**,** 616-622.

Alowitz, M. J. & Scherer, M. M. 2002. Kinetics of Nitrate, Nitrite, and Cr(VI) Reduction by Iron Metal. *Environ. Sci. Technol.,* 36**,** 299-306.

Anderson, R. A. 1989. Essentiality of chromium in humans. *Sci. Total Environ.,* 86**,** 75-81.

Armstrong, R. D. & Zhou, S. 1988. The corrosion inhibition of iron by silicate related materials. *Corros. Sci.,* 28**,** 1177-1181.

Bae, S. & Lee, W. 2013. Biotransformation of lepidocrocite in the presence of quinones and flavins. *Geochim. Cosmochim. Acta,* 114**,** 144-155.

Bartlett, R. & James, B. 1979. Behavior of chromium in soils: III. Oxidation. *J. Environ. Qual.,* 8**,** 31-35.

Bartlett, R. J. 1991. Chromium Cycling in Soils and Water: Links, Gaps, and Methods. *Environmental Health Perspectives,* 92**,** 17-24.

Battle, P. D., Bollen, S. K., Gibb, T. C. & Matsuo, M. 1991. The crystal and magnetic structures of Ca2Cr0.5Fe1.5O5 at 2.1 K. *J. Solid State Chem.,* 90**,** 42-46.

Bazylinski, D. A. & Frankel, R. B. 2000. Biologically Controlled Mineralization of Magnetic Iron Minerals by Magnetotactic Bacteria. *In:* Lovley, D. R. (ed.) *Environmental Microbe-Metal Interactions.*

Breeze, V. G. 1973. Land Reclamation and River Pollution Problems in the Croal Valley Caused by Waste from Chromate Manufacture. *J. Appl. Ecol.,* 10**,** 513-525.

Buerge, I. J. & Hug, S. J. 1999. Influence of Mineral Surfaces on Chromium(VI) Reduction by Iron(II). *Environ. Sci. Technol.,* 33**,** 4285-4291.

Burke, T. 1991. Chromite Ore Processing Residuein Hudson County, New Jersey. *Environ. Health Perspect.,* 92**,** 131-137.

Cantrell, K. J., Kaplan, D. I. & Wietsma, T. W. 1995. Zero-valent iron for the in situ remediation of selected metals in groundwater. *J. Hazard. Mater.,* 42**,** 201-212.

Cervantes, C., Campos-Garcia, J., Devars, S., Gutierrez-Corona, F., Loza-Tavera, H., Torres-Guzman, J. C. & Moreno-Sanchez, R. 2001. Interactions of chromium with microorganisms and plants. *FEMS Microbiology Reviews,* 25**,** 335-347.

Cervantes, C. & Silver, S. 1992. Plasmid chromate resistance and chromate reduction. *Plasmid,* 27**,** 65-71.

Chang, L.-Y. 2005. Chromate reduction in wastewater at different pH levels using thin iron wires—A laboratory study. *Environ. Prog.,* 24**,** 305-316.

Chrysochoou, M., Dermatas, D., Grubb, D., Moon, D. & Christodoulatos, C. 2010. Importance of Mineralogy in the Geoenvironmental Characterization and Treatment of Chromite Ore Processing Residue. *J. Geotech. Geoenviron. Eng.,* 136**,** 510-521.

Chrysochoou, M., Fakra, S. C., Marcus, M. A., Moon, D. H. & Dermatas, D. 2009. Microstructural Analyses of Cr(VI) Speciation in Chromite Ore Processing Residue (COPR). *Environ. Sci. Technol.,* 43**,** 5461-5466.

Cornell, R. M. & Schwertmann, U. 2006. *The Iron Oxides: Structure, Properties, Reactions, Occurrences and Uses*, Wiley.

Costa, M. 1997. Toxicity and Carcinogenicity of Cr(VI) in Animal Models and Humans. *Crit. Rev. Toxicol.,* 27**,** 431-442.

Csővári, M., Csicsák, J., Földing, G. & Simoncsics, G. 2005. Chapter 10 Experimental iron barrier in Pécs, Hungary. *In:* K.E. Roehl, T. M. F. G. S. & Stewart, D. I. (eds.) *Trace Metals and other Contaminants in the Environment.* Elsevier.

Cumin, N. 1827. Remarks on the medicinal properties of Madar and on the effects of bichromate of potassium on the human body. *Edinburgh Medical Surgery J.*

Darrie, G. 2001. Commercial Extraction Technology and Process Waste Disposal in the Manufacture of Chromium chemicals From Ore. *Environ. Geochem. Health,* 23**,** 187-193.

Daulton, T. L., Little, B. J., Jones-Meehan, J., Blom, D. A. & Allard, L. F. 2007. Microbial reduction of chromium from the hexavalent to divalent state. *Geochim. Cosmochim. Acta,* 71**,** 556-565.

Deng, B. & Stone, A. T. 1996. Surface-Catalyzed Chromium(VI) Reduction: Reactivity Comparisons of Different Organic Reductants and Different Oxide Surfaces. *Environ. Sci. Technol.,* 30**,** 2484-2494.

Dhal, B., Das, N. N., Thatoi, H. N. & Pandey, B. D. 2013a. Characterizing toxic Cr(VI) contamination in chromite mine overburden dump and its bacterial remediation. *Journal of Hazardous Materials,* 260**,** 141-149.

Dhal, B., Thatoi, H. N., Das, N. N. & Pandey, B. D. 2013b. Chemical and microbial remediation of hexavalent chromium from contaminated soil and mining/metallurgical solid waste: A review. *J. Hazard. Mater.,* 250–251**,** 272-291.

Dobbin, P. S., Carter, J. P., San Juan, C. G. S., von Hobe, M., Powell, A. K. & Richardson, D. J. 1999. Dissimilatory Fe(III) reduction by Clostridium beijerinckii isolated from freshwater sediment using Fe(III) maltol enrichment. *FEMS Microbiol. Lett.,* 176**,** 131-138.

Du, J., Lu, J., Wu, Q. & Jing, C. 2012. Reduction and immobilization of chromate in chromite ore processing residue with nanoscale zero-valent iron. *J. Hazard. Mater.,* 215–216**,** 152-158.

Evans, U. R. & Winterbottom, A. B. 1948. *Metallic corrosion, passivity and protection*, E. Arnold and co.

Farmer, J. G., Thomas, R. P., Graham, M. C., Geelhoed, J. S., Lumsdon, D. G. & Paterson, E. 2002. Chromium speciation and fractionation in ground and surface waters in the vicinity of chromite ore processing residue disposal sites. *J. Environ. Monit.,* 4**,** 235-243.

Fendorf, S. E. & Li, G. 1996. Kinetics of Chromate Reduction by Ferrous Iron. *Environ. Sci. Technol.,* 30**,** 1614-1617.

Fendorf, S. E. & Zasoski, R. J. 1992. Chromium(III) oxidation by .delta.-manganese oxide (MnO2). 1. Characterization. *Environ. Sci. Technol.,* 26**,** 79-85.

Fiuza, A., Silva, A., Carvalho, G., de la Fuente, A. V. & Delerue-Matos, C. 2010. Heterogeneous kinetics of the reduction of chromium (VI) by elemental iron. *J. Hazard. Mater.,* 175**,** 1042-1047.

Gao, H., Yang, Z. K., Barua, S., Reed, S. B., Romine, M. F., Nealson, K. H., Fredrickson, J. K., Tiedje, J. M. & Zhou, J. 2009. Reduction of nitrate in Shewanella oneidensis depends on atypical NAP and NRF systems with NapB as a preferred electron transport protein from CymA to NapA. *Isme. J.,* 3**,** 966-76.

Garnova, E. S., Zhilina, T. N., Tourova, T. P. & Lysenko, A. M. 2003. Anoxynatronum sibiricum gen.nov., sp.nov alkaliphilic saccharolytic anaerobe from cellulolytic community of Nizhnee Beloe (Transbaikal region). *Extremophiles,* 7**,** 213-220.

Geelhoed, J. S., Meeussen, J. C. L., Hillier, S., Lumsdon, D. G., Thomas, R. P., Farmer, J. G. & Paterson, E. 2002. Identification and geochemical modeling of processes controlling leaching of Cr(VI) and other major elements from chromite ore processing residue. *Geochim. Cosmochim. Acta,* 66**,** 3927-3942.

Gerlach, R., Cunningham, A. B. & Caccavo, F. 2000. Dissimilatory Iron-Reducing Bacteria Can Influence the Reduction of Carbon Tetrachloride by Iron Metal. *Environ. Sci. Technol.,* 34**,** 2461-2464.

Gheju, M. & Iovi, A. 2006. Kinetics of hexavalent chromium reduction by scrap iron. *J. Hazard. Mater.,* 135**,** 66-73.

Gillham, R. W. & O'Hannesin, S. F. 1994. Enhanced Degradation of Halogenated Aliphatics by Zero-Valent Iron. *Ground Water,* 32**,** 958-967.

Glasauer, S., Langley, S., Boyanov, M., Lai, B., Kemner, K. & Beveridge, T. J. 2007. Mixed-Valence Cytoplasmic Iron Granules Are Linked to Anaerobic Respiration. *Applied and Environmental Microbiology,* 73**,** 993-996.

Gorby, Y. A., Yanina, S., McLean, J. S., Rosso, K. M., Moyles, D., Dohnalkova, A., Beveridge, T. J., Chang, I. S., Kim, B. H., Kim, K. S., Culley, D. E., Reed, S. B., Romine, M. F., Saffarini, D. A., Hill, E. A., Shi, L., Elias, D. A., Kennedy,

D. W., Pinchuk, G., Watanabe, K., Ishii, S. i., Logan, B., Nealson, K. H. & Fredrickson, J. K. 2006. Electrically conductive bacterial nanowires produced by Shewanella oneidensis strain MR-1 and other microorganisms. *Proceedings of the National Academy of Sciences,* 103**,** 11358-11363.

Gorlenko, V., Tsapin, A., Namsaraev, Z., Teal, T., Tourova, T., Engler, D., Mielke, R. & Nealson, K. 2004. Anaerobranca californiensis sp nov., an anaerobic, alkalithermophilic, fermentative bacterium isolated from a hot spring on Mono Lake. *Int. J. Syst. Evol. Microbiol.,* 54**,** 739-743.

Gould, J. P. 1982. The kinetics of hexavalent chromium reduction by metallic iron. *Water Res.,* 16**,** 871-877.

Graham, M. C., Farmer, J. G., Anderson, P., Paterson, E., Hillier, S., Lumsdon, D. G. & Bewley, R. J. F. 2006. Calcium polysulfide remediation of hexavalent chromium contamination from chromite ore processing residue. *Sci. Total Environ.,* 364**,** 32-44.

Grant, W. D., Mwatha, W. E. & Jones, B. E. 1990. Alkaliphiles: Ecology, diversity and applications. *FEMS Microbiol. Lett.,* 75**,** 255-269.

Griffin, R. A., Au, A. K. & Frost, R. R. 1977. Effect of pH on adsorption of chromium from landfill-leachate by clay minerals. *J. Environ. Sci. Health A Environ. Sci. Eng Toxic Hazard Subst. Control,* 12**,** 431-449.

Grossl, P. R., Eick, M., Sparks, D. L., Goldberg, S. & Ainsworth, C. C. 1997. Arsenate and Chromate Retention Mechanisms on Goethite. 2. Kinetic Evaluation Using a Pressure-Jump Relaxation Technique. *Environ. Sci. Technol.,* 31**,** 321-326.

Guertin, J., Jacobs, J. A. & Avakian, C. P. 2004. *Chromium(VI) Handbook*, Taylor & Francis.

Harish, R., Samuel, J., Mishra, R., Chandrasekaran, N. & Mukherjee, A. 2012. Bio-reduction of Cr(VI) by exopolysaccharides (EPS) from indigenous bacterial species of Sukinda chromite mine, India. *Biodegradation,* 23**,** 487-496.

He, Y. T. & Traina, S. J. 2005. Cr(VI) Reduction and Immobilization by Magnetite under Alkaline pH Conditions: The Role of Passivation. *Environ. Sci. Technol.,* 39**,** 4499-4504.

Hillier, S., Roe, M. J., Geelhoed, J. S., Fraser, A. R., Farmer, J. G. & Paterson, E. 2003. Role of quantitative mineralogical analysis in the investigation of sites contaminated by chromite ore processing residue. *Sci. Total Environ.,* 308**,** 195-210.

Horikoshi, K. 1999. Alkaliphiles: Some Applications of Their Products for Biotechnology. *Microbiol. Mol. Biol. Rev.,* 63**,** 735-750.

Horikoshi, K. 2001. Alkaliphiles. John Wiley & Sons, Ltd.

James, B. R. 1996. Peer Reviewed: The Challenge of Remediating Chromium-Contaminated Soil. *Environmental Science & Technology,* 30**,** 248A-251A.

Jiann-Ruey, C., Huei-Yun, C., Yuh-Lin, L., Iua-Jou, Y., Jung-Chou, O. & Fu-Ming, P. 1991. Studies on carbon steel corrosion in molybdate and silicate solutions as corrosion inhibitors. *Surf. Sci.,* 247**,** 352-359.

Katz, S. A. & Salem, H. 1994. *The biological and environmental chemistry of chromium*, Wiley.

Kevbrin, V. V., Zhilina, T. N., Rainey, F. A. & Zavarzin, G. A. 1998. Tindallia magadii gen. nov., sp. nov.: An alkaliphilic anaerobic ammonifier from soda lake deposits. *Curr. Microbiol.,* 37**,** 94-100.

Kindness, A., Macias, A. & Glasser, F. P. 1994. Immobilization of chromium in cement matrices. *Waste Manage.,* 14**,** 3-11.

Kitsa, V., Lioy, P. J., Chow, J. C., Watson, J. G., Shupack, S., Howell, T. & Sanders, P. 1992. Particle-Size Distribution of Chromium: Total and Hexavalent Chromium in Inspirable, Thoracic, and Respirable Soil Particles from Contaminated Sites in New Jersey. *Aerosol Sci. Technol.,* 17**,** 213-229.

Kleikemper, J., Schroth, M. H., Sigler, W. V., Schmucki, M., Bernasconi, S. M. & Zeyer, J. 2002. Activity and Diversity of Sulfate-Reducing Bacteria in a Petroleum Hydrocarbon-Contaminated Aquifer. *Applied and Environmental Microbiology,* 68**,** 1516-1523.

Kotaś, J. & Stasicka, Z. 2000. Chromium occurrence in the environment and methods of its speciation. *Environ. Pollut.,* 107**,** 263-283.

Lahodny-Sarc, O. & Kastelan, L. 1981. The influence of pH on the inhibition of corrosion of iron and mild steel by sodium silicate. *Corros. Sci.,* 21**,** 265-271.

Lai, K. C. K. & Lo, I. M. C. 2008. Removal of Chromium (VI) by Acid-Washed Zero-Valent Iron under Various Groundwater Geochemistry Conditions. *Environ. Sci. Technol.,* 42**,** 1238-1244.

Langmuir, D. 1997. *Aqueous environmental geochemistry*, Prentice Hall.

Leonard, A. & Lauwerys, R. R. 1980. Carcinogenicity and Mutagenicity of Chromium. *Mutat. Res.,* 76**,** 227-239.

Liu, C., Gorby, Y. A., Zachara, J. M., Fredrickson, J. K. & Brown, C. F. 2002. Reduction kinetics of Fe(III), Co(III), U(VI), Cr(VI), and Tc(VII) in cultures of dissimilatory metal-reducing bacteria. *Biotechnol. Bioeng.,* 80**,** 637-649.

Liu, C. Y., Pagán, V. & Liu, N. H. S. 2011. The Terra Cotta Army of Qin Shi Huang. *World Neurosurg.,* 75**,** 352-353.

Lloyd, J. R. & Lovley, D. R. 2001. Microbial detoxification of metals and radionuclides. *Curr. Opin. Biotechnol.,* 12**,** 248-253.

Lovley, D. R. 1991. Dissimilatory Fe(III) and Mn(IV) reduction. *Microbiol. Mol. Biol. Rev.,* 55**,** 259-287.

Lovley, D. R. 1993. Dissimilatory Metal Reduction. *Annu. Rev. Microbiol.,* 47**,** 263-290.

Lovley, D. R. 2000. Fe(III) and Mn(IV) Reduction In: Environmental Microbe-Metal Interactions.

Lovley, D. R. 2001. Anaerobes to the Rescue. *Science,* 293**,** 1444-1446.

Lovley, D. R. 2006. *Dissimilatory Fe(III) and Mn(IV) reducing Prokaryotes. In: The Prokaryotes: A Handbook on the Biology of Bacteria: Vol. 2: Ecophysiology and Biochemistry*, Springer.

Lovley, D. R. 2008. Extracellular electron transfer: wires, capacitors, iron lungs, and more. *Geobiology,* 6**,** 225-231.

Lovley, D. R. & Phillips, E. J. P. 1994. Reduction of Chromate by Desulfovibro-Vulgaris and its C(3) Cytochrome. *Appl. Environ. Microbiol.,* 60**,** 726-728.

Lovley, D. R., Stolz, J. F., Nord, G. L. & Phillips, E. J. P. 1987. Anaerobic production of magnetite by a dissimilatory iron-reducing microorganism. *Nature,* 330**,** 252-254.

Loyaux-Lawniczak, S., Lecomte, P. & Ehrhardt, J.-J. 2001. Behavior of Hexavalent Chromium in a Polluted Groundwater: Redox Processes and Immobilization in Soils. *Environ. Sci. Technol.,* 35**,** 1350-1357.

Madeline, V., Kazem, K., Elizabeth, L. B.-H. & Derek, R. L. 1998. Microbiological evidence for Fe(III) reduction on early Earth. *Nature,* 395**,** 65-67.

Maier, R. M., Pepper, I. L. & Gerba, C. P. 2000. *Environmental microbiology*, Academic Press.

Marsili, E., Baron, D. B., Shikhare, I. D., Coursolle, D., Gralnick, J. A. & Bond, D. R. 2008. Shewanella Secretes Flavins That Mediate Extracellular Electron Transfer. *Proc. Natl. Acad. Sci. U.S.A.,* 105**,** 3968-3973.

Melitas, N., Chuffe-Moscoso, O. & Farrell, J. 2001. Kinetics of Soluble Chromium Removal from Contaminated Water by Zerovalent Iron Media: Corrosion Inhibition and Passive Oxide Effects. *Environ. Sci. Technol.,* 35**,** 3948-3953.

Mishra, A. K. & Mohanty, B. 2008. Acute toxicity impacts of hexavalent chromium on behavior and histopathology of gill, kidney and liver of the freshwater fish, Channa punctatus (Bloch). *Environ. Toxicol. Pharmacol.,* 26**,** 136-141.

Morrison, S. J. N., D. L. Davis, J. A. Fuller, C. C. 2002. Introduction to Groudwater Remediation of Metals, Radionuclides, and Nutrients with Permeable Reactive Barries. *In:* Naftz, D. M., S. J. Fuller, C. C. Davis J. A. (ed.) *Handbook of Groundwater Remediation using Permeable Reactive Barriers.*

Muyzer, G., Teske, A., Wirsen, C. & Jannasch, H. 1995. Phylogenetic relationships of Thiomicrospira species and their identification in deep-sea hydrothermal vent samples by denaturing gradient gel electrophoresis of 16S rDNA fragments. *Arch. Microbiol.,* 164**,** 165-172.

Myneni, S. C. B., Tokunaga, T. K. & Brown, G. E., Jr. 1997. Abiotic Selenium Redox Transformations in the Presence of Fe(II,III) Oxides. *Science,* 278**,** 1106-1109.

Nealson, K. H. & Saffarini, D. 1994. Iron and Manganese in Anaerobic Respiration: Environmental Significance, Physiology, and Regulation. *Annu. Rev. Microbiol.,* 48**,** 311-343.

Niederbacher, P. & Nahold, M. 2005. Installation and operation of an Adsorptive Reactor and Barrier (AR&B) system in Brunn am Gebirge, Austria. *Trace Metals and other Contaminants in the Environment,* 7**,** 283-309.

Noh, J. S. & Schwarz, J. A. 1989. Estimation of the point of zero charge of simple oxides by mass titration. *Journal of Colloid and Interface Science,* 130**,** 157-164.

O'Hannesin, S. F. & Gillham, R. W. 1998. Long-Term Performance of an In Situ "Iron Wall" for Remediation of VOCs. *Ground Water,* 36**,** 164-170.

Odziemkowski, M. S., Schuhmacher, T. T., Gillham, R. W. & Reardon, E. J. 1998. Mechanism of oxide film formation on iron in simulating groundwater solutions: Raman spectroscopic studies. *Corros. Sci.,* 40**,** 371-389.

Palmer, C. D. 2000. Precipitates in a Cr(VI)-Contaminated Concrete. *Environ. Sci. Technol.,* 34**,** 4185-4192.

Papp, J. F. 2010. 2010 Minerals Yearbook, Chromium. *United States Geological Survey*.

Pollock, J., Weber, K. A., Lack, J., Achenbach, L. A., Mormile, M. R. & Coates, J. D. 2007. Alkaline iron(III) reduction by a novel alkaliphilic, halotolerant, Bacillus sp. isolated from salt flat sediments of Soap Lake. *Appl. Microbiol. Biotechnol.,* 77**,** 927-34.

Powell, R. M. 1998. Permeable Reactive Barrier Technologies for Contaminant Remediation.

Powell, R. M., Puls, R. W., Hightower, S. K. & Sabatini, D. A. 1995. Coupled Iron Corrosion and Chromate Reduction: Mechanisms for Subsurface Remediation. *Environ. Sci. Technol.,* 29**,** 1913-1922.

Priscu, J. C., Adams, E. E., Lyons, W. B., Voytek, M. A., Mogk, D. W., Brown, R. L., McKay, C. P., Takacs, C. D., Welch, K. A., Wolf, C. F., Kirshtein, J. D. & Avci, R. 1999. Geomicrobiology of Subglacial Ice Above Lake Vostok, Antarctica. *Science,* 286**,** 2141-2144.

Puls, R. W., Paul, C. J. & Powell, R. M. 1999. The application of in situ permeable reactive (zero-valent iron) barrier technology for the remediation of chromate-contaminated groundwater: a field test. *Appl. Geochem.,* 14**,** 989-1000.

Qian, H., Wu, Y., Liu, Y. & Xu, X. 2008. Kinetics of hexavalent chromium reduction by iron metal. *Front. Environ. Sci. En.,* 2**,** 51-56.

Rabus, R. 2006. Dissimilatory Sulfate- and Sulfur-Reducing Prokaryotes. *In:* Martin Dworkin, S. F., Eugene Rosenberg, Karl-Heinz Schleifer (ed.) *The Prokaryotes.*

Rai, D., Eary, L. E. & Zachara, J. M. 1989. Environmental chemistry of chromium. *Sci. Total Environ.,* 86**,** 15-23.

Rai, D., Sass, B. M. & Moore, D. A. 1987. Chromium(III) Hydrolysis Constants and Solubility of Chromium(III) Hydroxide. *Inorg. Chem.,* 26**,** 345-349.

Rai, D. & Zachara, J. M. 1986. Geochemical behavior of chromium species.

Reardon, E. J. 1995. Anaerobic Corrosion of Granular Iron: Measurement and Interpretation of Hydrogen Evolution Rates. *Environ. Sci. Technol.,* 29**,** 2936-2945.

Richard, F. C. & Bourg, A. C. M. 1991. Aqueous geochemistry of chromium: A review. *Water Res.,* 25**,** 807-816.

Roehl, K. E. 2005. Permeable Reactive Barriers. *In:* K. E. Roehl, T. M., F-G. Simon, and D.I. Stewart (ed.) *Long-term Performance of Permeable Reactive Barriers.* Elsevier.

Roh, Y., Chon, C.-M. & Moon, J.-W. 2007. Metal reduction and biomineralization by an alkaliphilic metal-reducing bacterium,Alkaliphilus metalliredigens. *Geosci. J.,* 11**,** 415-423.

Roh, Y., Lee, S. Y. & Elless, M. P. 2000. Characterization of corrosion products in the permeable reactive barriers. *Environ. Geol.,* 40**,** 184-194.

Rushing, J. C., McNeill, L. S. & Edwards, M. 2003. Some effects of aqueous silica on the corrosion of iron. *Water Res.,* 37**,** 1080-1090.

Schmitz, R. A. 2006. The Anaerobic Way of Life. *In:* Martin Dworkin, S. F., Eugene Rosenberg, Karl-Heinz Schleifer (ed.) *The Prokaryotes*

Schrebler Guzmán, R. S., Vilche, J. R. & Arvía, A. J. 1979. The potentiodynamic behaviour of iron in alkaline solutions. *Electrochim. Acta,* 24**,** 395-403.

Schroeder, D. C. & Lee, G. F. 1975. Potential transformations of chromium in natural waters. *Water Air Soil Pollut.,* 4**,** 355-365.

Schroth, M. H., Kleikemper, J., Bolliger, C., Bernasconi, S. M. & Zeyer, J. 2001. In situ assessment of microbial sulfate reduction in a petroleum-contaminated aquifer using push–pull tests and stable sulfur isotope analyses. *Journal of Contaminant Hydrology,* 51**,** 179-195.

Shanker, A. K., Cervantes, C., Loza-Tavera, H. & Avudainayagam, S. 2005. Chromium toxicity in plants. *Environ. Int.,* 31**,** 739-753.

Shayne, C. 1989. Acute and chronic systemic chromium toxicity. *Sci. Total Environ.,* 86**,** 149-157.

Silva, R. J. N., H. 1995. Actinide Environmental Chemistry. *Radiochim. Acta,* 70/71**,** 377-396.

Sreeram, K. J. & Ramasami, T. 2001. Speciation and recovery of chromium from chromite ore processing residues. *J. Environ. Monit.,* 3**,** 526-530.

Stewart, D. I., Burke, I. T., Hughes-Berry, D. V. & Whittleston, R. A. 2010. Microbially mediated chromate reduction in soil contaminated by highly alkaline leachate from chromium containing waste. *Ecol. Eng.,* 36**,** 211-221.

Stewart, D. I., Burke, I. T. & Mortimer, R. J. G. 2007. Stimulation of Microbially Mediated Chromate Reduction in Alkaline Soil-Water Systems. *Geomicrobiol. J.,* 24**,** 655 - 669.

Stollenwerk, K. G. & Grove, D. B. 1985. Adsorption and Desorption of Hexavalent Chromium in an Alluvial Aquifer Near Telluride, Colorado. *J. Environ. Qual.,* 14**,** 150-155.

Suzuki, T., Miyata, N., Horitsu, H., Kawai, K., Takamizawa, K., Tai, Y. & Okazaki, M. 1992. NAD (P) H-dependent chromium (VI) reductase of Pseudomonas ambigua G-1: a Cr (V) intermediate is formed during the reduction of Cr (VI) to Cr (III). *J. Bacteriol.,* 174**,** 5340-5345.

Tandon, R. K., Crisp, P. T., Ellis, J. & Baker, R. S. 1984. Effect of pH on chromium(VI) species in solution. *Talanta,* 31**,** 227-228.

Taylor, D., Maddock, B. G. & Mance, G. 1985. The acute toxicity of nine 'grey list' metals (arsenic, boron, chromium, copper, lead, nickel, tin, vanadium and zinc) to two marine fish species: Dab (Limanda limanda) and grey mullet (Chelon labrosus). *Aquat. Toxicol.,* 7**,** 135-144.

Tinjum, J. M., Benson, C. H. & Edil, T. B. 2008. Mobilization of Cr(VI) from chromite ore processing residue through acid treatment. *Sci. Total Environ.,* 391**,** 13-25.

UK Environmental Agency 2002. Contaminants in soil: Collation of toxilogical data and intake values for humans. Chromium.

UKTAG 2008. Proposals For Environmental Quality Standards For Annex VIII Substances. UK Technical Advisory Group on the Water Framework Directive.

USEPA 1998. National Primary Drinking Water Regulations, Technical Factsheet on: Chromium.

USEPA 1999. Field Applications of In Situ Remediation Technologies: Permeable Reactive Barriers.

VanEngelen, M., Peyton, B., Mormile, M. & Pinkart, H. 2008. Fe(III), Cr(VI), and Fe(III) mediated Cr(VI) reduction in alkaline media using a Halomonas isolate from Soap Lake, Washington. *Biodegradation,* 19**,** 841-850.

Veeramani, H., Alessi, D. S., Suvorova, E. I., Lezama-Pacheco, J. S., Stubbs, J. E., Sharp, J. O., Dippon, U., Kappler, A., Bargar, J. R. & Bernier-Latmani, R. 2011. Products of abiotic U(VI) reduction by biogenic magnetite and vivianite. *Geochim. Cosmochim. Acta,* 75**,** 2512-2528.

von Canstein, H., Ogawa, J., Shimizu, S. & Lloyd, J. R. 2008. Secretion of Flavins by Shewanella Species and Their Role in Extracellular Electron Transfer. *Appl. Environ. Microbiol.,* 74**,** 615-623.

Wang, T., He, M. & Pan, Q. 2007. A new method for the treatment of chromite ore processing residues. *J. Hazard. Mater.,* 149**,** 440-444.

Wang, Y.-T. & Shen, H. 1997. Modelling Cr(VI) reduction by pure bacterial cultures. *Water Res.,* 31**,** 727-732.

Wang, Y. T. 2000. Microbial Reduction of Chromate. *In:* Lovley, D. R. (ed.) *Environmental Microbe-Metal Interactions.*

Weng, C. H., Huang, C. P., Allen, H. E., Cheng, A. H. D. & Sanders, P. F. 1994. Chromium leaching behavior in soil derived from chromite ore processing waste. *Sci. Total Environ.,* 154**,** 71-86.

Whitman, W. B., Coleman, D. C. & Wiebe, W. J. 1998. Prokaryotes: The unseen majority. *Proc. Natl. Acad. Sci. U.S.A.,* 95**,** 6578-6583.

Whittleston, R. A. 2011. *Bioremediation of chromate in alkaline sediment-water systems.* PhD thesis, University of Leeds.

Whittleston, R. A., Stewart, D. I., Mortimer, R. J. G., Tilt, Z. C., Brown, A. P., Geraki, K. & Burke, I. T. 2011a. Chromate reduction in Fe(II)-containing soil affected by hyperalkaline leachate from chromite ore processing residue. *J. Hazard. Mater.,* 194**,** 15-23.

Whittleston, R. A., Stewart, D. I., Mortimer, R. J. G., Tilt, Z. C., Brown, A. P., Geraki, K. & Burke, I. T. 2011b. Chromate reduction in Fe(II)-containing soil affected by hyperalkaline leachate from chromite ore processing residue. *J. Hazard. Mater.,* 194**,** 15-23.

Wilkin, R. T., Su, C., Ford, R. G. & Paul, C. J. 2005. Chromium-Removal Processes during Groundwater Remediation by a Zerovalent Iron Permeable Reactive Barrier. *Environ. Sci. Technol.,* 39**,** 4599-4605.

Williamson, A. J., Morris, K., Shaw, S., Byrne, J. M., Boothman, C. & Lloyd, J. R. 2013. Microbial Reduction of Fe(III) under Alkaline Conditions Relevant to Geological Disposal. *Applied and Environmental Microbiology,* 79**,** 3320-3326.

World Health Organisation 2000. Air Quality Guidlines for Europe, Second Edition.

World Health Organisation 2003. Chromium in Drinking-water, Background document for development of WHO Guidelines for Drinking-water Quality.

Xendis, A., Moirou, A., & Paspaliaris, I. 2002. A review on reactive materials and attenuation processes for permeable reactive barriers. *Mineral Wealth,* 123**,** 35-48.

Ye, Q., Roh, Y., Carroll, S. L., Blair, B., Zhou, J., Zhang, C. L. & Fields, M. W. 2004. Alkaline Anaerobic Respiration: Isolation and Characterization of a Novel Alkaliphilic and Metal-Reducing Bacterium. *Appl. Environ. Microbiol.,* 70**,** 5595-5602.

Zachara, J. M., Kukkadapu, R. K., Fredrickson, J. K., Gorby, Y. A. & Smith, S. C. 2002. Biomineralization of Poorly Crystalline Fe(III) Oxides by Dissimilatory Metal Reducing Bacteria (DMRB). *Geomicrobiol. J.,* 19**,** 179-207.

Zavarzina, D. G., Kolganova, T. V., Boulygina, E. S., Kostrikina, N. A., Tourova, T. P. & Zavarzin, G. A. 2006. Geoalkalibacter ferrihydriticus gen. nov. sp. nov., the first alkaliphilic representative of the family Geobacteraceae, isolated from a soda lake. *Microbiology,* 75**,** 673-682.

Zhilina, T. N., Zavarzina, D. G., Kolganova, T. V., Lysenko, A. M. & Tourova, T. P. 2009. Alkaliphilus peptidofermentans sp. nov., a new alkaliphilic bacterial soda lake isolate capable of peptide fermentation and Fe(III) reduction. *Microbiology,* 78**,** 445-454.

Zhu, W., Yang, Z., Ma, Z. & Chai, L. 2008. Reduction of high concentrations of chromate by Leucobacter sp. CRB1 isolated from Changsha, China. *World Journal of Microbiology and Biotechnology,* 24**,** 991-996.

Chapter 3 **Experimental Design, Analytical Methods and Materials**

3.1 Experimental Design

3.1.1 PRB Experimental Design

ZVI is known to react with Cr(VI) at neutral to acid pH to produce Cr(III)-hydroxides, removing Cr(VI) from solution (Fiuza et al., 2010, Gheju and Iovi, 2006). However, this reaction is assumed to be very slow at alkaline pH due to iron passivation and surface corrosion reactions (Alowitz and Scherer, 2002, Chang, 2005). Therefore, it was necessary to assess the performance of ZVI at alkaline pH if it is to be used at COPR sites. In order to achieve the stated aim it was important to utilise material actually from a highly alkaline COPR site so as to base this study on the real world. Therefore the Cr(VI) containing leachate used was collected from a historic COPR site in West Yorkshire. The results were contrasted with those using a simple Cr(VI) solution (as K-chromate) in order to determine how other solutes within the leachate affect the performance of the iron. Zero valent iron was sourced from a laboratory supplies company and acid washed before use to ensure minimal oxidation of the surface.

The reduction reaction was evaluated via a series of microcosm experiments with differing solid solution ratios. Periodical sampling allowed the concentration of Cr(VI) and pH to be determined with time in order to evaluate the performance of the iron. pH amended microcosms were also prepared in order to assess how the reaction changed with differing solution pH. Scanning electron microscopy (SEM) and X-ray photoelectron spectroscopy were employed to evaluate the surface of the iron post reaction.

3.1.2 Biobarrier Experimental Design

Several genera of anaerobic bacteria are known to facilitate the transformation of toxic Cr(VI) to insoluble Cr(III) hydroxides (Liu et al., 2002, Harish et al., 2012), but the viability of these reactions at high pH is not

certain. As the permeable reactive barrier study, it was important to base the work with on material collected from a historic COPR site. The bacteria consortium used in this study were initially cultured by Dr. Robert Whittleston from a clay layer beneath a historic COPR site in West Yorkshire (Whittleston, 2011). Whittleston et al (2011) presented evidence that microbial reduction processes, despite having a pH > 11, were occurring in this clay horizon that lead to elevated Fe(II) concentrations and a capacity to reduce Cr(VI) in influent alkaline waters. The potential to form a useful biobarrier depends on the genetic potential of these alkaliphile bacteria to control in-situ geochemical conditions such that Cr(VI) reduction is favoured. The present study therefore focuses on elucidating the physiological growth characteristics and metabolic pathways of this consortium of alkaliphile bacteria.

Since isolation (2009), the bacteria have been repeatedly grown in anaerobic alkaline Fe(III) containing media, with yeast extract as the electron donor (see chapter 3 for details). An Fe(III)-containing alluvial sand was recovered by Dr. Stewart from the below the clay layer and was used to test that the isolated consortia retained the ability to utilise natural Fe(III) minerals as an electron acceptor (Stewart et al., 2010). Microcosm tests were again used for the majority of this study as they allowed periodic sampling in order to determine concentrations of Cr(VI), Fe(II), ATP and riboflavin, as well as pH and cell numbers. These indicators were important for determining the growth of the bacteria and how that was affecting solutes within the microcosms. Being a closed system, microcosms allowed monitoring of the growth of the anaerobic bacteria whilst preventing infiltration by erroneous bacteria not from the COPR site. Microcosms also allow easy tailoring of the growth media in order to investigate the differing conditions in which the bacteria can live. Bacteria were also grown on solid agar plates in order to isolate those bacteria responsible for extracellular reduction of iron. The bacteria population was periodically characterised via sequencing of the 16s rRNA gene and compared to known type strains in order to create phylogenies. SEM analysis was used to identify the Fe(II) phase precipitated by the bacteria.

3.1.3 **Method Selection**

When deciding on the methods to utilise in this study it was important to focus on those that were robust, repeatable, and proven to give the required results. Therefore many of the techniques utilised were those previously used by members of the study group or highlighted by others in peer reviewed publications.

UV-VIS spectroscopy is the preferred method utilised by many to quantify concentrations of compounds within liquors. Indeed many working within this particular field have used it to measure concentrations of Cr(VI) and Fe(II) within liquors (Viollier et al., 2000, Lovley et al., 1987, Whittleston et al., 2011b, Chang, 2005, Stewart et al., 2007, Stewart et al., 2010, Alowitz and Scherer, 2002, Eary and Rai, 1988). The ease of use and repeatability, coupled with the ability to get meaningful results with minimal volumes of sample meant that it was ideal for this study.

Analysis of surfaces can be done by many spectroscopic techniques. Scanning electron microscopy (SEM) and X-ray photoelectron spectroscopy (XPS) were used to qualify the iron surface precipitates as they are able to give highly detailed information on the topology and elemental composition of any structures within the viewfinder. Whilst EDX can give good information on the elements present, it can give little information on their oxidation state or compounds that they are part of. Therefore X-ray diffraction spectroscopy (XRD) was utilised to identify the different oxidation states of the elements present.

Bacteria growth can be tracked by observing many different parameters. These include total cell counting, viable cell counting, accumulation of protein, ATP concentration, turbidity of the liquid, viscosity of the liquid and wet or dry weighing (Spencer and de Spencer, 2004). Many of these methods could be discounted immediately due to using media which included a coloured Fe(III) precipitate including the turbidity, viscosity and wet and dry weighing. Viable cell counting was discounted due to the extended time and skill required to grow the bacteria on separate anaerobic agar plates.

Therefore a trial was conducted whereby the growth of bacteria in AFe media was tracked by following the cell count, accumulation of protein, and ATP concentration. From this trial it was concluded that the accumulation of protein gave little usable information and was therefore discarded. The other two growth parameters gave useful information and were therefore deemed suitable for use.

Sequencing of bacteria populations is a relatively new pursuit made possible with the development of PCR in 1983. The techniques utilised in this study have been successfully used previously by members of the study group (Whittleston et al., 2013, Whittleston et al., 2011a, Stewart et al., 2010). Therefore it seemed prudent to continue using the same process which has a track record of success.

The isolation and identification of riboflavin was performed by Dr McMillan, using techniques that he has previously deployed with success (McMillan et al., 2010).

Utilising techniques already proved successful, ensured the highest degree of success and minimised the risk of wasting time and precious samples or materials.

3.1.4 **Data Quality**

All experimental work must be benchmarked against a known quantity in order to be able to derive value from it. Thus when performing any test the use of tightly controlled blanks and calibration curves were important to ensure good data quality. Calibration curves allow the comparison of samples to standards of known value thereby allowing the quantification of the sample. The use of blanks is also highly important as they allow the comparison of samples to baseline readings therefore highlighting any change that occurred during the test. Many of the methods used have well defined optimum operational windows which if not adhered to, can lead to erroneous and false data, therefore all detection limits for each method were strictly observed. Details of the calibration curves, blanks and detection limits are highlighted below, alongside descriptions of the methods used.

To ensure good quality data, it is important to repeat experiments as repetition of results gives a higher confidence that they are correct. However, for some large ranging experiments with 1000s of data points, repetition is impractical due to the excessive time required to do so. Therefore whenever possible, experiments were repeated three times with the standard deviation presented as the error from the mean. For larger data sets without repetition, the data was assessed for quality and any erroneous data discounted.

3.2 Materials

3.2.1 **Cr(VI) Leachate**

Cr(VI) leachate was obtained from a 19th century Chromite Ore Processing Residue (COPR) waste site in West Yorkshire. The leachate was taken from a borehole screened directly into the waste using a standpipe piezometer and was stored in a polythene barrel at room temperature (Whittleston et al., 2011b). The pH was recorded as 12.34 and the chemical composition of the leachate, determined by ICP-OES is shown in Table 3.1. Cr(VI) concentration was 0.994 mmol.L^{-1} as determined by UV-VIS (see below for details).

Element	Concentration ($mmol.L^{-1}$)	Concentration ($mg.L^{-1}$)
Na	0.543	12.5
Mg	3	73
K	1	39.1
Ca	13.77	552
Al	0.061	1.65
S	5.95	191
Si	1	28.1

Table 3.1: Chemical composition of the COPR leachate recovered from borehole 5.

3.2.2 **Cr(VI) Solution**

Cr(VI) solution was made by adding K_2CrO_4 to deionised water at a concentration of 1 $mmol.L^{-1}$. The pH of the solution was buffered using NaOH and HCl as required.

3.2.3 **Zero Valent Iron**

Two types of Zero Valent Iron (ZVI) were used for this study. Laboratory grade iron filings (sourced from Fisher Scientific, code I/0850/50) were used solely for batch reduction tests. These were highly uniform in size with 95% of the particles between 75-300 µm and had a BET determined surface area of 0.28 $m^2.g^{-1}$. Irregular shaped Iron coupons (Alfa Aesar, UK), roughly 10 x 10 x 2 mm in size were used as samples for SEM and XPS. Both types of iron were acid washed before use with 1 $mol.L^{-1}$ HCl for 30 mins. The coupons were then rinsed with deoxygenated deionised water three times.

3.2.4 **Bacteria Community**

The bacterial community used for work reported in this thesis was first isolated by Dr Robert Whittleston from a clay layer located directly beneath the waste of an historical COPR located in West Yorkshire (Whittleston, 2011). The initial extraction was achieved by suspending 5 mL soil in anaerobic growth media with yeast extract and Fe citrate added as the sole electron donor and acceptor respectively (see below for recipe). Colour

change of the Fe citrate from red to black indicated iron reduction. Once established, 1% v/v inoculate was taken from the microcosms and repeatedly grown on it the same media. Sequencing of the bacteria community showed that it consisted of 48% β-proteobacteria, 17% α-proteobacteria, 17% Bacteriodetes, 13% γ-proteobacteria and 7% unidentified.

3.2.5 **Aquifer Material from a Historic COPR Site**

Aquifer material from a historic COPR site in West Yorkshire was recovered during a commercial ground investigation in 2007. It was from a soil strata laying underneath the COPR waste material and was identified as alluvial sand and gravel. The gravel was subangular to subrounded fine to coarse of sandstone and mudstone. Since recovery it has been stored in a sealed plastic bucket. Visually the aquifer material resembled orange sand with much fine matter intermixed. X-ray diffraction (XRD) analysis of the sample revealed it to be predominantly quartz with minor traces of kaolinite. X-ray florescence spectroscopy (XRF) analysis (using an Innov-X X-5000 bench top XRF with Rh tube) showed it to contain ≈ 5% Fe (see Table 3.2 for full elemental analysis). Before use, the sample was sieved so that only particles <0.5 mm were used.

Element	Abundance (ppm)
Mg*	14000
Al*	76000
Si*	220000
P	<380
S	2700
K*	18000
Ca*	17000
Ti	5800
V	100
Cr	6800
Mn	5100
Fe*	51000
Ni	<4
Cu	20
Zn	180
As	15
Rb	130
Sr	420
Y	36
Zr	490
Cd	<2
Pb	53
Th	20

Table 3.2: Elemental composition of the aquifer material from the historic COPR site in West Yorkshire as determined by XRF (major elements (>1%) were determined using user defined calibration factors based on soil standards*; minor elements (<1%) were determined using Compton normalisation as programmed for by the instrument (all other elements)). < = less than given limit of detection.

3.2.6 **Anaerobic Alkaline Growth Media**

Anaerobic alkaline Fe(III) containing growth media was prepared by boiling 1L diH_2O for 30 mins before purging with N_2 for 30 mins in order to dispel any oxygen. 0.356 g.L^{-1} $NaH_2PO_4.H_2O$, 0.1 g.L^{-1} KCl and 10 mL.L^{-1} each of standard vitamin and mineral mixes were added (see Table 3.3 and 3.4 for mix recipes). The standard growth media had 2 g.L^{-1} iron (III) citrate ($C_6H_5FeO_7$) and 2 g.L^{-1} yeast extract added as the sole electron acceptor and donor respectively. The media was then buffered to a pH of 9.2 with the addition of sodium carbonate (Na_2CO_3). All headspaces in the microcosms were purged of O_2 by replacement with N_2, sealed with syringable rubber bungs and aluminium crimp caps and then heat sterilised by placing in the autoclave for 30 mins at 120°C.

Iron media with alternative electron donors was prepared in the same manner with the addition of ethanol, methanol, sucrose, acetate or lactate to a concentration of 20 mmol.L^{-1}. Yeast extract concentration was also added at 0.2 g.L^{-1} or removed completely as required.

Iron and chromate media used the same recipe as the iron media with the addition of 50 µmol. L^{-1} to 10 mmol.L^{-1} filter sterilised K_2CrO_4 post autoclave.

Chromate growth media was of the same recipe as the iron media however the Fe citrate was replaced with 200 µmol.L^{-1} filter sterilised potassium chromate (K_2CrO_4), as the sole electron acceptor.

Solid phase Fe(III) media was prepared to the same recipe as the AFe media however the Fe(III) citrate was replaced with the aquifer material recovered from the historic COPR site at a concentration of 100 g.L^{-1}.

Chemical	$mg.L^{-1}$
Biotin	2
Folic Acid	2
Pyridoxine HCl	10
Riboflavin	5
Thiamine	5
Nicotinic acid	5
Pantothenic acid	5
Vitamin B_{12}	0.1
p-aminobenzoic acid	5
Thioctic acid	5

Table 3.3: Vitamin Mix Recipe (Bruce et al., 1999).

Compound	$g.L^{-1}$
Nitrilotriacetic acid	1.5
$MgSO_4$	3.0
$MnSO_4.H_2O$	0.5
NaCl	1.0
$FeSO_4.7H_2O$	0.1
$CaCl_2.2H_2O$	0.1
$CoCl_2.6H_2O$	0.1
ZnCl	0.13
$CuSO_4$	0.01
$AlK(SO_4)_2.12H_2O$	0.01
H_3BO_2	0.01
Na_2MoO_4	0.025
$NiCl_2.6H_2O$	0.024
$Na_2WO_4.2H_2O$	0.025

Table 3.4: Mineral Mix Recipe (Bruce et al., 1999).

Anaerobic Agar Plates

AFe media was prepared in the same way as described above except with the addition of 20 $g.L^{-1}$ agar. After heat sterilisation in an autoclave, plates were pored keeping the agar <1.5 mm thick. 100 µL of media containing bacteria in the upper exponential phase of growth were taken from sealed microcosms using aseptic technique and spread over the surface. The plates were incubated anaerobically in a sealed box with an Anaerogen sachet to eliminate oxygen.

3.3 Methods

Ultraviolet-visible spectroscopy (UV-Vis) is a common analytical technique employed to the measure chemical concentrations in a solution. As light passes through a coloured solution, certain wavelengths of light are absorbed due to molecules contained within. Non bonded electrons are able to absorb the energy from photons and jump to higher molecular orbits. Those molecules with electrons which can be excited more easily, will be able to absorb photons with longer wavelengths. A UV-Vis spectrometer compares the intensity of the light before and after the coloured sample and gives a reading of the adsorbed light for a particular wavelength dependent on the samples colour. This behaviour is described by the Beer-Lambert Law:

$$A = \log_{10}\left(\frac{I_0}{I}\right) = \varepsilon . c . L \qquad (3.1)$$

Where A = absorbance, I_0 = the intensity of light at a given wavelength, I is the intensity of transmitted light, ε = extinction coefficient, c = concentration of the absorbing species and L = the path length through the sample. Thus the higher the concentration, the more light adsorbed by the sample.

When using UV-VIS spectrometry, calibration charts were constructed by running known concentrations of control substances through the same procedure in order to compute a calibration curve. These curves were then

used to convert readings from actual samples into concentrations with units. If any samples had concentrations higher than the maximum used for the calibration curve, they were diluted with deionised water in order to bring them within the range of the calibration curve. Before each test a blank was prepared using deionised water in place of an actual sample. These were subjected to exactly the same process as actual samples. As different reagents have different spectral properties, the blank mixture may register at the light wavelength specified without any concentration of the analyte present. Therefore this baseline reading must be removed from the sample readings in order to display a true reading. Modern UV-VIS spectrophotometers allow saving a blank baseline therefore this was done before each testing run. The ferrozine and diphenylcarbazide solutions used to measure Fe(II) and Cr(VI) respectively are age sensitive so each was made from stock reagents regularly to ensure full reactivity. A new calibration curve was constructed whenever reagents were changed.

3.3.1 **Aqueous Fe(II)**

UV-vis can be used to measure aqueous Fe(II) within a sample. When mixed with Ferrozine, aqueous Fe(II) creates a bright purple colour, the intensity of which directly corresponds to the aqueous Fe(II) concentration.

The method used was as described by Viollier et al., (2000). First the sample was placed in a 1.5 mL micro centrifuge tube and centrifuged at 13,300g for 5mins to pellet any precipitates or debris within the liquor. 100 µL of the supernatant was then placed in a disposable 1 mL cuvette and diluted with 900µl diH_2O. Finally 100 µL ferrozine solution was added, the solution mixed by inversion and then left for 15 mins to allow the colour to develop. Absorbance at 562 nm was then measured on a Thermo Scientific BioMate 3 UV/VIS spectrophotometer. The detection limit of the ferrozine method is estimated to be 0.3 µmol.L^{-1} thus any concentrations lower than this were treated as zero (Viollier et al., 2000).

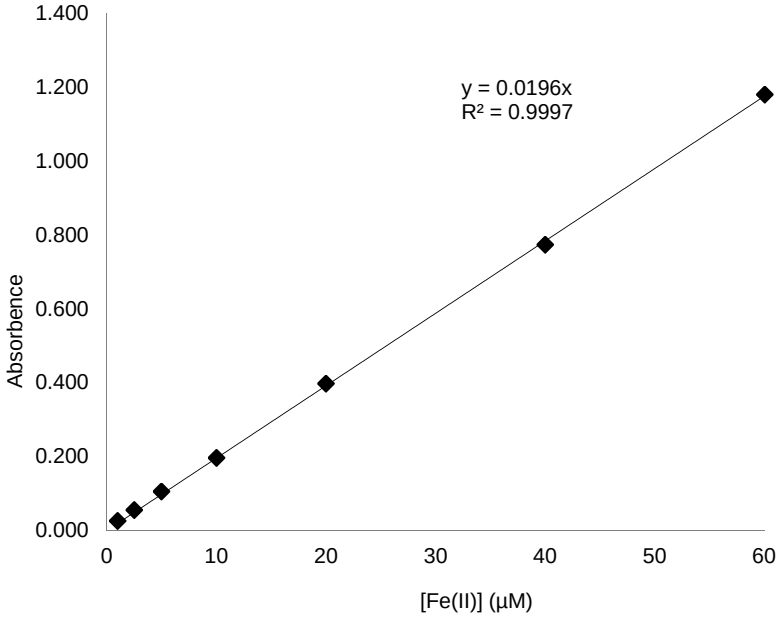

Figure 3.1: Example calibration chart used to convert the absorbances given by the UV-VIS spectrophotometer into usable concentrations of Fe(II) when using the ferrozine method.

3.3.2 **Total Fe(II)**

The method for determining total Fe(II) was adapted from that described by Lovely et al (Lovley and Phillips, 1986). 0.5 mL of sample was dissolved in 2 mL of 0.5N HCl for 1 hour. A 100 µL aliquot was then subjected to the same method as used for Aqueous Fe(II) determination.

3.3.3 **Aqueous Cr(VI)**

Aqueous Cr(VI) was determined using a UV-vis spectrometer and the diphenylcarbazide method as described in US Environmental Protection Agency Method 7196a (USEPA, 1992). First the sample was centrifuged at 13,300g for 5 mins to pellet any precipitates or debris within the liquor. 100 µL of the supernatant was placed in a clear 1.5 mL disposable cuvette, and then acidified with 900 µL of 10 mmol.L^{-1} H_2SO_4. 100 µL of diphenycarbazide (5 g.L^{-1} acetone) was added, before mixing by inversion and waiting 15 mins for the pink colour of the solution to develop. The cuvette was then placed in a UV-vis spectrometer and the amount of light absorbed at 540nm recorded.

A calibration curve was created by using prepared samples of Cr(VI) solution with molarities ranging from 0 to 300 µmol.L^{-1}. If the concentration of Cr(VI) within a sample was higher than the maximum used for the calibration curve, the test was repeated with the sample diluted with diH_2O to within the calibration range. The detection limit of the diphenylcarbazide method is ≈ 20 µmol.L^{-1}, therefore any readings under this amount were treated as zero (National Research Council, 1974).

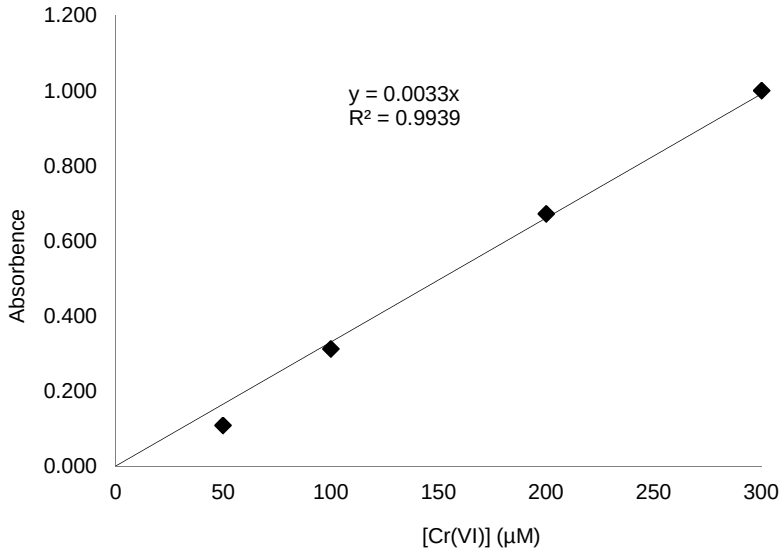

Figure 3.2: Example calibration chart used to convert absorbance readings displayed by the UV-VIS spectrophotometer into concentrations of Cr(VI) whilst using the diphenylcarbazide method.

3.3.4 **Brauner Emmett Teller (BET) Analysis**

BET analysis uses adsorption of nitrogen gas on a solid surface in order to determine the surface area of that surface. It uses adsorption theory as described by Stephen Brunauer, Paul Hugh Emmet and Edward Teller which subsequently gave the process its name (Brunauer et al., 1938). When exposing a surface to nitrogen gas at a certain pressure, adsorption reactions between the surface and gas remove nitrogen from the atmosphere resulting in a lower chamber pressure. The BET isotherm assumes that adsorption of

a gas onto a surface will occur in infinite layers of molecules with each layer forming via a Langmuir isotherm. The amount of nitrogen that is removed during monolayer adsorption (i.e. so as to cover a surface completely with one molecule of nitrogen), is directly related to the surface area of the material being tested and thus can by quantified. Thus:

$$\frac{1}{\left[V_a\left(\frac{P_0}{P}-1\right)\right]} = \frac{C-1}{V_m C} \times \frac{P}{P_0} \times \frac{1}{V_m C}$$

(3.2)

Where P = partial vapour pressure of nitrogen in equilibrium with the surface, P_0 = saturated pressure of nitrogen, V_a = volume of adsorbed nitrogen, V_m = volume of adsorbed gas and C = constant. BET analysis was performed using a Micromeritics Gemini V BET surface area analyser.

3.3.5 **Particle Size Analysis**

Particle size analysis was done using a sieve stack and shaker in accordance with BS 1377-2:1990 (British Standards Institute, 1990). A sample of material is weighed and then placed in the top of a sieve stack comprising of ever smaller meshes. The stack is then placed on a mechanical shaker for 30 mins and the particles retained on each subsequent sieve are weighed and given as a percentage of the total. A brush is used to ensure no particles get stuck within the mesh of each sieve.

3.3.6 **Aseptic Microcosm Sampling**

Aseptic microcosm sampling was achieved by first sealing the microcosms with syringable septums and aluminium crimp caps. Before sampling the bottle tops were placed in ethanol and passed through the flame of a Bunsen burner to sterilise them. Sterile syringes and needles were then used to sample liquid from the microcosm (Burke et al., 2006). To ensure non-discriminatory sampling, the microcosms were well shaken beforehand to re-suspend any precipitates present. When sampling anaerobic bottles, the sterile syringes were filled with nitrogen to the sample volume, and this was injected into the microcosm before withdrawing the sample. This ensured zero pressure difference between the atmospheres outside and within the microcosm, minimising the chance of oxygen ingress.

3.3.7 **Adenosine triphosphate concentration**

Adenosine triphosphate (ATP) concentration was measured as an indicator of cell activity in the bacterial microcosms. 0.5 mL sample was placed in a 1.5 mL eppendorf tube before being diluted with 0.5 mL of 1 mol.L^{-1} Tris-EDTA buffer (pH 7.2). This was then heated to 90°C using a dry heat block for 15 minutes in order to lyse any cells present. To remove cell debris from solution, the sample was then centrifuged at 13,300g for 15 mins. A luciferin luciferase assay (Invitrogen ATP determination Kit) was then used to measure ATP concentration within the supernatant. Luciferin, extracted from fireflies, reacts with any ATP present in the sample to produce oxyluciferin, adenosine monophosphate (AMP) and a light photon via the following reaction:

$$Luciferin + ATP \rightarrow Luciferyl\ Adenylate + PP_i \quad (3.3)$$

$$Luciferyl\ Adenylate + O_2 \rightarrow Oxyluciferin + AMP + Light \quad (3.4)$$

If there is abundant luciferin, the higher the concentration of ATP, the greater the intensity of light emitted. Thus the intensity of light emitted directly relates to the concentration of ATP within the sample. The intensity of light given off by samples was measured using a Glomax 20/20 luminometer. Luciferin luciferase degrades with time and exposure to light, therefore a calibration curve was made every time a sample was tested and reagents were replaced regularly. Concentrations of 1 to 1000 nmol.L^{-1} of ATP were used to create the calibration curve. Blanks were prepared with DNA free water. The manufacturers guidelines for the ATP determination kit used in this study state that it is sensitive enough to detect as little as 0.1 picomole of ATP. Thus any readings less than this amount were discarded as null.

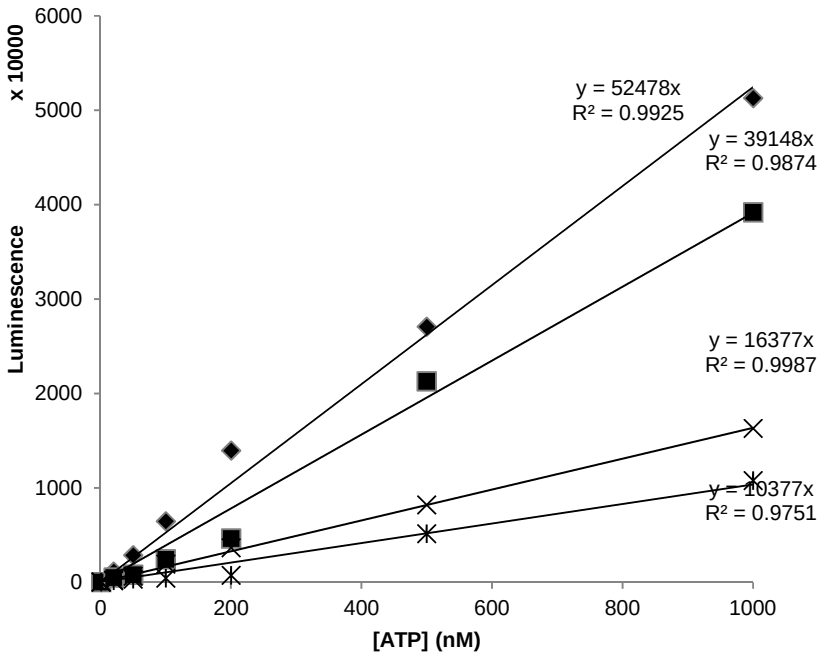

Figure 3.3: Example calibration chart used to convert the readings given from the luminometer into usable concentrations of ATP. A new chart was constructed every time the kit was used due to degradation of the reagents with time.

3.3.8 Cell Counting using an Improved Neubauer Haemocytometer

Cell counting was used to determine the number of cells within the anaerobic alkaline media and multiple samples were used to track the increase in cell numbers with time. An improved neubauer haemocytometer is a special microscope slide designed to help with the counting of cells. The slide has a machined stage in the middle that is lower than either side, allowing exactly 20 µL of water to be retained when a cover slip is placed on top. When viewed through a microscope, the lowered section of the slide has a square grid inscribed onto it allowing the number of cells contained within an aliquot of the liquid to be counted. As the specific volume of liquid above the grid is known, the amount of cells per unit volume can be calculated.

First an aliquot of media was removed from the microcosms using aseptic technique. 30 µL was then pipetted onto the central stage of the improved neubauer haemocytometer and a coverslip was carefully placed over the top. At this stage any excess media not retained by the coverslip flowed into

drainage changes machined around the central stage of the haemocytometer. Once mounted in the microscope the grid of the haemocytometer is then used to count the cells.

Starting from the top left of each square, cells are counted within that square. Any cells lying on the top and left lines of the square were counted, any bisecting the right and bottom lines were discounted. If the media contained >100 cells per square it was diluted an appropriate amount with deionised H_2O and recounted.

To calculate the amount of cells within the liquid the following equation is used:

$$\frac{Total\ cells\ counted\ \times\ dilution\ factor\ \times\ 4\ \times 10^8}{number\ of\ small\ squares\ counted\ \times\ filling\ depth} \qquad (3.5)$$

Cell counting was performed using an Olympus BH-2 microscope.

3.3.9 **Scanning Electron Microscopy**

Scanning electron microscopy (SEM) uses a highly focused and accelerated beam of electrons to produce images showing details as little as 1nm in size. The charged electrons are focused and fired at the sample, whereby they excite electrons within the surface. The kinetic energy of the electrons fired dislodges secondary electrons from within the sample that can be detected by the microscope to display the topology of the sample. SEM analysis was carried out using a FEI Quanta 650 FEG-ESEM.

Energy Dispersive X-ray (EDX) spectroscopy was used to characterise the elements and compounds present in the SEM samples tested. EDX measures x-ray emissions from materials when subject to the electron beam within an SEM. As the beams hits atoms within the sample, electrons from their inner sphere can be knocked out of place. This causes an electron from one of the atom's higher energy outer spheres to jump down to replace the electron that has been removed. The jump causes an x-ray emission that has the same energy as the difference in energy between the two electron shells. Each element has different energy gaps between their electron shells, thus the emitted x-rays energy can be measured and used to

characterise the atom it was released from. EDX can be used for spot analysis, to define the elements present in a single spot, or used for element mapping over larger areas. Typical detection limits are of the order of 100 to 200ppm (Bell and Garratt-Reed, 2003). Energy Dispersive X-ray spectra were collected with an Oxford X-max 80 SDD (liquid nitrogen free) EDS detector.

Zero valent iron samples were prepared for SEM by removing from the test liquor and drying by patting with a paper towel. The iron samples were then covered with a carbon coating in order to improve conductivity, before mounting in the machine. Blanks were prepared for SEM order to be able to compare results from the iron exposed to COPR and Cr(VI) solution with clean iron surfaces. Iron coupons were acid washed with 1 $mmol.L^{-1}$ HCl and cleaned with deoxygenated, deionised water. They were prepared just before analysis in order to minimise oxidation of the iron surface.

Bacterial precipitate was prepared for SEM by removing 2 mL liquor from each microcosm using aseptic technique and placing it in a clean 2 mL micro-centrifuge tube. The sample was then centrifuged at 13,300g for 5 mins to pellet the precipitate and the supernatant was removed. The precipitate was then suspended in 2 mL of diH_2O before being centrifuged again at 13,300g for 5mins. The supernatant was removed and the precipitate placed in a copper crucible and placed in the microscope. Environmental SEMs as used in this study are able to employ differential pumping of multiple chambers in order to allow samples to remain hydrated. Pumping of the upper electron column maintains a vacuum which the electron beam is fired through. An aperture allows the beam to descend into a lower chamber (where the sample is housed) which is kept at higher pressures than conventional SEMs. Whilst gaseous particles lower the intensity of the electron beam, the increased pressure of the lower chamber prevents the boiling of any water or hydrated phases within a sample allowing such phases to be imaged. All precipitate was imaged using this mode in order to prevent drying. The washing stage was required to remove solutes such as sodium carbonate which can precipitate when the sample is placed within the microscope, obscuring the iron crystals from view.

3.3.10 X-ray Photoelectron Spectroscopy

X-ray photoelectron spectroscopy (XPS) uses high powered x-rays, fired through a vacuum at a surface in order to evaluate elemental composition, chemical state and thickness of the surface. As the highly charged x-ray hits the sample surface, an electron is discharged into the vacuum at a specific kinetic energy that can be detected. The power of the x-ray used, directly affects the kinetic energy of the discharged electron, therefore the two are used to calculate the binding energy of the electron within the atom. The intensity of the electrons coming from the surface is measured and the results are plotted. Each element has a different electron binding energy, which can change due to the oxidation state and whether it is pure or part of a compound. Thus by comparing the binding energy of the sample to known standards, the type and oxidation state of any elements present can be determined. XPS machines are able to analyse an area of 0.2 to 1 mm in diameter to a depth of up to 50 Å. XPS is able to measure all atoms apart from H and He, requiring the presence of between 10^{13} to 10^{14} atoms in order to register as present (O'Connor et al., 2003).

All XPS analysis was performed at the Leeds EPSRC Nanoscience and Nanotechnology Facility in the School of Physics, using a VG Escalab 250 with a high intensity monochromated Al Kα source.

Samples were prepared for XPS by placing acid washed ZVI coupons in 1L of COPR leachate or chromate solution with minimal headspace. They were incubated for two months before taken out of the liquor and dried using a nitrogen gas stream and placed within the machine. Blanks were prepared for XPS in order to be able to compare results from the iron exposed to COPR and Cr(VI) solution with clean iron surfaces. Iron coupons were acid washed with 1 $mmol.L^{-1}$ HCl and cleaned with deoxygenated, deionised water and dried with a nitrogen air stream. They were prepared just before analysis in order to minimise oxidation of the iron surface.

3.3.11 X-ray Diffraction Spectroscopy

X-ray diffraction spectroscopy (XRD) is a technique that can be used to identify and characterise solid mineral and crystal phases within a material.

When X-rays are fired at a sample, electrons surrounding the atoms of the crystals diffract the X-rays causing them to take a different path. As crystals are generally a regular array of atoms, a regular array of secondary X-rays is emitted. Most of the X-rays cancel one another out, however at certain points, as determined by Bragg's law, the waves converge to produce a diffraction pattern:

$$2d \sin\theta = n\lambda \qquad (3.6)$$

Where d = the distance between diffracting planes, θ = the incidence angle, n = an integer and λ = the wavelength of the X-rays. The distance between the X-ray diffraction pattern is determined by the density of electron, thus the pattern given by a sample can be used to characterise the crystals present.

Aquifer material from the 19th century COPR site was analysed using a Phillips X'pert MPD pro diffractometer. The results given were analysed using X'pert highscore plus.

3.3.12 X-ray Florescence Spectroscopy

X-ray florescence spectroscopy (XRF) utilises the same principle as EDX. When bombarded with high energy short wave X-rays, electrons from the inner shell of an atom will be emitted from that shell. Electrons from outer shells will jump down to replace the emitted particle and in doing so will emit a photon of light equal to the energy difference between electron shells.

The aquifer material from the historic COPR site was analysed using an Innov-X X-5000 bench top XRF with Rh tube in both minor and major element modes.

3.3.13 DNA Extraction

Bacterial DNA was extracted from microcosm samples by using a 'FastDNA spin kit for soils' when there was a large amount of DNA available. 15 mL of sample was extracted using aseptic technique and placed in 15 mL centrifuge tubes. The tubes were then centrifuged for 15mins at 4000g to pellet any precipitate and cells. The pellet was then re-suspended in 978 µL

sodium phosphate buffer supplied within the FastDNA kit and the normal protocol for the kit applied.

When dealing with smaller amounts of DNA such as when sampling from a colony on an agar plate the following method was used, adapted from that used by (Corby et al., 2005). A plastic loop was used to scrape a colony off the agar plate, which was then placed in 50 µL of 50 mmol.L^{-1} TRIS-EDTA buffered to pH 7, with the addition of 0.5% Tween20. The sample was then incubated for 2 hours at 55°C and then 5 mins at 95°c using a dry heat block. The samples were removed from the heat and chilled on ice for 5 mins before being centrifuged at 13,300g for 10 seconds to separate the cell debris from the DNA in solution. The supernatant was transferred to a clean micro centrifuge tube ready for use.

3.3.14 Polymerase chain reactions

Polymerase chain reactions (PCR) are a way of amplifying a very small amount of a DNA into much larger, usable concentrations. It can take as little as one fragment of DNA and replicate into one of thousands or millions of replicates with the same sequence of base-pairs. PCR works by thermal cycling which melts and then rebuilds copy of DNA fragments with the help of enzymes. In order to select the area of DNA for replication, short strands of DNA called primers are used which complement the DNA in that area. PCR starts with an initial denaturation step which heats the DNA helix and melts the hydrogen bonds between each set of bases. Annealing follows where the primers are attached to the single strands of DNA and select the area of DNA to be replicated. Finally an extension phase synthesises a new DNA strand complementary to the existing strand via the use of enzyme polymerases. This process is cycled a number of times with each cycle yielding double the amount of DNA.

The PCR process is highly sensitive and can replicate one strand of DNA into millions. Thus there is a high risk of contamination from the human practising the technique or from environmental DNA in the workspace. Thus whenever a PCR was run, a blank was used to ensure that stray unwanted DNA had not contaminated the PCR mixture. For each blank, the sample was replaced with DNA free deionised water. After the PCR reaction had taken

place, the blank was run out on an TBE/agarose gel by electrophoresis and analysed with UV light. Any contamination would appear as a DNA band under UV light and therefore the other PCR reactions containing sample would be discarded.

3.3.15 **16s rRNA sequencing**

The 16S gene is ~1542bp long and is highly conserved between bacteria. However it contains hyper variable regions that make it ideal for the identification and comparison of bacterial species, and the creation of phylogenies. Amplification of 16S rRNA gene via PCR creates usable concentrations of DNA that can then be ligated and transformed into competent *E.coli* cells which can then be subsequently analysed to construct a sequence of the gene.

DNA was first extracted from the microcosms using the FastDNA method and from agar plates using the Tween20 method, both of which are described above. The DNA was stained with 6x loading dye and run out on a 1% w/v agarose/TBE gel with the addition of 1% ethidium bromide. DNA strands between 2000 to 20000 bp were cut from the gel and eluted in 30 µL solution via the use of a QIAquick gel extraction kit (Qiagen, Germany).

Differing PCR reaction mixtures and reaction conditions were used, dependent on the primers used. 1 µL of 5 $u.\mu L^{-1}$ GoTaq polymerase (Promega, USA) was mixed with 10 µL of 5x 'colourless' PCR reaction buffer (Promega, USA), 1 µL of 10 $mmol.L^{-1}$ Deoxynucleoside triphosphates (dNTPs, which contains 10 $mmol.L^{-1}$ of each deoxyribonucleotide (e.g. of dATP, dCTP, dGTP, and dTTP) to a total concentration of 40 $mmol.L^{-1}$), 1 µL of 25 $mmol.l^{-1}$ $MgCl_2$, and 29 µL ultrapure H_2O. 1.5 µL of 20 $\mu mol.L^{-1}$ 8f broad specificity primer (Eden et al., 1991) (5'-AGAGTTTGATCCTGGCTCAG-3') was added as well as either 1.5 µL of 20 $\mu mol.L^{-1}$ 1492r broad specificity primer (Weisburg et al., 1991) (5'-ACGGYTACCTTGTTACGA-3', where Y = C or T) or 1.5 µL of 20 $\mu mol.L^{-1}$ 1525r broad specificity primer (5'-AAGGAGGTGWTCCARCC-3' (Lane, 1991)). 5 µL of DNA sample was mixed with the PCR reagent, placed in a Mastercycler gradient thermal cycler, and subjected to the following thermal conditions. An initial denaturing phase of 95°C for 2 mins was followed by 30

cycles of 95°C for 45 secs to denature, 48°C for 1 min to anneal and 72°C for 2 mins to extend the DNA. A final extension was held at 72°C for 5 mins before cooling the mixture to 4°C post reaction.

When working with the 519r primer, the following PCR mixture and reaction conditions were used. 1 µL of 5 u.µL-1 GoTaq polymerase (Promega, USA) was mixed with 10 µL of 5x 'colourless' PCR reaction buffer (Promega, USA), 1 µL of 10 mmol.L-1 dNTPs and 30 µL ultrapure H_2O. 1.5 µL of 20 µmol.L^{-1} 8f broad specificity primer and 1.5 µL of 20 µmol.L^{-1} 519r broad specificity primer (5'-GWATTACCGCGGCKGCTG-3' where K = G or T, W = A or T (Lane et al., 1985)) were added as well as 5 µL of the DNA sample. The reaction conditions were 95°C for 2 mins to initial denature followed by 30 cycles of 95°C for 30 secs, 50°C for 30 secs, and 72°C for 45 secs. The final extension was held at 72°C for 7 mins before cooling to 4°C.

In all cases, the DNA was stained with 6x loading dye and run out on a 1% w/v agarose/TBE gel with the addition of 1% ethidium bromide and the band corresponding to 1500 bp cut out of the gel. A QIAquick gel extraction kit (Qiagen, Germany) was then used to elute the DNA into 30 µL solution.

3.3.16 Transformation and Cloning using *E.coli* Competent cells

Sequencing of mixed bacterial populations is often achieved by inserting a fragment of DNA from the original organism into a benign host (usually a strain of *E.coli*) which can then be grown to create a population of host bacteria, containing the original insert of DNA. This creates a population of clones which can then be used to identify the original DNA. The original DNA is usually ligated into a plasmid vector which is then transformed into *E.coli* competent cells. The vector includes a gene for antibiotic resistance, so those cells which do not incorporate a vector are killed once grown on ampicillin plates. The vector also includes the LacZ gene which causes the cell to take a blue colour upon growth. Upon successful ligation of the original DNA within the vector, this gene becomes interrupted, thus colonies without the blue colour are deemed to contain the successfully ligated plasmid and are suitable for sequencing.

The ~1500bp fragment of DNA, amplified via PCR, was ligated into the pGEM-T easy (Promega, USA) vector using the standard protocol. This vector was then transformed into XL1-Blue Competent Cells (Strategene, USA) via the recommended method.

LB Ampicillin agar plates were prepared by adding 10g NaCl, 10g tryptone, 5g yeast extract and 20g agar to 500 mL deionised H_2O before adjusting the pH to 7 with 5N NaOH. The liquor was then autoclaved to sterilise. Upon cooling to 55°C post sterilisation, 10 mL of 10 $mg.mL^{-1}$ filter sterilised ampicillin was added and then plates were poured to a depth of ≈ 5mm. Once cooled the plates were surface dressed with 100 µL of 10 $mmol.L^{-1}$ isopropyl-1-thio-β-D-galactopyranoside (IPTG) and 100 µL of 2% 5-bromo-4-chloro-3-inodlyl-β-D-galactopyranoside (X-gal) as required for the XL1-Blue colour screening. Transformed XL-1 Blue cells were spread onto the LB plates and incubated at 37°C for 24 hours. Single colonies which displayed a white colour indicating they had successfully incorporated the ligated vector were selected and re-streaked onto new plates to ensure isolate status. These streaked plates were then incubated for a further 24 hours at 37°C. Isolated colonies were then selected for analysis and stab inoculated onto 96-well LB-agar plates that contained ampicillin. The plates were sent to GATC Biotech LTD, (Germany) for sequencing.

3.3.17 Direct Sequencing using a PCR Product

When dealing with isolates, such as single colonies on an agar plate, cloning and sequencing using competent cells is not required. The 16s rRNA gene can be read directly from a PCR product. In these cases, once the PCR product had been extracted from within the electrophoresis gel, the concentration was measured using the Qubit method and sent directly to GATC Biotech, Germany for sequencing.

3.3.18 Analysis of Sequences and Construction of Phylogenic trees

Chimeras are an unwanted artefact created during the PCR process. They consist of two similar fragments of bacteria DNA which originate from different parent cells that have annealed to one another during the PCR process. This process creates a daughter chimera which although can look

like a true bacteria sequence, is an incorrect result and needs removing from the dataset before analysis. All sequence data was analysed using the Mallard (v1.02) chimera checker (Ashelford et al., 2006). Any sequences that were highlighted as being suspect were omitted from further analysis.

All non-chimeric sequences were classified using the Ribosomal Database Project (RDP) Classifier program (Cole et al., 2009) and then assigned to operational taxonomic units (OTUs) using the MOTHUR (v1.30.2) (Schloss et al., 2009) software, whilst employing a >98% nearest neighbour sequence similarity cut off. Representative sequences from each OTU were analysed using the Ribosomal Database Project (RDP) Seqmatch program (Cole et al., 2009) and closely related type strains were selected for use. Sequence data for the selected strains were recovered from the European Molecular Biology Laboratory, European Nucleotide Archive and *Bacillus Subtillus sp.* selected as a suitable out group for each phylogenic tree.

The selected sequences were aligned using ClustalX (v2.0) (Larkin et al., 2007) and a phylogenic tree created from the distance matrix via the neighbour joining method. Bootstrap analysis was performed on the tree using the same program with 2000 replicates in order to achieve over 95% reproducibility. The resulting file was inputted into Treeview (v1.6.6) (Page, 1996) which was used to create and edit the final phylogenic trees.

3.3.19 Measurement of DNA concentration

DNA concentration was determined using a Qubit 2.0 Fluorometer and the corresponding dsDNA high sensitivity assay (Invitrogen, USA). 2 µL DNA sample was tested using the standard protocol supplied with the kit.

3.3.20 Isolation and Quantification of Soluble Electron-Shuttling Compounds

The following was all conducted by Dr Duncan McMillan at the University Hospital Jena (Germany) along with help from his associates Marc Renz and Dr Martin Schmidt.

3.3.20.1 Isolation Purification of Soluble Electron-Shuttling Compounds

100 mL of culture was centrifuged at 9,000 x *g* for 15 min to separate cells from the growth medium. Culture supernatant was neutralized with HPLC-grade HCl to pH 7, and extracted with 100 mL of ethyl acetate. The bottom aqueous layer was discarded. The pooled organic phase was transferred into an acid-cleaned high-density polyethylene (HDPE) bottle and residual water was removed by drying over sodium sulphate (5 g) at 4°C overnight. The organic phase was then filtered through 0.45 µm polytetrafluoroethylene (PTFE) syringe filter (Sartorius) and dessicated using a rotary evaporator. The resulting residue was dissolved with MilliQ H_2O in an ultrasonic bath (Elma, Elmasonic S30).

A 10 mL column containing 8 g XAD-16 resin (Sigma) was pre-cleaned with 100 % methanol and rinsed thoroughly with deionised H_2O. The ethyl acetate soluble fraction extract was slowly transferred onto the column (XAD-16 is a non-ionic macroreticular resin is designed to adsorb small to medium MW organic substances from aqueous systems and polar solvents by hydrophobic and polar interactions). Compounds that bound to the resin were eluted sequentially with four bed volumes of 10%, 50% and 100% methanol (HPLC grade Merck). The 50% and 100% elutions were pooled and reduced to ~10 mL using a rotary evaporator at <30°C (previous work has shown that Flavins are retained in this fraction (McMillan et al., 2010)). This solution was then transferred to a 15 mL test tube and desiccated by speedvac (Savant SC210A). The resulting dark orange residue was resuspended in either 20 $mmol.L^{-1}$ 3-(*N*-morpholino)propanesulfonic acid (MOPS), 30 $mmol.L^{-1}$ Na_2SO_4 pH 7.4 or deionised H_2O for further spectroscopy, electrochemical assays and quantification.

As the AFe media contained a small amount of riboflavin it was important to differentiate between the flavin supplied by the media and that produced by the bacteria. Thus unused, autoclaved AFe media was used as a control and processed in exactly the same way as the actual samples in order to create a baseline of the riboflavin concentrations before bacteria growth had occurred.

Flavin quantification was performed by scanning wavelengths from 300 to 700 nm using a UV-2 UV/Vis spectrophotometer (Unicam). A standard curve was generated by observing known concentrations (0.05 µmol.L^{-1}, 0.125 µmol.L^{-1}, 0.25 µmol.L^{-1}, 0.5 µmol.L^{-1}, 1 µmol.L^{-1}) of riboflavin. An extinction coefficient at 455 nm (ε = 12,500 $cm^{-1}M^{-1}$) was used to quantify concentration (Otto et al., 1981).

3.3.20.2 Fluorescence Spectroscopy

Fluorescence spectra of purified culture supernatant were measured on a Quanta Master 30 (PTI/Photomed) fluorescence spectrometer using a 1 cm path length. Slit widths of 0.5 and 1.5 mm were used for excitation and emission wavelengths, respectively.

3.3.20.3 Electrochemical assays

Ultra-flat template-stripped gold (TSG) electrodes (surface area, A = 0.2 cm^2) were prepared and cleaned (see (Weiss et al., 2009) for details). Self-assembled monolayers (SAMs) were formed on electrodes by incubating them with 1 mmol.L^{-1} 8-mercaptooctanol in propanol for 16 hours. After rinsing with propanol and methanol, the electrodes were dried under a nitrogen gas flow and assembled in a bespoke glass electrochemical cell (Weiss et al., 2009). Voltammetry was conducted with a standard 3-electrode setup. A TSG working electrode was embedded in a PTFE holder with a rubber *O*-ring seal; a platinum wire counter electrode and a saturated silver/silver chloride electrode (Ag/AgCl) completed the circuit in the buffer volume (20 mmol.L^{-1} MOPS, 30 mmol.L^{-1} Na_2SO_4, pH 7.4) (McMillan et al., 2012). The electrochemical cell was surrounded by a steel mesh Faraday cage and operated inside an N_2 filled glovebox (MBraun MB 150 B-G) where the O_2 levels were <1 ppm. All solutions were purged with N_2 for 1 h and stored in the glovebox for at least 24 h before use. Electrochemical measurements were recorded at 21°C using an Autolab electrochemical analyser with a PGSTAT30 potentiostat, SCANGEN module and FRA2 frequency analyser (Ecochemie). Electrochemical impedance spectra were recorded for each SAM electrode prior to modification with flavin to control SAM quality. The electrodes were then incubated with approximately 0.1 µmol.L^{-1} flavin in 20 mmol.L^{-1} MOPS, 30 mmol.L^{-1} Na_2SO_4 pH 7.4 for 30 min.

The flavin-modified electrode was then washed 3 times with buffer solution to remove non surface-associated flavins.

Analogue cyclic voltammograms (CVs) were recorded by holding the potential at 0.2 V for 5 seconds before cycling at a scan rate (u) of 10 mV/s in the potential window from +200 mV to –600 mV (vs Ag/AgCl). Comparison of the CVs for SAM and flavin-modified electrodes indicate that a thin flavin layer remains bound to the electrode surface. The electroactive coverage of the flavin, Γ, was determined from the integration of the peak areas of the baseline-subtracted signals using SOAS software, available from Dr. C. Léger (Fourmond et al., 2009). The coverage is calculated from:

$$Q = nFA\Gamma \qquad (3.7)$$

Q is the total charge required for oxidation of the bound absorbate, F is the Faraday constant, and n is the number of electrons per flavin.

3.3.20.4 High performance liquid chromatography

For rapid discrimination of flavins a high performance liquid chromatography (HPLC) separation was used. The purified flavin, commercially available riboflavin (Sigma) and FMN (riboflavin-5′-phosphate; FLUKA, Buchs, Switzerland) were dissolved in water at a concentration of 10 µg.mL^{-1}. 10 µL samples (equivalent to 100 ng flavin) were injected into a HPLC system consisting of an online degasser DG-2080-53, a gradient former LG-1580-02, a PU-980 pump, an AS-1555 autosampler, a UV-975 UV-detector set at 420 nm (all from Jasco, Gross-Umstadt, Germany), and a RF-551 fluorescence-detector set at 450/520 nm (excitation/emission) (Shimadzu, Duisburg, Germany). Separations were performed at a flow-rate of 1 mL/min on a LiChrospher 100 RP-18e column (5 µm; 250 x 4 mm; Merck, Darmstadt, Germany) at 25°C. The solvent system consisted of water, 0.1 % trifluoroacetic acid (phase A) and acetonitrile (phase B) nominally applied as follows: 15 % B for 5 min, 15 % B to 50 % B in 2 min, 50 % B for 1 min, 50 % B to 15 % B in 1 min, and 15 % B for 4 min. Retention times (means ± SD, n = 3) of flavins in this solvent system were: 3.76 ± 0.01 min (FAD, riboflavin-5'-

diphosphate; which was present as a 6 % impurity in the FMN used), 4.64 ± 0.07 min (FMN), and 5.91 ± 0.03 min (riboflavin).

3.4 References

Alowitz, M. J. & Scherer, M. M. 2002. Kinetics of Nitrate, Nitrite, and Cr(VI) Reduction by Iron Metal. *Environ. Sci. Technol.,* 36**,** 299-306.

Ashelford, K. E., Chuzhanova, N. A., Fry, J. C., Jones, A. J. & Weightman, A. J. 2006. New Screening Software Shows that Most Recent Large 16S rRNA Gene Clone Libraries Contain Chimeras. *Appl. Environ. Microbiol.,* 72**,** 5734-5741.

Bell, D. & Garratt-Reed, A. 2003. *Energy Dispersive X-ray Analysis in the Electron Microscope*, Taylor & Francis.

British Standards Institute 1990. BS 1377-2: 1990 Methods of test for soils for civil engineering purposes. Classification tests.

Bruce, R. A., Achenbach, L. A. & Coates, J. D. 1999. Reduction of (per)chlorate by a novel organism isolated from paper mill waste. *Environ. Microbiol.,* 1**,** 319-329.

Brunauer, S., Emmett, P. H. & Teller, E. 1938. Adsorption of Gases in Multimolecular Layers. *J. ACS,* 60**,** 309-319.

Burke, I. T., Boothman, C., Lloyd, J. R., Livens, F. R., Charnock, J. M., McBeth, J. M., Mortimer, R. J. G. & Morris, K. 2006. Reoxidation Behavior of Technetium, Iron, and Sulfur in Estuarine Sediments. *Environ. Sci. Technol.,* 40**,** 3529-3535.

Chang, L.-Y. 2005. Chromate reduction in wastewater at different pH levels using thin iron wires—A laboratory study. *Environ. Prog.,* 24**,** 305-316.

Cole, J. R., Wang, Q., Cardenas, E., Fish, J., Chai, B., Farris, R. J., Kulam-Syed-Mohideen, A. S., McGarrell, D. M., Marsh, T., Garrity, G. M. & Tiedje, J. M. 2009. The Ribosomal Database Project: improved alignments and new tools for rRNA analysis. *Nucleic Acids Res.,* 37**,** D141-D145.

Corby, P. M., Lyons-Weiler, J., Bretz, W. A., Hart, T. C., Aas, J. A., Boumenna, T., Goss, J., Corby, A. L., Junior, H. M., Weyant, R. J. & Paster, B. J. 2005. Microbial Risk Indicators of Early Childhood Caries. *J. Clin. Microbiol.,* 43**,** 5753-5759.

Eary, L. E. & Rai, D. 1988. Chromate removal from aqueous wastes by reduction with ferrous ion. *Environ. Sci. Technol.,* 22**,** 972-977.

Eden, P. A., Schmidt, T. M., Blakemore, R. P. & Pace, N. R. 1991. Phylogenetic Analysis of Aquaspirillum magnetotacticum Using Polymerase Chain Reaction-Amplified 16S rRNA-Specific DNA. *Int. J. Syst. Bacteriol.,* 41**,** 324-325.

Fourmond, V., Hoke, K., Heering, H. A., Baffert, C., Leroux, F., Bertrand, P. & Léger, C. 2009. SOAS: A free program to analyze electrochemical data and other one-dimensional signals. *Bioelectrochemistry,* 76**,** 141-147.

Lane, D. J. 1991. 16S/23S rRNA sequencing. *In:* Goodfellow, E. S. M. (ed.) *Nucleic Acid Techniques in Bacterial Systematics.* Chichester: Wiley.

Lane, D. J., Pace, B., Olsen, G. J., Stahl, D. A., Sogin, M. L. & Pace, N. R. 1985. Rapid determination of 16S ribosomal RNA sequences for phylogenetic analyses. *Proceedings of the National Academy of Sciences,* 82**,** 6955-6959.

Larkin, M. A., Blackshields, G., Brown, N. P., Chenna, R., McGettigan, P. A., McWilliam, H., Valentin, F., Wallace, I. M., Wilm, A., Lopez, R., Thompson, J. D., Gibson, T. J. & Higgins, D. G. 2007. Clustal W and clustal X version 2.0. *Bioinformatics,* 23**,** 2947-2948.

Lovley, D. R. & Phillips, E. J. P. 1986. Availability of Ferric Iron for Microbial Reduction in Bottom Sediments of the Fresh-Water Tidal Potomac River. *Appl. Environ. Microbiol.,* 52**,** 751-757.

Lovley, D. R., Stolz, J. F., Nord, G. L. & Phillips, E. J. P. 1987. Anaerobic production of magnetite by a dissimilatory iron-reducing microorganism. *Nature,* 330**,** 252-254.

McMillan, D. G., Marritt, S. J., Butt, J. N. & Jeuken, L. J. 2012. Menaquinone-7 is specific cofactor in tetraheme quinol dehydrogenase CymA. *J. Biol. Chem.,* 287**,** 14215-25.

McMillan, D. G., Velasquez, I., Nunn, B. L., Goodlett, D. R., Hunter, K. A., Lamont, I., Sander, S. G. & Cook, G. M. 2010. Acquisition of iron by alkaliphilic bacillus species. *Appl. Environ. Microbiol.,* 76**,** 6955-61.

National Research Council 1974. *Chromium*, Committee on Biologic Effects of Atmospheric Pollutants - National Academy of Sciences.

O'Connor, J., Sexton, B. A. & Smart, R. S. C. 2003. *Surface Analysis Methods in Materials Science*, Springer.

Otto, M. K., Jayaram, M., Hamilton, R. M. & Delbruck, M. 1981. Replacement of riboflavin by an analogue in the blue-light photoreceptor of Phycomyces. *Proc. Natl. Acad. Sci. U.S.A.,* 78**,** 266-9.

Page, R. D. M. 1996. TreeView: An application to display phylogenetic trees on personal computers. *Comput. Appl. Biosci.,* 12**,** 357-358.

Schloss, P. D., Westcott, S. L., Ryabin, T., Hall, J. R., Hartmann, M., Hollister, E. B., Lesniewski, R. A., Oakley, B. B., Parks, D. H., Robinson, C. J., Sahl, J. W., Stres, B., Thallinger, G. G., Van Horn, D. J. & Weber, C. F. 2009. Introducing mothur: Open-Source, Platform-Independent, Community-Supported Software for Describing and Comparing Microbial Communities. *Appl. Environ. Microbiol.,* 75**,** 7537-7541.

Spencer, J. F. T. & de Spencer, A. L. R. 2004. *Environmental Microbiology: Methods and Protocols*, Humana Press.

Stewart, D. I., Burke, I. T., Hughes-Berry, D. V. & Whittleston, R. A. 2010. Microbially mediated chromate reduction in soil contaminated by highly alkaline leachate from chromium containing waste. *Ecol. Eng.,* 36**,** 211-221.

Stewart, D. I., Burke, I. T. & Mortimer, R. J. G. 2007. Stimulation of Microbially Mediated Chromate Reduction in Alkaline Soil-Water Systems. *Geomicrobiol. J.,* 24**,** 655 - 669.

USEPA 1992. SW-846 Manual: Method 7196a. Chromium hexavalent (colorimetric).

Viollier, E., Inglett, P. W., Hunter, K., Roychoudhury, A. N. & Van Cappellen, P. 2000. The ferrozine method revisited: Fe(II)/Fe(III) determination in natural waters. *Appl. Geochem.,* 15**,** 785-790.

Weisburg, W. G., Barns, S. M., Pelletier, D. A. & Lane, D. J. 1991. 16S ribosomal DNA amplification for phylogenetic study. *J. Bacteriol.,* 173**,** 697-703.

Weiss, S. A., Bushby, R. J., Evans, S. D., Henderson, P. J. & Jeuken, L. J. 2009. Characterization of cytochrome bo3 activity in a native-like surface-tethered membrane. *Biochem. J.,* 417**,** 555-60.

Whittleston, R. A. 2011. *Bioremediation of chromate in alkaline sediment-water systems.* PhD thesis, University of Leeds.

Whittleston, R. A., Stewart, D. I., Mortimer, R. J. G., Ashley, D. J. & Burke, I. T. 2011a. Effect of Microbially Induced Anoxia on Cr(VI) Mobility at a Site Contaminated with Hyperalkaline Residue from Chromite Ore Processing. *Geomicrobiol. J.,* 28**,** 68 - 82.

Whittleston, R. A., Stewart, D. I., Mortimer, R. J. G. & Burke, I. T. 2013. Enhancing microbial iron reduction in hyperalkaline, chromium contaminated sediments by pH amendment. *Appl. Geochem.,* 28**,** 135-144.

Whittleston, R. A., Stewart, D. I., Mortimer, R. J. G., Tilt, Z. C., Brown, A. P., Geraki, K. & Burke, I. T. 2011b. Chromate reduction in Fe(II)-containing soil affected by hyperalkaline leachate from chromite ore processing residue. *J. Hazard. Mater.,* 194**,** 15-23.

Chapter 4 **Chromate Reduction in Highly Alkaline Groundwater by Zero Valent Iron: Implications for its use in a permeable reactive barrier**

4.1 Abstract

It is not currently known if the widely used reaction of zero valent iron (ZVI) and Cr(VI) can be used in a permeable reactive barrier (PRB) to immobilise Cr leaching from hyper alkaline chromite ore processing residue (COPR). This chapter compares Cr(VI) removal from COPR leachate and chromate solution by ZVI at high pH. Cr(VI) removal occurs more rapidly from the chromate solution than from COPR leachate. The reaction is first order with respect to both [Cr(VI)] and the iron surface area, but iron surface reactivity is lost to the reaction. Buffering pH downwards produces little change in the removal rate or the specific capacity of iron until acidic conditions are reached. SEM and XPS analysis confirm that reaction products accumulate on the iron surface in both liquors, but that other surface precipitates also form in COPR leachate. Leachate from highly alkaline COPR contains Ca, Si and Al that precipitate on the iron surface and significantly reduce the specific capacity of iron to reduce Cr(VI). This chapter suggests that although Cr (VI) reduction by ZVI will occur at hyper alkaline pH, other solutes present in COPR leachate will limit the design life of a PRB.

4.2 Introduction

Chromium is widely used in the chemical and metal alloy industries (Y.T, 2000, Jacobs and Testa, 2005, Morales-Barrera and Cristiani-Urbina, 2008). Historically most chromium has been obtained by the “high-lime” process, in which the Cr(III) containing chromite ore is roasted with an alkali-carbonate and limestone to produce soluble Cr(VI), which is then extracted with water upon cooling (Burke, 1991, Darrie, 2001). Large volumes of chromium ore processing residues (COPR) are produced, (Darrie, 2001) that typically contains 2-7% chromium as a mixture of Cr(III) and Cr(VI) compounds (Geelhoed et al., 2002). Typical mineral phases include Calcite, Ettringite, Hydrogarnet and Brownmillerite, although the exact mineralogy depends on the initial processing mixture and whether constituents such as Brownmillerite have undergone hydration reactions post processing (Chrysochoou et al., 2010). Water in contact with high-lime COPR has a characteristically high pH of 11.5 to 12, (Geelhoed et al., 2002) and can contain up to 1.6 $mmol.L^{-1}$ Cr(VI) as chromate (Farmer et al., 2002). Until recently COPR has been used as a fill material for roads and other construction projects, (Burke, 1991, Geelhoed et al., 2002, Higgins et al., 1998) or was dumped in unlined tips (Breeze, 1973, Jeyasingh and Philip, 2005, Stewart et al., 2010, Stewart et al., 2007). As a result there are numerous sites around the world where water from COPR is contaminating the surrounding area with Cr(VI), which is a major concern as Cr(VI) is carcinogenic, mutagenic and toxic (Richard and Bourg, 1991, Fendorf, 1995). Removal of COPR waste by traditional “dig and dump” remediation strategies is not only financially costly due to the large volumes of waste involved, but also inadvisable due to the risk of forming Cr(VI) bearing dusts that are a confirmed human carcinogen through inhalation (USEPA, 1998). Thus remediation of COPR disposal sites will almost always involve two steps; placing a cover layer on the waste to prevent direct exposure and reduce rainwater infiltration, and treatment of any water that emerges from the waste.

A potentially cost-effective way to treat Cr(VI) contaminated groundwater is to construct a permeable reactive barrier (PRB) in the groundwater plume

downstream of the waste (Blowes et al., 2000, Gillham and O'Hannesin, 1994, Starr and Cherry, 1994). In a PRB the contaminant is removed from solution as the groundwater flows through in a high permeability treatment zone created in the ground. Elemental iron (usually called zero valent iron or ZVI) is a popular choice of reactive material where the contaminant can be treated by chemical reduction (Alowitz and Scherer, 2002, Cantrell et al., 1995). This is because iron oxidation is thermodynamically very favourable, and can be coupled to the reduction of a range of industrial contaminants. ZVI is relatively low cost material that can be readily supplied in a range of particle sizes to match the permeability requirements of a particular application. A similar approach for Cr(VI) contaminated groundwater currently under development is to inject nano sized iron particles directly into the ground in order to create a reactive zone (so-called nano zero valent iron, or nZVI, treatment) (Du et al., 2012, Chrysochoou et al., 2012). Much work has already been done to investigate the use of ZVI and nZVI to reduce Cr(VI) over the common environmental pH range of mildly acidic to moderately alkaline conditions (Du et al., 2012, Chrysochoou et al., 2012, Lee et al., 2003, Cantrell et al., 1995, Franco et al., 2009, Powell et al., 1995). In acidic conditions the reaction is relatively fast, but the rate of reaction is slower in neutral and mildly alkaline conditions (Chang, 2005).

The primary aim of this chapter was to extend understanding of the reaction between ZVI and Cr(VI) to the hyper alkaline conditions characteristic of COPR leachate. It reports on the rate of reaction between ZVI and Cr(VI) in hyper alkaline systems. It compares the behaviour of a simple chromate solution with that of high-lime COPR leachate. Scanning electron microscopy (SEM) and X-ray photo electron spectroscopy (XPS) on ZVI that has been exposed to each solution are presented. The effect of acidifying COPR leachate on ZVI reactivity is investigated, and the engineering implications for the use of ZVI in a PRB for highly alkaline COPR leachate are discussed.

4.3 Methods

Cr(VI) solution was made-up from analytical grade potassium chromate (K_2CrO_4) (Fisher Scientific UK Ltd) and deionised water that was deoxygenated by purging with N_2 for 30 minutes. The pH was adjusted with either HCl or NaOH. COPR leachate was obtained from a standpipe piezometer screened into COPR at a legacy COPR disposal site in the north of England (borehole 5; see (Whittleston et al., 2011) for details). The pH value of the COPR leachate was adjusted using HCl when required.

Iron metal fine filings were acid washed in 1 $mol.L^{-1}$ HCl for 30 minutes, rinsed three times with de-aerated, deionised water, and placed in 120 mL glass serum bottles (Wheaton Scientific, NJ, USA). Either chromate solution or COPR groundwater was added (100 mL), the head-space was purged with N_2, and the bottles were sealed. Solid solution ratios of 1 - 500 $g.L^{-1}$ were used. The bottles were kept at temperature 21 $\pm$ 1 °C. Periodically the bottles were sampled (2 mL) using nitrogen gas filled syringes and sterilised needles to maintain the oxygen free headspaces. Samples were centrifuged for three minutes at 12,000 g and the supernatant decanted for analysis

The particle size distribution of the iron filings was determined by dry sieving (BSI, 1990). The pH value was determined using a Corning pH meter 240 with electrodes calibrated using standard pH 7 and 10 buffer solutions. Aqueous Cr(VI) concentration was determined by the diphenylcarbazide method. Major element concentrations were determined on a Perkin Elmer 5300DV ICP-OES. Brunauer-Emmett-Teller (BET) analysis of the surface area of the ZVI granules was conducted using a Gemini V2365 system (Micromeritics Instrument Corp.) by the nitrogen adsorption method (Brunauer et al., 1938).

Iron coupons (approximately 20 x 10 x 2 mm) were washed in 1 $mol.L^{-1}$ HCl acid for 30 minutes with one set of coupons placed in a sealed 1 L bottles of COPR leachate and 1 $mmol.L^{-1}$ chromate solution with minimal headspace (the solid solution ratio in these bottle tests was approximately 1 $g.L^{-1}$ in order to minimise loss of Cr concentration with time). The iron coupons were exposed to the solutions for 2 months. Upon recovery coupons were rinsed in deionised water, dried by gentle patting with tissue paper, stored in dry

tissue paper for approximately one hour, and then mounted and carbon coated for scanning electron microscopy (SEM) analysis. A third set of acid washed iron coupons were prepared for SEM analysis without exposure to Cr(VI) solutions as controls. SEM analysis commenced 2.5 hours after sample recovery, and was carried out on a FEI Quanta 650 FEG-ESEM. Energy Dispersive X-ray spectra were collected with an Oxford X-max 80 SDD (liquid nitrogen free) EDS detector. Images were collected in secondary electron imaging mode.

A second set of iron coupons, prepared the same way, were analysed using X-ray photoelectron spectroscopy (XPS). These were removed from the test liquors 15 mins before analysis and were dried using a nitrogen airline. XPS analysis was performed on a VG Escalab 250 with a high intensity monochromated Al Kα source.

4.4 Results

4.4.1 **Materials Characterisation**

The particle size distribution of the iron filings was very uniform with 95% of the particles between 75 to 300 µm. Their specific surface area after acid washing, determined by B.E.T., was 0.28 $m^2.g^{-1}$. The COPR leachate had a pH of 12.3 and a Cr(VI) concentration of 994 $\mu mol.L^{-1}$. The chemical composition of the COPR leachate is reported in Table 4.1. The potassium chromate solution used for comparison with the COPR leachate was prepared with a pH of 12.0 and a Cr(VI) concentration of 1053 $\mu mol.L^{-1}$.

4.4.2 **Effect of Solid Solution Ratio on Cr(VI) Removal Rates**

Figure 4.1 shows the effect of ZVI on the aqueous Cr(VI) concentration in tests with chromate solution and COPR leachate at pH values of 12.0 ± 0.1 and 11.9 ± 0.2, respectively. Cr(VI) is removed from both solutions over time, with the time taken for complete Cr(VI) removal from solution increasing with decreasing solid to liquid ratio. In chromate solution, complete removal from the 50 $g.L^{-1}$ test was achieved within about 15 days, whereas in the

COPR leachate 92% removal had been achieved after 20 days. When the solid to liquid ratio was less than 50 $g.L^{-1}$, Cr(VI) removal was substantially incomplete after 20 days in both solutions. In all tests, the Cr(VI) removal rate was greatest at the start of the test and decreased steadily with time (the curves fitted to the data will be discussed later). At the same solid to liquid ratio Cr(VI) removal was slower in COPR leachate than in the chromate solution (for example aqueous Cr(VI) was undetectable after 48 hrs in the 500 $g.L^{-1}$ chromate solution test, whereas it took 72 hrs to reach the same point in the 500 $g.L^{-1}$ COPR leachate test).

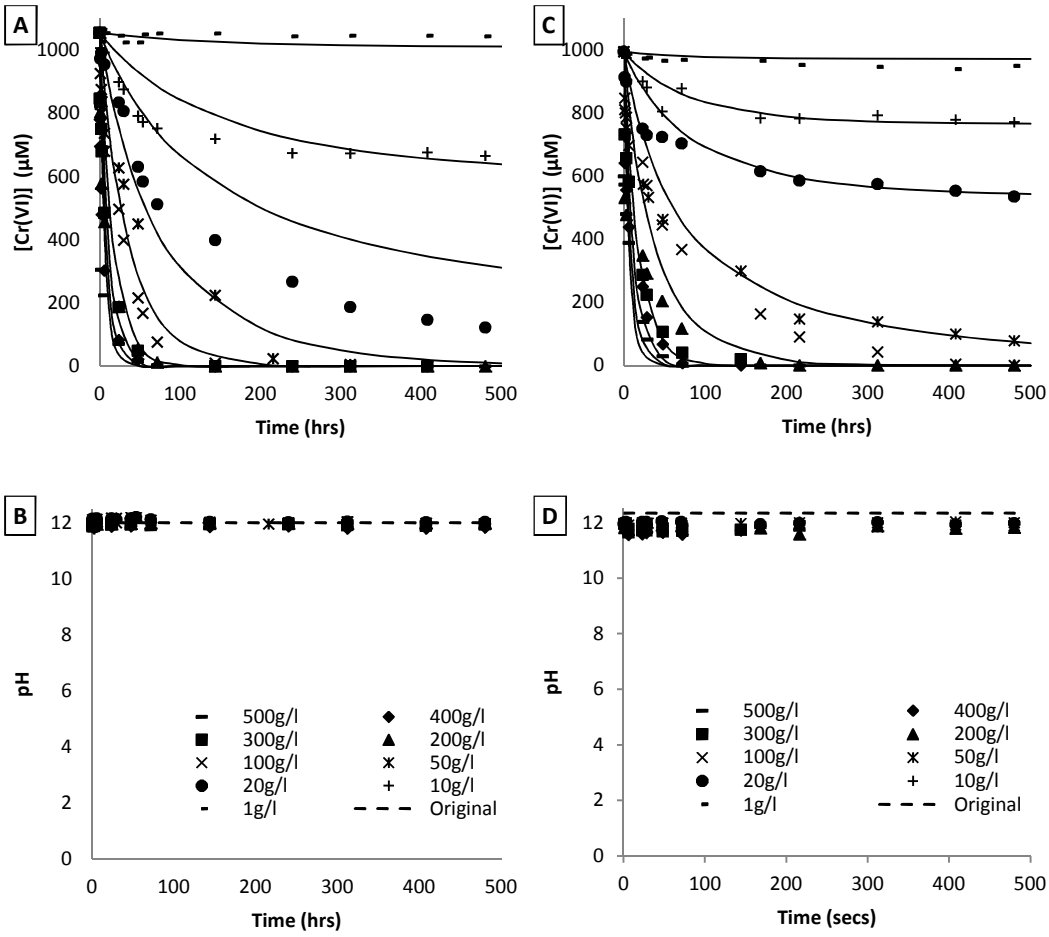

Figure 4.1: (A) Aqueous [Cr(VI)] vs. time for tests with different solid solution ratios in chromate solution. (B) pH vs. time for different solid solution ratios in chromate solution. (C) Aqueous [Cr(VI)] vs. time for tests with different solid solution ratios in COPR leachate. (D) pH vs. time for different solid solution ratios in COPR leachate.

For each test the instantaneous rate of aqueous Cr(VI) removal associated with each time point has been estimated by fitting a quadratic equation through the preceding, current and subsequent time points and differentiating that equation to determine the local gradient (data for time points where $[Cr(VI)]/[Cr(VI)]_o$ < 1% has been ignored). For the chromate solution tests there was an approximately linear relationship (r^2 > 0.91) between the logarithm of reaction rate and the logarithm of Cr(VI) concentration when the solid to liquid ratio was ≥ 100 $g.L^{-1}$. The average slope of the best-fit lines was 1.07 (standard deviation 0.16) indicating that the reaction is approximately first order with respect to the Cr(VI) concentration. There was also an approximately linear relationship (r^2 > 0.91) between the logarithm of reaction rate and the logarithm of Cr(VI) concentration for the COPR leachate tests when the solid to liquid ratio was ≥ 100 $g.L^{-1}$. The average slope the best-fit lines for these tests was 1.16 (with a standard deviation of 0.19) indicating that the reaction is again roughly first order with respect to the Cr(VI) concentration. The 50 $g.L^{-1}$ tests for both liquors also gave linear relationships that were roughly first order with respect to [Cr(VI)] although the data were more scattered (r^2 < 0.90). At solid solution ratios < 50 $g.L^{-1}$ the log of the reaction rate against the log of the gradient for the chromate solution gave only roughly linear relationships with lots of scatter (r^2 < 0.86) and slopes ≠ 1, indicating that all or part of these tests were not first order with respect to Cr(VI). Similarly the COPR leachate data for solid solutions of < 50g. L^{-1} showed scattered linear relationships (r^2 < 0.82) with slopes ≠ 1. If the reaction is first order with respect to [Cr(VI)] at solid solution ratios ≥ 100 $g.L^{-1}$ (i.e. α=1 in equation 2.8) the integrated rate equation will have the form:

$$[Cr\ (VI)] = \ [Cr\ (VI)]_o e^{-k_{obs}\, t} \quad [Cr(VI)] = \ [Cr(VI)]_o e^{-k_{obs} t}$$

(4.1)

Thus k_{obs} has been estimated by fitting an exponential line to the data, ignoring the data points where $[Cr(VI)]/\ [Cr(VI)]_o$ < 1% (see Figure 4.2). k_{obs} increased linearly with the solid to liquid ratio when removal was from COPR leachate (r^2 = 0.99, see Figure 4.3). k_{obs} increased approximately linearly with the solid to liquid ratio in simple chromate solution however there was much more scatter in the data (r^2= 0.79). That being the case, the rate

constant for the reaction of chromate solution with ZVI is approximately 50% higher than that for the reaction of COPR leachate with the same material. This was confirmed by running a t-test on the linear regressions applied to the data in Figure 4.3, which revealed a p-value of 0.049 indicating that the two data sets were significantly dissimilar. In those tests where the rate of Cr(VI) removal tended towards zero after 21 days without complete Cr(VI) removal from solution (solid to liquid ratios <50 $g.L^{-1}$), the amount of Cr(VI) removed from solution increases approximately linearly with the amount of iron present, with capacity of the iron in the chromate solution being about twice that in the COPR leachate (Figure 4.4). This was confirmed by a t-test p-value of 0.044 confirming that they were significantly dissimilar. Linear relationships between both the experimental rate constant (at high solid to liquid ratios), and the Cr(VI) reducing capacity (at low solid to liquid ratios), and the amount of iron present suggests that iron availability is the limiting factor for the reduction reaction.

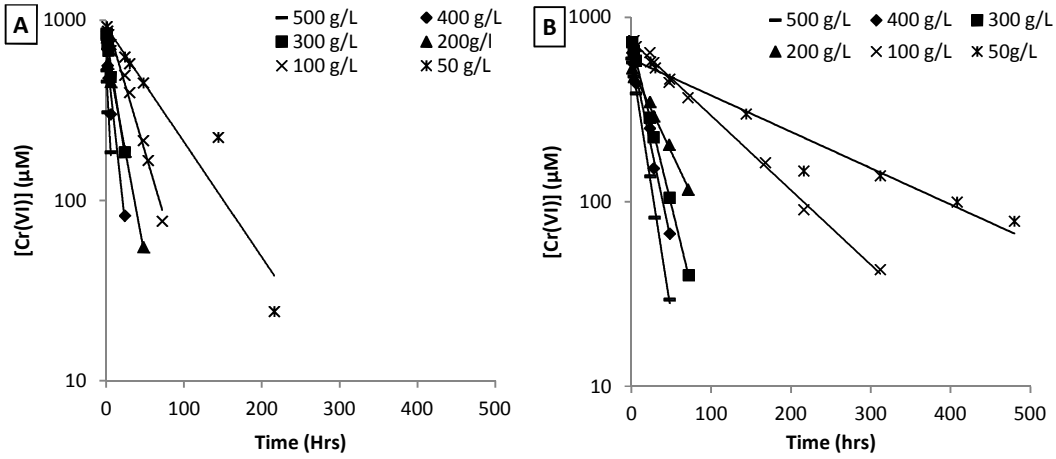

Figure 4.2: [Cr(VI)] vs. time for (A) 1mmol.L^{-1} chromate solution pH 12.0 ±0.1 and (B) 1mmol.L^{-1} COPR leachate pH 11.9 ± 0.2.

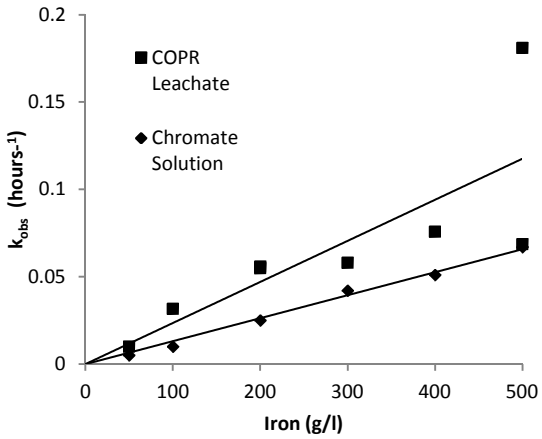

Figure 4.3: Variation in experimental 1st order rate constant, K_{obs}, with solid: liquid ratio (COPR leachate pH 11.9 ± 0.2, Chromate solution pH 12.0 ±0.1).

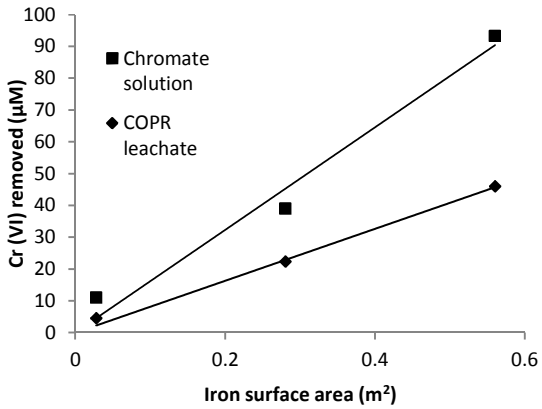

Figure 4.4: Variation in the Cr(VI) reduction capacity of the iron as a function of surface area for tests where the solid to liquid ratio <50 $g.L^{-1}$ (COPR leachate pH 11.9 ± 0.2, Chromate solution pH 12.0 ±0.1).

4.4.3 **Effect of Initial pH on Cr(VI) Removal Rates**

Figure 4.5 shows the removal of Cr(VI) from COPR leachate when the pH is lowered to different initial values. Tests were conducted with three solid to liquid ratios; 10, 20 and 100 $g.L^{-1}$. In all tests except those with an initial pH value of 12.0 (i.e. the unamended tests also shown in Figure 4.1), the pH value of the system buffered upwards with time. Typically the tests with higher solid to liquid ratios buffered to higher final pH values, and there is some evidence that buffering occurs more rapidly in these tests (although the data is not conclusive on this second point).

Cr(VI) was removed from solution at all initial pH values, at all three solid to liquid ratios, but only reached completion when the solid to liquid ratio was 100 $g.L^{-1}$ or the initial pH value was 2 (the 20 $g.L^{-1}$ test with an initial pH value of 4.0 was very close to completion after 20 days). The rate of reaction in the tests where the initial pH value was 2 was extremely high, and occurred before there was significant change in the pH value (the Cr(VI) concentration was below the detection limit after 6, 3 and 0.2 hours in the 10, 20 and 100 $g.L^{-1}$ tests, respectively). Otherwise Cr(VI) removal was contemporaneous with the change of pH.

When the solid to liquid ratio was 100 $g.L^{-1}$, Cr(VI) was completely removed from solution at a rate that generally increased with decreasing initial pH value, although tests with initial pH values of 10.0, 9.0, 8.0 and 6.0

responded in quite a similar manner, possibly because their pH values rapidly buffered to comparable values. In this test series then there was a roughly linear relationship (with one exception, $r^2 > 0.91$) between the logarithm of reaction rate and the logarithm of Cr(VI) concentration over the range $12.0 \geq pH \geq 4.0$ (in the pH2 tests the reaction was more than two orders of magnitude faster than in the other tests and, as a result, the kinetics were not accurately captured by the approach taken in this study). The average slope the best-fit lines was 1.12 (with a standard deviation of 0.13) indicating that the reaction is approximately first order with respect to the Cr(VI) concentration. k_{obs} values estimated by fitting an exponential line to the data (see Figure 4.6) are shown in Figure 4.7 as a function of pH (as the pH increased during these tests, the value when $[Cr(VI)]/[Cr(VI)]_0 = 50\%$ is plotted in Figure 4.7). The value of k_{obs} decreases from about 0.04 to 0.01 $hours^{-1}$ as initial pH increases from 4 to 12. A single trend-line has not been fitted to the data in Figure 4.7 as it is likely that the reaction mechanism will vary with the pH value due to changes in the reactants, for example chromate changing to hydrogen chromate or dichromate and Fe(II) becoming soluble at lower pH, however it is clear that the reaction rate is relatively insensitive to pH in the alkaline region (it decreases by a factor of two as the pH value increases from 7 to 12).

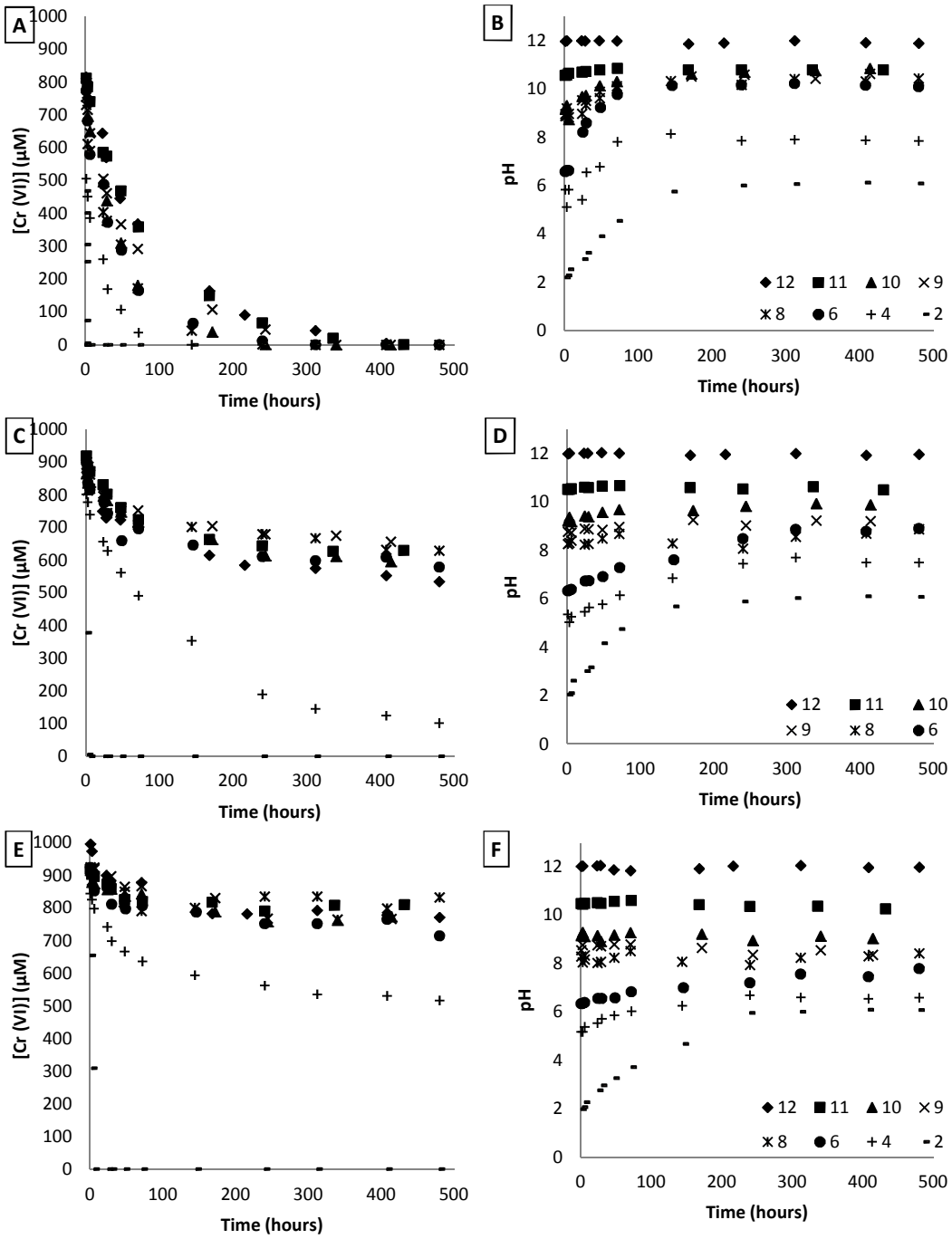

Figure 4.5: Variation of [Cr(VI)] and pH with time for COPR leachate lowered to different initial pH values: (A) and (B) solid solution ratio of 100 $g.L^{-1}$, (C) and (D) solid solution ratio of 20 $g.L^{-1}$, and (E) and (F) solid solution ratio of 10 $g.L^{-1}$.

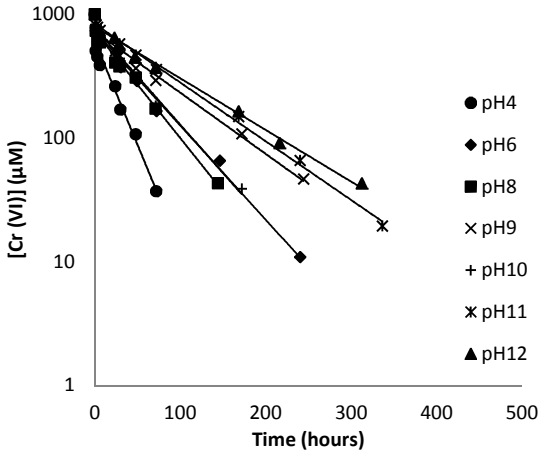

Figure 4.6: [Cr(VI)] vs. time for tests with 100 $g.L^{-1}$ ZVI in COPR leachate containing 1mmol.L^{-1} of Cr(VI) where the initial pH has been buffered to different values.

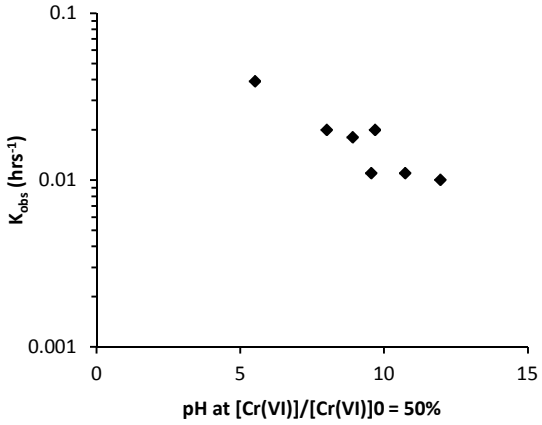

Figure 4.7: Variation in experimental rate constant K_{obs} with pH for COPR leachate when $[Cr(VI)]/[Cr(VI)]_o$ = 50%. ($[Cr(VI)]_0$ = 1mmol.L^{-1} ; 100 $g.L^{-1}$ iron).

4.4.4 **SEM Analysis of Cr-Reacted ZVI Coupons**

SEM images of an acid washed ZVI coupon and coupons exposed to K_2CrO_4 solution and COPR leachate (both containing ~1 mmol.L^{-1} of Cr(VI)) are shown in Figure 4.8. The unreacted sample was bright silvery grey in colour to the naked eye. Figure 4.8A shows a typical SEM image of the acid washed coupon and corresponding EDS spectra, which contained Fe peaks only. The coupons exposed to K_2CrO_4 solution were a uniform dull grey colour to the naked eye. Under the SEM the reacted surface was coated in a very thin speckled layer with EDS spot analysis containing weak Cr and O peaks in addition to prominent Fe peaks (Figure 4.8B). The iron coupons exposed to COPR were also a uniform dull grey colour upon recovery. High magnification SEM analysis revealed a variable surface coating that contained Cr, Ca, S, Al, Si and O in addition to Fe (Figure 4.8C). Lower magnification element maps (Figure 4.9) show three distinct types of surface coating were present, each with different combinations of the observed elements. Some regions considerably richer in Ca, Si and O show amorphous crystals, possibly a type of Calcium Silicate Hydrate, (Richardson, 2008) that form on top of the iron surface. Elongate prismatic crystals (approximately 5 x 1 x 1 μm) with Ca, S, Al and O-rich composition were also observed above the surface coating that have a morphology that is similar to ettringite (Myneni et al., 1998). Areas without any visible crystals had uniform EDS peaks of Cr, Fe and O, similar to those seen in the chromate solution. The area of the iron coupon that has been element mapped was selected because the three characteristic surface structures were in close proximity.

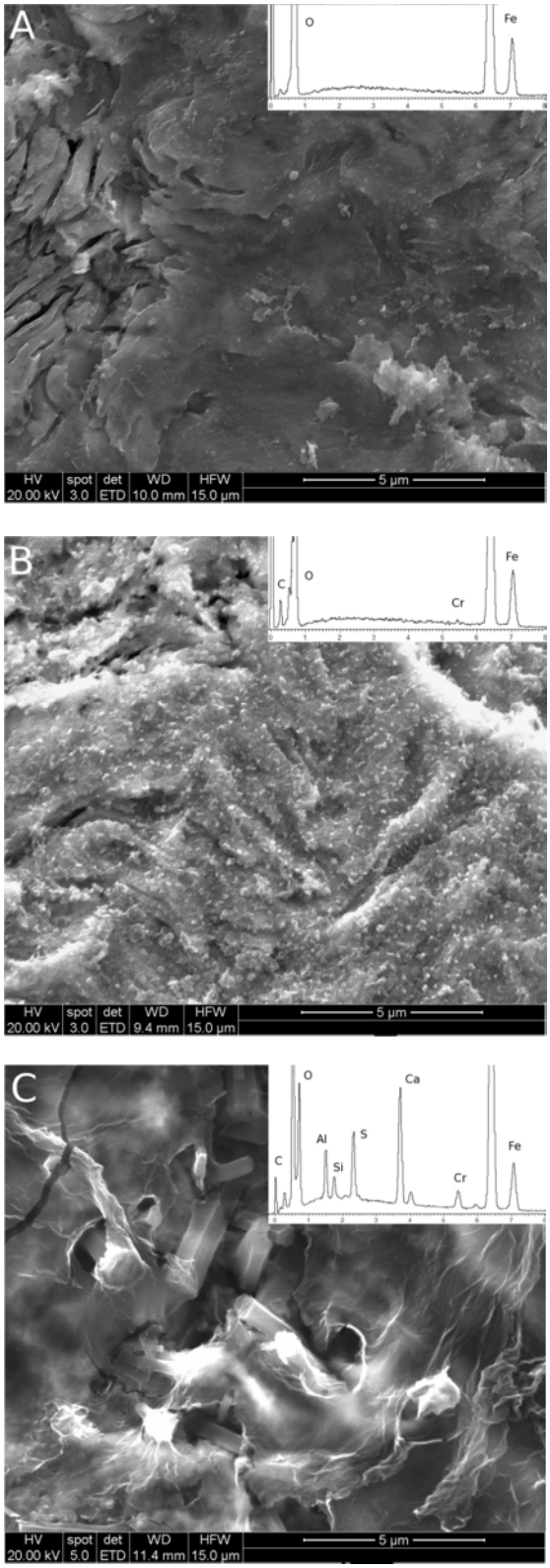

Figure 4.8: SEM images of Iron surfaces with corresponding EDS spectra inserts exposed to; (A) acid washed control specimen (B) 1 mmol.L^{-1}, pH12.0 Cr(VI) solution (C) 1 mmol.L^{-1}, ph 12.3, COPR leachate

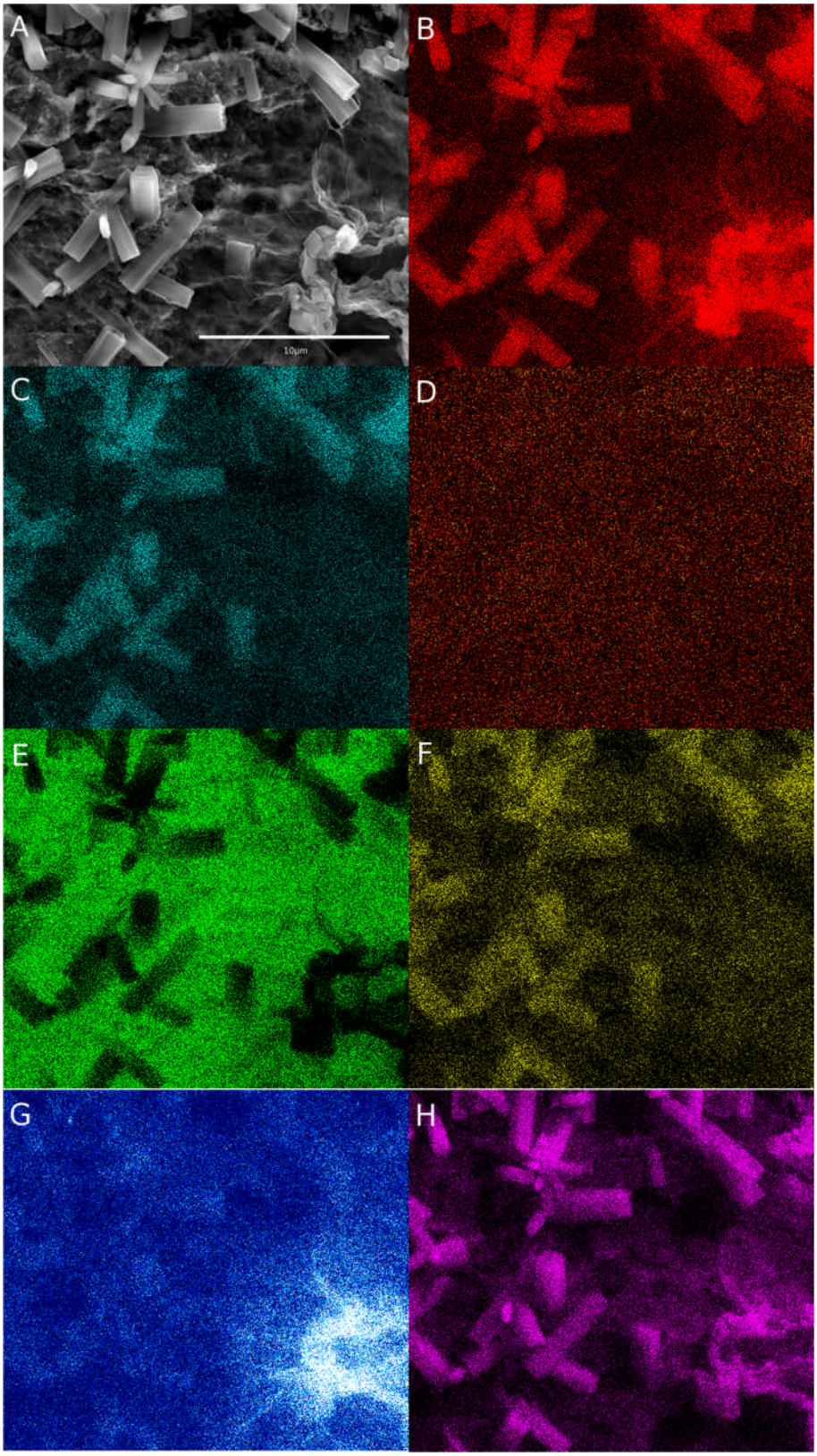

Figure 4.9: SEM image and EDS element mapping of an iron surface exposed to 1mmol.L^{-1}, pH 12.3 COPR leachate for 2 months. (A) Original SEM image, (B) Calcium, (C) Sulphur, (D) Chromium, (E) Iron, (F) Aluminium, (G) Silicon, (H) Oxygen.

4.4.5 **XPS Analysis of Cr(VI) Reacted Coupons**

XPS analysis of the coupon exposed to the chromate solution showed 85 ± 2% of the Cr present has a Cr 2p 3/2 peak with a binding energy of 577.2 eV (Figure 4.10); consistent with a number of Cr (III) hydroxides (Moulder and Chastain, 1995). The remaining 15 ± 2% of the Cr had a 2p 3/2 peak with a binding energy of 579.2 eV, indicating Cr (VI). Three Fe peaks with binding energies of 706.9, 711.1 and 713.3 eV were detected indicating the presence of elemental iron (5%) and two Fe (III) hydroxides (70% and 25%). There was a single O peak with a binding energy of 531.5 eV indicative of a hydroxide compound (Moulder and Chastain, 1995).

XPS analysis of the coupon exposed to the COPR groundwater showed Cr 2p 3/2 peaks with binding energies of 577.2 and 579.7 eV (Figure 4.10). Areas under the peaks indicated that 85 ± 2% was present as Cr (III) hydroxides, whereas 15 ± 2% was in the form of Cr (VI) (i.e. the same proportions as for the chromate solution). Fe peaks at 706.5 eV, 710.5 eV and 713.3 eV showed iron to be either elemental or one of two hydroxides. Oxygen had peaks at 531.5 and 529.7 eV showing that 90% was in the form of a hydroxide whereas 10% was in the form of an oxide (Moulder and Chastain, 1995).

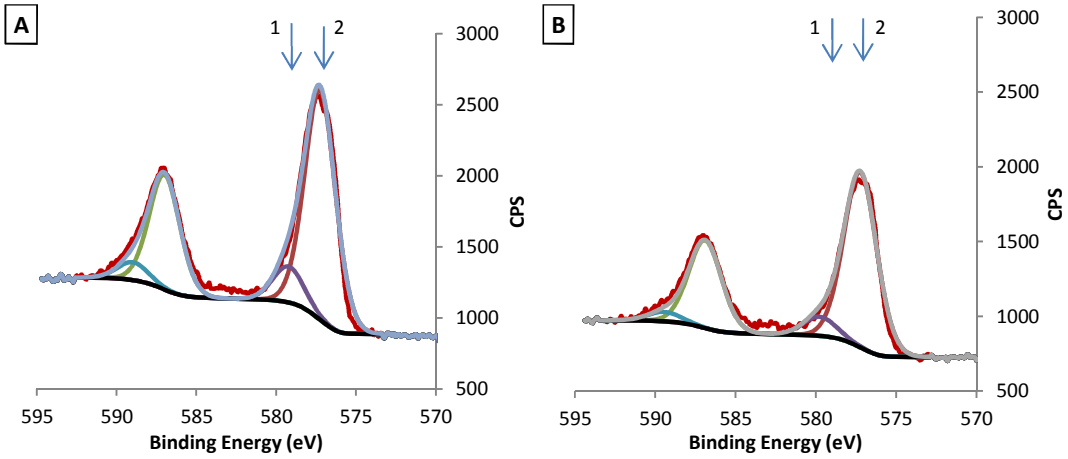

Figure 4.10: XPS Curves showing chromium peaks for an iron surface exposed to (A) 1mmol.L^{-1}, pH 12.0 chromate solution and (B) 1 mmol.L^{-1}, pH 12.3 COPR leachate, for 2 months. ↓ (1) shows expected 2p 3/2 peak position for Cr (VI) at 579eV, ↓ (2) shows expected 2p 3/2 peak position for Cr hydroxide at 577eV

4.5 Discussion

4.5.1 Kinetics of Cr(VI) Reduction by ZVI Under Hyper Alkaline Conditions

At pH 12 the experimental rate constant, k_{obs}, that is obtained by fitting a simple first-order rate equation (equation 4.1) to the data is directly proportional to the solid : solution ratio when that ratio is ≥ 50 g·L^{-1} (see Figure 4.3). This strongly suggests that the rate of reaction is proportional to the iron surface area, and thus involves a surface reaction. This is not surprising as iron species have very low solubility above pH9 (Langmuir, 1997); making a solution reaction unlikely.

The first step in any surface reaction is the sorption of the reactants onto the surface. In aqueous solution a hydroxylated film immediately forms on the surface of elemental iron (Muftikian et al., 1996, Fiedor et al., 1998). Some of these surface hydroxyls are exchangeable, and oxyanions, such as chromate, can form both monodentate surface complexes and biatomic-bidentate surface complexes where an oxygen is shared between the oxyanion and a surface iron atom (Grossl et al., 1997, Fendorf et al., 1997,

Singer et al., 2012). The net surface charge of a hydoxylated iron surface is pH dependant (protons readily exchange with the surface groups to produce $-OH^{2+}$, $-OH$, or $-O^{-}$ depending on pH (Fiedor et al., 1998). For most iron-containing minerals, the solution pH value that results in no net charge on the surface (i.e. the point of zero charge or pzc) is typically in the range of pH6 – 8 (Silva, 1995, Thorpe et al., 2012). Above the pzc, the net surface charge is negative, hindering the sorption of anionic species. Thus at pH 12 the amount of Cr(VI) retained by the surface by sorption is small,(Grossl et al., 1997) and probably localised to edge sites and surface deflects whose properties are less pH dependant. XPS analysis has confirmed that ≈15% of Cr associated with iron surfaces exposed to the hyperalkaline test liquors was the unreacted hexavalent form.

It has been widely reported that the removal of chromate from aqueous solution by elemental iron involves reduction of Cr(VI) to Cr(III) (Cantrell et al., 1995, Pratt et al., 1997, Wilkin et al., 2005). The precise mechanism whereby a sorbed metal ion is reduced on a hydroxylated iron surface is poorly understood, but it has been found that reduction of metals tends to occur preferentially at surface deflects, such as strained domain boundaries and cracks, that have intrinsically higher site reactivities (Singer et al., 2012). Reduction of Cr(VI) coupled to the oxidation of Fe(0) is thermodynamically favourable even at high pH (reaction 4), so provided sorption at these edge sites is not inhibited by high pH, chromate sorption should be followed by reduction of Cr(VI) to Cr(III). XPS data (Figure 4.10) that showed that ≈85 % of Cr present on the surface of the iron in both liquors tested is in the trivalent state, supports this theory.

Studies of the sorption and reduction of U(VI) on ZVI have shown that adsorption is significantly faster than the subsequent reduction step (Fiedor et al., 1998, Singer et al., 2012). Indeed most sorption studies investigating ZVI assume that sorption equilibrium is achieved in significantly less than 24hrs (Fendorf et al., 1997, Small et al., 1999). Thus the data Figure 4.1, which shows Cr(VI) removal over a period from about 2 to 20 days, strongly suggests that Cr(VI) sorption has time to reach equilibrium and that Cr(VI) reduction is the rate limiting step controlling the overall rate of Cr(VI) removal from solution. In such a system the rate at which individual sorbed species

react with a surface is not directly influenced by the bulk solution concentration, but the overall reaction rate is a function of surface coverage. Site-specific sorption that can be described by a Langmuir isotherm results in surface coverage that is directly proportional to the solution concentration when overall surface coverage is low (i.e. when a species weakly sorbs). Thus the overall rate equation is first order with respect to solution concentration.

When the solid to liquid ratio was less than 50 $g \cdot L^{-1}$ (see Figure 4.1), there was incomplete removal of Cr(VI) from solution, and the rate of reaction cannot be described by a simple first-order rate equation. After 20 days, when the continuing rate of reaction was very small, the amount of Cr(VI) that was removed from solution was proportional to amount of iron present. These low solid to liquid ratio tests suggest that an iron surface has a finite capacity for Cr(VI) reduction when the solution pH is high. SEM images of iron exposed to the chromate solution showed a speckled chromium-containing coating on the surface which the XPS data suggests is a mixed Fe(III) – Cr(III) hydroxide phase. It is therefore likely that the loss of reactivity is because the reaction products block the reactive sites on the iron surface. The problem with utilising a rate equation that is first order with respect to [Cr(VI)], such as equation 4.1, is that it implies that Cr(VI) reduction will go to completion regardless of the initial solid : solution ratio. If the reaction of Cr(VI) with ZVI is a surface reaction that is 1st order with respect to both [Cr(VI)] and surface area, A, then it would suggest a rate equation with the form:

$$\frac{d[Cr(VI)]}{dt} = - k_{12} [Cr(VI)] A \qquad (4.2)$$

Where k_{12} is the area-corrected rate constant at pH 12 and has the units of $m^{-2}.hrs^{-1}$. If the only reason that reactive surface area is lost is due to the surface reaction of Cr(VI) with Fe(0), the surface area can be described by an equation of the form:

$$A = A_0 - \frac{V}{B}([Cr(VI)]_0 - [Cr(VI)])$$

(4.3)

where A_0 is the initial reactive surface area (m^2), B is the specific capacity of the iron surface to reduce Cr(VI) ($mmol.m^{-2}$), and V is the volume of liquid in contact with the iron (it is implicit that $A \geq 0$). Thus:

$$\frac{d[Cr(VI)]}{dt} = -k_{12} \frac{A_0}{r} [Cr(VI)] \left(r - 1 + \frac{[Cr(VI)]}{[Cr(VI)]_0}\right)$$

(4.4)

Where $r = A_0B/C_0V$ is the "capacity ratio" of the system (i.e. the ratio of the amount of Cr(VI) that can be reduced to the amount of Cr(VI) present). Using substitutions $D = (r-1)C_0$ and $E = kA_0/(r.C_0)$ the equation simplifies to:

$$\frac{dC}{dt} = -E\ C\ (D + C)$$

(4.5)

Which, after variable separation can be integrated by use of partial fractions, provided $D \neq 0$:

$$\int \frac{dC}{C} - \int \frac{dC}{(D + C)} = -E\ D \int dt$$

(4.6)

Integration yields:

$$Ln\ C - Ln(D + C) = -EDt + constant$$

(4.7)

When $t = 0$, $C = C_0$:

$$\frac{C}{D + C} = \frac{C_0}{D + C_0} e^{-EDt}$$

(4.8)

Rearranging for C:

$$C = \frac{D\left(\frac{C_0}{D + C_0}\right) e^{-EDt}}{1 - \left(\frac{C_0}{D + C_0}\right) e^{-EDt}} \qquad (4.9)$$

Substituting for D:

$$\frac{C}{C_0} = \frac{(r-1)e^{-EDt}}{r - e^{-EDt}} \qquad (4.10)$$

Where ED= $kA_0(r-1)/r$:

$$\frac{C}{C_0} = \frac{(r-1)e^{-kA_0\left(\frac{r-1}{r}\right)t}}{r - e^{-kA_0\left(\frac{r-1}{r}\right)t}} \qquad (4.11)$$

Thus:

$$\frac{[Cr(VI)]}{[Cr(VI)]_0} = \frac{(r-1)e^{-k_{12}A_0\left(\frac{r-1}{r}\right)t}}{r - e^{-k_{12}A_0\left(\frac{r-1}{r}\right)t}} = \frac{(1-r)}{1 - re^{-k_{12}A_0\left(\frac{1-r}{r}\right)t}} \qquad (4.12)$$

This equation satisfies the boundary conditions that $[Cr(VI)] = [Cr(VI)]_0$ when $t = 0$, and that either $[Cr(VI)] \rightarrow 0$ as $t \rightarrow \infty$ when the capacity of the iron surface to reduce Cr(VI) exceeds the amount of Cr(VI) in solution (i.e. when $r > 1$), or that $[Cr(VI)] \rightarrow (1-r)[Cr(VI)]_0$ as $t \rightarrow \infty$ when the amount of Cr(VI) in solution exceeds the capacity of the iron surface to reduce Cr(VI) (i.e. when $r < 1$). Further when $r >> 1$, equation 4.12 simplifies to $[Cr(VI)]/[Cr(VI)]_0 \approx e^{-k12A_0t}$ (i.e. the variation of [Cr(VI)] with time can be described by a simple first order rate equation). Thus, at least qualitatively, equation 4.12 describes the observed behaviour of the system.

Equation 4.12 has been used to draw the curves shown in Figure 4.1A. The specific capacity of the iron surface to reduce Cr(VI) at pH 12 has been estimated from Figure 4.4 and the value of k_{12} estimated by correcting the

experimentally derived 1st order rate constants from the chromate solution tests with solid: solution ratios ≥ 100 $g.L^{-1}$ (reported in Figure 4.3) for A_0 and (r-1)/r. For solid solution ratios ≥ 100 $g.L^{-1}$ equation 4.5 yields curves that appear to be first order and fit the data well. Below 100$g.L^{-1}$ equation 4.12 predicts the general pattern of behavior quite well, with an initially rapid removal of Cr(VI) from solution tailing off as the tests progress, although the initial rate of reaction is greater than is predicted. The total amount of Cr(VI) removed from the 20 $g.L^{-1}$ test was also greater than predicted by equation 4.12. However, as small differences in the particle size distribution of the ZVI have disproportionately large effect on the surface area per unit weight of iron, the difference is not thought significant.

4.5.2 **The Effect of Solution Composition on Cr(VI) Reduction Rates**

Comparing data from Figures 4.1A and 4.1C reveals that for all solid solution ratios ≥100 $g.L^{-1}$, complete removal of Cr(VI) occurs more quickly from the chromate solution than the COPR leachate. Similarly for all solid solution ratios <100 $g.L^{-1}$ the amount of Cr(VI) removed was always greater from the chromate solution (Figure 4.4). XPS data from both testing solutions showed that ≈85% of Cr Present on the iron surface was in the form of a Cr(III) hydroxide, and that part of the Fe is present as Fe(III) hydroxide (O is also present as hydroxide). This suggests that Cr reduction results in precipitation of a mixed Fe(III)-Cr(III) hydroxide onto the iron surface which directly blocks the reaction site. SEM images of iron exposed to COPR leachate revealed that phases similar to ettringite and calcium silicate hydrate had been precipitated on a surface that was otherwise like the iron coupons exposed to a chromate solution. Thus it is believed that the reaction of Cr(VI) with the iron surface is not only inhibited by the reaction products from Cr(VI) reduction, but also by the reaction of other constituents of COPR leachate with the iron surface (SiO_3^- is reported to be an effective inhibitors of iron corrosion (Lehrman and Shuldener, 1952, Lahodny-Sarc and Kastelan, 1981)). As a result the iron surface has a lower capacity for Cr(VI) reduction.

It has been proposed that Cr(VI) reduction by elemental iron can be described by a two-step reaction: a fast sorption step that is in equilibrium, and a rate limiting reduction step. Where there is competition for reactive sites, it is reasonable to assume that there is a decrease in the number of reactive sites available for Cr(VI) sorption, but that the average time required to reduce a sorbed Cr(VI) molecule is unaffected. Equation 4.12 has therefore been used to produce the curves shown in Figure 4.1C by using a lower specific capacity for iron in contact with COPR leachate (estimated from Figure 4.4), but the same value for the area-corrected rate constant as used for modelling the behaviour in chromate solutions. For solid solution ratios ≤50 $g.L^{-1}$ the removal curves are a good fit to the data (see Figure 4.1C), accurately predicting the amount of Cr(VI) removed before the reaction ceases. For solid solution ratios >50$g.L^{-1}$ the curves slightly over predict the initial rate at which Cr(VI) is removed from solution and thus give a slightly optimistic evaluation of when total removal will occur. This approach implicitly assumes that the impact of competing ions on Cr sorption in the first step of the reaction mechanism can be determined from the decrease in Cr reduction capacity. In reality sorption equilibrium on reactive sites will reflect relative concentrations in solution, and thus will change over time if there are differences in the reaction rate of competing species. However the small differences between the model and data suggest the impact of this assumption is small, and thus is a reasonable engineering approximation for the system studied.

4.5.3 **The pH Dependence of Cr(VI) Reduction Rates**

Over the pH range 7 to 12, the rate of Cr(VI) removal from COPR leachate was relatively insensitive to the pH value. For the 100 $g.L^{-1}$ tests the first-order rate constant decreased by only a factor of 2 as the OH^- concentration increased by a factor of 10^5 (Figure 4.7). In the 20 and 10 $g.L^{-1}$ COPR leachate tests (where there was incomplete Cr(VI) removal) the specific capacity of the iron surface to remove Cr(VI) from solution did not vary significantly over this pH range. For Cr(VI) concentrations considered in this study the dominant Cr(VI) species in aqueous solution at pH values above

5.9 is the chromate anion ($Cr0_4^{2-}$), (Brito et al., 1997) and hydroxylated iron surfaces have a net negative surface charge in alkaline conditions, (Silva, 1995) restricting the sorption of anionic species to specific sites which remain available at high pH. Taken together the lack of pH sensitivity of both the rate of reaction and the specific capacity of the iron surface suggest that the Cr(VI) is removed from solution by the same reaction mechanism across the pH range 7-12. The slight pH sensitivity of the rate of reaction probably reflects the slight increases in the activation energy of the reaction as the pH increases (the reaction constant for an elementary reaction is a function of the increase Gibbs free energy that is required to form the reaction intermediate).

When the initial pH value was 4 the rate of Cr(VI) removal from COPR leachate was faster than in alkaline conditions (Figure 4.5). The first-order rate constant determined for the 100 $g.L^{-1}$ test (where there was complete Cr(VI) removal) was about twice the value at pH 7. The specific capacity of the iron determined in the 20 and 10 $g.L^{-1}$ tests (where there was incomplete Cr(VI) removal) was 2-3 times greater than that in the alkaline range. Cr(VI) removal in the tests that started with a pH value of 2 was too fast for the rate constant to be quantified accurately, but the rate was orders of magnitude greater than in the higher pH tests. Also there was complete Cr(VI) removal at all three a solid to liquid ratios. In the acidic pH range chromate will exist as either $Cr_2O_7^{2-}$, $HCrO_4^-$ or H_2CrO_4 (see Figure 2.3) meaning that the reaction between these and the ZVI will be slightly different in form. Similarly the iron surface will be dominated with sorbed H^+ ions, meaning that there will be a net positive charge across that surface. This means that the negatively charged Cr(VI) anions will be attracted to the iron surface meaning that the effects from adsorbtion reactions become important in the acidic pH range. As the rate of reaction was considerably faster in acidic conditions, as demonstrated by an increase in rate constants in Figure 4.7, it seems reasonable to infer that the reaction mechanism in acidic conditions is different from that in alkaline systems.

4.5.4 **Engineering Implications**

ZVI barriers have been deployed at several field sites where the groundwater pH is initially mildly alkaline without reported problems (Wilkin et al., 2003, Csovari, 2005). The data presented in this paper suggests that the use of ZVI to treat Cr(VI) contaminated groundwater could also be successful at more alkaline pH values provided the water does not contain solutes that compete with Cr(VI) for the reactive sites on the iron. As many soils contain silicates which become increasingly soluble above about pH 9.5, (Langmuir, 1997) this pH value may represent upper pH limit at which iron can be deployed in a conventionally designed PRB.

Solutes in COPR leachate slow the reaction of Cr(VI) with iron and significantly reduce the specific capacity of the iron surface. The implications for using iron as the reactive media within a PRB are that longer residence times will be required, and that effective barrier thickness will be lost more quickly due to passivation of the iron. Thus significantly thicker barriers will be required to treat COPR leachate than would otherwise be required with groundwater contaminated with Cr. There is probably no engineering reason why a thicker reactive zone should not be used within a PRB, but this will impact on the overall cost of the barrier, and may make such a solution uneconomic.

4.5.5 **Conclusions**

The rate at which Cr(VI) is removed from aqueous solution by reaction with elemental iron is independent of pH over the range 7 to 12. In this range the reaction is first order with respect to both [Cr(VI)] and the iron surface area. Iron surface reactivity is lost to the reaction, but the specific capacity of iron to reduce Cr(VI) is relatively independent of pH over the same range. As the reactive Cr(VI) species and the surface properties of iron do not vary significantly over this pH range, the pH independence of the reaction rate and specific capacity suggest that the reaction mechanism is the same from pH7 to pH12. Leachate from highly alkaline COPR contains solutes that significantly reduce the specific capacity of iron to reduce Cr(VI), probably because the solutes (e.g. silicate) compete with Cr(VI) for reactive sites on the iron.

4.6 References

Alowitz, M. J.; Scherer, M. M. Kinetics of nitrate, nitrite, and Cr(VI) reduction by iron metal. *Environ. Sci. Technol.* 2002, 36, (3), 299-306.

Blowes, D. W.; Ptacek, C. J.; Benner, S. G.; McRae, C. W. T.; Bennett, T. A.; Puls, R. W. Treatment of inorganic contaminants using permeable reactive barriers. *J. Contam. Hydrol.* 2000, 45, (1-2), 123-137

Brunauer, S.; Emmett, P. H.; Teller, E. Adsorption of Gases in Multimolecular Layers. *J. Am. Chem. Soc.* 1938, 60, (2), 309-319.

Breeze, V. G. Land Reclamation and River Pollution Problems in the Croal Valley Caused by Waste from Chromate Manufacture. *J. Appl. Ecol.* 1973, 10, (2), 513-525.

British Standards Institution., BS 1377-2:1990 Methods of test for soils for civil engineering purposes. Classification tests. BSI: London, 1990.

Brito, F.; Ascanio, J.; Mateo, S.; Hernández, C.; Araujo, L.; Gili, P.; Martín-Zarza, P.; Domínguez, S.; Mederos, A. Equilibria of chromate(VI) species in acid medium and ab initio studies of these species. *Polyhedron* 1997, 16, (21), 3835-3846.

Burke, T. Chromite Ore Processing Residuein Hudson County, New Jersey. Environ. *Health Perspect.* 1991, 92, 131-137.

Cantrell, K. J.; Kaplan, D. I.; Wietsma, T. W. Zero-Valent Iron For The In-situ Remediation Of Selected Metals In Groundwater. *J. Hazard. Mater.* 1995, 42, (2), 201-212.

Castle, J. E.; Mann, G. M. W. The mechanism of formation of a porous oxide film on steel. *Corros. Sci.* 1966, 6, (6), 253-262.

Chang, L.-Y. Chromate reduction in wastewater at different pH levels using thin iron wires—A laboratory study. *Environ. Prog.* 2005, 24, (3), 305-316.

Chrysochoou, M.; Johnston, C. P.; Dahal, G. A comparative evaluation of hexavalent chromium treatment in contaminated soil by calcium polysulfide and green-tea nanoscale zero-valent iron. *J. Hazard. Mater.* 2012, 201–202, (0), 33-42.

Chrysochoou, M.; Dermatas, D.; Grubb, D.; Moon, D.; Christodoulatos, C. Importance of Mineralogy in the Geoenvironmental Characterization and Treatment of Chromite Ore Processing Residue. *J. Geotech. Geoenviron. Eng.* 2010, 136, (3), 510-521.

Csovari, M., J. Csicsak, G. Folding and G. Simoncsics, Experimental iron barrier in Pecs, Hungary. In *Long-Term Performance Of Permeable Reactive Barriers;* Roehl, K. E., Meggyes, T., Simon, F. G., Stewart, D. I., Eds.; Elsevier: 2005;

Darrie, G. Commercial Extraction Technology and Process Waste Disposal in the Manufacture of Chromium chemicals From Ore. *Environ. Geochem. Health.* 2001, 23, 187-193.

Drissi, S. H.; Refait, P.; Abdelmoula, M.; Génin, J. M. R. The preparation and thermodynamic properties of Fe(II)/Fe(III) hydroxide-carbonate (green rust 1); Pourbaix diagram of iron in carbonate-containing aqueous media. *Corros. Sci.* 1995, 37, (12), 2025-2041.

Du, J.; Lu, J.; Wu, Q.; Jing, C. Reduction and immobilization of chromate in chromite ore processing residue with nanoscale zero-valent iron. *J. Hazard. Mater.* 2012, 215–216, (0), 152-158.

Evans, U. R.; Winterbottom, A. B. *Metallic corrosion, passivity and protection*. E. Arnold and co.: 1948.

Farmer, J. G.; Thomas, R. P.; Graham, M. C.; Geelhoed, J. S.; Lumsdon, D. G.; Paterson, E. Chromium speciation and fractionation in ground and surface waters in the vicinity of chromite ore processing residue disposal sites. *J. Environ. Monit.* 2002, 4, (2), 235-243.

Fendorf, S.; Eick, M. J.; Grossl, P.; Sparks, D. L. Arsenate and Chromate Retention Mechanisms on Goethite. 1. Surface Structure. *Environ. Sci. Technol.* 1997, 31, (2), 315-320.

Fendorf, S. E. Surface reactions of chromium in soils and waters. *Geoderma* 1995, 67, (1-2), 55-71.

Fiedor, J. N.; Bostick, W. D.; Jarabek, R. J.; Farrell, J. Understanding the Mechanism of Uranium Removal from Groundwater by Zero-Valent Iron Using X-ray Photoelectron Spectroscopy. *Environ. Sci. Technol.* 1998, 32, (10), 1466-1473.

Franco, D.; Da Silva, L.; Jardim, W. Reduction of Hexavalent Chromium in Soil and Ground Water Using Zero-Valent Iron Under Batch and Semi-Batch Conditions. *Water, Air, Soil Pollut.* 2009, 197, (1), 49-60.

Geelhoed, J. S.; Meeussen, J. C. L.; Hillier, S.; Lumsdon, D. G.; Thomas, R. P.; Farmer, J. G.; Paterson, E. Identification and geochemical modeling of processes controlling leaching of Cr(VI) and other major elements from chromite ore processing residue. *Geochim. Cosmochim. Acta* 2002, 66, (22), 3927-3942.

Gheju, M.; Iovi, A. Kinetics of hexavalent chromium reduction by scrap iron. *J. Hazard. Mater.* 2006, 135, (1-3), 66-73.

Gillham, R. W.; O'Hannesin, S. F. Enhanced Degradation of Halogenated Aliphatics by Zero-Valent Iron. *Ground Water* 1994, 32, (6), 958-967.

Gould, J. P. The kinetics of hexavalent chromium reduction by metallic iron. *Water Res.* 1982, 16, (6), 871-877.

Grossl, P. R.; Eick, M.; Sparks, D. L.; Goldberg, S.; Ainsworth, C. C. Arsenate and Chromate Retention Mechanisms on Goethite. 2. Kinetic Evaluation Using a Pressure-Jump Relaxation Technique. *Environ. Sci. Technol.* 1997, 31, (2), 321-326.

Higgins, T. E.; Halloran, A. R.; Dobbins, M. E.; Pittignano, A. J. In situ reduction of hexavalent chromium in alkaline soils enriched with chromite ore processing residue. *J. Air Waste Manage. Assoc.* 1998, 48, (11), 1100-1106.

Jacobs, J. A.; Testa, S. M. Overview of chromium (VI) in the environment: Background and history. In *Chromium (VI) handbook;* Guertin, E. J., Jacobs, J. A., Avakian C. P., Eds.; CRC Press: 2005

Jeyasingh, J.; Philip, L. Bioremediation of chromium contaminated soil: optimization of operating parameters under laboratory conditions. *J. Hazard. Mater.* 2005, 118, (1-3), 113-120.

Lahodny-Sarc, O.; Kastelan, L. The influence of pH on the inhibition of corrosion of iron and mild steel by sodium silicate. *Corros. Sci.* 1981, 21, (4), 265-271.

Langmuir, D. *Aqueous environmental geochemistry.* Prentice Hall: 1997.

Lee, T. R.; Wilkin, R. T. Iron hydroxy carbonate formation in zerovalent iron permeable reactive barriers: Characterization and evaluation of phase stability. *J. Contam. Hydrol.* 2010, 116, (1-4), 47-57.

Lee, T.; Lim, H.; Lee, Y.; Park, J.-W. Use of waste iron metal for removal of Cr(VI) from water. *Chemosphere* 2003, 53, (5), 479-485.

Lehrman, L.; Shuldener, H. L. Action of Sodium Silicate as a Corrosion Inhibitor in Water Piping. *Ind. Eng. Chem.* 1952, 44, (8), 1765-1769.

Matheson, L. J.; Tratnyek, P. G. Reductive Dehalogenation of Chlorinated Methanes by Iron Metal. Environ. *Sci. Technol.* 1994, 28, (12), 2045-2053.

Melitas, N.; Chuffe-Moscoso, O.; Farrell, J. Kinetics of Soluble Chromium Removal from Contaminated Water by Zerovalent Iron Media: Corrosion Inhibition and Passive Oxide Effects. *Environ. Sci. Technol.* 2001, 35, (19), 3948-3953.

Morales-Barrera, L.; Cristiani-Urbina, E. Hexavalent Chromium Removal by a Trichoderma inhamatum Fungal Strain Isolated from Tannery Effluent. *Water, Air, Soil Pollut.* 2008, 187, (1), 327-336.

Moulder, J. F.; Chastain, J. *Handbook of X-ray Photoelectron Spectroscopy: A Reference Book of Standard Spectra for Identification and Interpretation of XPS Data*. Physical Electronics: 1995.

Muftikian, R.; Nebesny, K.; Fernando, Q.; Korte, N. X-ray Photoelectron Spectra of the Palladium−Iron Bimetallic Surface Used for the Rapid Dechlorination of Chlorinated Organic Environmental Contaminants. *Environ. Sci. Technol.* 1996, 30, (12), 3593-3596.

Myneni, S. C. B.; Traina, S. J.; Logan, T. J. Ettringite solubility and geochemistry of the $Ca(OH)_2$–$Al_2(SO_4)_3$–H_2O system at 1 atm pressure and 298 K. *Chem. Geol.* 1998, 148, (1–2), 1-19.

Odziemkowski, M. S.; Schuhmacher, T. T.; Gillham, R. W.; Reardon, E. J. Mechanism of oxide film formation on iron in simulating groundwater solutions: Raman spectroscopic studies. *Corros. Sci.* 1998, 40, (2-3), 371-389.

Powell, R. M.; Puls, R. W.; Hightower, S. K.; Sabatini, D. A. Coupled Iron Corrosion and Chromate Reduction: Mechanisms for Subsurface Remediation. *Environ. Sci. Technol.* 1995, 29, (8), 1913-1922.

Pratt, A. R.; Blowes, D. W.; Ptacek, C. J. Products of Chromate Reduction on Proposed Subsurface Remediation Material. *Environ. Sci. Technol.* 1997, 31, (9), 2492-2498.

Qian, H.; Wu, Y.; Liu, Y.; Xu, X. Kinetics of hexavalent chromium reduction by iron metal. *Front. Environ. Sci. Eng. China* 2008, 2, (1), 51-56.

Richard, F. C.; Bourg, A. C. M. Aqueous geochemistry of chromium: A review. *Water Res.* 1991, 25, (7), 807-816.

Richardson, I. G. The calcium silicate hydrates. *Cem. Concr. Res.* 2008, 38, (2), 137-158.

Roh, Y.; Lee, S. Y.; Elless, M. P. Characterization of corrosion products in the permeable reactive barriers. *Environ. Geol. (Heidelberg, Ger.)* 2000, 40, (1/2), 184-194.

Silva, R. J. N., H. Actinide Environmental Chemistry. *Radiochim. Acta* 1995, 70/71, 377-396.

Singer, D. M.; Chatman, S. M.; Ilton, E. S.; Rosso, K. M.; Banfield, J. F.; Waychunas, G. A. Identification of Simultaneous U(VI) Sorption Complexes and U(IV) Nanoprecipitates on the Magnetite (111) Surface. *Environ. Sci. Technol.* 2012, 46, (7), 3811-3820.

Small, T. D.; Warren, L. A.; Roden, E. E.; Ferris, F. G. Sorption of Strontium by Bacteria, Fe(III) Oxide, and Bacteria−Fe(III) Oxide Composites. *Environ. Sci. Technol.* 1999, 33, (24), 4465-4470.

Starr, R. C.; Cherry, J. A. In Situ Remediation of Contaminated Ground Water: The Funnel-and-Gate System. *Ground Water* 1994, 32, (3), 465-476.

Stewart, D. I.; Burke, I. T.; Hughes-Berry, D. V.; Whittleston, R. A. Microbially mediated chromate reduction in soil contaminated by highly alkaline leachate from chromium containing waste. *Ecol. Eng.* 2010, 36, (2), 211-221.

Stewart, D. I.; Burke, I. T.; Mortimer, R. J. G. Stimulation of Microbially Mediated Chromate Reduction in Alkaline Soil-Water Systems. *Geomicrobiol. J.* 2007, 24, (7), 655 - 669.

Stumm, W.; Morgan, J. J. *Aquatic chemistry: chemical equilibria and rates in natural waters*. Wiley: 1996.

Thorpe, C. L.; Lloyd, J. R.; Law, G. T. W.; Burke, I. T.; Shaw, S.; Bryan, N. D.; Morris, K. Strontium sorption and precipitation behaviour during bioreduction in nitrate impacted sediments. *Chem. Geol.* 2012, 306–307, (0), 114-122.

USEPA, SW-846 Manual: Method 7196a. Chromium hexavalent (colorimetric). 1992.

USEPA, Toxicological Review of Hexavalent Chromium. 1998.

Wang, Y. T. Microbial reduction of chromate. In *Environmental microbe-metal interactions*; Lovley D. R. ASM Press: Washington, DC, 2000; pp 225-235.

Whittleston, R. A.; Stewart, D. I.; Mortimer, R. J. G.; Tilt, Z. C.; Brown, A. P.; Geraki, K.; Burke, I. T. Chromate reduction in Fe(II)-containing soil affected by hyperalkaline leachate from chromite ore processing residue. *J. Hazard. Mater.* 2011, 194, 15-23.

Wilkin, R. T.; Su, C.; Ford, R. G.; Paul, C. J. Chromium-Removal Processes during Groundwater Remediation by a Zerovalent Iron Permeable Reactive Barrier. *Environ. Sci. Technol.* 2005, 39, (12), 4599-4605.

Wilkin, R. T.; Puls, R. W.; Sewell, G. W. Long-Term Performance of Permeable Reactive Barriers Using Zero-Valent Iron: Geochemical and Microbiological Effects. *Ground Water* 2003, 41, (4), 493-503.

Chapter 5 **Extracellular electron transport mediated Fe(III) reduction by a community of alkaliphilic bacteria that use flavins as electron shuttles.**

5.1 Abstract

The biochemical and molecular mechanisms used by alkaliphilic bacterial communities to reduce metals in the environment are currently unknown. This chapter demonstrates that an alkaliphilic (pH > 9) consortium dominated by *Tissierella, Clostridium* and *Alkaliphilus* sp. are capable of using iron (Fe(III)) as a final electron acceptor under anaerobic conditions. This is important from a remediation standpoint as Fe(II) is able to reduce Cr(VI) abiotically Iron reduction is associated with the production of a freely diffusible species that upon rudimentary purification and subsequent spectroscopic, HPLC and electrochemical analysis has been identified as a flavin species displaying properties indistinguishable from riboflavin. Due to the link between iron reduction and the onset of flavin production, it is likely that riboflavin has an import role in extracellular metal reduction by this alkaliphilic community.

5.2 Introduction

Iron is the most abundant redox-active metal in soils (Stucki et al., 2007) with two oxidation states that are stable under the geochemical conditions found in soils: Fe(III) under relatively oxic conditions and Fe(II) under reducing conditions (Langmuir, 1997). Fe-reducing microorganisms can couple the oxidation of a wide variety of organic compounds to the reduction of Fe(III) to Fe(II) during dissimilative metabolism (Lovley, 2006). Due to the ubiquity of iron in the subsurface the oxidation of a significant portion of all organic matter in submerged soils and aquatic sediments is coupled to reduction of Fe(III) (Lovley, 2006). Numerous Fe-reducing microorganisms from a range of microbial taxa have been isolated from a broad range of environments (Roh et al., 2007, Pollock et al., 2007, Zavarzina et al., 2006). This is an important process when considering the use of a biobarrier for the treatment of highly alkaline COPR sites, as Fe(II) is highly effective at reducing Cr(VI) to Cr(III) (Eary and Rai, 1988, Fendorf and Li, 1996). Previous work has shown that increased concentrations of Fe(II) were present in a soil layer beneath a historic COPR site (Whittleston et al., 2011). This was accompanied by Cr(III) accumulation, suggesting that Fe(III) reducing bacteria were respiring and the resultant Fe(II) was reacting with soluble Cr(VI) abiotically. This finding, coupled with the fact that Fe(III) reduction is so prevalent within the natural environment suggests that it may be a significant bacterial process on a COPR site and thus investigating the iron reducing capability of bacteria hailing from such a site is necessary in order to fully understand the biological processes beneficial to a biobarrier.

During anaerobic respiration, bacteria transfer electrons from organic carbon to an electron acceptor that originates outside the cell and use the energy released from these coupled reactions to translocate protons from the cytoplasm to the periplasm (Madigan et al., 2003). This results in an electrochemical gradient (or electromotive force), composed of a membrane potential, $\Delta\Psi$, and a proton concentration gradient across the cytoplasmic membrane, which is used to drive bioenergetic processes such as solute transport and ATP synthesis via oxidative phosphorylation (Kim and Gadd,

2008). Some alkaliphilic bacteria can exploit the transmembrane electrochemical gradient that arises from a sodium concentration gradient to drive bioenergetic processes in conditions where it is challenging to maintain a proton gradient (Mulkidjanian et al., 2008). In aerobic conditions the electron acceptor is oxygen, however in anaerobic conditions, such as found in saturated soils, bacteria can use other electron acceptors, commonly fumarate, nitrate, arsenate, DMSO, Fe(III), Mn(IV), Cr(IV) V(V) oxides and various forms of other carbonaceous and sulfur-based compounds (Myers and Nealson, 1990, Nealson and Saffarini, 1994, Viamajala et al., 2002, Gralnick et al., 2006, Murphy and Saltikov, 2007, Carpentier et al., 2005, Burns and DiChristina, 2009, McMillan et al., 2012).

Bacteria often respire with electron acceptors that are passively transported into the periplasmic space. Such respiration involves a lipophilic proton/electron carrier commonly referred to as the quinone/quinol pool located in the cytoplasmic membrane, which transfers electrons to an inner-membrane bound, periplasm facing multi-heme *c*-type cytochrome (Richardson, 2000, McMillan et al., 2013). A number of different terminal reductases can then complete the membrane associated electron transport system (Schwalb et al., 2002, Schwalb et al., 2003, Ross et al., 2007, Gao et al., 2009, McMillan et al., 2013). In pH neutral and acidic environments, bacteria have also been shown to facilitate the transfer of electrons to various compounds that are outside the cell. During extracellular electron transport the inner-membrane bound *c*-type cytochrome is thought to transfer electrons to a series of other multi-heme cytochromes, and by that mechanism, across the periplasm and through the outer membrane (Field et al., 2000, Myers and Myers, 1992, Pitts et al., 2003, Clarke et al., 2008). It has been proposed multi-heme cytochromes then have a central role in electron transfer to metal oxides outside the cell and can be achieved by two mechanisms. The first is by direct attachment of the cell to the electron acceptor, such as metal oxides (Lovley, 2006), and has been elegantly demonstrated in the case of the Mtr complex where direct electron transfer was shown by Mtr contact with minerals (White et al., 2013). The second is by the production of soluble extracellular electron shuttles, such as flavins, which are released into the

immediate environment around the cell (Marsili et al., 2008, von Canstein et al., 2008, Coursolle et al., 2010, Newman and Kolter, 2000).

Electron-shuttling compounds are usually organic molecules external to the bacterial cells that can be reversibly oxidized and reduced. These compounds can thus carry electron carriers between bacterial cells and insoluble electron acceptors, enabling long-distance electron transfer (Watanabe et al., 2009). As the oxidation and reduction of electron-shuttling compounds are reversible, small catalytic amounts can undergo multiple reduction-oxidation cycles (Nevin and Lovley, 2002). Humic substances that contain quinone moieties were the first electron-shuttling compounds reported to stimulate Fe(III) oxide reduction (Lovley et al., 1996). To date it has been shown that *Shewanella* sp. and several methanotrophic bacteria can release flavins (i.e. flavin mononucleotide and riboflavin (von Canstein et al., 2008, Balasubramanian et al., 2010) as electron shuttles. As yet it is uncertain whether bacteria can also release quinone-like compounds as electron shuttles in response to a metabolic requirement (Myers and Myers, 2004), or whether this is an opportunistic use of substances found in the environment. Quinone groups in humic acids can act as electron shuttling compounds during the reductive dechlorination of chlorinated solvents, but the reduction rate is pH sensitive in the range 7.2 to 8.0 (Van der Zee and Cervantes, 2009). This was attributed to the varying ease of deprotonation of the redox active groups in the electron shuttling compounds. Further, humic substances contain several different functional groups, which can act as electron shuttling compounds in the range 6.6 - 8.0, and the pH value at which a particular type of functional group is active dependent on substituents neighbouring the redox centre (Ratasuk and Nanny, 2007).

Several species of bacteria have been shown to reduce Fe(III) in alkaline growth media over the pH range $9 \leq$ pH ≤ 11 (e.g. *Geoalkalibacter ferrihydriticus* (Zavarzina et al., 2006); *Alkaliphilus metalliredigens* (Ye et al., 2004); *Tindallia magadii* (Kevbrin et al., 1998); *Clostridium beirjerinckii* (Dobbin et al., 1999); *Anoxynatronum sibiricum* (Garnova et al., 2003); *Anaerobranca californiensis* (Gorlenko et al., 2004)). However, as yet, there is little detailed information on the mechanisms of how anaerobic bacteria

growing at high pH use iron as a final electron acceptor. Utilising iron is particularly challenging as most Fe(III) phases are relatively insoluble in this pH range (Langmuir, 1997). Indeed the amount of iron in aqueous solution is estimated to be approximately 10^{-23} mol.L^{-1} at pH 10 (McMillan et al., 2010). Thus it is speculated that the iron reduction mechanisms of alkaliphilic bacteria must be extremely efficient. Recently it has been shown that adding riboflavin to a community of alkaliphilic soil bacteria grown in-vitro at pH 10 increased the rate at which Fe(III) was reduced suggesting that members of the community might be able to use riboflavin as an electron shuttle in alkaline conditions (Williamson et al., 2013). However, as electron shuttle catalysed reactions are very pH sensitive (Van der Zee and Cervantes, 2009, Ratasuk and Nanny, 2007), it may not be appropriate to extrapolate what is known about the process from near neutral studies to high pH environments.

This chapter investigates the growth characteristics of a community of bacteria recovered from beneath a waste tip where highly alkaline chromium ore processing residue (COPR) has been dumped. It characterises the bacterial consortium that has become established after repeated growth in an alkaline Fe(III)-containing growth media. Growth of the bacterial consortium by iron reduction is linked to the production of a soluble species that was detected in the growth media. This species was isolated and characterised by spectroscopic and electrochemical analyses.

5.3 Methods

5.3.1 **Alkaline Fe(III)(AFe) Media**

The AFe media was made to the recipe described in chapter 3. Riboflavin spiked media was made by adding 3.76 x10^{-2} g.L^{-1} riboflavin to AFe media.

5.3.2 **Alkaliphilic Fe(III)-Reducing Bacterial Community**

A community of alkaliphilic anaerobic bacterial capable of Fe(III) reduction was cultured from soil taken from beneath a 19th Century COPR waste tip using the AFe media used in this study (see (Whittleston et al., 2011, Whittleston, 2011) for details). This community was grown on several times in AFe media, with subsequent bottles inoculated with 1% (v/v) of cell

suspension from a culture in the upper exponential phase of growth. Upper exponential growth was determined by colour change of the precipitate in the media from red to black.

5.3.3 **Growth Characterisation**

Bottles containing AFe media were inoculated with the alkaliphilic Fe(III) reducing bacterial community. The bottles were kept at a temperature of 21 ± 1 °C. Periodically they were sampled using needles and syringes and aseptic technique (Burke et al., 2006). The pH was measured using a HQ40d pH meter (Hach). Total Fe(II) was measured by using the ferrozine method and a Thermo Scientific BioMate 3 UV/VIS Spectrophotometer (Lovley and Phillips, 1986). The total amount of Adenosine Triphosphate (ATP) was determined using a Molecular Probes ATP Determination Kit (Life Technologies, USA). Cell counting was performed using an improved Neubauer haemocytometer on an Olympus BH-2 microscope.

5.3.4 **Growth of the Community with Alternative Electron Donors**

AFe Media was prepared with alternative electron donors and inoculated with 1 % (v/v) of cell suspension from a bacterial community grown on AFe media that was in the upper exponential phase of growth. The bottles were incubated for one week, and 1 % (v/v) was transferred into fresh media and grown on for a second week. Colour change of the media from red to black was taken to indicate iron reduction. Those that showed colour change were grown on into media containing no yeast extract and assessed for iron reduction after a further week.

5.3.5 **Bacteria growth on Plates**

AFe media was prepared with the addition of 20 $g.L^{-1}$ agar. After heat sterilisation at 120°C for 20 min, plates were poured keeping the agar media <1.5 mm thick. A cell suspension of the community in the upper exponential growth phase was diluted 100x using autoclaved AFe media and 100 µL spread onto the plates. The plates were stored in a sealed box, with an Anaerogen sachet (Oxoid Ltd, UK) to eliminate oxygen, at a temperature of 37˚C. After 2 weeks, single colonies were picked-off and re-streaked on new

plates which were then kept under the same conditions. Iron reduction was identified by areas of agar discolouring from red to clear.

5.3.6 DNA Extraction and Sequencing of the 16S rRNA Gene

DNA was extracted from the bacterial community growing in the AFe media as well as from colonies growing on agar plates. A 1.5 kb fragment of the 16s rRNA gene was amplified by Polymerase Chain Reaction (PCR) inserted into e.coli competent cells and sequenced.

The quality of gene sequences was evaluated (Ashelford et al., 2006), and putative chimeras were excluded from subsequent analyses. Sequences were grouped into operational taxonomic units (OTUs) (Schloss et al., 2009), and phylogenetic trees were constructed for representative sequences (Larkin et al., 2007, Page, 1996). Sequences were classified using the Ribosomal Database Project (RDP) naïve Bayesian Classifier (Wang et al., 2007). Sequences were submitted to the GenBank database (Genbank Numbers: KF362050-KF362117) (Wang et al., 2007).

5.3.7 Scanning Electron Microscopy (SEM)

Precipitate taken from a bottle of AFe media in the upper exponential phase of growth was transferred to a copper crucible and SEM analysis was performed using a FEI Quanta 650 FEG-ESEM. Energy Dispersive X-ray spectra were collected with an Oxford X-max 80 SDD (liquid nitrogen free) EDS detector and images were collected in secondary electron imaging mode.

5.3.8 Isolation and Quantification of Soluble Electron-Shuttling Compounds

Isolation of soluble electron shuttling compounds was achieved via the XAD-16 resin method detailed in chapter 3.

Flavin quantification was performed by scanning wavelengths from 300 to 700 nm using a UV-2 UV/Vis spectrophotometer (Unicam). An extinction coefficient at 455 nm (ε = 12,500 $cm^{-1}M^{-1}$) was used to quantify concentration (Otto et al., 1981).

5.3.8.1 Fluorescence Spectroscopy

Fluorescence spectra of purified culture supernatant were measured on a Quanta Master 30 (PTI/Photomed) fluorescence spectrometer using a 1 cm path length. Slit widths of 0.5 and 1.5 mm were used for excitation and emission wavelengths, respectively.

5.3.8.2 Electrochemical assays

Electrochemical measurements were recorded using an Autolab electrochemical analyser with a PGSTAT30 potentiostat, SCANGEN module and FRA2 frequency analyser (Ecochemie). Analogue cyclic voltammograms (CVs) were recorded by holding the potential at 0.2 V for 5 seconds before cycling at a scan rate (u) of 10 mV/s in the potential window from +200 mV to –600 mV (vs Ag/AgCl). Comparison of the CVs for SAM and flavin-modified electrodes indicate that a thin flavin layer remains bound to the electrode surface.

5.3.8.3 High performance liquid chromatography

For rapid discrimination of flavins a high performance liquid chromatography (HPLC) separation was used. 10 µL samples (equivalent to 100 ng flavin) were injected into a HPLC system consisting of an online degasser DG-2080-53, a gradient former LG-1580-02, a PU-980 pump, an AS-1555 autosampler, a UV-975 UV-detector set at 420 nm (all from Jasco, Gross-Umstadt, Germany), and a RF-551 fluorescence-detector set at 450/520 nm (excitation/emission) (Shimadzu, Duisburg, Germany).

5.4 Results

5.4.1 Bacteria growth characteristics

Growth of the community of alkaliphilic Fe(III)-reducing bacteria in alkaline Fe(III) containing (AFe) media was characterised by enumeration of cell numbers, ATP and total Fe(II) concentration in the media. Cell numbers, ATP and total Fe(II) showed the same trend. After initial inoculation, there was a lag phase where cells.L^{-1} stayed roughly constant for 72 hours, after which cell numbers exponentially increased to a peak of ~200 x 10^9 cells.L^{-1} at 168 hours (Figure 5.1*A*). Cell numbers stayed at similar levels until 500

hours when they started to slowly decrease. Negligible Fe(II) was recorded until 96 hours had elapsed then the concentration increased to a maximum of ~3500 µmol.L^{-1} at 216 hours (Figure 5.1*C*) and subsequently stayed relatively constant until 500 hours. After this time Fe(II) levels started to decrease (data after 600 hours not shown). Trace amounts of ATP were observed until 96 hours at which point the concentration exponentially increased to the maximum of 1-2 nmol.L^{-1} after 192 hours (Figure 5.1*D*). The pH was consistently 9.1 until 72 hours had elapsed when it started to decrease and reached a final value of 8.5 by ~360 hours (Figure 5.1*B*). The growth phase of the iron reducing culture was modelled using a logistic sigmoidal growth function (Zwietering et al., 1990);

$$y = \frac{A}{\left\{1 + exp\left[\frac{4\,\mu_m}{A}(\lambda - t) + 2\right]\right\}} \qquad (5.2)$$

Where A= average maximum cell numbers (cells.L^{-1}), μ_m = maximum specific growth rate (unit), λ= lag time (hours) and t = time (hours). This growth function was to fit the cell numbers in Figure 5.1*A* using A = 166.7 x 10^6 cells.L^{-1}, λ = 72 hours and μ_m = 0.6 x 10^6 cells.L^{-1}.h^{-1}. The same growth function was used to fit the total Fe(II) data for the population in AFe media in Figure 5.1*C* and Figure 5.8 using the average maximum amount of Fe(II) (3500 µmol.L^{-1}) for A, and a maximum specific reduction rate of 29 µM.h^{-1} for μ_m, and a lag time of 96 hours. The same function was fitted to the total Fe(II) data for the population in AFe + riboflavin media in Figure 5.8 with A = 3500 µmol.L^{-1}, λ = 48 hours and μ_m = 41 µmol.L^{-1}.h^{-1}.

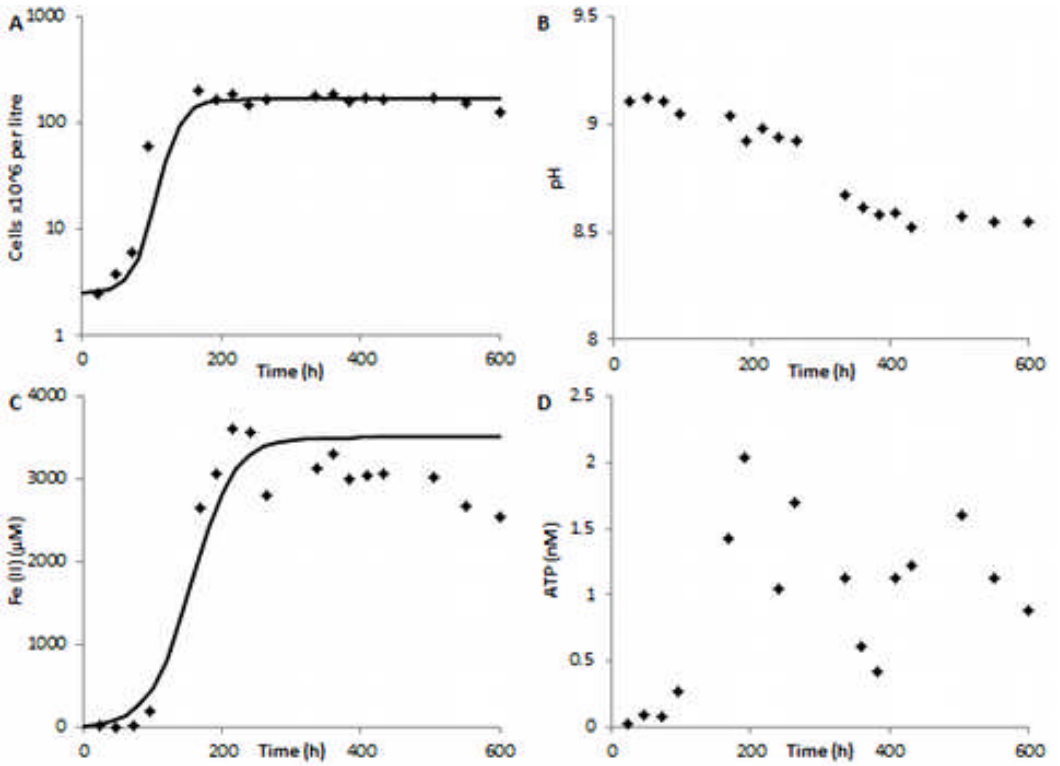

Figure 5.1: Growth of the iron reducing consortia in AFe media: Variation of (A): Cell numbers $x10^6.L^{-1}$ (B) pH, (C) Fe(II) ($\mu mol.L^{-1}$) and (D) ATP ($nmol.L^{-1}$) with time. Sigmoidal growth curves have been fitted to the cell count and Fe(II) data.

5.4.2 **Growth with Alternative Electron Donors**

Growth was observed in the majority of media containing an alternative electron donor after one week (Table 5.1). When inocula from these bottles were transferred into fresh media, only bottles where either sucrose or ethanol were the primary electron donor exhibited colour change after a further week of incubation. Transfer of inocula from the growth positive bottles to media containing either sucrose or ethanol (as appropriate) as the sole electron donor resulted in no colour change.

Electron Donor	Week 1	Week 2	Week 3
Acetate	++-	---	
Lactate	++-	---	
Ethanol	+++	+++	---
Methanol	++-	---	
Sucrose	+++	+++	---

Table 5.1: Iron reduction by the alkaliphilic bacterial community when grown on different electron donors (+/– indicates a positive and negative outcome in each replicate).

5.4.3 **Agar Plates and isolate Analysis**

Growth of 1 μL of the AFe media culture on agar plates resulted in small colourless colonies on the surface of the plate after 2 weeks. A lessening in the colour density of media/agar plates and the formation of very small dark particles in the agar was associated with colony growth (Figure 5.2). The colour change is due to reduction of aqueous Fe(III) in the AFe media and precipitation of Fe(II). SEM analysis of the spent AFe media (see below) suggests that the particles in the agar-AFe media were Vivianite crystals (hydrated Fe(II) phosphate). The reduction in colour density extended across wide areas of the plate, so individual colonies were picked off the plates with sterile toothpicks and streaked onto new plates. For about 25 % of these streaks there was a reduction in the colour density of media/agar in the immediate vicinity of the streak, which extended about 2mm beyond the boundary of the cell colonies. Colonies were randomly selected from these plates for rRNA gene sequence analysis.

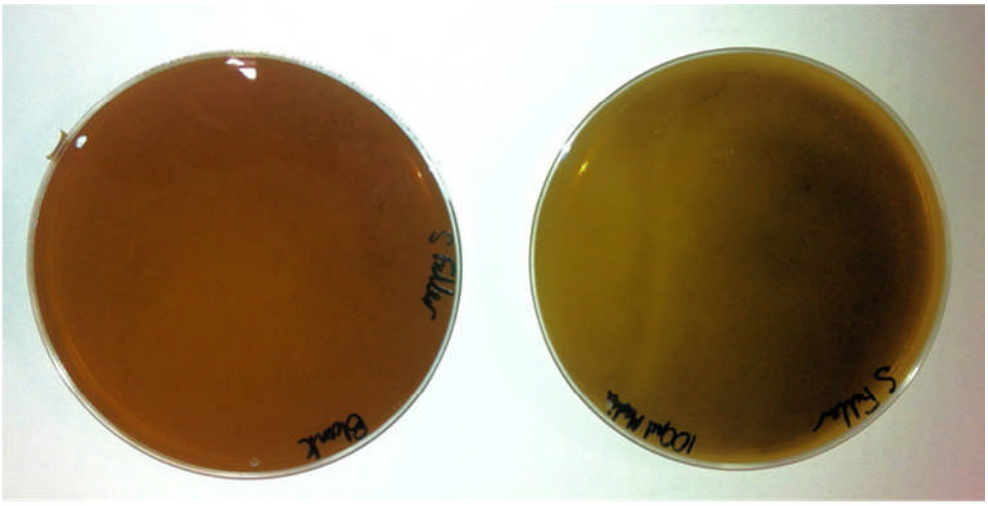

Figure 5.2: Anaerobic growth of the iron reducing consortia on AFe media-agar plates.

5.4.4 **Community analysis and Streak analysis**

The 16s rRNA gene sequences extracted from the AFe media show that all the bacteria within the consortium were from the order Clostridiales within the phylum Firmicutes. Analysis of the 59 sequences using the RDP Classifier (Cole et al., 2009) indicated that there were three genera represented; 40% of the sequences were *Tissierella* sp. 53% were *Clostridium* sp. and 7% were *Alkaliphilus* sp.). MOTHUR analysis further classified the sequences into 5 OTUs. The *Tissierella* genus contained three OTUs, of which representative samples were picked and analysed again using the RDP classifier. This showed two of the OTUs to be *Tissierella* sp. (from now on called *Tissierella* strain A and B) with a confidence threshold of 100% and the other, with a threshold of 87% (*Tissierella* strain C). The Clostridia and Alkaliphillus genera both contained one OTU with a confidence threshold of 100% (Figure 5.3). Representative sequences were selected from each OTU and a taxonomic tree showing their relationship with closely related type strain was constructed (Figure 5.4).

Direct PCR sequencing of bacteria grown on agar plates showed that the bacteria associated with a reduction in the colour density of media/agar (5 sequences) were all from the genus *Tissierella*. Comparative MOTHUR analysis of these sequences and those from the AFe media showed them to be all from the *Tissierella* strain C. The bacteria from the streaks where there was no change in the colour density of media/agar were much harder to isolate and sequence. Four sequences were characterised using the RDP classifier, two were from the genus Actinomyces, one from the genus Ochrobactrum, and the other was an unclassified Actinomycetaceae.

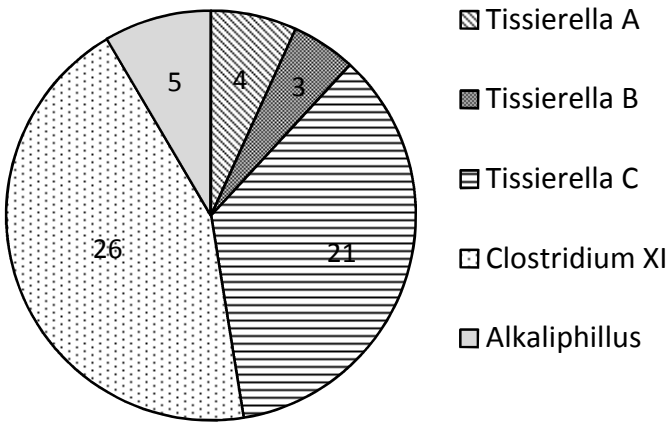

Figure 5.3: Microbial community grown on alkaline Fe(III) containing media; sequence allocation to Operation Taxonomic Units was determined by the MOTHUR program.

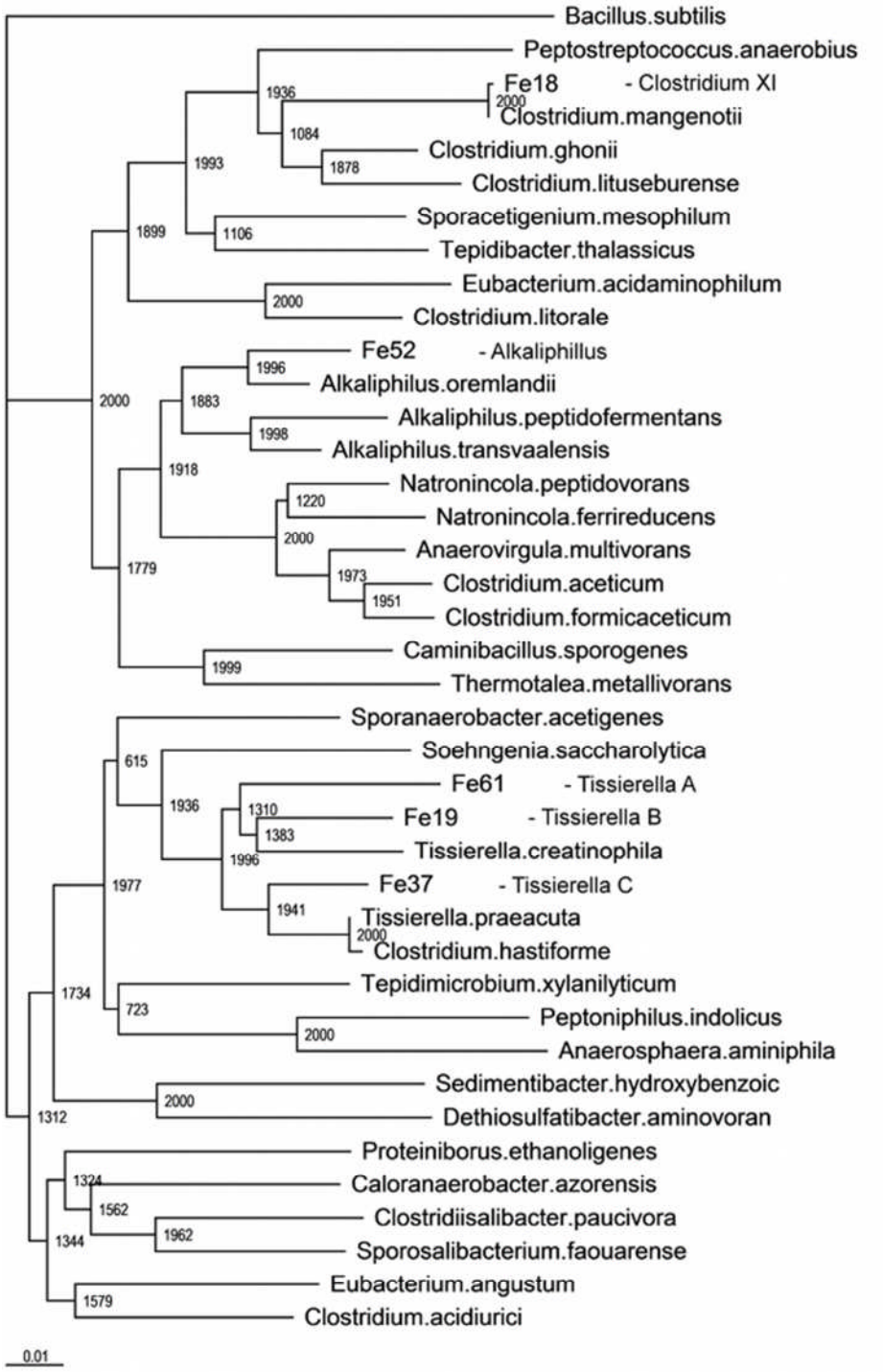

Figure 5.4: Taxonomic tree showing the relationships between representative sequences from each OTU and closley related type strains (the scale bar corresponds to 0.01 nucleotide substitutions per site and bootstrap values from 2000 replications are shown at branch points).

5.4.5 **Analysis for of Soluble Electron-Shuttling Compounds**

To investigate whether a soluble electron shuttling compound was involved in Fe(III) by the consortium, the spectral properties of spent media were studied at four stages of growth. Time points at 24, 72, 168 and 336 h (1, 3, 7 and 14 days) were examined for optical signatures indicative of quinones or flavins (unused AFe media was used as the control). Scanning the culture supernatants over a wavelength range 200 to 700 nm revealed spectral features that increased in amplitude with the age of the culture that is compatible with accumulation of flavinoids in the media (Figure 5.5*A*). The extracts from XAD-column purification exhibited spectral features (Figure 5.5*B*) indistinguishable from those exhibited by commercially available riboflavin (Posadaz et al., 2000) (the extract from the unused media produced no detectable peaks). Upon excitation at 441 nm, the XAD-column extract exhibited a broad emission peak between 475 and 650 nm in its fluorescence spectra with a maximum at 517 nm (Figure 5.5*D*). This feature, exhibited by commercially available riboflavin (also shown in Figure 5.5*D*), is diagnostic for the isoalloxazine ring structure in flavin species (Harbury and Foley, 1958). To corroborate these findings with the Fe(II)-dependent growth of the culture, the amount of flavin produced at each stage of growth was compared to Fe(II) accumulation in the culture medium. Interestingly, there is a direct correlation between the appearance of flavin and generation of Fe(II) during the growth phrase of the bacterial consortium (Figure 5.5*C*).

Cyclic voltammetry (Figure 5.6*A*) revealed that the surface immobilized XAD-column extract is capable of transferring electrons to and from a metal species, with oxidation and reduction peak potentials of -0.18 mV and -0.25 mV vs. SHE respectively. Furthermore, the electrochemical profile of the column extract is very similar to that obtained from commercially available pure riboflavin. Once the peaks were baseline corrected to remove any slope bias from the scans (Figure 5.6*B*), it was revealed that the electrochemical coverage and peak potentials of the column extract were almost identical to those of commercially available riboflavin (Figure 5.6*A* and 5.6*B*). Thus both the surface adsorption and packing characteristics of the column extract are indistinguishable from riboflavin.

However, the spectral, fluorescence and electrochemical properties investigated here are common to FAD, FMN and riboflavin, so to further discern the identity of the flavin species HPLC spectroscopy was performed. HPLC analysis of the surface immobilized XAD-column extract revealed a single peak which, when compared to commercially available riboflavin, FMN and FAD eluted at the same retention volume as riboflavin (Figure 5.7).

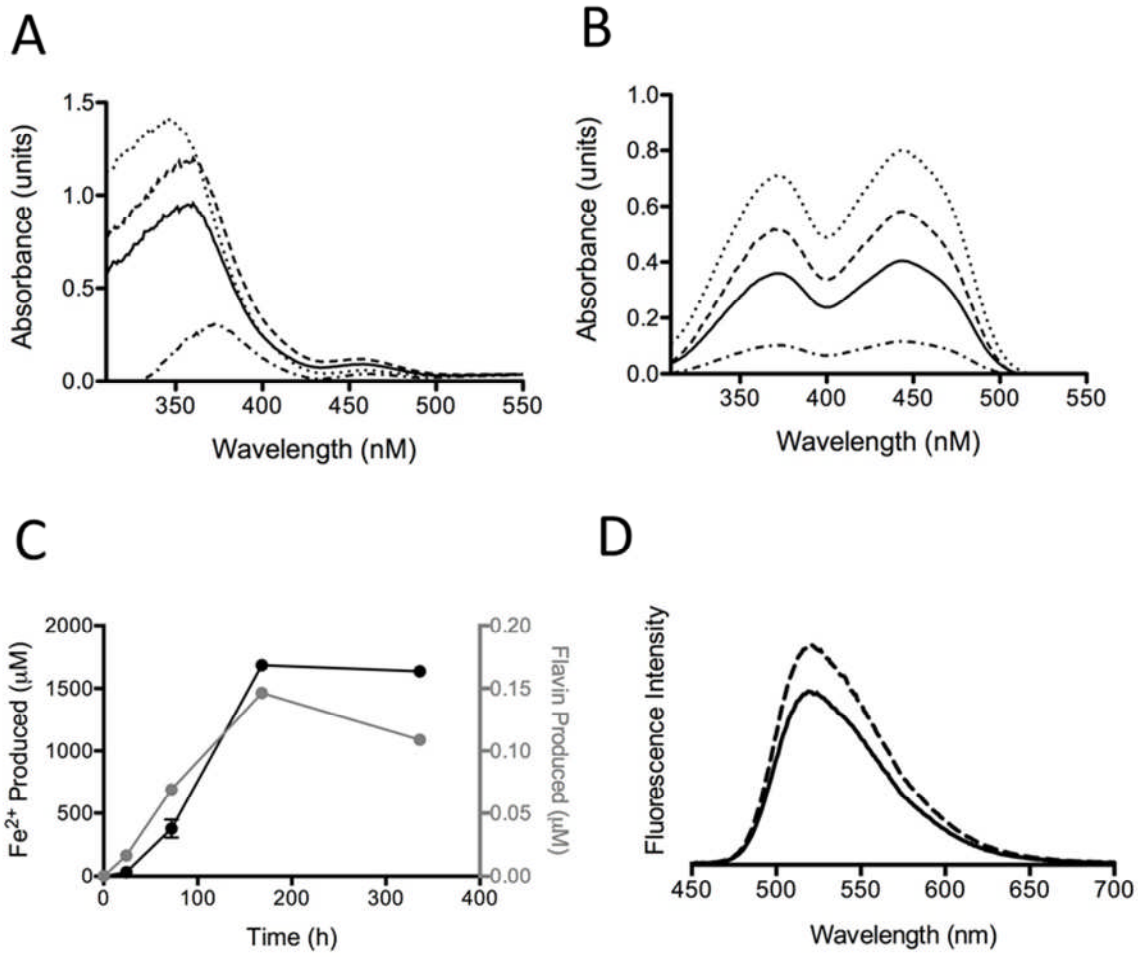

Figure 5.5: Spectroscopy of culture supernatants. UV-visible spectra of (*A*) culture media supernatant at various stages of alkaliphilic consortium growth or (*B*) extracellular compounds isolated. Data is shown from samples taken as day 1 (dash-dot lines), day 3 (solid lines), day 7 (dotted lines) and day 14 (dashed lines). (*C*) Compares the flavin produced with Fe(III) conversion to Fe(II) using the quantification information from (*B*). (*D*) Fluorescence spectra of extracellular compounds isolated from culture media supernatant (dashed line) compared to those from commercial pure riboflavin (solid line). Upon excitation at 441 nm, the emission spectra were monitored between 450 and 700 nm. Results shown are representative of two biological replicates.

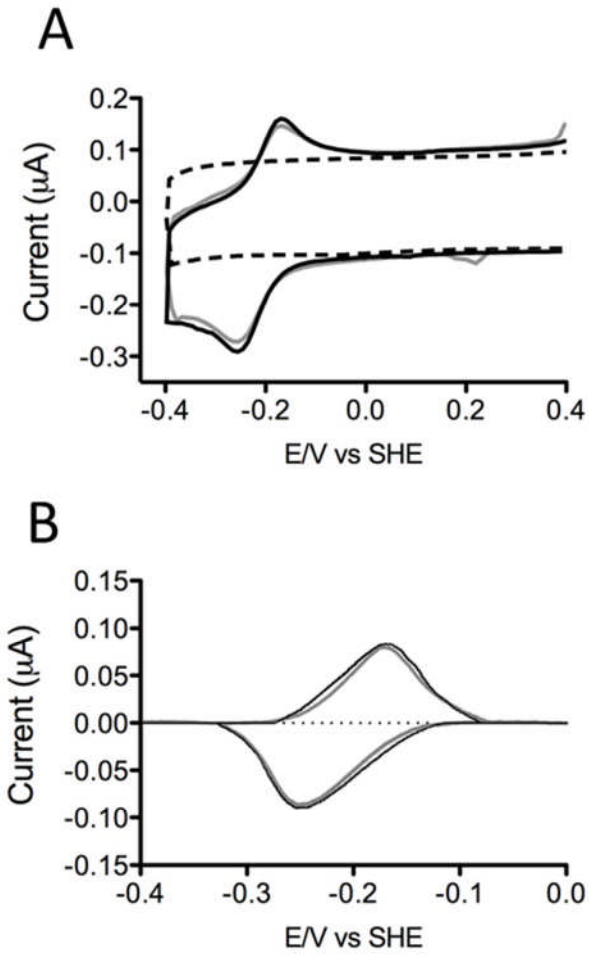

Figure 5.6: Cyclic voltammetry (CV) of 8-OH-modified TSG electrode before (blank) and after formation of a flavin film. All CVs were recorded in 20 mmol.L^{-1} MOPS, 30 mmol.L^{-1} Na_2SO_4 buffer (pH 7.4) at a 10 mV.s^{-1} scan rate. (*A*) CVs showing redox chemistry of immobilized purified flavin extract (*grey lines*) compared to commercially pure riboflavin (*black lines*) and a blank SAM (*dashed lines*). (*B*) Baseline correct voltammogram for immobilized purified flavin extract from the CV presented in (*A*). Results shown are representative of three replicate experiments.

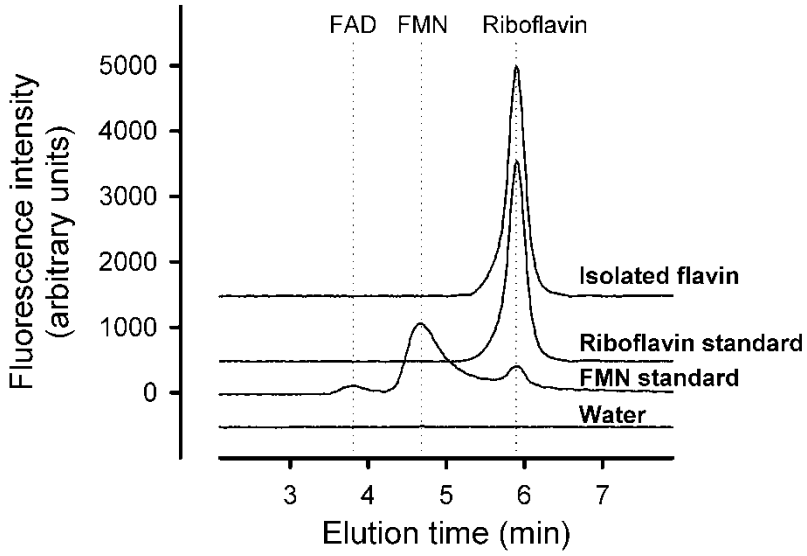

Figure 5.7: Reversed phase HPLC of the isolated flavin. (A) riboflavin standard. (B) and an FMN preparation, which contains sizeable amounts of riboflavin and FAD, respectively. (C) 100 ng of each sample were analysed. (D) Water injection only.

5.4.5.1 Growth in Media Spiked with Riboflavin

To further corroborate the role of riboflavin in Fe(III) reduction, growth media was spiked with riboflavin. Bacteria grown in AFe media supplemented with riboflavin resulted in the production of Fe(II) after 48 hours, half the time of the bacteria in the base AFe media (Figure 5.8). The exponential phase of growth for the bacteria in riboflavin amended media was complete after 144 hours.

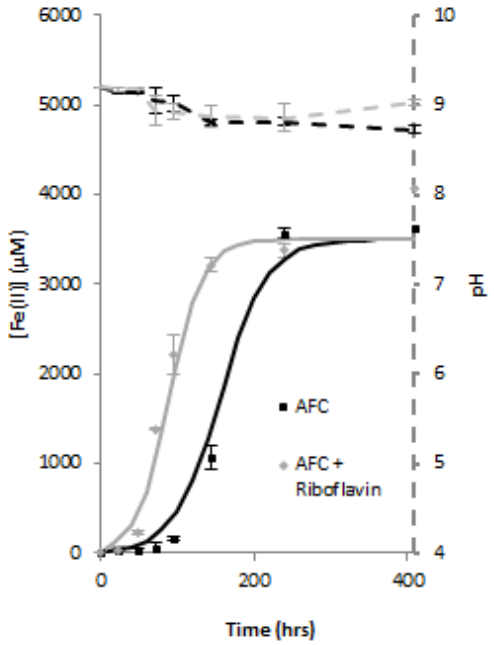

Figure 5.8: Average Fe(II) production and pH value during the growth of the iron reducing consortia in AFe media spiked with riboflavin. Sigmoidal growth curves are fitted to the Fe(II) data. Error bars indicate one standard deviation from the mean.

5.4.5.2 SEM

The precipitate recovered from the microcosms containing AFe media after cell growth appeared to be black in colour and crystalline in nature. Under SEM analysis the primary features seen were flattened prismatic crystals, roughly 30 x 5 x 5 µm in size (Figure 5.9). Between the crystals was an amorphous gel which cracked as the sample was dried. EDS spot analysis of crystals (insert in Figure 5.9) gave similar spectra with distinct peaks for O, P, and Fe, and a small S peak (there were also Cu peaks associated with the copper crucible which contained the sample). The flattened prismatic crystals have the morphology of Vivianite ($Fe_3(PO_4)_2.8H_2O$) (Dana et al., 1997) (the sulphur peak in the EDS spectra is probably associated with the amorphous background phase). Vivianite is a common phase when Fe(III) is bio-reduced in the media containing high concentrations of soluble phosphate (Bae and Lee, 2013).

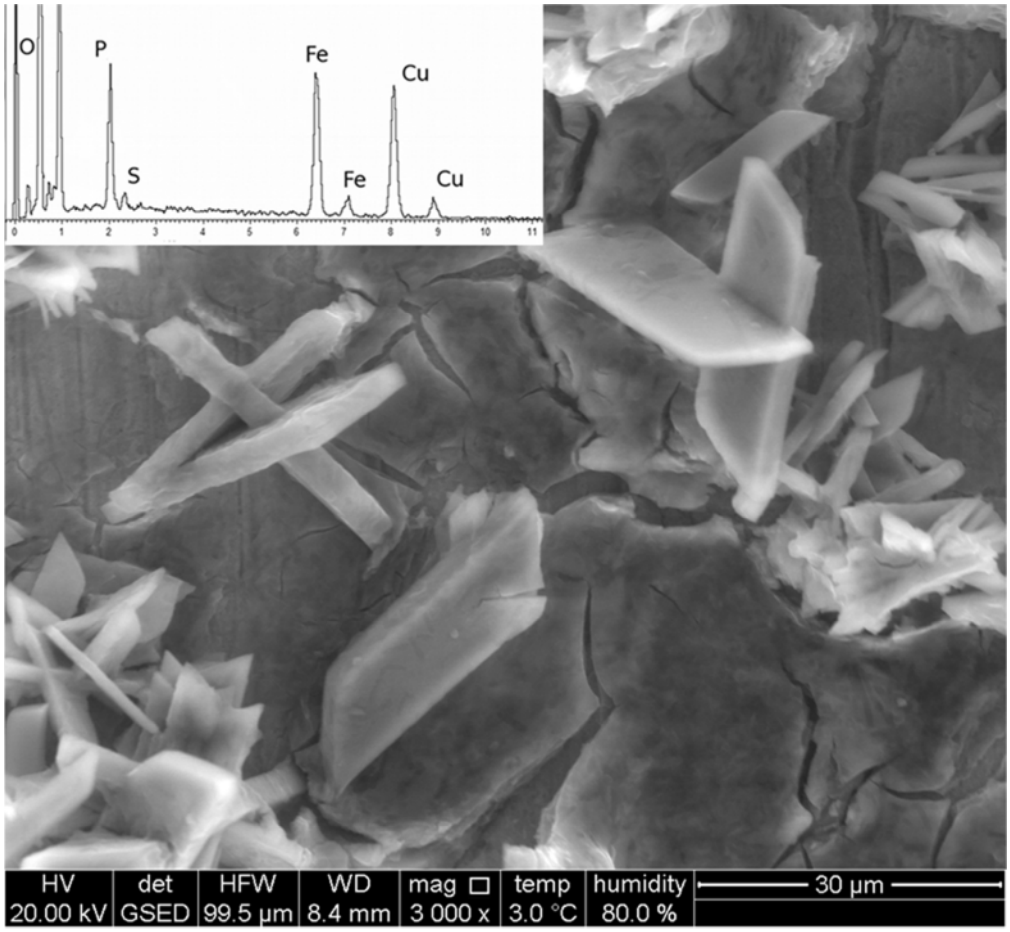

Figure 5.9: Electron micrograph of the precipitate recovered from the spent AFe media.

5.5 Discussion

5.5.1 **The identity of alkaliphilic community**

After repeated growth on AFe media (50+ growth cycles since isolation from the soil), sequencing data shows that there are still several genera of bacteria in the iron reducing community. This suggests that either all the bacteria present are able to respire independently using the AFe media or a symbiotic relationship has developed between the differing types of bacteria whereby one requires the respiration products of another for growth. The AFe media contained yeast extract which is a complex mixture of organic compounds, including amino acids and polysaccharides (Edens et al., 2002). Yeast extract can support a wide range of metabolic processes, and this may

explain the range of species in the consortium. None of the alternative electron donors supported long-term growth of the consortium. In media containing sucrose or ethanol with a low concentration of yeast extract, bacterial growth was recorded however no growth was observed without it. Thus it is clear that yeast extract contains something that is vital for iron reduction that is not supplied by the base media. Several other alkaliphilic organisms are reported to grow poorly on single organic compounds and require the presence of complex electron donor species (Horikoshi and Akiba, 1982, McMillan et al., 2009).

Nearly half (48%) of the sequences characterised from the AFe were from the genus *Tissierella* with Mothur analysis showing they could be further separated into three OTUs, *Tissierella* A, B and C. *Tissierella sp.* are obligate anaerobic, gram negative, non-sporeforming rods (Collins and Shah, 1986). All OTUs were most closely related to the type strain Tissierella Preacuta (seqmatch scores are A = 75%, B = 80% and C = 86%). 44% of the sequences characterised were from a single OTU in the genus Clostridium XI and were up to 100% similar to type strain *Clostridium mangenoti*. Found in many soils around the world (Smith, 1975), *Clostridium mangenoti* is an extremely hardy anaerobe whose spores are able to resist low temperature, vacuums and high levels of radiation (Koike and Oshima, 1993). Therefore it is no surprise that it can exist in the harsh geochemical environment in the original soil with high pH and in the presence of chromate. 8% of the bacteria sequenced were from a single OTU in the genus the Alkaliphilus most closely related to the type strain *Alkaliphilus oremlandii* (seqmatch score 83%) (Fisher et al., 2008). Bacteria from the Alkaliphilus genus are obligate alkaliphilic anaerobes that have been found in deep subsurface alkaline environments (Takai et al., 2001). Members of this genus have been shown to reduce numerous Fe(III) phases (Roh et al., 2007, Ye et al., 2004), as well as groundwater contaminants such as arsenic (Fisher et al., 2008).

The isolation of bacterial colonies in streaks on agar plates identified species that can reduce iron remote from the cell location. The streaks that visibly cleared the media contained bacteria the genus *Tissierella*, which MOTHER

analysis showed to be part of the OTU C. This fact, together with the observation that *Tissierella* forms a significant part of the AFe media consortium, suggests that *Tissierella* may be the principle bacteria producing the electron-shuttling compound. Extensive efforts to reintroduce these Tissierella C streaks into AFe media for further investigation were unsuccessful possibly due to factors such as accidental exposure to oxygen, which these bacteria may not be able to tolerate. It should be noted that these data do not preclude the possibility that other bacteria species in the consortium are also producing a soluble electron-shuttling compound as the relatively small sample size could mean that other bacteria capable of flavin production were not seen by chance.

The sequences characterised from the streaks which did not clear were identified as bacteria not seen in the initial population from the AFe media. This is not a surprise as environmental samples usually contain many different bacteria strains which can tolerate the media in which they are cultured, but never reach the exponential stage of growth. When growth conditions and competitive pressures are changed initially minor constituents of a bacterial population can become more significant.

5.5.2 **The alkaliphilic community secrete flavins to transfer electrons extracellularly**

When the bacterial community is grown on AFe media at pH 9.2, cell growth occurs contemporaneously with an increase in Fe(II) (both have been modelled in Figure 5.1 using the same lag time by a logistic sigmoidal growth function (Zwietering et al., 1990). During the period of cell growth and Fe(III) reduction a water soluble organic compound was released into solution. The concentration of this extracellular compound increased during the exponential growth phase, but decreased slightly in late stationary phase (see Figure 5.5*A* and 5.5*B*) suggesting its release is not associated with cell lysis. Reasons for the decrease after peaking at 168 hours could be due to riboflavin's sensitivity to UV radiation. Whilst generally kept in the dark, these microcosms were exposed to light whilst sampling, potentially allowing the breakdown of the flavin molecule. As available Fe(III) was exhausted, the

iron reducing bacteria were unable to respire thus could not replenish the concentration which subsequently decreased. Thus the slight decrease is not deemed to be significant.

The extracellular compound exhibited UV/vis spectral features indistinguishable from those of commercially available riboflavin. Further it has surface adsorption characteristics and surface packing on TSG electrodes, and oxidises and reduces with essentially the same redox potentials, as riboflavin. Lastly, HPLC analysis showed this to be a single compound a chromatogram matching the retention time of commercially available riboflavin. Thus, taking into account the overwhelming agreement in the data, it is deduced that the extracellular compound is riboflavin. When riboflavin was spiked into AFe media containing the bacterial community Fe(III) reduction started sooner and was quicker than in unspiked media, strongly suggesting that the riboflavin is involved in the mechanism of Fe(III) reduction. When isolates from the community were grown on AFe-agar plates the media cleared at mm scale distances from the “streaks” demonstrating that iron reduction was occurring remote from the cell location (see Figure 5.10).

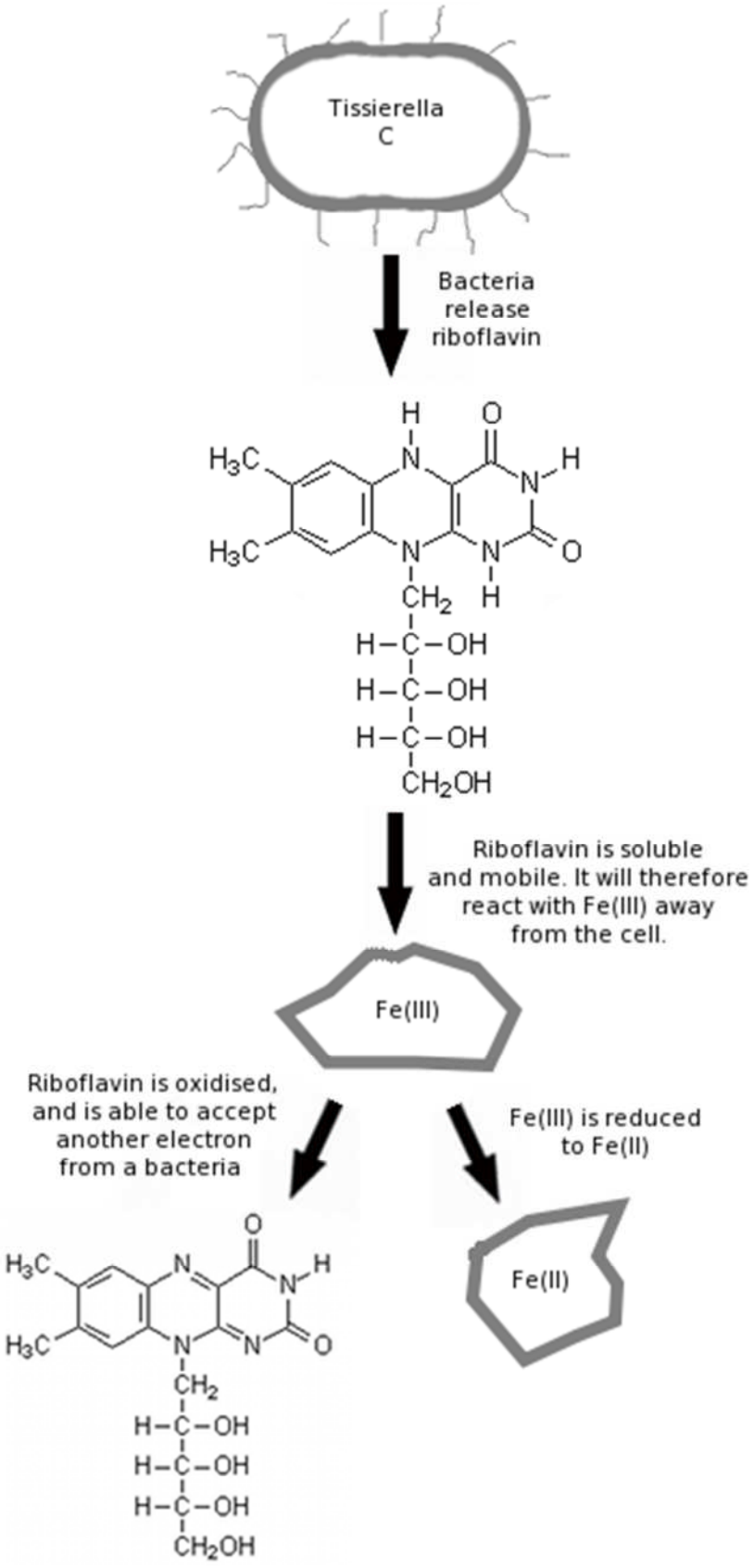

Figure 5.10: Schematic showing how riboflavin released by bacteria can reduce Fe(III) externally away from the cell.

There is a wide body of evidence that flavins can act as an electron shuttling compound during extracellular electron transport to iron in circum-neutral pH environments. For example *Shewanella* species release flavins and this increases the ability of cells to reduce Fe(III) oxides into Fe(II) in cellular respiration (von Canstein et al., 2008, Coursolle et al., 2010, Newman and Kolter, 2000, Marsili et al., 2008). Thus it seems extremely likely that the flavin-like compound released to solution by the alkaliphilic iron reducing community during growth is acting as an electron-shuttling compound, and has a role in Fe(III) reduction; the first time that this has been shown to occur at alkaline pH. Given that even mesophilic bacteria can adopt a wide variety of mechanisms to perform similar roles physiological functions when interacting with their environment (Drechsel and Jung, 1998), and the stress of a challenging environment has led extremophilic bacteria to evolve distinctly different mechanisms in many cases (McMillan et al., 2010, Temirov et al., 2003), it is striking that the electron shuttling compound found in this study of alkaliphiles is indistinguishable from that used by mesophiles. Interestingly flavins have also been found in the culture supernatants of several methanotrophic species (Balasubramanian et al., 2010), indicating that this method of extracellular electron transfer may be more widespread among anaerobic communities living on the brink of life than first thought.

5.6 Bioremediative potential

The bacterial consortium investigated in this study was recovered from beneath a waste tip where alkaline, Cr(VI) containing COPR leachate has been migrating into the underlying soil layer for over 100 years (Stewart et al., 2010). Chromium has accumulated in this soil within a mixed Cr(III)–Fe(III) oxy-hydroxide phase. The most likely mechanism of chromium retention is abiotic reduction by microbially produced soil associated Fe(II) (Whittleston et al., 2011). Hence, microbially Fe(III) reduction at high pH can have important consequences for the mobility of redox sensitive contaminants at alkaline contaminated sites, and promoting microbial Fe(III)

reduction could form the basis of a treatment strategy for such sites in the future.

An issue at some industrially contaminated sites is that the waste can be very high pH. Common industrial processes, such as iron and steel making, aluminium and chromium extraction, and lime and cement manufacture, produce a waste form with a pH > 12 (Burke et al., 2013, Burke et al., 2012, Stewart et al., 2010, Mayes et al., 2006). Many of these wastes contain elevated concentration of redox-sensitive, potentially mobile, toxic metals (e.g. As, V, Cr). Thus the near-waste environment is particularly harsh, so soil bacteria will tend to favour micro-habitats where they are protected from the bulk chemical flux by buffering reactions occurring with the soil minerals and respiration products (Nunan et al., 2006, Ranjard et al., 2000). The production of a soluble electron-shuttling compound enhances the potential success of any bioremediation scheme, as the electron shuttling compounds can diffuse out from these niche environments where the bacteria respire, and produce reduced iron even where the soil is highly leachate affected. There is some evidence of this at the sampling site, where 45→75% of the microbially available iron is Fe(II) despite an average soil pH value of 11→12.5, and this may account for why the soil has accumulated 0.3%→0.5% (w/w) Cr(III), despite the soil receiving a continual flux of Cr(VI) containing leachate from the waste (Whittleston et al., 2011). The use of a soluble electron-shuttling compound will increase the amount of soil Fe(III) available for bioreduction many fold, even where it is present in high pH zones unsuitable for bacterial respiration, thus increasing the overall bioreduction capacity of the soil. Another interesting point to note is that although flavin electron-shuttles are well suited to perform one or two electron transfers (i.e. those interactions involving Fe(III)-minerals and cell cytochromes;(Marsili et al., 2008), flavin electron-shuttles do not specifically target Fe(III) compounds. Flavins will react with the other oxidised compound they encounter with a high enough reductive potential, thus direct reduction of some groundwater contaminants (e.g. Cr(VI) → Cr(III)) by this bacteria community may be possible.

5.7 References

Ashelford, K. E., Chuzhanova, N. A., Fry, J. C., Jones, A. J. & Weightman, A. J. 2006. New Screening Software Shows that Most Recent Large 16S rRNA Gene Clone Libraries Contain Chimeras. *Appl. Environ. Microbiol.,* 72**,** 5734-5741.

Bae, S. & Lee, W. 2013. Biotransformation of lepidocrocite in the presence of quinones and flavins. *Geochim. Cosmochim. Acta,* 114**,** 144-155.

Balasubramanian, R., Levinson, B. T. & Rosenzweig, A. C. 2010. Secretion of Flavins by Three Species of Methanotrophic Bacteria. *Appl. Environ. Microbiol.,* 76**,** 7356-7358.

Burke, I. T., Boothman, C., Lloyd, J. R., Livens, F. R., Charnock, J. M., McBeth, J. M., Mortimer, R. J. G. & Morris, K. 2006. Reoxidation Behavior of Technetium, Iron, and Sulfur in Estuarine Sediments. *Environ. Sci. Technol.,* 40**,** 3529-3535.

Burke, I. T., Mortimer, R. J., Palaniyandi, S., Whittleston, R. A., Lockwood, C. L., Ashley, D. J. & Stewart, D. I. 2012. Biogeochemical Reduction Processes in a Hyper-Alkaline Leachate Affected Soil Profile. *Geomicrobiol. J.,* 29**,** 769-779.

Burke, I. T., Peacock, C. L., Lockwood, C. L., Stewart, D. I., Mortimer, R. J. G., Ward, M. B., Renforth, P., Gruiz, K. & Mayes, W. M. 2013. Behavior of Aluminum, Arsenic, and Vanadium during the Neutralization of Red Mud Leachate by HCl, Gypsum, or Seawater. *Environ. Sci. Technol.,* 47**,** 6527-6535.

Burns, J. L. & DiChristina, T. J. 2009. Anaerobic Respiration of Elemental Sulfur and Thiosulfate by Shewanella oneidensis MR-1 Requires psrA, a Homolog of the phsA Gene of Salmonella enterica Serovar Typhimurium LT2. *Appl. Environ. Microbiol.,* 75**,** 5209-5217.

Carpentier, W., De Smet, L., Van Beeumen, J. & Brige, A. 2005. Respiration and growth of Shewanella oneidensis MR-1 using vanadate as the sole electron acceptor. *J. Bacteriol.,* 187**,** 3293-301.

Clarke, T. A., Holley, T., Hartshorne, R. S., Fredrickson, J. K., Zachara, J. M., Shi, L. & Richardson, D. J. 2008. The role of multihaem cytochromes in the respiration of nitrite in Escherichia coli and Fe(III) in Shewanella oneidensis. *Biochem Soc Trans,* 36**,** 1005-10.

Cole, J. R., Wang, Q., Cardenas, E., Fish, J., Chai, B., Farris, R. J., Kulam-Syed-Mohideen, A. S., McGarrell, D. M., Marsh, T., Garrity, G. M. & Tiedje, J. M. 2009. The Ribosomal Database Project: improved alignments and new tools for rRNA analysis. *Nucleic Acids Res.,* 37**,** D141-D145.

Collins, M. D. & Shah, H. N. 1986. NOTES: Reclassification of Bacteroides praeacutus Tissier (Holdeman and Moore) in a New Genus, Tissierella, as Tissierella praeacuta comb. nov. *Int. J. Syst. Bacteriol.,* 36**,** 461-463.

Coursolle, D., Baron, D. B., Bond, D. R. & Gralnick, J. A. 2010. The Mtr respiratory pathway is essential for reducing flavins and electrodes in Shewanella oneidensis. *J. Bacteriol.,* 192**,** 467-74.

Dana, J. D., Dana, E. S. & Gaines, R. V. 1997. *Dana's New Mineralogy: The System of Mineralogy of James Dwight Dana and Edward Salisbury Dana*, Wiley.

Dobbin, P. S., Carter, J. P., San Juan, C. G. S., von Hobe, M., Powell, A. K. & Richardson, D. J. 1999. Dissimilatory Fe(III) reduction by Clostridium beijerinckii isolated from freshwater sediment using Fe(III) maltol enrichment. *FEMS Microbiol. Lett.,* 176**,** 131-138.

Drechsel, H. & Jung, G. 1998. Peptide siderophores. *J. Pept. Sci.,* 4**,** 147-181.

Eary, L. E. & Rai, D. 1988. Chromate removal from aqueous wastes by reduction with ferrous ion. *Environ. Sci. Technol.,* 22**,** 972-977.

Edens, N. K., Reaves, L. A., Bergana, M. S., Reyzer, I. L., O'Mara, P., Baxter, J. H. & Snowden, M. K. 2002. Yeast extract stimulates glucose metabolism and inhibits lipolysis in rat adipocytes in vitro. *J. Nutr.,* 132**,** 1141-8.

Fendorf, S. E. & Li, G. 1996. Kinetics of Chromate Reduction by Ferrous Iron. *Environ. Sci. Technol.,* 30**,** 1614-1617.

Field, S. J., Dobbin, P. S., Cheesman, M. R., Watmough, N. J., Thomson, A. J. & Richardson, D. J. 2000. Purification and magneto-optical spectroscopic characterization of cytoplasmic membrane and outer membrane multiheme c-type cytochromes from Shewanella frigidimarina NCIMB400. *J. Biol. Chem.,* 275**,** 8515-22.

Fisher, E., Dawson, A. M., Polshyna, G., Lisak, J., Crable, B., Perera, E., Ranganathan, M., Thangavelu, M., Basu, P. & Stolz, J. F. 2008. Transformation of Inorganic and Organic Arsenic byAlkaliphilus oremlandiisp. nov. Strain OhILAs. *Ann. N. Y. Acad. Sci.,* 1125**,** 230-241.

Gao, H., Yang, Z. K., Barua, S., Reed, S. B., Romine, M. F., Nealson, K. H., Fredrickson, J. K., Tiedje, J. M. & Zhou, J. 2009. Reduction of nitrate in Shewanella oneidensis depends on atypical NAP and NRF systems with NapB as a preferred electron transport protein from CymA to NapA. *Isme. J.,* 3**,** 966-76.

Garnova, E. S., Zhilina, T. N., Tourova, T. P. & Lysenko, A. M. 2003. Anoxynatronum sibiricum gen.nov., sp.nov alkaliphilic saccharolytic anaerobe from cellulolytic community of Nizhnee Beloe (Transbaikal region). *Extremophiles,* 7**,** 213-220.

Gorlenko, V., Tsapin, A., Namsaraev, Z., Teal, T., Tourova, T., Engler, D., Mielke, R. & Nealson, K. 2004. Anaerobranca californiensis sp nov., an anaerobic, alkalithermophilic, fermentative bacterium isolated from a hot spring on Mono Lake. *Int. J. Syst. Evol. Microbiol.,* 54**,** 739-743.

Gralnick, J. A., Vali, H., Lies, D. P. & Newman, D. K. 2006. Extracellular respiration of dimethyl sulfoxide by Shewanella oneidensis strain MR-1. *Proc. Natl. Acad. Sci. U.S.A.,* 103**,** 4669-4674.

Harbury, H. A. & Foley, K. A. 1958. Molecular interaction of isoalloxazine derivatives. *Proc. Natl. Acad. Sci. U.S.A.,* 44**,** 662.

Horikoshi, K. & Akiba, T. 1982. *Alkalophilic microorganisms: a new microbial world*, Japan Scientific Societies Press.

Kevbrin, V. V., Zhilina, T. N., Rainey, F. A. & Zavarzin, G. A. 1998. Tindallia magadii gen. nov., sp. nov.: An alkaliphilic anaerobic ammonifier from soda lake deposits. *Curr. Microbiol.,* 37**,** 94-100.

Kim, B. H. & Gadd, G. M. 2008. *Bacterial physiology and metabolism*, Cambridge university press Cambridge.

Koike, J. & Oshima, T. 1993. Planetary quarantine in the solar system. Survival rates of some terrestrial organisms under simulated space conditions by proton irradiation. *Acta Astronaut.,* 29**,** 629-632.

Langmuir, D. 1997. *Aqueous Environmental Geochemistry*, Prentice-Hall.

Larkin, M. A., Blackshields, G., Brown, N. P., Chenna, R., McGettigan, P. A., McWilliam, H., Valentin, F., Wallace, I. M., Wilm, A., Lopez, R., Thompson, J. D., Gibson, T. J. & Higgins, D. G. 2007. Clustal W and clustal X version 2.0. *Bioinformatics,* 23**,** 2947-2948.

Lovley, D. R. 2006. *Dissimilatory Fe(III) and Mn(IV) reducing Prokaryotes. In: The Prokaryotes: A Handbook on the Biology of Bacteria: Vol. 2: Ecophysiology and Biochemistry*, Springer.

Lovley, D. R., Coates, J. D., Blunt-Harris, E. L., Phillips, E. J. & Woodward, J. C. 1996. Humic substances as electron acceptors for microbial respiration. *Nature,* 382**,** 445-448.

Lovley, D. R. & Phillips, E. J. P. 1986. Availability of Ferric Iron for Microbial Reduction in Bottom Sediments of the Fresh-Water Tidal Potomac River. *Appl. Environ. Microbiol.,* 52**,** 751-757.

Madigan, M. T., Martinko, J. M. & Parker, J. 2003. *Brock biology of microorganisms*, Prentice Hall/Pearson Education.

Marsili, E., Baron, D. B., Shikhare, I. D., Coursolle, D., Gralnick, J. A. & Bond, D. R. 2008. Shewanella Secretes Flavins That Mediate Extracellular Electron Transfer. *Proc. Natl. Acad. Sci. U.S.A.,* 105**,** 3968-3973.

Mayes, W. M., Younger, P. L. & Aumo, J. 2006. Buffering of alkaline steel slag leachate across a natural wetland. *Environ. Sci. Technol.,* 40**,** 1237-1243.

McMillan, D. G., Keis, S., Berney, M. & Cook, G. M. 2009. Nonfermentative thermoalkaliphilic growth is restricted to alkaline environments. *Appl. Environ. Microbiol.,* 75**,** 7649-54.

McMillan, D. G., Marritt, S. J., Butt, J. N. & Jeuken, L. J. 2012. Menaquinone-7 is specific cofactor in tetraheme quinol dehydrogenase CymA. *J. Biol. Chem.,* 287**,** 14215-25.

McMillan, D. G., Velasquez, I., Nunn, B. L., Goodlett, D. R., Hunter, K. A., Lamont, I., Sander, S. G. & Cook, G. M. 2010. Acquisition of iron by alkaliphilic bacillus species. *Appl. Environ. Microbiol.,* 76**,** 6955-61.

McMillan, D. G. G., Marritt, S. J., Firer-Sherwood, M. A., Shi, L., Richardson, D. J., Evans, S. D., Elliott, S. J., Butt, J. N. & Jeuken, L. J. C. 2013. Protein-protein interaction regulates the direction of catalysis and electron transfer in a redox enzyme complex. *J. ACS*.

Mulkidjanian, A. Y., Dibrov, P. & Galperin, M. Y. 2008. The past and present of sodium energetics: May the sodium-motive force be with you. *Biochim. Biophys. Acta,* 1777**,** 985-992.

Murphy, J. N. & Saltikov, C. W. 2007. The cymA gene, encoding a tetraheme c-type cytochrome, is required for arsenate respiration in Shewanella species. *J. Bacteriol.,* 189**,** 2283-90.

Myers, C. R. & Myers, J. M. 1992. Localization of cytochromes to the outer membrane of anaerobically grown Shewanella putrefaciens MR-1. *J. Bacteriol.,* 174**,** 3429-3438.

Myers, C. R. & Myers, J. M. 2004. Shewanella oneidensis MR-1 Restores Menaquinone Synthesis to a Menaquinone-Negative Mutant. *Applied and Environmental Microbiology,* 70**,** 5415-5425.

Myers, C. R. & Nealson, K. H. 1990. Respiration-linked proton translocation coupled to anaerobic reduction of manganese(IV) and iron(III) in Shewanella putrefaciens MR-1. *J. Bacteriol.,* 172**,** 6232-8.

Nealson, K. H. & Saffarini, D. 1994. Iron and Manganese in Anaerobic Respiration: Environmental Significance, Physiology, and Regulation. *Annu. Rev. Microbiol.,* 48**,** 311-343.

Nevin, K. P. & Lovley, D. R. 2002. Mechanisms for Fe(III) Oxide Reduction in Sedimentary Environments. *Geomicrobiol. J.,* 19**,** 141-159.

Newman, D. K. & Kolter, R. 2000. A role for excreted quinones in extracellular electron transfer. *Nature,* 405**,** 94-7.

Nunan, N., Ritz, K., Rivers, M., Feeney, D. S. & Young, I. M. 2006. Investigating microbial micro-habitat structure using X-ray computed tomography. *Geoderma,* 133**,** 398-407.

Otto, M. K., Jayaram, M., Hamilton, R. M. & Delbruck, M. 1981. Replacement of riboflavin by an analogue in the blue-light photoreceptor of Phycomyces. *Proc. Natl. Acad. Sci. U.S.A.,* 78**,** 266-9.

Page, R. D. M. 1996. TreeView: An application to display phylogenetic trees on personal computers. *Comput. Appl. Biosci.,* 12**,** 357-358.

Pitts, K. E., Dobbin, P. S., Reyes-Ramirez, F., Thomson, A. J., Richardson, D. J. & Seward, H. E. 2003. Characterization of the Shewanella oneidensis MR-1 decaheme cytochrome MtrA: expression in Escherichia coli confers the ability to reduce soluble Fe(III) chelates. *J. Biol. Chem.,* 278**,** 27758-65.

Pollock, J., Weber, K. A., Lack, J., Achenbach, L. A., Mormile, M. R. & Coates, J. D. 2007. Alkaline iron(III) reduction by a novel alkaliphilic, halotolerant, Bacillus sp. isolated from salt flat sediments of Soap Lake. *Appl. Microbiol. Biotechnol.,* 77**,** 927-34.

Posadaz, A., Sánchez, E., Gutiérrez, M. I., Calderón, M., Bertolotti, S., Biasutti, M. A. & García, N. A. 2000. Riboflavin and rose bengal sensitised photooxidation of sulfathiazole and succinylsulfathiazoleKinetic study and microbiological implications. *Dyes. Pigm.,* 45**,** 219-228.

Ranjard, L., Nazaret, S., Gourbiere, F., Thioulouse, J., Linet, P. & Richaume, A. 2000. A soil microscale study to reveal the heterogeneity of Hg(II) impact on indigenous bacteria by quantification of adapted phenotypes and analysis of community DNA fingerprints. *FEMS Microbiol. Ecol.,* 31**,** 107-115.

Ratasuk, N. & Nanny, M. A. 2007. Characterization and Quantification of Reversible Redox Sites in Humic Substances. *Environ. Sci. Technol.,* 41**,** 7844-7850.

Richardson, D. J. 2000. Bacterial respiration: a flexible process for a changing environment. *Microbiology,* 146**,** 551-571.

Roh, Y., Chon, C.-M. & Moon, J.-W. 2007. Metal reduction and biomineralization by an alkaliphilic metal-reducing bacterium,Alkaliphilus metalliredigens. *Geosci. J.,* 11**,** 415-423.

Ross, D. E., Ruebush, S. S., Brantley, S. L., Hartshorne, R. S., Clarke, T. A., Richardson, D. J. & Tien, M. 2007. Characterization of protein-protein interactions involved in iron reduction by Shewanella oneidensis MR-1. *Appl. Environ. Microbiol.,* 73**,** 5797-808.

Schloss, P. D., Westcott, S. L., Ryabin, T., Hall, J. R., Hartmann, M., Hollister, E. B., Lesniewski, R. A., Oakley, B. B., Parks, D. H., Robinson, C. J., Sahl, J. W., Stres, B., Thallinger, G. G., Van Horn, D. J. & Weber, C. F. 2009. Introducing mothur: Open-Source, Platform-Independent, Community-Supported Software for Describing and Comparing Microbial Communities. *Appl. Environ. Microbiol.,* 75**,** 7537-7541.

Schwalb, C., Chapman, S. K. & Reid, G. A. 2002. The membrane-bound tetrahaem c-type cytochrome CymA interacts directly with the soluble fumarate reductase in Shewanella. *Biochem Soc Trans,* 30**,** 658-62.

Schwalb, C., Chapman, S. K. & Reid, G. A. 2003. The tetraheme cytochrome CymA is required for anaerobic respiration with dimethyl sulfoxide and nitrite in Shewanella oneidensis. *Biochem.,* 42**,** 9491-7.

Smith, L. D. 1975. Common mesophilic anaerobes, including Clostridium botulinum and Clostridium tetani, in 21 soil specimens. *Appl. Microbiol.,* 29**,** 590-594.

Stewart, D. I., Burke, I. T., Hughes-Berry, D. V. & Whittleston, R. A. 2010. Microbially mediated chromate reduction in soil contaminated by highly alkaline leachate from chromium containing waste. *Ecol. Eng.,* 36**,** 211-221.

Stucki, J. W., Lee, K., Goodman, B. A. & Kostka, J. E. 2007. Effects of in situ biostimulation on iron mineral speciation in a sub-surface soil. *Geochim. Cosmochim. Acta,* 71**,** 835-843.

Takai, K., Moser, D. P., Onstott, T. C., Spoelstra, N., Pfiffner, S. M., Dohnalkova, A. & Fredrickson, J. K. 2001. Alkaliphilus transvaalensis gen. nov., sp. nov., an extremely alkaliphilic bacterium isolated from a deep South African gold mine. *Int. J. Syst. Evol. Microbiol.,* 51**,** 1245-56.

Temirov, Y. V., Esikova, T. Z., Kashparov, I. A., Balashova, T. A., Vinokurov, L. M. & Alakhov, Y. B. 2003. A Catecholic Siderophore Produced by the Thermoresistant Bacillus licheniformis VK21 Strain. *Russ. J. Bioorganic Chem.,* 29**,** 542-549.

Van der Zee, F. P. & Cervantes, F. J. 2009. Impact and application of electron shuttles on the redox (bio)transformation of contaminants: A review. *Biotechnol. Adv.,* 27**,** 256-277.

Viamajala, S., Peyton, B. M., Apel, W. A. & Petersen, J. N. 2002. Chromate reduction in Shewanella oneidensis MR-1 is an inducible process associated with anaerobic growth. *Biotechnol. Prog.,* 18**,** 290-5.

von Canstein, H., Ogawa, J., Shimizu, S. & Lloyd, J. R. 2008. Secretion of Flavins by Shewanella Species and Their Role in Extracellular Electron Transfer. *Appl. Environ. Microbiol.,* 74**,** 615-623.

Wang, Q., Garrity, G. M., Tiedje, J. M. & Cole, J. R. 2007. Naïve Bayesian Classifier for Rapid Assignment of rRNA Sequences into the New Bacterial Taxonomy. *Appl. Environ. Microbiol.,* 73**,** 5261-5267.

Watanabe, K., Manefield, M., Lee, M. & Kouzuma, A. 2009. Electron shuttles in biotechnology. *Curr. Opin. Biotechnol.,* 20**,** 633-641.

White, G. F., Shi, Z., Shi, L., Wang, Z., Dohnalkova, A. C., Marshall, M. J., Fredrickson, J. K., Zachara, J. M., Butt, J. N., Richardson, D. J. & Clarke, T. A. 2013. Rapid electron exchange between surface-exposed bacterial cytochromes and Fe(III) minerals. *Proc. Natl. Acad. Sci. U.S.A.*

Whittleston, R. A. 2011. *Bioremediation of chromate in alkaline sediment-water systems.* PhD thesis, University of Leeds.

Whittleston, R. A., Stewart, D. I., Mortimer, R. J. G., Tilt, Z. C., Brown, A. P., Geraki, K. & Burke, I. T. 2011. Chromate reduction in Fe(II)-containing soil affected by hyperalkaline leachate from chromite ore processing residue. *J. Hazard. Mater.,* 194**,** 15-23.

Williamson, A. J., Morris, K., Shaw, S., Byrne, J. M., Boothman, C. & Lloyd, J. R. 2013. Microbial Reduction of Fe(III) under Alkaline Conditions Relevant to Geological Disposal. *Applied and Environmental Microbiology,* 79**,** 3320-3326.

Ye, Q., Roh, Y., Carroll, S. L., Blair, B., Zhou, J., Zhang, C. L. & Fields, M. W. 2004. Alkaline Anaerobic Respiration: Isolation and Characterization of a Novel Alkaliphilic and Metal-Reducing Bacterium. *Appl. Environ. Microbiol.,* 70**,** 5595-5602.

Zavarzina, D. G., Kolganova, T. V., Boulygina, E. S., Kostrikina, N. A., Tourova, T. P. & Zavarzin, G. A. 2006. Geoalkalibacter ferrihydriticus gen. nov. sp. nov.,

the first alkaliphilic representative of the family Geobacteraceae, isolated from a soda lake. *Microbiology,* 75**,** 673-682.

Zwietering, M. H., Jongenburger, I., Rombouts, F. M. & VAN 'T Riet, K. 1990. Modeling of the Bacterial Growth Curve. *Appl. Environ. Microbiol.,* 56**,** 1875-1881.

Chapter 6 **Bioreduction of Hexavalent Chromium by Alkaliphilic Bacteria Recovered from a Chromite Ore Processing Residue Disposal Site**

6.1 Abstract

A community of alkaliphilic Fe(III)-reducing bacteria (principally *Tissierella*, *Clostridium XI* and *Alkaliphilus* sp.) have been isolated from highly alkaline soil found beneath a Chromate Ore Processing Reside (COPR) waste tip. The growth of this community in media containing Cr(VI), and the resulting changes in community composition, are reported. The growth of the community in sediment suspensions where the only Fe(III) available was in the solid phase is also reported. The bacterial community were able to completely remove Cr(VI) from alkaline Fe(III) containing (AFe) media containing 2000 $\mu mol.L^{-1}$ chromate. Partial Cr(VI) removal was recorded from AFe with 8500 $\mu mol.L^{-1}$ Cr(VI). Members of population were also able to grow with Cr(VI) as the sole electron donor. The bacterial community can also reduce solid phase Fe(III) contained within sediments collected from the same site. Population data shows that as Cr(VI) is introduced into the growth media the diversity of the community is reduced as the *Tissierella*, sp. appear to have a low tolerance for Cr(VI). The only species to be able to use Cr(VI) as the sole electron donor were *Clostridium XI*. Conversely growth on solid phase iron favoured a single species of Tissierella which releases riboflavin, probably as an extracellular electron shuttle, to mediate reduction of solid phase iron. This chapter suggests that bioreduction of Cr(VI) can occur as a direct enzymatically mediated process, but this process did not support long term growth. Cr(VI) reduction also occurred as part of Fe(III)/Fe(II) cycling that does support long term growth, even in the presence of high Cr(VI) concentrations. Therefore, it is the indirect mechanism involving microbial Fe(III) reduction that is more likely to account for the low Cr(VI) mobility found at the COPR waste site.

6.2 Introduction

Whilst the previous chapter has established the Fe(III) reducing capabilities of bacteria isolated from a historical COPR site, little is known about their ability to grow in the presence of and ability to reduce Cr(VI). The contamination of potable groundwater with toxic trace metals/metalloids such as Cr(VI) is a major concern (Karim, 2000, Costa, 1997). Microbial Fe(III) reduction can have a major impact on the solubility and mobility of many trace metal/metalloid contaminants in the geosphere, particularly those that form stable oxyanions such as Cr, V, Mo, W, Tc and Se (Lovley, 2001). Reduced Fe(II) is able to react with these contaminants, producing less mobile and in some cases less toxic phases (Veeramani et al., 2011).

During anaerobic dissimilatory metabolism, bacteria take electrons from organic carbon (an electron donor) and transfer them to a substrate (an electron acceptor) which is reduced (Liermann et al., 2007). The energy released during this reaction is used by the cell in order to drive internal processes such as ATP synthesis (Madigan et al., 2003, Kim and Gadd, 2008). Bacteria usually use those electron acceptors that have the highest oxidation potential first, as these release the most energy to the cell. In aerobic conditions they use oxygen, however in the subsurface, any O_2 is quickly exhausted by geochemical and biological reactions (Lovley, 2001). Thus anaerobic dissimilatory bacteria will respire and reduce a number of common compounds such as nitrate, Fe(III) and sulphate (Lovley, 1997, Gao et al., 2009, Rabus, 2006), as well as anthropogenic contaminants including Cr(VI), Tc(VII), V(V), Molybdate and U(VI) (Harish et al., 2012, Abdelouas et al., 1998, Burke et al., 2006, Carpentier et al., 2005, Shukor et al., 2010). Bacteria use many different mechanisms to reduce electron acceptors, and reactions can occur either internally and externally to the cell. For example Fe(III) reduction can be facilitated by many different bacterial mechanisms. Intercellular reduction has been observed by *Shewanella Putrefaciens* CN32 which stores Fe(III) in ‘lungs’ before use (Glasauer et al., 2007). Other bacteria, such as *Shewanella Putrefaciens,* reduce Fe(III) on contact via *c*-type cytochromes located within their cell wall (Lovley, 2008, Bae and Lee, 2013). As has already been seen in Chapter 5, some produce soluble

electron shuttles such as quinones and flavins to transfer electrons outside the cell to more distant Fe(III) sources (Bae and Lee, 2013, von Canstein et al., 2008). *Geobacter metallireducens* is another highlighted bacteria capable of using humic substances as electron shuttles (Lovley et al., 1998). Other bacteria facilitate Fe(III) reduction remotely by transferring electrons along conductive appendages extending from the cell walls (so called 'nanowires') (Gorby et al., 2006). In natural systems, the electron donors used by most soil bacteria are organic molecules derived from the breakdown of soil organic matter. Introducing supplementary electron donors into a contaminated aquifer may encourage the proliferation of the indigenous bacteria population. Increased respiration will increase the demand for electron acceptors; promote increased anoxia, and the transition to the use of electron acceptors with lower oxidation potentials. Under the right conditions this can result in immobilisation of a contaminant as a consequence of their respiration processes (e.g. the reductive precipitation of Cr (Richard and Bourg, 1991)).

Many industrial processes produce highly alkaline wastes (e.g. coal combustion, lime production, chromium ore processing, cement production, iron and steel manufacture, and bauxite refining, to name but a few), (Mayes and Younger, 2006, Burke et al., 2013, Deakin et al., 2001, Jankowski et al., 2006). However, until recently these bulk wastes were often poorly disposed of; frequently in unlined tips (Higgins et al., 1998, Mayes et al., 2008, Stewart et al., 2006). When rainwater infiltrates the waste it can often leach these toxic elements transporting them downwards into the groundwater beneath disposal sites. Thus the fate of toxic metals in this alkaline leachate depends on the biogeochemical reactions that take place in the soil beneath the site. Sites such as those containing chromite ore processing residue (COPR), a legacy of chromium chemical manufacture, have been identified as being suitable for bioremediation. COPR contains toxic and soluble Cr(VI) compounds, which can be reduced to Cr(III) by microbial mediated reactions. Cr(III) readily sorbs to soil minerals, and (co)-precipitates as insoluble Cr(III) hydroxides in neutral and alkaline environments (Richard and Bourg, 1991, Rai et al., 1987).

Many bacteria have been isolated which can respire using Fe(III) as the sole electron acceptor in alkaline conditions (e.g. *Alkaliphilus metalliredigens* (Roh et al., 2007), *Alkaliphilus peptidofermentans* (Zhilina et al., 2009), *Anaerobranca californiensis* (Gorlenko et al., 2004), with the formation of Fe(II) containing phases such as vivianite, magnetite and siderite. Neo-formed Fe(II) phases can reduce some contaminant oxyanions (e.g. vanadate, pertechnetate, chromate, selenite (Charlet et al., 2007, Whittleston et al., 2011, White and Peterson, 1996, Burke et al., 2006)), while other oxyanions form ferrous complexes on hydrated Fe(II) minerals (e.g. molybdate, tungstate (Rey and Reggiani, 2005, O'Loughlin et al., 2010)). As yet, there is little detailed information on the mechanisms of how anaerobic bacteria growing at high pH use iron as a final electron acceptor. Work highlighted in Chapter 5 discovered that some alkaliphillic bacteria have the ability to use riboflavin to mediate extracellular electron transfer, which is advantageous as most Fe(III) phases are relatively insoluble at alkaline pH. Williamson et al. (2013) found that addition of electron transfer mediators can speed up Fe(III) reduction in alkaline soil.

Some trace metals can also be reduced directly as part of microbial metabolism. For example selenite and pertechnetate can be reduced directly by dissimilatory bacteria (Lovley, 1993, Lloyd et al., 2000). Many different types of bacteria can enzymatically reduce Cr(VI) (the contaminant at COPR sites) in both aerobic and anaerobic conditions (e.g. *Pyrobaculum islandicum* (Lloyd and Lovley, 2001), *Desulfovibrio vulgaris* (Lovley and Phillips, 1994), *Enterobacter cloacae* (Harish et al., 2012), *Shewanella putrefaciens* and *Shewanella alga* (Liu et al., 2002)). However, very few bacteria strains are able to use Cr(VI) as the sole electron acceptor on which to respire (Daulton et al., 2007). Cr(VI) is toxic to many forms of bacteria as it is able to pass through the cell membrane via the sulphate transport system (Daulton et al., 2007). Once inside the cell wall, it will readily react with DNA and other intercellular agents which are subsequently damaged via binding with the newly formed Cr(III) (Cervantes and Silver, 1992, Wang and Shen, 1997, Dhal et al., 2013). Thus although some bacteria can reduce Cr(VI), the act of reduction can damage the cell, leading to mutations and cell death.

Mineralogical analysis of soil from directly below a 19th century chromium ore processing residue (COPR) disposal site in West Yorkshire showed that there was rapid attenuation of Cr(VI) and accumulation of Cr(III) within the organic rich former topsoil layer beneath the tip (Stewart et al., 2010). Within this soil layer a large proportion of the 0.5 N HCl extractable Fe (a proxy for microbial available Fe, (Weber et al., 2001)) was in the Fe(II) oxidation state. The persistence of the Fe(II) oxidation state in the presence of a Cr(VI) flux suggests that microbial iron reduction was occurring. XAS analysis of soil samples indicated that Cr is present as a mixed Cr(III)–Fe(III) oxyhydroxide phase, suggesting that the elevated soil Cr content is due to reductive precipitation of Cr(VI) by Fe(II) (Whittleston et al., 2011). Chapter 5 detailed how these bacteria, isolated from this same soil horizon, have been repeatedly grown in alkaline anaerobic media with Fe(III) as the sole electron donor resulting in the accumulation of Fe(II)-containing phases in spent media.

This chapter takes the same community of bacteria as used in Chapter 5 and investigates Cr(VI) removal from alkaline anaerobic media containing Cr(VI) and Fe(III) as electron acceptors and with Cr(VI) as the sole electron acceptor. It also reports on Fe(II) production in media containing aquifer sand to provide solid phase Fe(III) as an electron acceptor. Changes to the bacteria population as a result of changes to the growth media are presented. Finally it discusses the significance of the results with regards to bioremediation of COPR sites.

6.3 Materials and Method

6.3.1 **Alkaliphilic Fe(III) reducing Bacteria Community**

The bacteria community used in this study was recovered from a soil horizon that is immediately beneath a 19th century COPR tip (see (Whittleston et al., 2011, Whittleston, 2011) for details). This horizon is thought to be the former top soil layer that was buried by deposition of the waste. Water in contact with COPR has a pH value >12 and contains approximately 1000 µmol.L^{-1} of

Cr(VI) (see Chapter 3). Due to a perched water table in the waste, this water is seeping downwards into the soil horizon of interest.

Since its recovery, the bacteria community used in this study has been repeatedly grown anaerobically in alkaline growth media containing Fe(III) (AFe media). Chapter 5 showed the community to contain bacteria of the genera Tissierella, Clostridium XI and Alkaliphillus which could be further classified into 5 operational taxonomic units (OTUs); from now on referred to as Tissierella A (7% of the population), Tissierella B (5%), Tissierella C (36%), Alkaliphillus (8%) and Clostridium XI (44%) (Genbank numbers KF362050-KF362117). The representative sequences from Tissierella A, B, and C are 75.9, 80.7 and 86.6% similar to the type species *Tissierella Praecuta*. The representative sequence from the Clostridium XI OTU is 98.8% similar to *Clostrisdium mangenoti* and the representative sequence from the Alkaliphillus OTU is 83.3% similar to *Alkaliphilus oremlandii*.

6.3.2 **Growth Media**

Alkaline Fe(III) containing (AFe), Alkaline Cr(VI) containing (ACr) media and alkaline Fe(III) and Cr(VI) containing (AFeCr) media were prepared to the recipes highlighted in chapter 3. Alkaline solid phase Fe(III) (SFe) media was prepared to the same recipe as the AFe media except the Fe(III) citrate was omitted and alluvial sand was added which was recovered from beneath the 19th century COPR waste tip in order to provide the electron acceptor (Stewart et al., 2010). It contained 5% Fe as determined by X-ray fluorescence (XRF) (for full elemental analysis see Table 3.2). This solid phase Fe(III) is present as fine particles and grain coatings is presumed to be the main electron acceptor present.

6.3.3 **Growth Characterisation**

Growth media bottles were inoculated with 1% media containing bacteria in the upper exponential phase of growth. Microcosms were kept at a constant temperature of 21 ± 1°C. The bottles were sampled using sterile needles and aseptic, anaerobic technique (Burke et al., 2006). Total Fe(II) was determined by the ferrozine method with the absorbance at 562 nm read

using a Thermo Scientific BioMate 3 UV/VIS Spectrophotometer. Aqueous Cr(VI) concentration was measured by the diphenylcarbazide method and the absorbance measured at 540 nm (USEPA, 1992). A Hach HQ40d pH meter was used to measure pH.

6.3.4 **Sequencing using the 16s Gene**

DNA was recovered from the microcosms using a FastDNA spin kit for soils (MP Biomedicals, USA).).

Polymerase chain reaction (PCR) was used to amplify a 1.5 kb fragment of the 16s rRNA gene using broad specificity primers. This was then ligated and transformed into XL1-blue competent *E.coli* cells UK Ltd) which were subsequently sent for sequencing.

Sequences were checked for chimeras using Mallard (v1.02) (Ashelford et al., 2006) before being grouped into operational taxonomic units (OTUs) using MOTHUR (v1.30.2)(Schloss et al., 2009). Sequences were classified using the Ribosomal Database Project (RDP) naïve Bayesian Classifier (Wang et al., 2007).ClustalX (v2.0) (Larkin et al., 2007) was used to align representative sequences from each OTU with selected type sequences, and then create a distance matrix by the neighbour joining method. Treeview (v1.6.6)(Page, 1996) was used to create and edit the final phylogenic trees. All sequences were submitted to the Genbank database with accession numbers KF797922 – KF798171.

6.3.5 **Isolation and Quantification of Soluble Electron-Shuttling Compounds**

Soluble electron shuttling compounds were extracted using the XAD-15 resin method as described in Chapter 3. Unused AFe media was subjected to the same extraction and used as a control.

Flavin quantification was performed by scanning wavelengths from 300-700 nm using a UV-2 UV/Vis spectrophotometer (Unicam). A standard curve was generated by observing known concentrations (0.05, 0.125, 0.25, 0.5, 1 $\mu mol.L^{-1}$) of riboflavin. An extinction coefficient at 455 nm (ε = 12,500 $cm^{-1}.M^{-1}$) was used to quantify concentration (Otto et al., 1981).

6.4 Results

6.4.1 **Bacteria Growth in Iron (III) Media (AFe)**

Since isolation, the bacteria have been repeatedly grown in AFe media. As detailed in Chapter 5, the average time before there is an increase in the Fe(II) concentration was ~100 hours. Iron reduction was accompanied with a reduction in pH from 9.2 to ~8.5. To aid comparison with growth characteristics in other media, part of Figure 5.8 has been reproduced here as Figure 6.1.

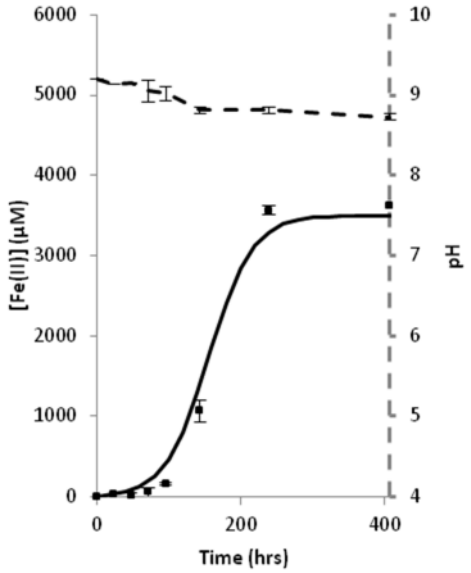

Figure 6.1: Fe(II) production and pH of the bacteria population grown in AFe media. Error bars indicate one standard deviation from the mean.

6.4.2 **Bacteria Growth in Iron(III) and Chromate Media (AFeCr)**

When the alkaliphilic iron reducing community was grown in AFeCr media essentially all the Cr(VI) was removed from the media where the initial Cr(VI) concentration was between 100 and 2000 µmol.L^{-1}. Cr(VI) removal started after ~500 hours, but the time taken for complete Cr(VI) increased with the initial Cr(VI) concentration, taking from 100 to 1000 hours (Figure 6.2A). Partial Cr(VI) reduction was seen in microcosms with initial Cr(VI) concentrations of 4500 and 8500 µmol.L^{-1}. It started after 720 and 1224 hours respectively, and after 1500 hours the Cr(VI) concentrations were 2800 and 7500 µmol.L^{-1}.

When the initial Cr(VI) concentration was ≤2000 µmol.L^{-1} an increased Fe(II) concentration followed the removal of Cr(VI) from solution (Figure 6.2B). Thus the time taken before Fe(II) production commenced increased with increasing initial Cr(VI) concentration. In the tests containing 100 to 2000 µmol.L^{-1} Cr(VI), growth in cell numbers is closely linked to the start of Fe(II) production. In tests where the initial Cr(VI) concentration was ≥4500 µmol.L^{-1}, growth in cell numbers commenced after ~1000 hours, before all the Cr(VI) was removed from solution, and before any Fe(II) was produced (Figure 6.2C). The pH value of all the tests remained fairly constant at 9.2 for ~400 hours before decreasing slightly to an average final pH of 8.5 (Figure 6.2D). Standard sigmoidal growth curves are shown in Figure 6.2C and D to represent the variation cell numbers and Fe(II) concentration with time (see equation 5.2 for full explanation (Zwietering et al., 1990)).

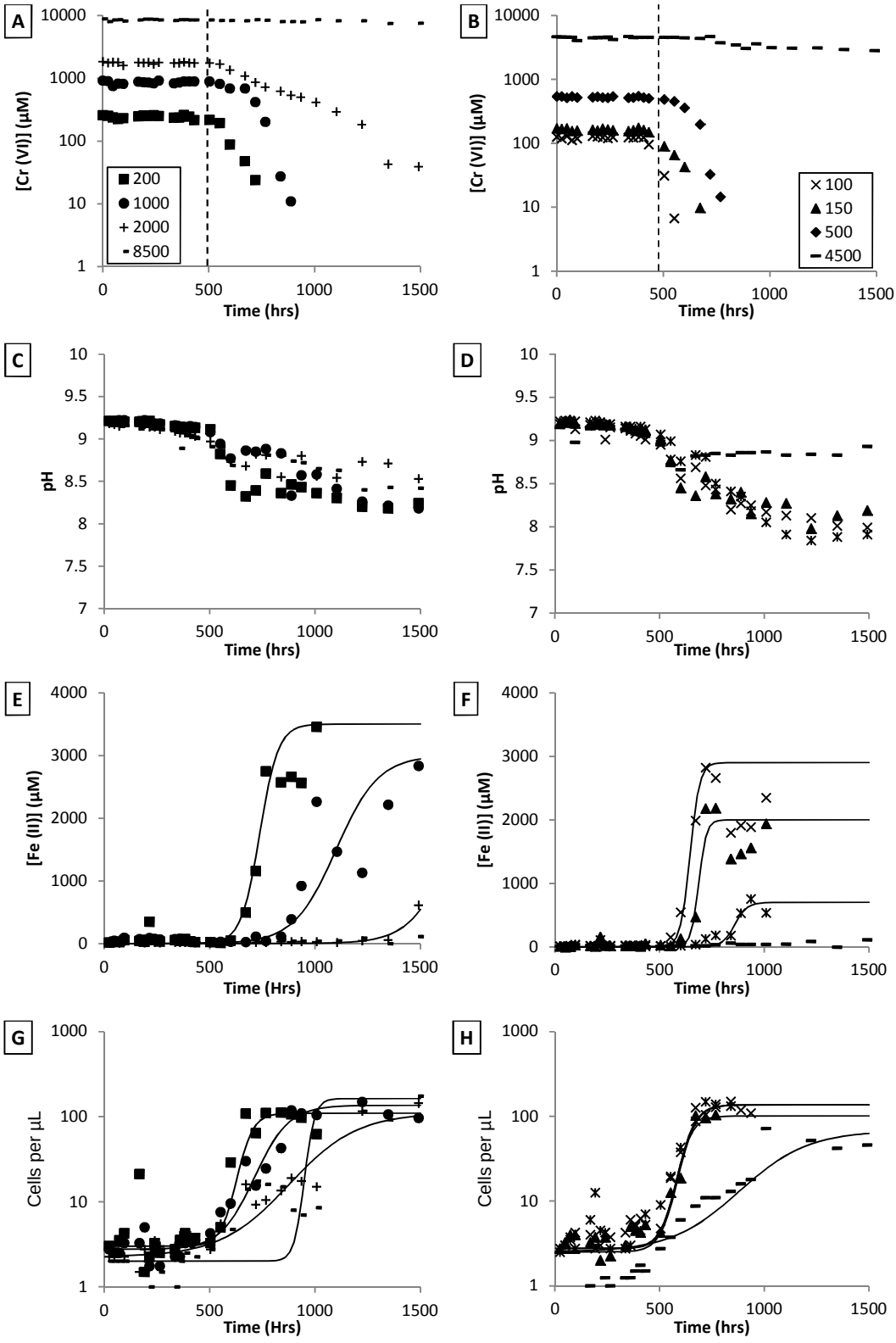

Figure 6.2: Growth of the Fe(III) reducing bacteria in AFeCr media with initial Cr concentrations ranging from 100 to 8500 µmol.L^{-1} (A,B) Cr(VI) concentration with time. The dashed line indicates when Cr(VI) reduction commenced for those tests with 100 to 2000 µmol.L^{-1} (C,D) Total Fe(II) concentration with time (E,F) cell numbers with time (G,H) pH with time.

6.4.3 **Bacteria Growth in Cr Media**

Bacteria in the upper exponential phase of growth were taken from AFe media and grown repeatedly in ACr media (this contains 200 µmol.L^{-1} Cr(VI) as the sole electron donor). Colour change of the media from yellow to clear was taken to indicate that Cr(VI) reduction had occurred (spectroscopic measurements on the cleared media from selected bottles confirmed that Cr(VI) < 20 µmol.L^{-1}). The bacteria were able to sustain fragile growth coupled to Cr(VI) reduction for 10 cycles before Cr(VI) reduction ceased (see Table 6.1 for success rates). In growth positive tests the time taken for complete Cr(VI) removal was about 25 days. Once growth coupled to Cr(VI) reduction had ceased, an aliquot of media from the 7th growth cycle was inoculated back into AFe media and grown on repeatedly. Sustained growth in AFe media was observed (the revived bacterial community will be referred to as the Cr(VI) reducing community).

Growth Cycle	1	2	3	4	5	6	7	8	9	10
Outcome	+++	++-	+--	++-	+--	+--	+--	++-	++-	---

Table 6.1: Record of growth of bacteria in media containing Cr(VI) as the sole electron donor. + denotes final concentration of Cr(VI) recorded as <10% of the initial concentration. – Indicates zero Cr(VI) reduction recorded.

6.4.4 **Bacteria Growth in Solid Phase Iron(III) Media**

The alkaliphilic Fe(III) reducing community and the Cr(VI) reducing community were inoculated into SFe media. Initially the amount of Fe(II) was very low because the Fe in the aquifer sand was predominantly in the Fe(III) oxidation state (Figure 6.3). In both systems there was an increase in the amount of Fe(II) after 250 hours. In the system inoculated with the alkaliphilic Fe(III) reducing community, the amount of Fe(II) increased to ~4000 µmol.L^{-1} after ~1000 hours. In the system inoculated with the Cr(VI)

reducing community, the amount of Fe(II) increased to ~1500 μmol.L^{-1} after ~1200 hours. In both systems the average pH dropped from 9.2 to ~8 during the first 250 hours and then remained steady while the amount of Fe(II) increased.

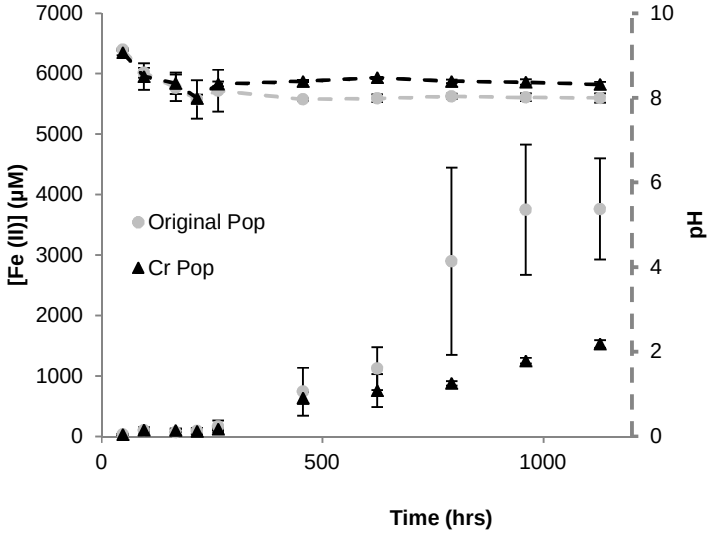

Figure 6.3: Average Fe (II) concentration and pH for bacteria grown in Fe (III) Solid phase media.○ denotes bacteria inoculated from the original AFe media. △ denotes bacteria inoculated from Cr(VI) media. Error bars indicate one standard deviation from the mean.

6.4.5 **Sequencing of the Bacteria population**

Cloning and sequencing of the bacteria from the AFeCr200 media (i.e. AFe media containing 200 μmol.L^{-1} Cr(VI)) produced 28 sequences from three different genera of bacteria presented. Mothur analysis indicated there 4 OTUs (based on >98% nearest neighbour similarity). These were the same as the Tissierella B, Tissierella C, Clostridium XI and Alkaliphillus OTUs in the original bacterial community (the representative sequences of each OTU from this population were FeCr200-11, FeCr200-19, FeCr200-23 and FeCr200-6, respectively).

Sixty sequences were obtained from the ACr media, and 59 were from genus Clostridium XI (representative sequence Cr44). These belonged to the same OTU as the Clostridium XI in the original bacterial community. One sequence was from genus Micrococcus (sequence Cr25, which was 97% similar to *Micrococcus luteus*). When this population was inoculated back into AFe media all 47 sequences were Clostridium XI (representative sequence CFe61). When it was then grown on solid phase Fe(III) all 32 sequences were Clostridium XI (representative sequence SCr1). In both cases these sequences were part of the same OTU as the Clostridium XI in the original bacterial community.

When the alkaliphilic Fe(III) reducing community was grown on solid phase Fe(III) 59 sequences were obtained from three different genera of bacteria. There are four different OTUs, 3 from the original population (5 Tissierella B sequences, 37 Tissierella C sequences and 2 Clostridium XI sequences) plus an OTU containing 15 Actinomycetales sequences (representative sequence SFE88 is 71% similar to *Actinomyces marimammalium*).

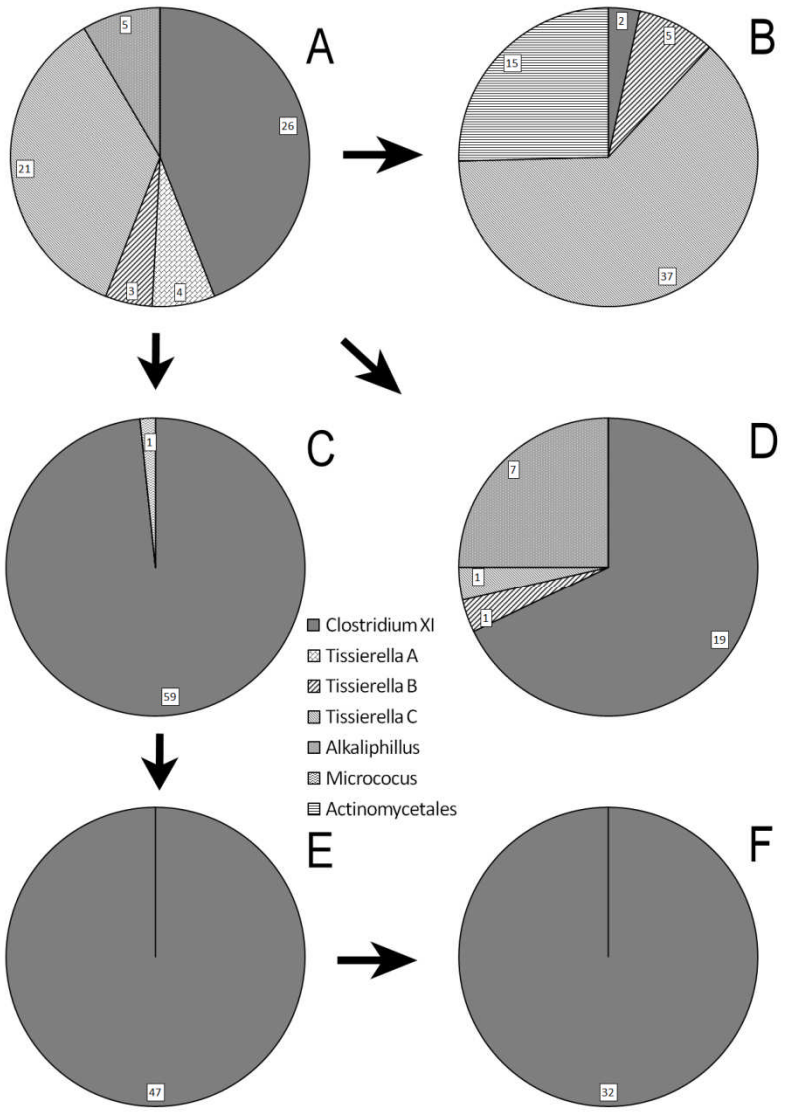

Figure 6.4: Pie charts showing the percentage of the bacterial population assigned to each OTU from (A) AFe media (B) Bacteria from A grown in SFe media. (C) Bacteria from A grown in Cr media (D) Bacteria from A grown in AFeCr200 media (E) bacteria from C grown in AFe media (F) Bacteria from E grown in SFe media.

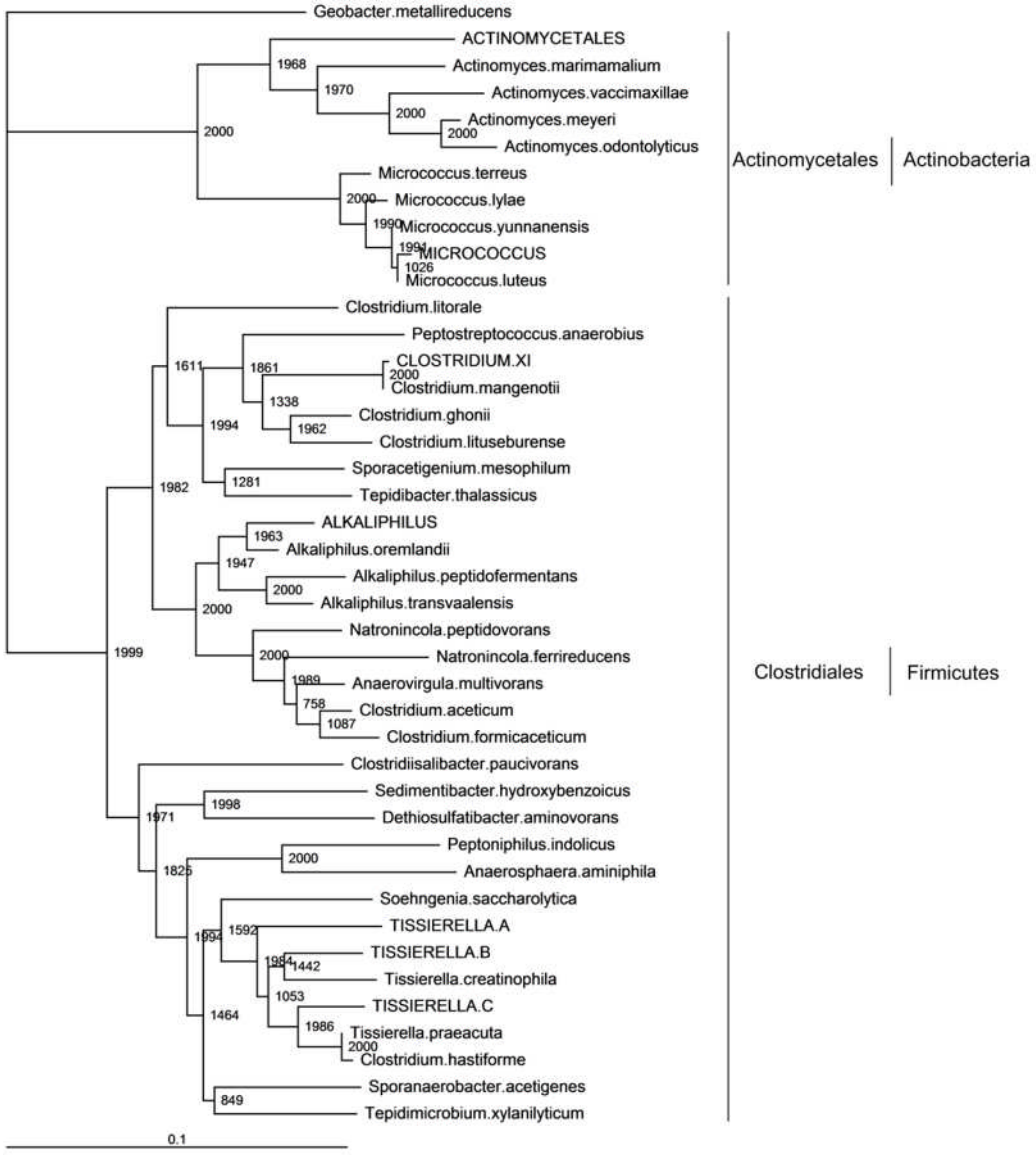

Figure 6.5: Phylogenic tree showing the relationship between representative sequences from each OTU and select type strains.

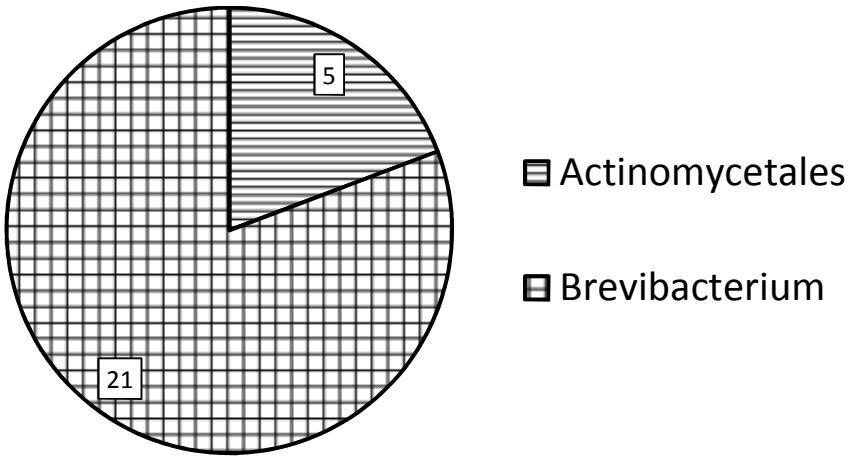

Figure 6.6: Pie chart showing the percentage of bacteria sequenced and assigned to each OTU from the AFeCr8500 media.

6.4.6 **Analysis for of Soluble Electron-Shuttling Compounds**

To investigate whether a soluble electron shuttling compound was involved in Fe(III) reduction, the spectral properties of spent media from the growth experiments with solid phase iron were studied. Scanning the culture supernatants over a wavelength range 300-550 nm revealed a large double peak from the Fe consortia whereas there was only a very slight peak from the Cr population (Figure 6.7A). Extraction of the extracellular compounds from the XAD-column showed a large double peak from the original Fe consortia whereas there was minimal associated with the Cr consortia (Figure 6.7B). Upon excitation at 441 nm the emission spectra from the extracellular compounds was found to be indistinguishable from those exhibited by commercially available riboflavin (Figure 6.7C). Quantification of the flavin compounds revealed there to be approximately 0.11 $\mu mol.L^{-1}$ in the Fe supernatant, and less than 0.01 $\mu mol.L^{-1}$ in the Cr.

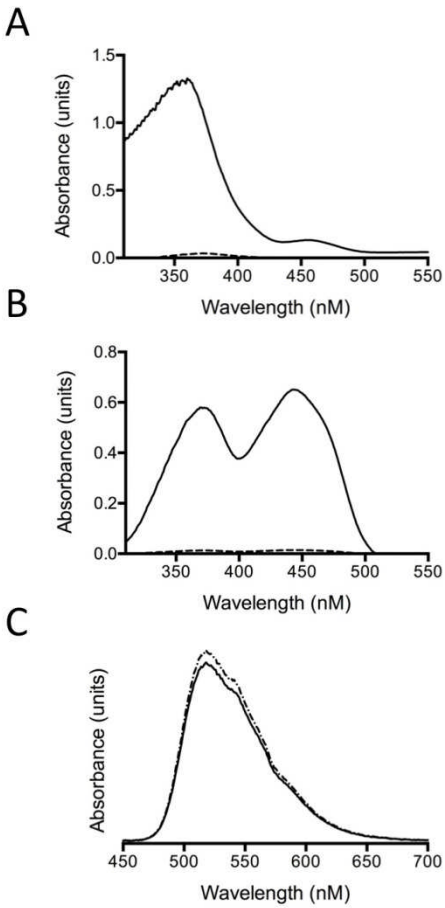

Figure 6.7: UV-visible spectra of (*A*) culture media supernatant after alkaliphilic consortium growth or (*B*) extracellular compounds isolated. Data is shown from samples taken from either iron consortia (solid lines) or chromium consortia (dotted lines). (*C*) Fluorescence spectra of extracellular compounds isolated from culture media supernatant (dashed line) compared to those from commercial pure riboflavin (solid line). Upon excitation at 441 nm, the emission spectra were monitored between 450 and 700 nm. Results shown are representative of two biological replicates.

6.5 Discussion

The alkaliphilic Fe(III)-reducing community has evolved very little since it was first isolated by Whittleston (2011) despite numerous further growth cycles in AFe media. Therefore the population of this community is now considered stable when grown in AFe media. It consists principally of three species of Tissierella (A, B and C), one species of Clostridium XI and one species of Alkaliphillus (however the sequencing density used does not preclude small numbers of other species, as evidenced by the actinomycetales bacteria found on agar plates in Chapter 5). When cultured in AFe media the lag time before exponential growth of the alkaliphilic Fe(III)-reducing community is about 3 days, and Fe(III) reduction was contemporaneous with that growth (see Chapter 5). Thus it is assumed that all dominant species in the community can respire with Fe(III) as the electron acceptor.

Introducing Cr(VI) into this media (i.e. AFeCr200 media) put a stress on this population, as growth in cell numbers was significantly delayed (the lag time increased from about 3 days to about 25 days). Cr(VI) removal started after about 20 days and was substantially complete before there was a significant change in the cell numbers. Fe(III) reduction started as the Cr(VI) was becoming exhausted, and was contemporaneous with an increase in cell numbers. The cell numbers after complete Fe(III) reduction were of similar order of magnitude in both AFe and AFeCr200 media, although the proportion of the population that were *Tissierella* species is much smaller in AFeCr200 media. The increased lag time in the presence of Cr(VI) suggests that it restricts cell growth, corroborated by the fact that cell numbers did not substantially increase until after Cr(VI) was removed from the media. This correlates with much of the literature which states that Cr(VI) is toxic and mutagenic to cells meaning that a high proportion of the population will have died on exposure to chromate (Dhal et al., 2013, Cervantes and Silver, 1992). This being the case, the bacteria in this study were originally exposed to Cr(VI) at the COPR site (Whittleston, 2011) and it has been reported that bacteria from contaminated sites are more resistant to toxic elements than others (Martins et al., 2010, Jeyasingh and Philip, 2005). Thus presumably all bacteria studied must have become tolerant to Cr(VI) in order to survive at

the original site. The change in community composition suggests that the *Tissierella* species are less tolerant of Cr than the *Clostridium XI* and *Alkaliphillus* species. Indeed other bacteria of these genus have demonstrated the ability to live in and reduce Cr(VI) (Roh et al., 2007, Martins et al., 2010) whereas there is no supporting literature to suggest the same of Tissierella bacteria, signifying Cr(VI) tolerance is possibly atypical of these bacteria.

All the AFeCr media tests with initial Cr(VI) concentrations from 100 to 2000 $\mu mol.L^{-1}$ exhibited similar patterns in Cr(VI) and Fe(III) reduction, and cell growth. Cr(VI) reduction commenced at roughly the same time (~20 days (see Figure 6.2A and B dashed line)) regardless of the initial Cr(VI) concentration and occurred without an appreciable change in the cell numbers. The time taken for complete Cr(VI) removal increased with Cr(VI) concentration, but data scatter makes it difficult to discern a trend in the rate of removal. Fe(III) reduction started as the Cr(VI) was becoming exhausted, and was contemporaneous with a significant increase in cell numbers. The similarities in growth characteristics of the alkaliphilic Fe(III)-reducing consortium in these media suggests that the initial Cr(VI) concentration affected the community in essentially the same way and the increased time it took for Cr(VI) removal to occur was only due to the time it took for the bacteria to reduce the increased concentrations of metal.

The AFeCr media tests with very high initial Cr(VI) concentrations (4,500 and 8,500 $\mu mol.L^{-1}$) behaved differently from those containing lower concentrations. In the test containing 4500 $\mu mol.L^{-1}$ Cr(VI), the removal of Cr(VI) from solution started after about 32 days and was only 60% complete after 56 days, yet cell numbers started to increase after 39 days. In the test containing 8500 $\mu mol.L^{-1}$ Cr(VI), there was very little change in the Cr(VI) concentration (it decreased by <10% over the test), yet cell numbers started to increase after ~60 days (cell numbers were only ~20% of the numbers seen after Fe(III) reduction in the lower Cr(VI) concentration tests). The microbial population of the 8500 $\mu mol.L^{-1}$ microcosm consisted of Brevibacterium and Actinomycetales bacteria (see Figure 6.6). Brevibacterium are both rod and cocoid of shape, gram positive and isolated

from many environments including those with high salt content (Collins, 2006) whereas Actinomycetales bacteria are also gram positive bacteria isolated from many different sources (Cummins and Harris, 1958). The soil organisms seen in this study, may have grown fermentatively using yeast extract, as other members of these genus' have previously been shown to respire in this way (Nampoothiri and Pandey, 1995, Pine and Georg, 1965, Collins, 2006). This being the case, other *Brevibacterium sp*. have been found able to reduce Cr(VI) (Das and Mishra, 2010) which if similar to the bacteria in this study would account for the small reduction in Cr(VI) in these microcosms. Either theory would explain why the increase in cell numbers is not associated with Fe(II) production. Both species were presumably a very small component of the initial population and were either highly adapted to living with Cr(VI) or extremely hardy.

Attempts to grow the alkaliphilic Fe(III)-reducing community in ACr media (200 $\mu mol.L^{-1}$ Cr(VI)) were only partially successful, with no growth in some replicates and attempts to culture-on the community failing completely after 10 growth cycles. This is not a surprise as very few bacteria have been found which are able to respire using Cr(VI) as the sole electron donor (Daulton et al., 2007). Failure to get a community that grew reliably meant that growth could not be characterised in detail, but the time taken for complete Cr(VI) reduction in the ACr media was very similar to the time taken for complete Cr(VI) reduction AFeCr200 (in both case about ~25 to 30 days). After 7 growth cycles the population was dominated by Clostridium XI, indicating that this species can respire using Cr(VI) as the sole electron acceptor however, the fragile nature of the growth suggests that this may be an unintentional result of reductive mechanisms within the cell not specifically designed for Cr(VI) reduction.

When the alkaliphilic Fe(III)-reducing community was cultured in SFe media (i.e. aquifer sand as a source of solid phase iron), Fe(III) reduction to Fe(II) became apparent after about 10 days. Growth in SFe media led to an increased abundance of Tissierella C species (from ~1/3 to >2/3 of sequences). When the Cr(VI)-reducing community was cultured in the same media Fe(II) production became apparent after a similar time period, however

after 50 days, the amount of Fe(II) produced by the original community was nearly 3 times greater than by the Cr(VI)-reducing community. Results from Chapter 5 showed that when the alkaliphilic Fe(III)-reducing community was grown in AFe media, cell growth and Fe(III)-reduction occurred contemporaneously with the release of riboflavin into the media. It was demonstrated that the Tissierella C species could release this compound, which is able to act as an electron shuttling compound during extracellular Fe(III) reduction (Marsili et al., 2008, von Canstein et al., 2008). These results show that growth of the alkaliphilic Fe(III)-reducing community in SFe media resulted in the release of the same riboflavin like molecule into the media, whereas growth of the Clostridium XI dominated Cr(VI)-reducing community did not. This result convincingly shows that the Clostridium XI bacteria do not reduce Fe(III) by the production of riboflavin. However, the increased dominance of Tissierella C species in the SFe media strongly supports the hypothesis that this species releases this electron shuttling compound. The increased rate of Fe(III) reduction (in comparison with the Clostridium XI dominated system), supports the hypothesis that the riboflavin-like molecule acts as an electron shuttling compound during extracellular Fe(III) reduction and is therefore an advantage when reducing solid phase Fe(III) electron acceptors as riboflavin is able to reduce most Fe(III) oxides as well as many soluble forms of the metal (Marsili et al., 2008).

It is clear that the *Clostridium XI* sp. has the ability reduce solid phase iron, as Fe(III) is very sparingly soluble at pH values above pH8 in the absence of complexing ligands such a citrate (Langmuir, 1997); thus it is speculated that Clostridium XI must interact with solid phase iron by another mechanism. These bacteria, being gram positive in design, lack the outer membrane required for c-type cytosomes; already identified as essential for contact reduction of Fe(III) (Williamson et al., 2013, Lovley, 2008). Thus further work must be done in order to identify the reductive mechanism of these bacteria.

6.6 Implications for the Bioremediation of COPR impacted sites

This paper clearly shows that bioremediation has great potential for the treatment of highly alkaline COPR impacted sites. Leachate from the historical COPR site whence the bacteria were isolated has a Cr(VI) concentration of 1000 µmol.L^{-1} within the waste and 200 µmol.L^{-1} within the drainage ditch adjacent to the site (Stewart et al., 2010). These results show that bacteria from the same site are able to grow and reduce chromate in liquors containing up to 2000 µmol.L^{-1} Cr(VI). This ability surpasses the maximum chromate concentration of leachate reported on any COPR disposal site thus far (Whittleston et al., 2011). In most microcosms, pH buffered downwards to around 8.5 before the exponential phase of growth indicating that the bacteria in this study are most comfortable at lower pH. This is interesting as others have found that buffering the pH of aquifers down to ~9, results in more robust Fe(III) reduction (Whittleston et al., 2013).

The high pH of COPR leachate in comparison with the pH range used in this study may seem to point to a poor prognosis for bioremediation at such sites, however rapid buffering of COPR leachate by soil minerals means that pH quickly drops whilst moving away from a COPR site (Whittleston, 2011). Therefore the area in which a biobarrier should be implemented may be slightly downstream from the waste in less alkaline conditions in order to achieve maximum bacteria growth. Less alkaline areas are likely to host a much more diverse bacteria population compared to the highly alkaline COPR waste, further enhancing the likelihood of success. Another option to improve the chances of success could be reducing the pH of affected groundwater by the addition of acid or bicarbonate (Whittleston et al., 2013).

Whilst the changes to the bacteria population in these microcosms have been significant when grown in the differing media, in the natural environment the bacterial population native to COPR sites (especially those been in place for some time) are likely to be stable, highly adapted to their surroundings and resistant to Cr(VI) toxicity (Martins et al., 2010). The fact that the bacteria in this study were originally growing by a COPR site indicates that at this location were all the ingredients required to sustain

them. Thus augmenting a contaminated subsurface with a complex electron donor such as yeast extract (which is likely to support the growth of more varieties of bacteria than simpler electron donors (see Chapter 5)) is likely to result in an increase in cell growth and as a consequence the required remediative effect.

This study highlights *Clostridium mangenoti* as a bacteria capable of alkaline Fe(III) and Cr(VI) reduction which is important as this particular strain has been found in many different soils around the world and has been described as ubiquitous (Smith, 1975). Indeed it has been found in similar studies on bacteria hailing from a highly alkaline, lime processing site and been shown to reduce Fe(III), indicating that it is comfortable in the alkaline environment (Williamson et al., 2013). This means that it is highly likely to be present in soil close to other COPR sites. Bacterially produced riboflavin electron shuttles, being soluble, will propagate until they are reduced; effectively creating a biobarrier wider than the immediate cell habitat. As Chapter 5 has shown, as well as others such as Williamson et al. (2013), that spiking alkaliphilic bacteria with riboflavin resulted in more robust Fe(III) reduction, it may be beneficial to add riboflavin to contaminated soils to achieve the same affect.

Whilst this study has concentrated on Fe(III) and Cr(VI) reduction with respect to COPR contaminated sites, the results have important and far reaching implications for the bioremediation of all the oxyanions highlighted in the introduction of this chapter. Direct reduction of these contaminants will probably be facilitated by a select few, highly adapted bacteria at each site, however results from this study show that Fe(III) reduction is likely to be a much more significant process within an alkaline contaminated geosphere. This means that the success of a bioremediation scheme will depend primarily on Fe(III) reducing bacteria which only have to be tolerant to the contaminant in which they grow. Iron's ubiquity in nature (and therefore the presence of Fe(III) reducing bacteria in most environments) coupled with the fact that bacteria are notoriously quick to adapt to challenging environments means that bioremediation holds much promise for the treatment of all the oxyanion contaminants mentioned.

6.7 Conclusions

Bacteria were able to completely remove Cr(VI) from liquors containing 2000 $\mu mol.L^{-1}$ Cr(VI) with part removal recorded in liquors containing 8500 $\mu mol.L^{-1}$. Exponential cell growth was associated with Fe(II) reduction suggesting this is the significant process whilst dealing with the bacteria. Bacteria were able to sustain fragile growth whilst using Cr(VI) as the sole electron acceptor. As the population of bacteria were introduced to Cr(VI), the diversity fell and Clostridium XI bacteria dominated. Growth of the consortia in solid phase Fe(III) media caused the population to shift towards those bacteria which produce riboflavin electron shuttles. Thus bioremediation holds much promise for the treatment of alkaline affected sites where redox active contaminants are found

6.8 References

Abdelouas, A., Lu, Y., Lutze, W. & Nuttall, H. E. 1998. Reduction of U(VI) to U(IV) by indigenous bacteria in contaminated ground water. *J. Contam. Hydrol.,* 35**,** 217-233.

Ashelford, K. E., Chuzhanova, N. A., Fry, J. C., Jones, A. J. & Weightman, A. J. 2006. New Screening Software Shows that Most Recent Large 16S rRNA Gene Clone Libraries Contain Chimeras. *Appl. Environ. Microbiol.,* 72**,** 5734-5741.

Bae, S. & Lee, W. 2013. Biotransformation of lepidocrocite in the presence of quinones and flavins. *Geochim. Cosmochim. Acta,* 114**,** 144-155.

Burke, I. T., Boothman, C., Lloyd, J. R., Livens, F. R., Charnock, J. M., McBeth, J. M., Mortimer, R. J. G. & Morris, K. 2006. Reoxidation Behavior of Technetium, Iron, and Sulfur in Estuarine Sediments. *Environ. Sci. Technol.,* 40**,** 3529-3535.

Burke, I. T., Peacock, C. L., Lockwood, C. L., Stewart, D. I., Mortimer, R. J. G., Ward, M. B., Renforth, P., Gruiz, K. & Mayes, W. M. 2013. Behavior of Aluminum, Arsenic, and Vanadium during the Neutralization of Red Mud Leachate by HCl, Gypsum, or Seawater. *Environ. Sci. Technol.,* 47**,** 6527-6535.

Carpentier, W., De Smet, L., Van Beeumen, J. & Brigé, A. 2005. Respiration and Growth of Shewanella oneidensis MR-1 Using Vanadate as the Sole Electron Acceptor. *Journal of Bacteriology,* 187**,** 3293-3301.

Cervantes, C. & Silver, S. 1992. Plasmid chromate resistance and chromate reduction. *Plasmid,* 27**,** 65-71.

Charlet, L., Scheinost, A. C., Tournassat, C., Greneche, J. M., Géhin, A., Fernández-Martı´nez, A., Coudert, S., Tisserand, D. & Brendle, J. 2007. Electron transfer at the mineral/water interface: Selenium reduction by ferrous iron sorbed on clay. *Geochimica et Cosmochimica Acta,* 71**,** 5731-5749.

Collins, M. D. 2006. The Genus Brevibacterium. *In:* Dworkin, M. & Falkow, S. (eds.) *The Prokaryotes: Vol. 3: Archaea. Bacteria: Firmicutes, Actinomycetes.* Springer.

Costa, M. 1997. Toxicity and Carcinogenicity of Cr(VI) in Animal Models and Humans. *Crit. Rev. Toxicol.,* 27**,** 431-442.

Cummins, C. S. & Harris, H. 1958. Studies on the Cell-Wall Composition and Taxonomy of Actinomycetales and Related Groups. *Journal of General Microbiology,* 18**,** 173-189.

Das, A. P. & Mishra, S. 2010. Biodegradation of the metallic carcinogen hexavalent chromium Cr(VI) by an indigenously isolated bacterial strain. *J Carcinog,* 9**,** 1477-3163.

Daulton, T. L., Little, B. J., Jones-Meehan, J., Blom, D. A. & Allard, L. F. 2007. Microbial reduction of chromium from the hexavalent to divalent state. *Geochim. Cosmochim. Acta,* 71**,** 556-565.

Deakin, D., West, L. J., Stewart, D. I. & Yardley, B. W. D. 2001. Leaching behaviour of a chromium smelter waste heap. *Waste Management,* 21**,** 265-270.

Dhal, B., Thatoi, H. N., Das, N. N. & Pandey, B. D. 2013. Chemical and microbial remediation of hexavalent chromium from contaminated soil and mining/metallurgical solid waste: A review. *J. Hazard. Mater.,* 250–251**,** 272-291.

Gao, H., Yang, Z. K., Barua, S., Reed, S. B., Romine, M. F., Nealson, K. H., Fredrickson, J. K., Tiedje, J. M. & Zhou, J. 2009. Reduction of nitrate in Shewanella oneidensis depends on atypical NAP and NRF systems with NapB as a preferred electron transport protein from CymA to NapA. *Isme. J.,* 3**,** 966-76.

Glasauer, S., Langley, S., Boyanov, M., Lai, B., Kemner, K. & Beveridge, T. J. 2007. Mixed-Valence Cytoplasmic Iron Granules Are Linked to Anaerobic Respiration. *Applied and Environmental Microbiology,* 73**,** 993-996.

Gorby, Y. A., Yanina, S., McLean, J. S., Rosso, K. M., Moyles, D., Dohnalkova, A., Beveridge, T. J., Chang, I. S., Kim, B. H., Kim, K. S., Culley, D. E., Reed, S. B., Romine, M. F., Saffarini, D. A., Hill, E. A., Shi, L., Elias, D. A., Kennedy, D. W., Pinchuk, G., Watanabe, K., Ishii, S. i., Logan, B., Nealson, K. H. & Fredrickson, J. K. 2006. Electrically conductive bacterial nanowires produced by Shewanella oneidensis strain MR-1 and other microorganisms. *Proceedings of the National Academy of Sciences,* 103**,** 11358-11363.

Gorlenko, V., Tsapin, A., Namsaraev, Z., Teal, T., Tourova, T., Engler, D., Mielke, R. & Nealson, K. 2004. Anaerobranca californiensis sp nov., an anaerobic, alkalithermophilic, fermentative bacterium isolated from a hot spring on Mono Lake. *Int. J. Syst. Evol. Microbiol.,* 54**,** 739-743.

Harish, R., Samuel, J., Mishra, R., Chandrasekaran, N. & Mukherjee, A. 2012. Bio-reduction of Cr(VI) by exopolysaccharides (EPS) from indigenous bacterial species of Sukinda chromite mine, India. *Biodegradation,* 23**,** 487-496.

Higgins, T. E., Halloran, A. R., Dobbins, M. E. & Pittignano, A. J. 1998. In situ reduction of hexavalent chromium in alkaline soils enriched with chromite ore processing residue. *J. Air Waste Manag. Assoc.,* 48**,** 1100-1106.

Jankowski, J., Ward, C. R., French, D. & Groves, S. 2006. Mobility of trace elements from selected Australian fly ashes and its potential impact on aquatic ecosystems. *Fuel,* 85**,** 243-256.

Jeyasingh, J. & Philip, L. 2005. Bioremediation of chromium contaminated soil: optimization of operating parameters under laboratory conditions. *J. Hazard. Mater.,* 118**,** 113-120.

Karim, M. M. 2000. Arsenic in groundwater and health problems in Bangladesh. *Water Research,* 34**,** 304-310.

Kim, B. H. & Gadd, G. M. 2008. *Bacterial Physiology and Metabolism*, Cambridge University Press.

Langmuir, D. 1997. *Aqueous environmental geochemistry*, Prentice Hall.

Larkin, M. A., Blackshields, G., Brown, N. P., Chenna, R., McGettigan, P. A., McWilliam, H., Valentin, F., Wallace, I. M., Wilm, A., Lopez, R., Thompson, J. D., Gibson, T. J. & Higgins, D. G. 2007. Clustal W and clustal X version 2.0. *Bioinformatics,* 23**,** 2947-2948.

Liermann, L. J., Hausrath, E. M., Anbar, A. D. & Brantley, S. L. 2007. Assimilatory and dissimilatory processes of microorganisms affecting metals in the environment. *Journal of Analytical Atomic Spectrometry,* 22**,** 867-877.

Liu, C., Gorby, Y. A., Zachara, J. M., Fredrickson, J. K. & Brown, C. F. 2002. Reduction kinetics of Fe(III), Co(III), U(VI), Cr(VI), and Tc(VII) in cultures of dissimilatory metal-reducing bacteria. *Biotechnol. Bioeng.,* 80**,** 637-649.

Lloyd, J. R. & Lovley, D. R. 2001. Microbial detoxification of metals and radionuclides. *Curr. Opin. Biotechnol.,* 12**,** 248-253.

Lloyd, J. R., Sole, V. A., Van Praagh, C. V. G. & Lovley, D. R. 2000. Direct and Fe(II)-Mediated Reduction of Technetium by Fe(III)-Reducing Bacteria. *Applied and Environmental Microbiology,* 66**,** 3743-3749.

Lovley, D. R. 1993. Dissimilatory Metal Reduction. *Annu. Rev. Microbiol.,* 47**,** 263-290.

Lovley, D. R. 1997. Microbial Fe(III) reduction in subsurface environments. *FEMS Microbiol. Rev.,* 20**,** 305-313.

Lovley, D. R. 2001. Anaerobes to the Rescue. *Science,* 293**,** 1444-1446.

Lovley, D. R. 2008. Extracellular electron transfer: wires, capacitors, iron lungs, and more. *Geobiology,* 6**,** 225-231.

Lovley, D. R., Fraga, J. L., Blunt-Harris, E. L., Hayes, L. A., Phillips, E. J. P. & Coates, J. D. 1998. Humic substances as a mediator for microbially catalyzed metal reduction. *Acta Hydrochimica et Hydrobiologica,* 26**,** 152-157.

Lovley, D. R. & Phillips, E. J. P. 1994. Reduction of Chromate by Desulfovibro-Vulgaris and its C(3) Cytochrome. *Appl. Environ. Microbiol.,* 60**,** 726-728.

Madigan, M. T., Martinko, J. M. & Parker, J. 2003. *Brock biology of microorganisms*, Prentice Hall/Pearson Education.

Marsili, E., Baron, D. B., Shikhare, I. D., Coursolle, D., Gralnick, J. A. & Bond, D. R. 2008. Shewanella Secretes Flavins That Mediate Extracellular Electron Transfer. *Proc. Natl. Acad. Sci. U.S.A.,* 105**,** 3968-3973.

Martins, M., Faleiro, M. L., Chaves, S., Tenreiro, R., Santos, E. & Costa, M. C. 2010. Anaerobic bio-removal of uranium (VI) and chromium (VI): Comparison of microbial community structure. *Journal of Hazardous Materials,* 176**,** 1065-1072.

Mayes, W. M. & Younger, P. L. 2006. Buffering of Alkaline Steel Slag Leachate across a Natural Wetland. *Environmental Science & Technology,* 40**,** 1237-1243.

Mayes, W. M., Younger, P. L. & Aumônier, J. 2008. Hydrogeochemistry of Alkaline Steel Slag Leachates in the UK. *Water, Air, and Soil Pollution,* 195**,** 35-50.

Nampoothiri, K. M. & Pandey, A. 1995. Effect of different carbon sources on growth and glutamic acid fermentation by Brevibacterium sp. *Journal of Basic Microbiology,* 35**,** 249-254.

O'Loughlin, E. J., Gorski, C. A., Scherer, M. M., Boyanov, M. I. & Kemner, K. M. 2010. Effects of Oxyanions, Natural Organic Matter, and Bacterial Cell Numbers on the Bioreduction of Lepidocrocite (γ-FeOOH) and the Formation of Secondary Mineralization Products. *Environmental Science & Technology,* 44**,** 4570-4576.

Otto, M. K., Jayaram, M., Hamilton, R. M. & Delbruck, M. 1981. Replacement of riboflavin by an analogue in the blue-light photoreceptor of Phycomyces. *Proc. Natl. Acad. Sci. U.S.A.,* 78**,** 266-9.

Page, R. D. M. 1996. TreeView: An application to display phylogenetic trees on personal computers. *Comput. Appl. Biosci.,* 12**,** 357-358.

Pine, L. & Georg, L. 1965. The classification and phylogenetic relationships of the Actinomycetales. *International Bulletin of Bacteriological Nomenclature and Taxonomy,* 15**,** 143-164.

Rabus, R. 2006. Dissimilatory Sulfate- and Sulfur-Reducing Prokaryotes. *In:* Martin Dworkin, S. F., Eugene Rosenberg, Karl-Heinz Schleifer (ed.) *The Prokaryotes.*

Rai, D., Sass, B. M. & Moore, D. A. 1987. Chromium(III) Hydrolysis Constants and Solubility of Chromium(III) Hydroxide. *Inorg. Chem.,* 26**,** 345-349.

Rey, S. & Reggiani, G. M. 2005. Molybdate and Non-Molybdate Options for Closed Systems – Part II. *AWT Annual Convention.* Palm Springs: Cooling Water Subcommittee of the AWT Technical Committee.

Richard, F. C. & Bourg, A. C. M. 1991. Aqueous geochemistry of chromium: A review. *Water Res.,* 25**,** 807-816.

Roh, Y., Chon, C.-M. & Moon, J.-W. 2007. Metal reduction and biomineralization by an alkaliphilic metal-reducing bacterium,Alkaliphilus metalliredigens. *Geosci. J.,* 11**,** 415-423.

Schloss, P. D., Westcott, S. L., Ryabin, T., Hall, J. R., Hartmann, M., Hollister, E. B., Lesniewski, R. A., Oakley, B. B., Parks, D. H., Robinson, C. J., Sahl, J. W., Stres, B., Thallinger, G. G., Van Horn, D. J. & Weber, C. F. 2009. Introducing mothur: Open-Source, Platform-Independent, Community-Supported Software for Describing and Comparing Microbial Communities. *Appl. Environ. Microbiol.,* 75**,** 7537-7541.

Shukor, M. Y., Ahmad, S. A., Nadzir, M. M. M., Abdullah, M. P., Shamaan, N. A. & Syed, M. A. 2010. Molybdate reduction by Pseudomonas sp strain DRY2. *Journal of Applied Microbiology,* 108**,** 2050-2058.

Smith, L. D. 1975. Common Mesophilic Anaerobes, Including Clostridium botulinum and Clostridium tetani, in 21 Soil Specimens. *Appl. Environ. Microbiol.,* 29**,** 590-594.

Stewart, D. I., Burke, I. T., Hughes-Berry, D. V. & Whittleston, R. A. 2010. Microbially mediated chromate reduction in soil contaminated by highly alkaline leachate from chromium containing waste. *Ecol. Eng.,* 36**,** 211-221.

Stewart, D. I., Cousens, T. W. & Charles-Cruz, C. A. 2006. The interpretation of CPT data from hydraulically placed PFA. *Engineering Geology,* 85**,** 184-196.

USEPA 1992. SW-846 Manual: Method 7196a. Chromium hexavalent (colorimetric).

Veeramani, H., Alessi, D. S., Suvorova, E. I., Lezama-Pacheco, J. S., Stubbs, J. E., Sharp, J. O., Dippon, U., Kappler, A., Bargar, J. R. & Bernier-Latmani, R. 2011. Products of abiotic U(VI) reduction by biogenic magnetite and vivianite. *Geochim. Cosmochim. Acta,* 75**,** 2512-2528.

von Canstein, H., Ogawa, J., Shimizu, S. & Lloyd, J. R. 2008. Secretion of Flavins by Shewanella Species and Their Role in Extracellular Electron Transfer. *Appl. Environ. Microbiol.,* 74**,** 615-623.

Wang, Q., Garrity, G. M., Tiedje, J. M. & Cole, J. R. 2007. Naïve Bayesian Classifier for Rapid Assignment of rRNA Sequences into the New Bacterial Taxonomy. *Appl. Environ. Microbiol.,* 73**,** 5261-5267.

Wang, Y.-T. & Shen, H. 1997. Modelling Cr(VI) reduction by pure bacterial cultures. *Water Res.,* 31**,** 727-732.

Weber, K. A., Picardal, F. W. & Roden, E. E. 2001. Microbially Catalyzed Nitrate-Dependent Oxidation of Biogenic Solid-Phase Fe(II) Compounds. *Environmental Science & Technology,* 35**,** 1644-1650.

White, A. F. & Peterson, M. L. 1996. Reduction of aqueous transition metal species on the surfaces of Fe(II) -containing oxides. *Geochimica et Cosmochimica Acta,* 60**,** 3799-3814.

Whittleston, R. A. 2011. *Bioremediation of chromate in alkaline sediment-water systems.* PhD thesis, University of Leeds.

Whittleston, R. A., Stewart, D. I., Mortimer, R. J. G. & Burke, I. T. 2013. Enhancing microbial iron reduction in hyperalkaline, chromium contaminated sediments by pH amendment. *Appl. Geochem.,* 28**,** 135-144.

Whittleston, R. A., Stewart, D. I., Mortimer, R. J. G., Tilt, Z. C., Brown, A. P., Geraki, K. & Burke, I. T. 2011. Chromate reduction in Fe(II)-containing soil affected by hyperalkaline leachate from chromite ore processing residue. *J. Hazard. Mater.,* 194**,** 15-23.

Williamson, A. J., Morris, K., Shaw, S., Byrne, J. M., Boothman, C. & Lloyd, J. R. 2013. Microbial Reduction of Fe(III) under Alkaline Conditions Relevant to Geological Disposal. *Applied and Environmental Microbiology,* 79**,** 3320-3326.

Zhilina, T. N., Zavarzina, D. G., Kolganova, T. V., Lysenko, A. M. & Tourova, T. P. 2009. Alkaliphilus peptidofermentans sp. nov., a new alkaliphilic bacterial

soda lake isolate capable of peptide fermentation and Fe(III) reduction. *Microbiology,* 78**,** 445-454.

Zwietering, M. H., Jongenburger, I., Rombouts, F. M. & VAN 'T Riet, K. 1990. Modeling of the Bacterial Growth Curve. *Appl. Environ. Microbiol.,* 56**,** 1875-1881.

Chapter 7 **Conclusions and Future Work**

The desire of this study was to present research so that a workable, sustainable remediation strategy for highly alkaline chromite ore processing residue (COPR) waste could be found and enacted by practicing engineers. Due to the health implications of aerating Cr(VI) containing dust, strategies whereby the leachate leaving COPR sites is treated and the waste left undisturbed were deemed to be the only ones suitable. This study concentrated on zero valent iron permeable reactive barriers (ZVI-PRBs) and biobarriers, and assessed their suitability to remediate Cr(VI) impacted leachate. The major findings of this work are represented below.

7.1 Conclusions

7.1.1 **Permeable Reactive Barriers**

PRBs already have a successful track record in treating a number of different groundwater contaminants (Morrison, 2002) and are potentially an ideal solution for COPR sites as their installation requires minimal ground disruption. ZVI barriers have been deployed at a number of Cr(VI) contaminated sites however these have always been in either acid or neutral conditions (Wilkin et al., 2005). Thus this study sort to evaluate the performance of ZVIPRBs in hyper alkaline conditions, as found at COPR sites.

Results from Chapter 4 show that reduction of Cr(VI) by ZVI is possible at pH 12, however the reaction is slow and will cease at low solid:solution ratios. Lowering the leachate pH appeared to have little effect on the Cr(VI) reduction rate until the acidic range was reached. Rate coefficients presented in Figure 4.7 suggest that the reaction mechanism changes as pH enters the acidic range, however, there are insufficient data in the acidic range to definitively prove this point. Although theoretically possible to amend pH on site, implementation would be problematic as large volumes of

acid would be required due to the massive buffering capacity of COPR (Tinjum et al., 2008). An unwanted consequence of buffering the pH so low would be the liberation of many other metals from the surrounding minerals (Weng et al., 1994). Similarly Cr(III) becomes soluble at low pH meaning that it is unlikely to be retained within a barrier.

Comparing reduction at pH 12 between Cr(VI) solutions and COPR leachate found that removal occurred quicker and for longer from simple Cr(VI) solutions. SEM and XPS analysis of iron exposed to the two liquors showed that whilst both sets of iron retained Cr(III) compounds on the surface (as a remnant of Cr(VI) reduction), the iron exposed to COPR leachate also had many other compounds precipitated on its surface. Results suggest that these compounds, predominantly consisting of silica and calcium, were blocking potential reaction sites and thus reducing the specific reactive capacity of the iron.

These data indicate that upon construction, unwanted surface reactions would result in a reduced design life for a ZVI-PRB as the iron would quickly become inert. Thus either a strategy of implementing a wide barrier to increase the available iron, or one whereby the iron is replaced regularly could be possible; however both require extra cost, complicate an otherwise very simple design and could therefore make such a scheme unviable. The wider implications of this work are important for all ZVI barrier designs in hyperalkaline conditions, as when the pH of groundwater increases, the incidence of other soil derived minerals becoming soluble within the leachate (eg. Si) will also increase; thereby escalating the likelihood of the iron becoming inhibited. For example the pH at which the solubility of silica becomes significant in groundwater is 9.5 (Langmuir, 1997). This pH could represent the upper limit for which ZVI can be successfully applied in any PRB scheme.

7.1.2 **Biobarriers**

Biobarriers utilise the natural bacteria population within the subsurface to reduce contaminants as a result of their respiration processes. By augmenting a contaminated groundscape with extra electron donor, bacteria growth is encouraged, leading to an increase in bacterial activity and as a

consequence dissimilatory reduction reactions. The advantages of this technique include minimal cost and lack of disruption to the ground – vital for the remediation of COPR.

Chapter 5 shows how a population of bacteria isolated from soils below a 19th century COPR site were able to reduce soluble Fe(III) (ferric citrate) and produce Fe(II). This is important for remediation as Fe(II) is capable of reducing Cr(VI) to Cr(III) abiotically. Iron reduction was linked with the exponential phase of cell growth, lowering of pH and an increase in ATP concentration. SEM and EDX analysis of the Fe(II) mineral produced by the bacteria revealed that it was most likely to be vivianite (an Fe(II) phase which has previously been shown to be produced by bioreduction of Fe(III) in the presence of phosphates (Bae and Lee, 2013)). The bacteria population was characterised revealing bacteria representing three different genera which was further divided into 5 different OTUs (*Clostridium XI*, *Alkaliphilus* and *Tissierella* A, B and C). Analysis of the supernatant from these microcosms showed that the production of riboflavin, a soluble electron shuttle, accompanied the accumulation of Fe(II), indicating that this was an important respiration process for some of the bacteria within the population. This is significant as it is the first time riboflavin production has been documented in the alkaline pH range. Augmenting the growth media with extra riboflavin reduced the lag phase of growth and increased the rate at which Fe(III) was reduced by the bacteria population. In order to identify those species which were producing riboflavin, the population was transferred to solid agar plates. Fe(III) reduction resulted in colour change of the plates from orange to clear accompanied by the production of very fine black particulates. Isolated colonies were streaked on fresh plates resulting in some streaks which cleared the area around them and some which did not. For those streaks that cleared, the reduction in colour was visible beyond the confines of cell growth indicating that reduction was occurring away from the cell – indicative behaviour of an external electron shuttle. Sequencing of the streaks which cleared showed them all to be from the same OTU, *Tissierella* C.

The production of a soluble electron shuttle is important from a Bioremediative perspective as it means that the bacteria do not have to be

physically connected to the electron acceptor that they are reducing. This potentially opens up a much greater body of iron on which the bacteria can respire and increases the area in which a biobarrier will be active. This behaviour is an advantage for the bacteria as some Fe(III) phases are less amenable to bioreduction than others (Lovley, 1991, Zachara et al., 2002). Similarly iron surfaces can become swamped with sorbed Fe(II), blocking access to the Fe(III) below (Fredrickson et al., 1998). In both cases, bacteria that require contact with an electron acceptor would be unable to respire and would die. The soluble flavin electron shuttle negates this affect as it will travel in groundwaters until it reaches a suitable electron acceptor. Thus the amount of potential Fe(III) available for reduction in a contaminated area would greatly increase via the use of an external electron shuttle. That said, flavins will not discriminate against other compounds in order to react with ferric iron and should react with the first electron acceptor they meet; theoretically allowing the bacteria to respire on not just Fe(III). The population was grown with a range of different electron donors and found that only yeast extract yielded strong and repeated Fe(III) reduction. As yeast extract is a complex mixture of organic compounds (Edens et al., 2002), it is clear that it provides a metabolite critical to alkaliphilic growth which other electrons donors cannot.

Chapter 6 details how the bacteria population responded to the presence of Cr(VI). Chromate reduction was observed in AFC microcosms with up to 8500µmol.L^{-1} initial Cr(VI) concentration. Full removal was recorded from those microcosms with 100 to 2000 µmol.L^{-1} Cr(VI). Fe(II) production, accompanied by exponential cell growth, started when full Cr(VI) removal was achieved, indicating that iron reduction is the more significant process. Transferring the population to media with Cr(VI) as the sole electron acceptor yielded fragile growth which terminated with the 10^{th} media cycle. Growing the Fe(III)-reducing population in media with solid phase iron yielded cell growth accompanied by Fe(II) production. Analysis of the supernatant from these tests showed the accumulation of riboflavin within the media. Tracking the species of bacteria as they were introduced to different media showed how Cr(VI) caused specialisation within the population. *Clostridium XI*

bacteria were the only ones who were tolerant and able to reduce Cr(VI). *Alklaiphilus* bacteria were tolerant to Cr(VI) but unable to reduce Cr(VI). *Tissierella* bacteria were less tolerant of Cr(VI) however when grown in solid phase Fe(III) media, those from the C OTU dominated, a potential effect of being able to produce riboflavin as an electron shuttle.

It is clear from the data presented that biobarriers hold much promise for the treatment of highly alkaline COPR waste sites. The results presented suggest that Fe(III) reduction may be the most significant reductive process near COPR sites. This is no surprise as iron reduction has been described as the most important dissimilatory reaction in the natural environment and can be responsible for up to 100% of organic substrate oxidation in the subsurface (Lovley, 2001, Lovley, 2006). The ability of these bacteria to comfortably live in Fe(III) media containing 2000 $\mu mol.L^{-1}$ chromate exceeds the maximum Cr(VI) concentrations so far reported on COPR sites (Stewart et al., 2007, Whittleston, 2011). Thus injecting yeast extract and riboflavin into such a contaminated site could give the required remediative effect.

7.2 Future Work

7.2.1 **Permeable Reactive Barriers**

This study into the kinetics of the ZVI and Cr(VI) reaction suggests that there is a change in the reaction mechanism as pH is amended from the alkaline to acidic region. However the evidence presented does not provide conclusive proof of this fact as the focus of the work was reactions in the hyperalkaline pH range and minimal investigations were undertaken into the kinetics of the acidic pH range. To prove conclusively that this theorem is viable, an investigation should be planned which captures the kinetics of this reaction throughout the pH range. Once completed, Figure 4.7 could be updated and any change in trend with pH would indicate a change in the reaction speed. Whilst not proof itself of a change in mechanism, large scale changes in reaction kinetics often indicate when this is the case and investigations into the mechanism could be made accordingly.

Whilst the results of this study suggest that the near COPR environment presents a less than ideal situation in which to build a ZVI-PRB, it is clear that this remediation strategy would work, albeit not for the desired timeframe. Usually a PRBs design life would be measured in decades whereas the work presented indicates that in COPR leachate the design life would be significantly less. Figure 4.3 gives a rough estimate of 80 $\mu mol.L^{-1}.m^2$ as being the specific reduction capacity per unit area of ZVI in the leachate from the West Yorkshire site. However in order to quantify a definitive design life for ZVI in these liquors, continuously pumped column tests would be the natural technique to employ.

Other limitations include the fact that this study has concentrated on the abiotic processes within a PRB. Organic matter and microorganisms can have a significant effect on iron in the ground. The build-up of organic matter within a barrier, so called biofouling, can reduce activity and permeability within the barrier (Niederbacher and Nahold, 2005). This study also ignores the effect of natural bacteria which could reduce Fe(III) within the barrier, potentially increasing the design life of the iron. Thus the only way to model the actual behaviour of iron within a contaminated subsurface would be to construct a trial barrier and monitor its performance over a number of months.

7.2.2 **Biobarriers**

The production of riboflavin by a bacteria in alkaline conditions is an important finding, however we still know little about the *Tissierella* sp. capable of this feat. Growth of the population on agar plates allowed the isolation of this species however all attempts re-inoculate back into aqueous media failed. Further attempts to isolate this bacteria should be made in order to fully characterise this species. Growing the population in media with solid phase iron caused this species to dominate, thus repeated growth may yield an isolate. Indeed most of the bacteria in the study were novel and every effort should be made to isolate and fully characterise them.

This work has uncovered the reductive mechanism of one bacteria from the population, however little is known about the respiration processes of the majority of the species present. Identifying how the *Clostridium XI* sp. is able to reduce both Fe(III) and Cr(VI) for example, could identify novel alkaliphilic bacterial processes and further the understanding of these prokaryotes. Gram positive bacteria such as these Clostridium XI lack the cell membrane required to house already identified reductive mechanisms such as c-type cytochromes (Williamson et al., 2013) thus novel reductive mechanisms could be in play and therefore it may be highly advantages to investigate them further.

This study suggests that bioremediation is a possible management strategy for COPR waste sites, however much work is yet to be done before one can be confidently prescribed to treat a contaminated site.. Whilst bacteria in these studies have been shown to reduce nominal amounts of Cr(VI), a biobarrier would rely on sustained and robust growth of the bacteria so that Cr(VI) reduction continues.

The approach used in this study was to use microcosms to grow bacteria originally isolated from soils beneath a historic COPR site. Whilst a good proxy, the media used is not an exact replicate of the conditions found in natural environment. The initial extraction process coupled with the chemical composition of the media used will cause a bias in the study towards those bacteria which are hardy enough to survive, and which are able to continue to grow within the selected media. The bacteria population within a soil horizon is likely to be far more complex than represented in the population data of this study. By using a media with soluble Fe(III) as the sole electron donor for the initial isolation could mean that any bacteria which do not respire via this mechanism would soon be out-competed and not be represented in the population. If in the COPR environment these non Fe(III) reducers dominate, then the majority of electron donor introduced into the environment will be utilised by these bacteria and the remediative effect will be minimal. As previous work has shown Fe(II) accumulation to occur beneath the historic COPR site in West Yorkshire (Stewart et al., 2010Stewart et al., 2010, Whittleston, 2011) it would appear that Fe(III)

reduction is an important method of respiration for the bacteria that reside there. To give definitive proof to this theory, sampling from other sites than the one in West Yorkshire and conducting a similar set of experiments would establish whether the behaviour of the bacteria population in this study is an exception or the norm. The presence of Fe(II) in soils surrounding a site would give an indication that this is the case. Once confirmed, the logical next step would be push pull tests in a borehole on such a site. Injecting a cocktail of yeast extract and riboflavin into a contaminated aquifer and then analysing the liquor after a certain time frame for reduced iron and chromium would indicate whether bioreduction was occurring and whether it would be a suitable treatment option.

The results of this study also have far reaching implications for the treatment of many other contaminants in highly alkaline areas. As bacteria are able to reduce Cr(VI) and Fe(III) at high pH, they may also be able to facilitate the transformation of other redox active contaminants (such as vanadate, pertechnate and uranium). This being the case, bioreduction could also be a suitable treatment for these waste streams and conducting a similar study on bacteria isolated from sites contaminated with these other waste streams, could confirm this theorem.

7.3 References

Bae, S. & Lee, W. 2013. Biotransformation of lepidocrocite in the presence of quinones and flavins. *Geochim. Cosmochim. Acta,* 114**,** 144-155.

Edens, N. K., Reaves, L. A., Bergana, M. S., Reyzer, I. L., O'Mara, P., Baxter, J. H. & Snowden, M. K. 2002. Yeast extract stimulates glucose metabolism and inhibits lipolysis in rat adipocytes in vitro. *J. Nutr.,* 132**,** 1141-8.

Fredrickson, J. K., Zachara, J. M., Kennedy, D. W., Dong, H., Onstott, T. C., Hinman, N. W. & Li, S.-m. 1998. Biogenic iron mineralization accompanying the dissimilatory reduction of hydrous ferric oxide by a groundwater bacterium. *Geochim. Cosmochim. Acta,* 62**,** 3239-3257.

Langmuir, D. 1997. *Aqueous environmental geochemistry*, Prentice Hall.

Lovley, D. R. 1991. Dissimilatory Fe(III) and Mn(IV) reduction. *Microbiol. Mol. Biol. Rev.,* 55**,** 259-287.

Lovley, D. R. 2001. Anaerobes to the Rescue. *Science,* 293**,** 1444-1446.

Lovley, D. R. 2006. *Dissimilatory Fe(III) and Mn(IV) reducing Prokaryotes. In: The Prokaryotes: A Handbook on the Biology of Bacteria: Vol. 2: Ecophysiology and Biochemistry*, Springer.

Morrison, S. J. N., D. L. Davis, J. A. Fuller, C. C. 2002. Introduction to Groudwater Remediation of Metals, Radionuclides, and Nutrients with Permeable Reactive Barries. *In:* Naftz, D. M., S. J. Fuller, C. C. Davis J. A. (ed.) *Handbook of Groundwater Remediation using Permeable Reactive Barriers.*

Niederbacher, P. & Nahold, M. 2005. Installation and operation of an Adsorptive Reactor and Barrier (AR&B) system in Brunn am Gebirge, Austria. *Trace Metals and other Contaminants in the Environment,* 7**,** 283-309.

Stewart, D. I., Burke, I. T., Hughes-Berry, D. V. & Whittleston, R. A. 2010. Microbially mediated chromate reduction in soil contaminated by highly alkaline leachate from chromium containing waste. *Ecol. Eng.,* 36**,** 211-221.

Stewart, D. I., Burke, I. T. & Mortimer, R. J. G. 2007. Stimulation of Microbially Mediated Chromate Reduction in Alkaline Soil-Water Systems. *Geomicrobiol. J.,* 24**,** 655 - 669.

Tinjum, J. M., Benson, C. H. & Edil, T. B. 2008. Mobilization of Cr(VI) from chromite ore processing residue through acid treatment. *Sci. Total Environ.,* 391**,** 13-25.

Weng, C. H., Huang, C. P., Allen, H. E., Cheng, A. H. D. & Sanders, P. F. 1994. Chromium leaching behavior in soil derived from chromite ore processing waste. *Sci. Total Environ.,* 154**,** 71-86.

Whittleston, R. A. 2011. *Bioremediation of chromate in alkaline sediment-water systems.* PhD thesis, University of Leeds.

Wilkin, R. T., Su, C., Ford, R. G. & Paul, C. J. 2005. Chromium-Removal Processes during Groundwater Remediation by a Zerovalent Iron Permeable Reactive Barrier. *Environ. Sci. Technol.,* 39**,** 4599-4605.

Williamson, A. J., Morris, K., Shaw, S., Byrne, J. M., Boothman, C. & Lloyd, J. R. 2013. Microbial Reduction of Fe(III) under Alkaline Conditions Relevant to Geological Disposal. *Applied and Environmental Microbiology,* 79**,** 3320-3326.

Zachara, J. M., Kukkadapu, R. K., Fredrickson, J. K., Gorby, Y. A. & Smith, S. C. 2002. Biomineralization of Poorly Crystalline Fe(III) Oxides by Dissimilatory Metal Reducing Bacteria (DMRB). *Geomicrobiol. J.,* 19**,** 179-207.

Appendix A List of Bacteria Sequences Referred to in the Text

The following is a complete list of bacteria 16s rRNA gene sequences referred to in the main body of text. Sequences can be reviewed by searching for the accession numbers on the GenBank database (http://www.ncbi.nlm.nih.gov/genbank/).

A.1 Bacteria Sequences from Chapter 5

ID	Accession Number	Length (bp)	Classification using the RDP classifier (95% Confidence threshold)	OTU
Fe1	KF362050	1467	Firmicutes, Clostridia, Clostridiales, Peptostreptococcaceae, Clostridium XI	Clostridium XI
Fe2	KF362051	1467	Firmicutes, Clostridia, Clostridiales, Peptostreptococcaceae, Clostridium XI	Clostridium XI
Fe3	KF362052	1466	Firmicutes, Clostridia, Clostridiales, Peptostreptococcaceae, Clostridium XI	Clostridium XI
Fe4	KF362053	1495	Firmicutes, Clostridia, Clostridiales	Tissierella C
Fe5	KF362054	1495	Firmicutes, Clostridia, Clostridiales, Incertae Sedis XI, Tissierella	Tissierella C
Fe6	KF362055	1467	Firmicutes, Clostridia, Clostridiales, Peptostreptococcaceae, Clostridium XI	Clostridium XI
Fe8	KF362056	1489	Firmicutes, Clostridia, Clostridiales, Clostridiaceae 2, Alkaliphilus	Alkaliphilus
Fe9	KF362057	1467	Firmicutes, Clostridia, Clostridiales, Peptostreptococcaceae, Clostridium XI	Clostridium XI
Fe10	KF362058	1467	Firmicutes, Clostridia, Clostridiales, Peptostreptococcaceae, Clostridium XI	Clostridium XI
Fe11	KF362059	1495	Firmicutes, Clostridia, Clostridiales	Tissierella C
Fe12	KF362060	1495	Firmicutes, Clostridia, Clostridiales	Tissierella C
Fe14	KF362061	1467	Firmicutes, Clostridia, Clostridiales, Peptostreptococcaceae, Clostridium XI	Clostridium XI
Fe15	KF362062	1467	Firmicutes, Clostridia, Clostridiales, Peptostreptococcaceae, Clostridium XI	Clostridium XI
Fe16	KF362063	1467	Firmicutes, Clostridia, Clostridiales, Peptostreptococcaceae, Clostridium XI	Clostridium XI
Fe17	KF362064	1496	Firmicutes, Clostridia, Clostridiales, Incertae Sedis XI, Tissierella	Tissierella A
Fe18	KF362065	1467	Firmicutes, Clostridia, Clostridiales, Peptostreptococcaceae, Clostridium XI	Clostridium XI
Fe19	KF362066	1496	Firmicutes, Clostridia, Clostridiales, Incertae Sedis XI, Tissierella	Tissierella B
Fe20	KF362067	1467	Firmicutes, Clostridia, Clostridiales, Peptostreptococcaceae, Clostridium XI	Clostridium XI
Fe21	KF362068	1495	Firmicutes, Clostridia, Clostridiales	Tissierella C
Fe22	KF362069	1467	Firmicutes, Clostridia, Clostridiales, Peptostreptococcaceae, Clostridium XI	Clostridium XI
Fe25	KF362070	1496	Firmicutes, Clostridia, Clostridiales, Incertae Sedis XI, Tissierella	Tissierella B
Fe26	KF362071	1495	Firmicutes, Clostridia, Clostridiales	Tissierella C
Fe27	KF362072	1496	Firmicutes, Clostridia, Clostridiales, Incertae Sedis XI, Tissierella	Tissierella A
Fe28	KF362073	1495	Firmicutes, Clostridia, Clostridiales	Tissierella C
Fe29	KF362074	1467	Firmicutes, Clostridia, Clostridiales, Peptostreptococcaceae, Clostridium XI	Clostridium XI
Fe30	KF362075	1488	Firmicutes, Clostridia, Clostridiales, Clostridiaceae 2, Alkaliphilus	Alkaliphilus
Fe31	KF362076	1496	Firmicutes, Clostridia, Clostridiales, Incertae Sedis XI, Tissierella	Tissierella B
Fe32	KF362077	1468	Firmicutes, Clostridia, Clostridiales, Peptostreptococcaceae, Clostridium XI	Clostridium XI
Fe33	KF362078	1467	Firmicutes, Clostridia, Clostridiales, Peptostreptococcaceae, Clostridium XI	Clostridium XI
Fe34	KF362079	1495	Firmicutes, Clostridia, Clostridiales, Incertae Sedis XI, Tissierella	Tissierella C

ID	Accession Number	Length (bp)	Classification using the RDP classifier (95% Confidence threshold)	OTU
Fe35	KF362080	1467	Firmicutes, Clostridia, Clostridiales, Peptostreptococcaceae, Clostridium XI	Clostridium XI
Fe36	KF362081	1467	Firmicutes, Clostridia, Clostridiales, Peptostreptococcaceae, Clostridium XI	Clostridium XI
Fe37	KF362082	1495	Firmicutes, Clostridia, Clostridiales	Tissierella C
Fe39	KF362083	1467	Firmicutes, Clostridia, Clostridiales, Peptostreptococcaceae, Clostridium XI	Clostridium XI
Fe41	KF362084	1495	Firmicutes, Clostridia, Clostridiales	Tissierella C
Fe42	KF362085	1467	Firmicutes, Clostridia, Clostridiales, Peptostreptococcaceae, Clostridium XI	Clostridium XI
Fe43	KF362086	1495	Firmicutes, Clostridia, Clostridiales	Tissierella C
Fe44	KF362087	1487	Firmicutes, Clostridia, Clostridiales, Clostridiaceae 2, Alkaliphilus	Alkaliphilus
Fe45	KF362088	1495	Firmicutes, Clostridia, Clostridiales	Tissierella C
Fe47	KF362089	1467	Firmicutes, Clostridia, Clostridiales, Peptostreptococcaceae, Clostridium XI	Clostridium XI
Fe48	KF362090	1495	Firmicutes, Clostridia, Clostridiales	Tissierella C
Fe49	KF362091	1495	Firmicutes, Clostridia, Clostridiales	Tissierella C
Fe50	KF362092	1495	Firmicutes, Clostridia, Clostridiales	Tissierella C
Fe51	KF362093	1495	Firmicutes, Clostridia, Clostridiales	Tissierella C
Fe52	KF362094	1489	Firmicutes, Clostridia, Clostridiales, Clostridiaceae 2, Alkaliphilus	Alkaliphilus
Fe53	KF362095	1494	Firmicutes, Clostridia, Clostridiales	Tissierella C
Fe54	KF362096	1466	Firmicutes, Clostridia, Clostridiales, Peptostreptococcaceae, Clostridium XI	Clostridium XI
Fe55	KF362097	1467	Firmicutes, Clostridia, Clostridiales, Peptostreptococcaceae, Clostridium XI	Clostridium XI
Fe56	KF362098	1495	Firmicutes, Clostridia, Clostridiales	Tissierella C
Fe57	KF362099	1466	Firmicutes, Clostridia, Clostridiales, Peptostreptococcaceae, Clostridium XI	Clostridium XI
Fe58	KF362100	1495	Firmicutes, Clostridia, Clostridiales	Tissierella C
Fe59	KF362101	1495	Firmicutes, Clostridia, Clostridiales	Tissierella C
Fe60	KF362102	1465	Firmicutes, Clostridia, Clostridiales, Peptostreptococcaceae, Clostridium XI	Clostridium XI
Fe61	KF362103	1496	Firmicutes, Clostridia, Clostridiales, Incertae Sedis XI, Tissierella	Tissierella A
Fe63	KF362104	1495	Firmicutes, Clostridia, Clostridiales	Tissierella C
Fe64	KF362105	1496	Firmicutes, Clostridia, Clostridiales, Incertae Sedis XI, Tissierella	Tissierella A
Fe65	KF362106	1489	Firmicutes, Clostridia, Clostridiales, Clostridiaceae 2, Alkaliphilus	Alkaliphilus
Fe66	KF362107	1467	Firmicutes, Clostridia, Clostridiales, Peptostreptococcaceae, Clostridium XI	Clostridium XI
Fe68	KF362108	1467	Firmicutes, Clostridia, Clostridiales, Peptostreptococcaceae, Clostridium XI	Clostridium XI

Table A.1: Classification and OTU for bacteria sequences obtained from AFe media.

ID	Accession Number	Length (bp)	Classification using the RDP classifier (95% Confidence threshold)	OTU
Str5	KF362109	1402	Firmicutes, Clostridia, Clostridiales, Incertae Sedis XI, Tissierella	Tissierella C
Str6	KF362110	1315	Firmicutes, Clostridia, Clostridiales, Incertae Sedis XI, Tissierella	Tissierella C
Str9	KF362111	1234	Firmicutes, Clostridia, Clostridiales, Incertae Sedis XI, Tissierella	Tissierella C
Str20	KF362112	1398	Firmicutes, Clostridia, Clostridiales, Incertae Sedis XI, Tissierella	Tissierella C
Str26	KF362113	1400	Firmicutes, Clostridia, Clostridiales, Incertae Sedis XI, Tissierella	Tissierella C

Table A.2: Classification and OTU for bacteria sequences obtained from streaks on AFe agar plates which cleared the surrounding gel.

ID	Accession Number	Length (bp)	Classification using the RDP classifier (95% Confidence threshold)	OTU
Str3	KF362114	1304	Actinobacteria, Actinobacteridae, Actinomycetales	Actinomycetales
Str4	KF362115	462	Actinobacteria, Actinobacteridae, Actinomycetales	Actinomycetales
Str10	KF362116	515	Actinobacteria, Actinobacteridae, Actinomycetales	Actinomycetales
Str48	KF362117	1359	Proteobacteria, Alphaproteobacteria, Rhizobiales, Brucellaceae, Ochrobactrum	Ochrobactrum

Table A.3: Classification and OTU for bacteria sequences obtained from streaks on AFe agar plates which did not clear the surrounding gel.

A.2 Bacteria Sequences from Chapter 6

ID	Accession Number	Length (bp)	Classification using the RDP classifier (95% Confidence threshold)	OTU
ACr1	KF797922	1467	Firmicutes, Clostridia, Clostridiales, Peptostreptococcaceae, Clostridium XI	Clostridium XI
ACr2	KF797923	1467	Firmicutes, Clostridia, Clostridiales, Peptostreptococcaceae, Clostridium XI	Clostridium XI
ACr3	KF797924	1467	Firmicutes, Clostridia, Clostridiales, Peptostreptococcaceae, Clostridium XI	Clostridium XI
ACr4	KF797925	1467	Firmicutes, Clostridia, Clostridiales, Peptostreptococcaceae, Clostridium XI	Clostridium XI
ACr5	KF797926	1467	Firmicutes, Clostridia, Clostridiales, Peptostreptococcaceae, Clostridium XI	Clostridium XI
ACr6	KF797927	1467	Firmicutes, Clostridia, Clostridiales, Peptostreptococcaceae, Clostridium XI	Clostridium XI
ACr7	KF797928	1467	Firmicutes, Clostridia, Clostridiales, Peptostreptococcaceae, Clostridium XI	Clostridium XI
ACr8	KF797929	1466	Firmicutes, Clostridia, Clostridiales, Peptostreptococcaceae, Clostridium XI	Clostridium XI
ACr9	KF797930	1466	Firmicutes, Clostridia, Clostridiales, Peptostreptococcaceae, Clostridium XI	Clostridium XI
ACr10	KF797931	1467	Firmicutes, Clostridia, Clostridiales, Peptostreptococcaceae, Clostridium XI	Clostridium XI
ACr11	KF797932	1467	Firmicutes, Clostridia, Clostridiales, Peptostreptococcaceae, Clostridium XI	Clostridium XI
ACr12	KF797933	1467	Firmicutes, Clostridia, Clostridiales, Peptostreptococcaceae, Clostridium XI	Clostridium XI
ACr13	KF797934	1467	Firmicutes, Clostridia, Clostridiales, Peptostreptococcaceae, Clostridium XI	Clostridium XI
ACr14	KF797935	1467	Firmicutes, Clostridia, Clostridiales, Peptostreptococcaceae, Clostridium XI	Clostridium XI
ACr15	KF797936	1467	Firmicutes, Clostridia, Clostridiales, Peptostreptococcaceae, Clostridium XI	Clostridium XI
ACr16	KF797937	1467	Firmicutes, Clostridia, Clostridiales, Peptostreptococcaceae, Clostridium XI	Clostridium XI
ACr17	KF797938	1466	Firmicutes, Clostridia, Clostridiales, Peptostreptococcaceae, Clostridium XI	Clostridium XI
ACr18	KF797939	1467	Firmicutes, Clostridia, Clostridiales, Peptostreptococcaceae, Clostridium XI	Clostridium XI
ACr20	KF797940	1467	Firmicutes, Clostridia, Clostridiales, Peptostreptococcaceae, Clostridium XI	Clostridium XI
ACr21	KF797941	1467	Firmicutes, Clostridia, Clostridiales, Peptostreptococcaceae, Clostridium XI	Clostridium XI
ACr22	KF797942	1467	Firmicutes, Clostridia, Clostridiales, Peptostreptococcaceae, Clostridium XI	Clostridium XI
ACr23	KF797943	1467	Firmicutes, Clostridia, Clostridiales, Peptostreptococcaceae, Clostridium XI	Clostridium XI
ACr24	KF797944	1467	Firmicutes, Clostridia, Clostridiales, Peptostreptococcaceae, Clostridium XI	Clostridium XI
ACr25	KF797945	1485	Actinobacteria, Actinobacteridae, Actinomycetales, Micrococcineae, Micrococcaceae, Micrococcus	Clostridium XI
ACr26	KF797946	1467	Firmicutes, Clostridia, Clostridiales, Peptostreptococcaceae, Clostridium XI	Clostridium XI
ACr27	KF797947	1467	Firmicutes, Clostridia, Clostridiales, Peptostreptococcaceae, Clostridium XI	Clostridium XI

ID	Accession Number	Length (bp)	Classification using the RDP classifier (95% Confidence threshold)	OTU
ACr28	KF797948	1467	Firmicutes, Clostridia, Clostridiales, Peptostreptococcaceae, Clostridium XI	Clostridium XI
ACr29	KF797949	1467	Firmicutes, Clostridia, Clostridiales, Peptostreptococcaceae, Clostridium XI	Clostridium XI
ACr30	KF797950	1467	Firmicutes, Clostridia, Clostridiales, Peptostreptococcaceae, Clostridium XI	Clostridium XI
ACr31	KF797951	1467	Firmicutes, Clostridia, Clostridiales, Peptostreptococcaceae, Clostridium XI	Clostridium XI
ACr32	KF797952	1467	Firmicutes, Clostridia, Clostridiales, Peptostreptococcaceae, Clostridium XI	Clostridium XI
ACr33	KF797953	1467	Firmicutes, Clostridia, Clostridiales, Peptostreptococcaceae, Clostridium XI	Clostridium XI
ACr34	KF797954	1467	Firmicutes, Clostridia, Clostridiales, Peptostreptococcaceae, Clostridium XI	Clostridium XI
ACr35	KF797955	1467	Firmicutes, Clostridia, Clostridiales, Peptostreptococcaceae, Clostridium XI	Clostridium XI
ACr36	KF797956	1467	Firmicutes, Clostridia, Clostridiales, Peptostreptococcaceae, Clostridium XI	Clostridium XI
ACr37	KF797957	1467	Firmicutes, Clostridia, Clostridiales, Peptostreptococcaceae, Clostridium XI	Clostridium XI
ACr39	KF797958	1467	Firmicutes, Clostridia, Clostridiales, Peptostreptococcaceae, Clostridium XI	Clostridium XI
ACr40	KF797959	1467	Firmicutes, Clostridia, Clostridiales, Peptostreptococcaceae, Clostridium XI	Clostridium XI
ACr41	KF797960	1467	Firmicutes, Clostridia, Clostridiales, Peptostreptococcaceae, Clostridium XI	Clostridium XI
ACr42	KF797961	1467	Firmicutes, Clostridia, Clostridiales, Peptostreptococcaceae, Clostridium XI	Clostridium XI
ACr43	KF797962	1467	Firmicutes, Clostridia, Clostridiales, Peptostreptococcaceae, Clostridium XI	Clostridium XI
ACr44	KF797963	1467	Firmicutes, Clostridia, Clostridiales, Peptostreptococcaceae, Clostridium XI	Clostridium XI
ACr45	KF797964	1467	Firmicutes, Clostridia, Clostridiales, Peptostreptococcaceae, Clostridium XI	Clostridium XI
ACr46	KF797965	1467	Firmicutes, Clostridia, Clostridiales, Peptostreptococcaceae, Clostridium XI	Clostridium XI
ACr47	KF797966	1468	Firmicutes, Clostridia, Clostridiales, Peptostreptococcaceae, Clostridium XI	Clostridium XI
ACr49	KF797967	1467	Firmicutes, Clostridia, Clostridiales, Peptostreptococcaceae, Clostridium XI	Clostridium XI
ACr50	KF797968	1467	Firmicutes, Clostridia, Clostridiales, Peptostreptococcaceae, Clostridium XI	Clostridium XI
ACr51	KF797969	1467	Firmicutes, Clostridia, Clostridiales, Peptostreptococcaceae, Clostridium XI	Clostridium XI
ACr52	KF797970	1466	Firmicutes, Clostridia, Clostridiales, Peptostreptococcaceae, Clostridium XI	Clostridium XI
ACr53	KF797971	1468	Firmicutes, Clostridia, Clostridiales, Peptostreptococcaceae, Clostridium XI	Clostridium XI
ACr54	KF797972	1467	Firmicutes, Clostridia, Clostridiales, Peptostreptococcaceae, Clostridium XI	Clostridium XI
ACr55	KF797973	1467	Firmicutes, Clostridia, Clostridiales, Peptostreptococcaceae, Clostridium XI	Clostridium XI
ACr56	KF797974	1467	Firmicutes, Clostridia, Clostridiales, Peptostreptococcaceae, Clostridium XI	Clostridium XI
ACr57	KF797975	1467	Firmicutes, Clostridia, Clostridiales, Peptostreptococcaceae, Clostridium XI	Clostridium XI
ACr58	KF797976	1467	Firmicutes, Clostridia, Clostridiales, Peptostreptococcaceae, Clostridium XI	Clostridium XI

ID	Accession Number	Length (bp)	Classification using the RDP classifier (95% Confidence threshold)	OTU
ACr59	KF797977	1467	Firmicutes, Clostridia, Clostridiales, Peptostreptococcaceae, Clostridium XI	Clostridium XI
ACr60	KF797978	1468	Firmicutes, Clostridia, Clostridiales, Peptostreptococcaceae, Clostridium XI	Clostridium XI
ACr61	KF797979	1469	Firmicutes, Clostridia, Clostridiales, Peptostreptococcaceae, Clostridium XI	Clostridium XI
ACr62	KF797980	1467	Firmicutes, Clostridia, Clostridiales, Peptostreptococcaceae, Clostridium XI	Clostridium XI
ACr63	KF797981	1467	Firmicutes, Clostridia, Clostridiales, Peptostreptococcaceae, Clostridium XI	Clostridium XI

Table A.4: Classification and OTU for bacteria sequences obtained from Cr(VI) media

ID	Accession Number	Length (bp)	Classification using the RDP classifier (95% Confidence threshold)	OTU
AFeCr200-1	KF797982	1490	Firmicutes, Clostridia, Clostridiales, Clostridiaceae 2, Alkaliphilus	Alkaliphilus
AFeCr200-3	KF797983	1467	Firmicutes, Clostridia, Clostridiales, Peptostreptococcaceae, Clostridium XI	Clostridium XI
AFeCr200-4	KF797984	1467	Firmicutes, Clostridia, Clostridiales, Peptostreptococcaceae, Clostridium XI	Clostridium XI
AFeCr200-5	KF797985	1467	Firmicutes, Clostridia, Clostridiales, Peptostreptococcaceae, Clostridium XI	Clostridium XI
AFeCr200-6	KF797986	1489	Firmicutes, Clostridia, Clostridiales, Clostridiaceae 2, Alkaliphilus	Alkaliphilus
AFeCr200-8	KF797987	1467	Firmicutes, Clostridia, Clostridiales, Peptostreptococcaceae, Clostridium XI	Clostridium XI
AFeCr200-9	KF797988	1305	Firmicutes, Clostridia, Clostridiales, Peptostreptococcaceae, Clostridium XI	Clostridium XI
AFeCr200-10	KF797989	1467	Firmicutes, Clostridia, Clostridiales, Peptostreptococcaceae, Clostridium XI	Clostridium XI
AFeCr200-11	KF797990	1496	Firmicutes, Clostridia, Clostridiales, IncertaeSedis XI, Tissierella	Tissierella B
AFeCr200-12	KF797991	1467	Firmicutes, Clostridia, Clostridiales, Peptostreptococcaceae, Clostridium XI	Clostridium XI
AFeCr200-13	KF797992	1365	Firmicutes, Clostridia, Clostridiales, Peptostreptococcaceae, Clostridium XI	Clostridium XI
AFeCr200-15	KF797993	1467	Firmicutes, Clostridia, Clostridiales, Peptostreptococcaceae, Clostridium XI	Clostridium XI
AFeCr200-16	KF797994	1468	Firmicutes, Clostridia, Clostridiales, Peptostreptococcaceae, Clostridium XI	Clostridium XI
AFeCr200-17	KF797995	1467	Firmicutes, Clostridia, Clostridiales, Peptostreptococcaceae, Clostridium XI	Clostridium XI
AFeCr200-18	KF797996	1467	Firmicutes, Clostridia, Clostridiales, Peptostreptococcaceae, Clostridium XI	Clostridium XI
AFeCr200-19	KF797997	1495	Firmicutes, Clostridia, Clostridiales	Tissierella C
AFeCr200-20	KF797998	1489	Firmicutes, Clostridia, Clostridiales, Clostridiaceae 2, Alkaliphilus	Alkaliphilus
AFeCr200-21	KF797999	1467	Firmicutes, Clostridia, Clostridiales, Peptostreptococcaceae, Clostridium XI	Clostridium XI
AFeCr200-22	KF798000	1467	Firmicutes, Clostridia, Clostridiales, Peptostreptococcaceae, Clostridium XI	Clostridium XI
AFeCr200-23	KF798001	1467	Firmicutes, Clostridia, Clostridiales, Peptostreptococcaceae, Clostridium XI	Clostridium XI
AFeCr200-24	KF798002	1489	Firmicutes, Clostridia, Clostridiales, Clostridiaceae 2, Alkaliphilus	Alkaliphilus

ID	Accession Number	Length (bp)	Classification using the RDP classifier (95% Confidence threshold)	OTU
AFeCr200-25	KF798003	1467	Firmicutes, Clostridia, Clostridiales, Peptostreptococcaceae, Clostridium XI	Clostridium XI
AFeCr200-26	KF798004	1467	Firmicutes, Clostridia, Clostridiales, Peptostreptococcaceae, Clostridium XI	Clostridium XI
AFeCr200-27	KF798005	1434	Firmicutes, Clostridia, Clostridiales, Clostridiaceae 2, Alkaliphilus	Alkaliphilus
AFeCr200-28	KF798006	1464	Firmicutes, Clostridia, Clostridiales, Clostridiaceae 2, Alkaliphilus	Alkaliphilus
AFeCr200-30	KF798007	1489	Firmicutes, Clostridia, Clostridiales, Clostridiaceae 2, Alkaliphilus	Alkaliphilus
AFeCr200-31	KF798008	1466	Firmicutes, Clostridia, Clostridiales, Peptostreptococcaceae, Clostridium XI	Clostridium XI
AFeCr200-32	KF798009	1468	Firmicutes, Clostridia, Clostridiales, Peptostreptococcaceae, Clostridium XI	Clostridium XI

Table A.5: Classification and OTU for bacteria sequences obtained from AFe Cr200 media.

ID	Accession Number	Sequence length	Classification using the RDP classifier (95% Confidence threshold)	OTU
AFeCr8500-1	KF798010	1502	Actinobacteria, Actinobacteridae, Actinomycetales	Actinomycetales
AFeCr8500-2	KF798011	1490	Actinobacteria, Actinobacteridae, Actinomycetales, Micrococcineae, Brevibacteriaceae, Brevibacterium	Brevibacterium
AFeCr8500-3	KF798012	1490	Actinobacteria, Actinobacteridae, Actinomycetales, Micrococcineae, Brevibacteriaceae, Brevibacterium	Brevibacterium
AFeCr8500-5	KF798013	1481	Actinobacteria, Actinobacteridae, Actinomycetales, Micrococcineae, Brevibacteriaceae, Brevibacterium	Brevibacterium
AFeCr8500-6	KF798014	1532	Actinobacteria, Actinobacteridae, Actinomycetales	Actinomycetales
AFeCr8500-7	KF798015	1490	Actinobacteria, Actinobacteridae, Actinomycetales, Micrococcineae, Brevibacteriaceae, Brevibacterium	Brevibacterium
AFeCr8500-8	KF798016	1502	Actinobacteria, Actinobacteridae, Actinomycetales	Actinomycetales
AFeCr8500-11	KF798017	1490	Actinobacteria, Actinobacteridae, Actinomycetales, Micrococcineae, Brevibacteriaceae, Brevibacterium	Brevibacterium
AFeCr8500-15	KF798018	1502	Actinobacteria, Actinobacteridae, Actinomycetales	Actinomycetales
AFeCr8500-17	KF798019	1489	Actinobacteria, Actinobacteridae, Actinomycetales, Micrococcineae, Brevibacteriaceae, Brevibacterium	Brevibacterium
AFeCr8500-18	KF798020	1490	Actinobacteria, Actinobacteridae, Actinomycetales, Micrococcineae, Brevibacteriaceae, Brevibacterium	Brevibacterium

ID	Accession Number	Sequence length	Classification using the RDP classifier (95% Confidence threshold)	OTU
AFeCr8500-19	KF798021	1490	Actinobacteria, Actinobacteridae, Actinomycetales, Micrococcineae, Brevibacteriaceae, Brevibacterium	Brevibacterium
AFeCr8500-20	KF798022	1490	Actinobacteria, Actinobacteridae, Actinomycetales, Micrococcineae, Brevibacteriaceae, Brevibacterium	Brevibacterium
AFeCr8500-21	KF798023	1490	Actinobacteria, Actinobacteridae, Actinomycetales, Micrococcineae, Brevibacteriaceae, Brevibacterium	Brevibacterium
AFeCr8500-22	KF798024	1490	Actinobacteria, Actinobacteridae, Actinomycetales, Micrococcineae, Brevibacteriaceae, Brevibacterium	Brevibacterium
AFeCr8500-23	KF798025	1490	Actinobacteria, Actinobacteridae, Actinomycetales, Micrococcineae, Brevibacteriaceae, Brevibacterium	Brevibacterium
AFeCr8500-24	KF798026	1490	Actinobacteria, Actinobacteridae, Actinomycetales, Micrococcineae, Brevibacteriaceae, Brevibacterium	Brevibacterium
AFeCr8500-26	KF798027	1490	Actinobacteria, Actinobacteridae, Actinomycetales, Micrococcineae, Brevibacteriaceae, Brevibacterium	Brevibacterium
AFeCr8500-27	KF798028	1502	Actinobacteria, Actinobacteridae, Actinomycetales	Actinomycetales
AFeCr8500-28	KF798029	1490	Actinobacteria, Actinobacteridae, Actinomycetales, Micrococcineae, Brevibacteriaceae, Brevibacterium	Brevibacterium
AFeCr8500-29	KF798030	1490	Actinobacteria, Actinobacteridae, Actinomycetales, Micrococcineae, Brevibacteriaceae, Brevibacterium	Brevibacterium

ID	Accession Number	Sequence length	Classification using the RDP classifier (95% Confidence threshold)	OTU
AFeCr8500-31	KF798031	1490	Actinobacteria, Actinobacteridae, Actinomycetales, Micrococcineae, Brevibacteriaceae, Brevibacterium	Brevibacterium
AFeCr8500-32	KF798032	1490	Actinobacteria, Actinobacteridae, Actinomycetales, Micrococcineae, Brevibacteriaceae, Brevibacterium	Brevibacterium
AFeCr8500-34	KF798033	1490	Actinobacteria, Actinobacteridae, Actinomycetales, Micrococcineae, Brevibacteriaceae, Brevibacterium	Brevibacterium
AFeCr8500-36	KF798034	1490	Actinobacteria, Actinobacteridae, Actinomycetales, Micrococcineae, Brevibacteriaceae, Brevibacterium	Brevibacterium
AFeCr8500-37	KF798035	1490	Actinobacteria, Actinobacteridae, Actinomycetales, Micrococcineae, Brevibacteriaceae, Brevibacterium	Brevibacterium

Table A.6: Classification and OTU for bacteria sequences obtained from AFeCr8500 media.

ID	Accession Number	Length (bp)	Classification using the RDP classifier (95% Confidence threshold)	OTU
Cr-AFE3	KF798036	628	Firmicutes, Clostridia, Clostridiales, Peptostreptococcaceae, Clostridium XI	Clostridium XI
Cr-AFE4	KF798037	1126	Firmicutes, Clostridia, Clostridiales, Peptostreptococcaceae, Clostridium XI	Clostridium XI
Cr-AFE5	KF798038	1496	Firmicutes, Clostridia, Clostridiales, Peptostreptococcaceae, Clostridium XI	Clostridium XI
Cr-AFE6	KF798039	1496	Firmicutes, Clostridia, Clostridiales, Peptostreptococcaceae, Clostridium XI	Clostridium XI
Cr-AFE7	KF798040	1496	Firmicutes, Clostridia, Clostridiales, Peptostreptococcaceae, Clostridium XI	Clostridium XI
Cr-AFE9	KF798041	1496	Firmicutes, Clostridia, Clostridiales, Peptostreptococcaceae, Clostridium XI	Clostridium XI
Cr-AFE10	KF798042	300	Firmicutes, Clostridia, Clostridiales, Peptostreptococcaceae, Clostridium XI	Clostridium XI
Cr-AFE11	KF798043	1496	Firmicutes, Clostridia, Clostridiales, Peptostreptococcaceae, Clostridium XI	Clostridium XI
Cr-AFE12	KF798044	1496	Firmicutes, Clostridia, Clostridiales, Peptostreptococcaceae, Clostridium XI	Clostridium XI
Cr-AFE13	KF798045	1496	Firmicutes, Clostridia, Clostridiales, Peptostreptococcaceae, Clostridium XI	Clostridium XI
Cr-AFE14	KF798046	1496	Firmicutes, Clostridia, Clostridiales, Peptostreptococcaceae, Clostridium XI	Clostridium XI
Cr-AFE15	KF798047	1496	Firmicutes, Clostridia, Clostridiales, Peptostreptococcaceae, Clostridium XI	Clostridium XI
Cr-AFE16	KF798048	1496	Firmicutes, Clostridia, Clostridiales, Peptostreptococcaceae, Clostridium XI	Clostridium XI
Cr-AFE17	KF798049	1496	Firmicutes, Clostridia, Clostridiales, Peptostreptococcaceae, Clostridium XI	Clostridium XI
Cr-AFE18	KF798050	787	Firmicutes, Clostridia, Clostridiales, Peptostreptococcaceae, Clostridium XI	Clostridium XI
Cr-AFE19	KF798051	1496	Firmicutes, Clostridia, Clostridiales, Peptostreptococcaceae, Clostridium XI	Clostridium XI
Cr-AFE20	KF798052	895	Firmicutes, Clostridia, Clostridiales, Peptostreptococcaceae, Clostridium XI	Clostridium XI
Cr-AFE22	KF798053	1496	Firmicutes, Clostridia, Clostridiales, Peptostreptococcaceae, Clostridium XI	Clostridium XI
Cr-AFE24	KF798054	1496	Firmicutes, Clostridia, Clostridiales, Peptostreptococcaceae, Clostridium XI	Clostridium XI

ID	Accession Number	Length (bp)	Classification using the RDP classifier (95% Confidence threshold)	OTU
Cr-AFE25	KF798055	934	Firmicutes, Clostridia, Clostridiales, Peptostreptococcaceae, Clostridium XI	Clostridium XI
Cr-AFE27	KF798056	1496	Firmicutes, Clostridia, Clostridiales, Peptostreptococcaceae, Clostridium XI	Clostridium XI
Cr-AFE28	KF798057	981	Firmicutes, Clostridia, Clostridiales, Peptostreptococcaceae, Clostridium XI	Clostridium XI
Cr-AFE29	KF798058	1495	Firmicutes, Clostridia, Clostridiales, Peptostreptococcaceae, Clostridium XI	Clostridium XI
Cr-AFE30	KF798059	1118	Firmicutes, Clostridia, Clostridiales, Peptostreptococcaceae, Clostridium XI	Clostridium XI
Cr-AFE31	KF798060	1496	Firmicutes, Clostridia, Clostridiales, Peptostreptococcaceae, Clostridium XI	Clostridium XI
Cr-AFE34	KF798061	1496	Firmicutes, Clostridia, Clostridiales, Peptostreptococcaceae, Clostridium XI	Clostridium XI
Cr-AFE36	KF798062	1496	Firmicutes, Clostridia, Clostridiales, Peptostreptococcaceae, Clostridium XI	Clostridium XI
Cr-AFE38	KF798063	1496	Firmicutes, Clostridia, Clostridiales, Peptostreptococcaceae, Clostridium XI	Clostridium XI
Cr-AFE39	KF798064	1496	Firmicutes, Clostridia, Clostridiales, Peptostreptococcaceae, Clostridium XI	Clostridium XI
Cr-AFE41	KF798065	1225	Firmicutes, Clostridia, Clostridiales, Peptostreptococcaceae, Clostridium XI	Clostridium XI
Cr-AFE42	KF798066	1496	Firmicutes, Clostridia, Clostridiales, Peptostreptococcaceae, Clostridium XI	Clostridium XI
Cr-AFE43	KF798067	965	Firmicutes, Clostridia, Clostridiales, Peptostreptococcaceae, Clostridium XI	Clostridium XI
Cr-AFE44	KF798068	1496	Firmicutes, Clostridia, Clostridiales, Peptostreptococcaceae, Clostridium XI	Clostridium XI
Cr-AFE45	KF798069	1496	Firmicutes, Clostridia, Clostridiales, Peptostreptococcaceae, Clostridium XI	Clostridium XI
Cr-AFE46	KF798070	1496	Firmicutes, Clostridia, Clostridiales, Peptostreptococcaceae, Clostridium XI	Clostridium XI
Cr-AFE47	KF798071	895	Firmicutes, Clostridia, Clostridiales, Peptostreptococcaceae, Clostridium XI	Clostridium XI
Cr-AFE48	KF798072	1496	Firmicutes, Clostridia, Clostridiales, Peptostreptococcaceae, Clostridium XI	Clostridium XI
Cr-AFE50	KF798073	1496	Firmicutes, Clostridia, Clostridiales, Peptostreptococcaceae, Clostridium XI	Clostridium XI

ID	Accession Number	Length (bp)	Classification using the RDP classifier (95% Confidence threshold)	OTU
Cr-AFE52	KF798074	1496	Firmicutes, Clostridia, Clostridiales, Peptostreptococcaceae, Clostridium XI	Clostridium XI
Cr-AFE53	KF798075	1496	Firmicutes, Clostridia, Clostridiales, Peptostreptococcaceae, Clostridium XI	Clostridium XI
Cr-AFE54	KF798076	1496	Firmicutes, Clostridia, Clostridiales, Peptostreptococcaceae, Clostridium XI	Clostridium XI
Cr-AFE55	KF798077	1496	Firmicutes, Clostridia, Clostridiales, Peptostreptococcaceae, Clostridium XI	Clostridium XI
Cr-AFE56	KF798078	1496	Firmicutes, Clostridia, Clostridiales, Peptostreptococcaceae, Clostridium XI	Clostridium XI
Cr-AFE57	KF798079	1496	Firmicutes, Clostridia, Clostridiales, Peptostreptococcaceae, Clostridium XI	Clostridium XI
Cr-AFE58	KF798080	1496	Firmicutes, Clostridia, Clostridiales, Peptostreptococcaceae, Clostridium XI	Clostridium XI
Cr-AFE59	KF798081	426	Firmicutes, Clostridia, Clostridiales, Peptostreptococcaceae, Clostridium XI	Clostridium XI
Cr-AFE60	KF798082	1496	Firmicutes, Clostridia, Clostridiales, Peptostreptococcaceae, Clostridium XI	Clostridium XI
Cr-AFE61	KF798083	1496	Firmicutes, Clostridia, Clostridiales, Peptostreptococcaceae, Clostridium XI	Clostridium XI

Table A.7: Classification and OTU for bacteria sequences obtained from Bacteria initially grown in Cr only media and then regrown in AFC media.

ID	Accession Number	Length (bp)	Classification using the RDP classifier (95% Confidence threshold)	OTU
Cr-SFe1	KF798143	1496	Firmicutes, Clostridia, Clostridiales, Peptostreptococcaceae, Clostridium XI	Clostridium XI
Cr-SFe2	KF798144	1496	Firmicutes, Clostridia, Clostridiales, Peptostreptococcaceae, Clostridium XI	Clostridium XI
Cr-SFe3	KF798145	1496	Firmicutes, Clostridia, Clostridiales, Peptostreptococcaceae, Clostridium XI	Clostridium XI
Cr-SFe5	KF798146	1496	Firmicutes, Clostridia, Clostridiales, Peptostreptococcaceae, Clostridium XI	Clostridium XI
Cr-SFe6	KF798147	1496	Firmicutes, Clostridia, Clostridiales, Peptostreptococcaceae, Clostridium XI	Clostridium XI
Cr-SFe7	KF798148	1496	Firmicutes, Clostridia, Clostridiales, Peptostreptococcaceae, Clostridium XI	Clostridium XI
Cr-SFe8	KF798149	1496	Firmicutes, Clostridia, Clostridiales, Peptostreptococcaceae, Clostridium XI	Clostridium XI
Cr-SFe9	KF798150	1493	Firmicutes, Clostridia, Clostridiales, Peptostreptococcaceae, Clostridium XI	Clostridium XI
Cr-SFe10	KF798151	1496	Firmicutes, Clostridia, Clostridiales, Peptostreptococcaceae, Clostridium XI	Clostridium XI
Cr-SFe11	KF798152	1496	Firmicutes, Clostridia, Clostridiales, Peptostreptococcaceae, Clostridium XI	Clostridium XI
Cr-SFe12	KF798153	1496	Firmicutes, Clostridia, Clostridiales, Peptostreptococcaceae, Clostridium XI	Clostridium XI
Cr-SFe13	KF798154	1496	Firmicutes, Clostridia, Clostridiales, Peptostreptococcaceae, Clostridium XI	Clostridium XI
Cr-SFe14	KF798155	1496	Firmicutes, Clostridia, Clostridiales, Peptostreptococcaceae, Clostridium XI	Clostridium XI
Cr-SFe15	KF798156	1496	Firmicutes, Clostridia, Clostridiales, Peptostreptococcaceae, Clostridium XI	Clostridium XI
Cr-SFe16	KF798157	1496	Firmicutes, Clostridia, Clostridiales, Peptostreptococcaceae, Clostridium XI	Clostridium XI
Cr-SFe17	KF798158	1496	Firmicutes, Clostridia, Clostridiales, Peptostreptococcaceae, Clostridium XI	Clostridium XI
Cr-SFe18	KF798159	1496	Firmicutes, Clostridia, Clostridiales, Peptostreptococcaceae, Clostridium XI	Clostridium XI
Cr-SFe19	KF798160	1496	Firmicutes, Clostridia, Clostridiales, Peptostreptococcaceae, Clostridium XI	Clostridium XI
Cr-SFe20	KF798161	1495	Firmicutes, Clostridia, Clostridiales, Peptostreptococcaceae, Clostridium XI	Clostridium XI

ID	Accession Number	Length (bp)	Classification using the RDP classifier (95% Confidence threshold)	OTU
Cr-SFe21	KF798162	1496	Firmicutes, Clostridia, Clostridiales, Peptostreptococcaceae, Clostridium XI	Clostridium XI
Cr-SFe22	KF798163	1496	Firmicutes, Clostridia, Clostridiales, Peptostreptococcaceae, Clostridium XI	Clostridium XI
Cr-SFe23	KF798164	1496	Firmicutes, Clostridia, Clostridiales, Peptostreptococcaceae, Clostridium XI	Clostridium XI
Cr-SFe24	KF798165	1496	Firmicutes, Clostridia, Clostridiales, Peptostreptococcaceae, Clostridium XI	Clostridium XI
Cr-SFe26	KF798166	1496	Firmicutes, Clostridia, Clostridiales, Peptostreptococcaceae, Clostridium XI	Clostridium XI
Cr-SFe28	KF798167	1497	Firmicutes, Clostridia, Clostridiales, Peptostreptococcaceae, Clostridium XI	Clostridium XI
Cr-SFe29	KF798168	1496	Firmicutes, Clostridia, Clostridiales, Peptostreptococcaceae, Clostridium XI	Clostridium XI
Cr-SFe30	KF798169	1496	Firmicutes, Clostridia, Clostridiales, Peptostreptococcaceae, Clostridium XI	Clostridium XI
Cr-SFe31	KF798170	1495	Firmicutes, Clostridia, Clostridiales, Peptostreptococcaceae, Clostridium XI	Clostridium XI
Cr-SFe32	KF798171	1496	Firmicutes, Clostridia, Clostridiales, Peptostreptococcaceae, Clostridium XI	Clostridium XI

Table A.8: Classification and OTU for bacteria sequences from the Cr(VI) consortia grown in SFe media.

ID	Accession Number	Sequence length	Classification using the RDP classifier (95% Confidence threshold)	OTU
Fe-SFe7	KF798084	1524	Firmicutes, Clostridia, Clostridiales	Tissierella C
Fe-SFe9	KF798085	1524	Firmicutes, Clostridia, Clostridiales	Tissierella C
Fe-SFe10	KF798086	1524	Firmicutes, Clostridia, Clostridiales	Tissierella C
Fe-SFe12	KF798087	1523	Firmicutes, Clostridia, Clostridiales	Tissierella C
Fe-SFe14	KF798088	1524	Firmicutes, Clostridia, Clostridiales	Tissierella C
Fe-SFe15	KF798089	1524	Firmicutes, Clostridia, Clostridiales	Tissierella C
Fe-SFe21	KF798090	1524	Firmicutes, Clostridia, Clostridiales	Tissierella C
Fe-SFe24	KF798091	1524	Firmicutes, Clostridia, Clostridiales	Tissierella C
Fe-SFe26	KF798092	1524	Firmicutes, Clostridia, Clostridiales	Tissierella C
Fe-SFe29	KF798093	1531	Actinobacteria, Actinobacteridae, Actinomycetales	Actinomycetales
Fe-SFe30	KF798094	1525	Firmicutes, Clostridia, Clostridiales, Incertae Sedis XI, Tissierella	Tissierella B
Fe-SFe31	KF798095	1496	Firmicutes, Clostridia, Clostridiales, Peptostreptococcaceae, Clostridium XI	Clostridium XI
Fe-SFe32	KF798096	1530	Actinobacteria, Actinobacteridae, Actinomycetales	Actinomycetales
Fe-SFe34	KF798097	1524	Firmicutes, Clostridia, Clostridiales	Tissierella C
Fe-SFe37	KF798098	1525	Firmicutes, Clostridia, Clostridiales	Tissierella C
Fe-SFe38	KF798099	1524	Firmicutes, Clostridia, Clostridiales	Tissierella C
Fe-SFe39	KF798100	1524	Firmicutes, Clostridia, Clostridiales	Tissierella C
Fe-SFe40	KF798101	1530	Actinobacteria, Actinobacteridae, Actinomycetales, Actinomycineae, Actinomycetaceae	Actinomycetales
Fe-SFe41	KF798102	1525	Firmicutes, Clostridia, Clostridiales, Incertae Sedis XI, Tissierella	Tissierella B
Fe-SFe43	KF798103	1524	Firmicutes, Clostridia, Clostridiales	Tissierella C
Fe-SFe45	KF798104	1524	Firmicutes, Clostridia, Clostridiales	Tissierella C
Fe-SFe47	KF798105	1524	Firmicutes, Clostridia, Clostridiales	Tissierella C

ID	Accession Number	Sequence length	Classification using the RDP classifier (95% Confidence threshold)	OTU
Fe-SFe52	KF798106	1524	Firmicutes, Clostridia, Clostridiales	Tissierella C
Fe-SFe55	KF798107	1524	Firmicutes, Clostridia, Clostridiales	Tissierella C
Fe-SFe57	KF798108	1531	Actinobacteria, Actinobacteridae, Actinomycetales	Actinomycetales
Fe-SFe58	KF798109	1524	Firmicutes, Clostridia, Clostridiales	Tissierella C
Fe-SFe61	KF798110	1525	Firmicutes, Clostridia, Clostridiales, Incertae Sedis XI, Tissierella	Tissierella B
Fe-SFe62	KF798111	1524	Firmicutes, Clostridia, Clostridiales	Tissierella C
Fe-SFe64	KF798112	1524	Firmicutes, Clostridia, Clostridiales	Tissierella C
Fe-SFe65	KF798113	1161	Actinobacteria, Actinobacteridae, Actinomycetales	Actinomycetales
Fe-SFe66	KF798114	1531	Actinobacteria, Actinobacteridae, Actinomycetales	Actinomycetales
Fe-SFe67	KF798115	1523	Firmicutes, Clostridia, Clostridiales	Tissierella C
Fe-SFe68	KF798116	1524	Firmicutes, Clostridia, Clostridiales	Tissierella C
Fe-SFe69	KF798117	1524	Firmicutes, Clostridia, Clostridiales	Tissierella C
Fe-SFe70	KF798118	1525	Firmicutes, Clostridia, Clostridiales	Tissierella C
Fe-SFe71	KF798119	1524	Firmicutes, Clostridia, Clostridiales	Tissierella C
Fe-SFe73	KF798120	1531	Actinobacteria, Actinobacteridae, Actinomycetales	Actinomycetales
Fe-SFe74	KF798121	1531	Actinobacteria, Actinobacteridae, Actinomycetales	Actinomycetales
Fe-SFe75	KF798122	1531	Actinobacteria, Actinobacteridae, Actinomycetales	Actinomycetales
Fe-SFe76	KF798123	1524	Firmicutes, Clostridia, Clostridiales, Incertae Sedis XI, Tissierella	Tissierella B
Fe-SFe77	KF798124	1524	Firmicutes, Clostridia, Clostridiales	Tissierella C
Fe-SFe78	KF798125	1523	Firmicutes, Clostridia, Clostridiales	Tissierella C
Fe-SFe79	KF798126	1523	Firmicutes, Clostridia, Clostridiales	Tissierella C
Fe-SFe80	KF798127	1523	Firmicutes, Clostridia, Clostridiales	Tissierella C
Fe-SFe81	KF798128	1523	Firmicutes, Clostridia, Clostridiales	Tissierella C

ID	Accession Number	Sequence length	Classification using the RDP classifier (95% Confidence threshold)	OTU
Fe-SFe82	KF798129	1524	Firmicutes, Clostridia, Clostridiales, Incertae Sedis XI, Tissierella	Tissierella B
Fe-SFe83	KF798130	1530	Actinobacteria, Actinobacteridae, Actinomycetales	Actinomycetales
Fe-SFe84	KF798131	1530	Actinobacteria, Actinobacteridae, Actinomycetales	Actinomycetales
Fe-SFe85	KF798132	1524	Firmicutes, Clostridia, Clostridiales	Tissierella C
Fe-SFe86	KF798133	1523	Firmicutes, Clostridia, Clostridiales	Tissierella C
Fe-SFe87	KF798134	1523	Firmicutes, Clostridia, Clostridiales	Tissierella C
Fe-SFe88	KF798135	1530	Actinobacteria, Actinobacteridae, Actinomycetales	Actinomycetales
Fe-SFe89	KF798136	1496	Firmicutes, Clostridia, Clostridiales, Peptostreptococcaceae, Clostridium XI	Clostridium XI
Fe-SFe90	KF798137	1529	Actinobacteria, Actinobacteridae, Actinomycetales	Actinomycetales
Fe-SFe91	KF798138	1523	Firmicutes, Clostridia, Clostridiales	Tissierella C
Fe-SFe92	KF798139	1530	Actinobacteria, Actinobacteridae, Actinomycetales	Actinomycetales
Fe-SFe93	KF798140	1530	Actinobacteria, Actinobacteridae, Actinomycetales	Actinomycetales
Fe-SFe94	KF798141	1524	Firmicutes, Clostridia, Clostridiales	Tissierella C
Fe-SFe95	KF798142	1524	Firmicutes, Clostridia, Clostridiales	Tissierella C

Table A.9: Classification and OTU for bacteria sequences from the Fe reducing consortia grown in SFe media.